The molecular evolution of DEDDh exonucleases reveals novel functions in innate immune signalling

by

Sabateeshan Mathavarajah

Submitted in partial fulfilment of the requirements

For Degree of Doctor of Philosophy

Dalhousie University

Halifax, Nova Scotia

December 2023

Table of Contents

List of Figures

Abstract

The Promyelocytic Leukemia (PML) protein is the major constituent of PML nuclear bodies (NBs), a subnuclear compartment involved in regulating a diverse array of cellular processes. PML NBs have tumour suppressive functions through their regulation of post-translational modifications, cell cycle progression, senescence, maintenance of genome stability, and apoptosis. However, there are many remaining questions about the functions of the PML-I isoform and its role in the cytoplasm. Work presented in this thesis examines the molecular evolution of *PML* and identifies a new role for PML-I and a novel family of related genes, PML-like exon 9 (Plex9), in repressing LINE-1 retroelements and regulating cGAS-STING signalling in jawed vertebrates.

Duplication of DNA encoding the PML C-terminus gave rise to *Plex9* genes in Teleostei, which lack homologs of both PML and the TREX1 DEDDh exonuclease (a regulatory of cGAS-STING). In an example of convergent evolution, zebrafish (*Danio rerio*) Plex9.1 functionally replaces TREX1 to suppress LINE-1. We then characterize an ortholog of PML encoded in the genome of the spotted gar (*Lepisosteus oculatus*). Gar Pml is a cytoplasmic exonuclease belonging to the DEDDh family that also suppresses LINE-1 retrotransposition. The PML protein lost exonuclease activity but evolved SUMOylation sites to form NBs in amniote species. However, human PML-I retained the ability to restrict LINE-1 by shuttling in a CRM1-dependent manner to the cytoplasm. Thus, we shed new light on the molecular evolution and functional divergence of PML protein over the course of vertebrate evolution.

cGAS-STING signalling is involved in mammalian wound healing and age-related senescence, but it has not been examined in other vertebrate species. We examine the expression of these suppressors of cGAS-STING, as well as inflammatory genes and cGAS activity during caudal fin and limb regeneration using the spotted gar and axolotl (*Ambystoma mexicanum*) model species, and during age-related senescence in the hearts of zebrafish. During the early stages of limb-fin regeneration and age-related senescence, Pml, Trex1 and Plex9.1 exonucleases are downregulated, presumably to allow cGAS-STING activation. Therefore, in jawed vertebrates, negative regulation of cGAS-STING activity is accomplished by the collective actions of Trex1, Pml and Plex9 DEDDh exonucleases.

List of abbreviations used

PML	Promyelocytic Leukemia
NB	Nuclear body
SUMO	Small ubiquitin-like modifier
SIM	SUMO interacting motif
RBCC	RING, B-box, Coiled coil
NLS	Nuclear localization sequence
NES	Nuclear export sequence
DAXX	Death domain-associated protein 6
TRIM	Tripartite motif
LD	Lipid droplet
ALT	Alternative lengthening of telomeres
MAPP	Mitotic accumulations of PML protein
Plex9	PML-like exon 9-like
TREX1	Three prime exonuclease 1
CGAS	Cyclic GMP-AMP synthase
CGAMP	2',3'-Cylic GMP-AMP
STING	Stimulator of interferon genes
IFN	Interferon
UPS	Ubiquitin-proteasome system
APL	Acute Promyelocytic Leukemia
BTR	BLM-TOPO3a-RMI
ATRA	All-trans retinoic acid
ATO	Arsenic trioxide
PPAR	Peroxisome proliferator-activated receptor
NF-κB	Nuclear factor kappa light chain enhancer of activated B cells

ER	Endoplasmic Reticulum
L1	LINE-1, Long interspersed nuclear element 1
TREX1	Three prime repair exonuclease 1
HIV	Human immunodeficiency virus
AGS	Aicardi-Goutières syndrome
CDE	C-terminal DEDDh exonuclease domain
ExoIII	Exonuclease III
HMT	Hexahistidine-maltose binding protein-tobacco etch virus protease recognition sequence
zfPlex9	Zebrafish Plex9
sgPml	Spotted gar PML
axTREX1	Axolotl TREX1
qPML	Japanese quail PML
L2	LINE-2
dsDNA	Double-stranded DNA
ssDNA	Single-stranded DNA
DSB	Double-stranded break
ATM	Ataxia-telangiectasia mutated
EMT	Epithelial-Mesenchymal transition
SMAD	Suppressor of Mothers against Decapentaplegic transcription factor
IFN-γ	Interferon γ
IFN-β	Interferon β
IFN-α	Interferon α
UTR	Untranslated region
TPRT	Target-primed reverse transcription
SASP	Senescence Associated Secretory Phenotype
IL6	Interleukin 6
IL8	Interleukin 8

Acknowledgements

I want to acknowledge firstly my supervisor and mentor Dr. Graham Dellaire. When I first started in his lab, I was completely clueless as to how science was properly done. Under your mentorship, I learned how to better plan experiments and think rationally about what I am trying to answer. Your excitement for science is always motivating and I will try to hold at least half of that excitement as I continue, as that is an important part to making this a satisfying career.

In addition, I want to thank my two best colleagues/friends in the lab, Joyce and Jayme. I can't think of many days where I haven't bugged you two with a question. You both have been pillars for me. I also want to thank all the former lab members who have taught me most of what I know or helped me with experiments. This includes Dudley, Carter, Livia, Ally, and Elias who I can dedicate many lab lessons and memories to. Finally, I want to thank the Pathology department that has made my research possible, especially the Marcato and Waisman labs who have shared equipment for my experiments.

In addition, I'd like to thank the Langelaan lab, Braasch lab (University of Michigan), Roy Lab (University of Montreal), Roger lab, Berman lab (University of Ottawa), and Quinn lab for all the collaborations and support they have provided to my thesis over the years. I also want to thank my previous supervisor Dr. Robert J. Huber for his constant support throughout my graduate studies.

I want to thank my family for all their support over the years. My closest friends Ahmed, Taran, and Alex, who have supported me since I first learned how to use a pipette in undergrad. Then, the friends who kept me motivated here in Halifax. I am lucky for all the support I have received throughout my PhD.

Finally, thank you to the funding agencies (BHCRI and the Cancer Research Training Program, NSERC, NSHRF, and Killam Trusts) who have provided financial support for this work.

Chapter 1 – Introduction

This chapter contains material (sections 1.2, 1.4, 1.6; Figures 1.4 and 1.6) originally published in 2 manuscripts:

"McPhee, M.J., Salsman, J., Foster, J., Thompson, J., Mathavarajah, S., Dellaire, G. and Ridgway, N.D., 2022. Running 'LAPS' around nLD: nuclear lipid droplet form and function. *Frontiers in Cell and Developmental Biology*, *10*, p.837406."

"Mathavarajah, Sabateeshan, and Graham Dellaire. "LINE-1: an emerging initiator of cGAS-STING signalling and inflammation that is dysregulated in disease." *Biochemistry and Cell Biology* (2023). e-First."

1.1 Preface

Deciphering the molecular evolution of the promyelocytic leukemia (PML) protein to improve our understanding of how it contributes to genome stability and innate immune signalling is the central focus of this thesis. This chapter introduces PML nuclear bodies (NBs) and how they form, their regulation of cellular processes, the subset of different PML NBs formed, and the different PML isoforms. In addition to reviewing the literature revolving around PML from a biochemical and cellular perspective, the chapter will discuss how PML is involved in cancer. Throughout my thesis, I link PML to a pathway known as cGAS-STING, which I will also review in this chapter.

The chapters which follow will present our findings on the evolution of PML, the identification and characterization of a novel PML-related gene family (the PML-like exon 9-like (Plex9) genes) in teleost fishes, conserved functions for the PML gene in

maintaining genome stability and finally a new role for PML and Plex9 in aquatic vertebrate limb-fin regeneration and age-related senescence.

1.2 PML Nuclear Bodies

The nucleus is spatially organized, with the positioning of chromosomes having distinct territories and there being heterogenous localizations of nuclear proteins. The variety of protein localizations within the nucleus are possible through subnuclear compartments, with some structures being stable and others being more dynamic. These different compartments form in part because of a biophysical phenomenon known as phase-separation, leading to the formation of "membrane-less" compartments (Lee et al., 2022). These phase-separated structures in the nucleus include nucleoli, nuclear speckles, Cajal bodies and PML NBs, all with distinct regulatory functions that help dictate cellular progression and cell fate decisions (Banani et al., 2016; Brangwynne et al., 2011; Courchaine et al., 2021; Kim et al., 2019).

PML NBs are compact subnuclear compartments ranging in diameter from 0.1 to 1 μm, with mammalian cells hosting 4-30 bodies (Banani et al., 2016; Hoischen et al., 2018). PML NBs are structures that differ in number and composition depending on the cell type, cell cycle phase, and differentiation stage (Dellaire & Bazett-Jones, 2004). For example, this can be as extreme as PML NBs being absent in cells after myogenic or neuron differentiation (Lam et al., 1995; Salsman et al., 2017). Electron microscopy and super-resolution techniques revealed that PML NBs typically form an insoluble spherical shell that tethers to chromatin (Corpet et al., 2020; Hoischen et al., 2018; Stuurman et al., 1992).

The tethering to surrounding chromatin occurs through multiple contact sites and contributes to the integrity and stability of the PML NBs (Eskiw et al., 2004). Cellular events or stresses that cause chromatin condensation result in the fission of small bodies from the detached and destabilized PML NB structure (Ching et al., 2005; Eskiw et al., 2004).

PML is part of the tripartite motif (TRIM) family, where proteins harbor a similar N-terminal motif that is characterized by a RING domain, two B-box domains (B1 and B2), and a Coiled-coil domain, also known as the RBCC domain (as they occur in that order within the protein sequence) (Ugge et al., 2022). In contrast, the C-terminus of PML differs depending on the protein isoform, of which there are seven main isoforms. The RING domain is a cysteine rich tandem zinc-finger domain that spans 40–60 residues (Borden et al., 1995; Wang et al., 2018). The B-box domain is a zinc-binding protein domain that is characterized by conserved cysteine and histidine residues (Borden et al., 1996; Bregnard et al., 2022). Finally, there is the Coiled-coil domain that essentially has 2–5 α-helices that twist on another to produce a supercoil structure that promotes subunit oligomerization (Antolini et al., 2003; Occhionorelli et al., 2011).

The PML protein contains at least seven validated sites on lysine residues for conjugation to the Small ubiquitin-like modifier (SUMO) protein. In addition, the protein encodes a C-terminal SUMO-interacting motif (SIM). This allows SUMO-modified PML to homo-multimerize through their SIMs (Cheng & Kao, 2012; Song et al., 2004). Phosphorylation of the PML SIM enhances its interaction to SUMO1, as positively charged residues of SUMO1 interact with the phosphorylated serine residues of the SIM (Cappadocia et al., 2015). Additional regulatory factors exist that affect the SUMO-SIM

interaction, such as the zinc binding to SUMO1, that relieves its autoinhibitory state and then promotes consequent binding to the phosphorylated SIM of PML (Mathieu Lussier-Price et al., 2022). SUMOylation contributes to PML NB formation but it is not essential for PML NB oligomerization, with multimerization occurring primarily via the N-terminal RBCC domain (**Figure 1.1**) (Sahin et al., 2014). The PML NB shell results from self-oligomerization that occurs through three steps (**Figure 1.1**); (1) the N-terminal RBCC domain of PML facilitates self-oligomerization between PML monomers via oxidation-drive disulfide bridges and noncovalent binding of RBCC domains (through RING and B1 domains) and (2) further multimerization promoted by PML post-translational modification by SUMO (e.g., via UBC9, a SUMO E2 protein), driven by SUMO-SIM interactions and (3) the recruitment of client proteins that are SUMOylated or SIM-containing to the nuclear bodies to form mature PML NBs (Hoischen et al., 2018; Li et al., 2019; Wang et al., 2018). Afterwards, there is polySUMOylation of PML proteins, that can trigger the degradation of PML via RNF4, an E3 ubiquitin ligase that senses polySUMOylated targets (Gärtner & Muller, 2014; Geoffroy et al., 2010; M. H. Tatham et al., 2008). Ubiquitinated PML is then degraded through the ubiquitin-proteasome system (UPS). The result is a dynamic structure that is constantly being remodelled by the incorporation of new PML protein, changes in the repertoire of interacting/localizing proteins, and degradation of residing PML protein. Therefore, both the RBCC domain and SUMO:SIM interactions allow for PML protein self-oligomerization and the consequent formation of the nuclear bodies (**Figure 1.1**).

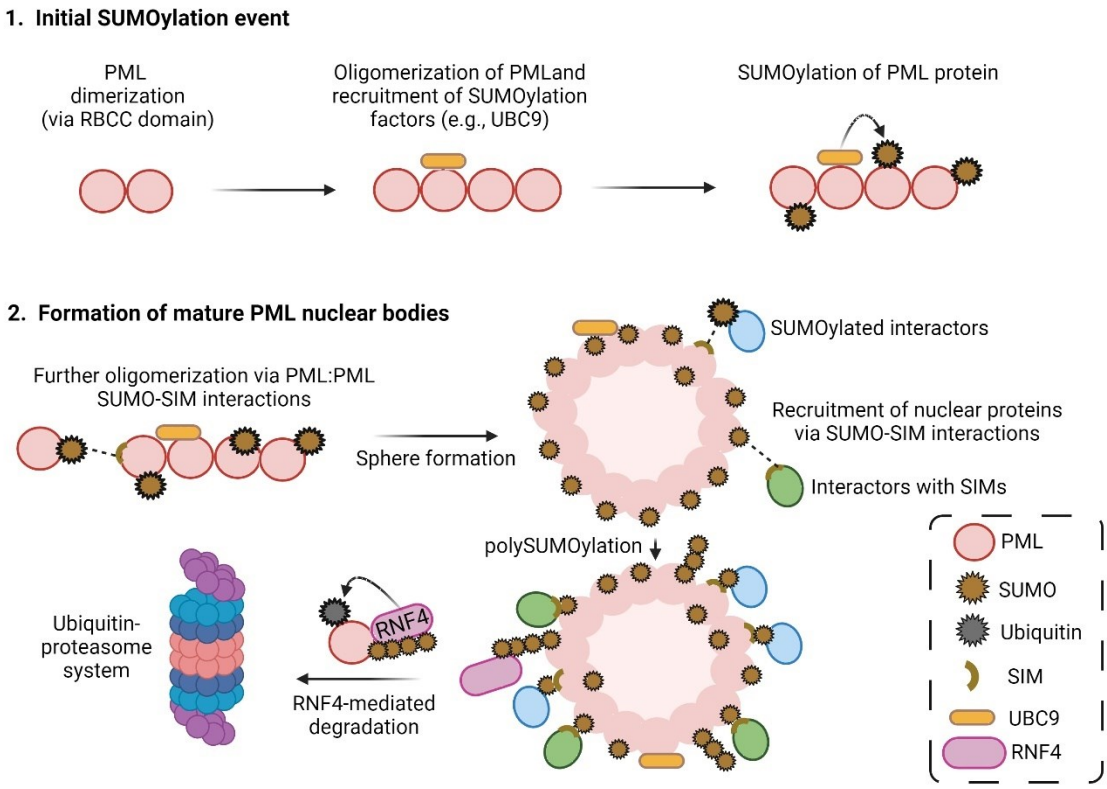

Figure 1.1. Steps in forming PML NBs. PML NBs form through a multi-step process that begins homodimerization between two monomers via their N-terminal RBCC domains. The resulting chain is then modified by SUMO through recruited factors such as UBC9, which causes SUMO-SIM interactions between other PML protein and the eventual formation of the PML NB sphere. Afterwards, there is recruitment of resident proteins at PML NBs via SUMO-SIM interactions. Finally, the structures can be regulated and PML can be sent for degradation with polySUMOylation, that leads to RNF4-mediated ubiquitination of PML for degradation.

These dynamic structures serve as regulatory hubs for over 150 nuclear proteins that are known to constitutively and transiently associate (**Figure 1.2**) (Van Damme et al., 2010). Proteins known to localize and interact with PML have functions in cell cycle regulation (including cell fate decisions such as senescence), apoptosis, SUMOylation modifications, Telomere maintenance, DNA repair, antiviral response, chromatin remodelling and transcription (**Figure 1.2**) (Attwood et al., 2020; Bernardi et al., 2008; Bischof et al., 2002; Dellaire & Bazett-Jones, 2004; Dellaire, Ching, et al., 2006; Everett & Chelbi-Alix, 2007; Pearson & Pelicci, 2001; Villagra et al., 2006). Important cell fate regulators such as p53 and Rb also localize to PML, where they are regulated (de Stanchina et al., 2004; Dellaire et al., 2003; Vernier et al., 2011). Many PML NB client proteins associate with PML NB in a SUMOylation- and/or SIM-dependent manner. For example, two well established PML NB interactors that consistently localize and comprise the "classical" PML NBs are Death domain-associated protein 6 (DAXX) and SP100 (Khelifi et al., 2005; Szostecki et al., 1990) (Figure 2). SP100 is SUMOylated and interacts with PML NB through the SIM on PML. Conversely, DAXX possesses its own SIM that allows for binding to SUMOylated PML. In addition, many components of the SUMOylation machinery localize to NBs such as SUMO proteases (i.e. SENPs) and SUMO ligases (i.e. UBC9 and PIAS proteins) which regulate these interactions in terms of timing and functional outcomes (Barroso-Gomila et al., 2021; Brown et al., 2016; Hattersley et al., 2011; Sahin et al., 2014; Van Damme et al., 2010). Such SUMO-SIM interactions between partner proteins are fundamental to how classical PML NBs interact with other protein constituents and thus SUMO-SIM interactions are an important part of PML biology.

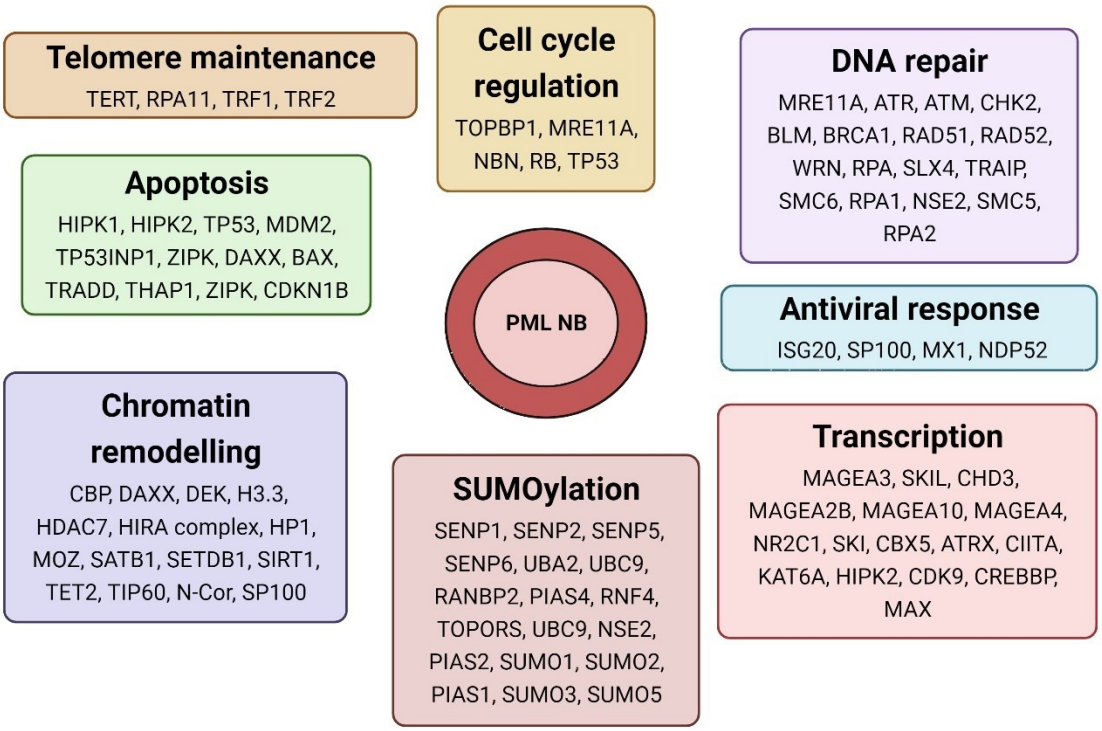

Figure 1.2. Nuclear proteins that localize to PML NBs. Over 150 nuclear proteins localize to PML NBs and regulate various cellular processes, as indicated. PML NB regulation of these proteins contributes to how these subcellular compartments regulate a wide array of cellular processes. The following is a list of known interactors and PML NB localizing proteins curated from publications (Chang et al., 2018; Corpet et al., 2020; Dellaire & Bazett-Jones, 2004; Van Damme et al., 2010) and the Gene Ontology annotation database (under the term PML body Gene Ontology Term (GO:0016605)).

1.3 PML protein architecture and isoforms

The *PML* gene (also known as *TRIM19*) is located on chromosome 15q and contains 9 exons which are subjected extensive alternative mRNA splicing, resulting in the formation of seven main protein isoforms that have a common tripartite RBCC motif (encoded by the first 3 exons) and variable C-terminal tails that are a result of alternative splicing (Exons 7-9) (Jensen et al., 2001; Nisole et al., 2013) (**Figure 1.3A**). Early work identified that alternative splicing of exons 4-6 may occur in various combinations for each of the seven main isoforms, but there has not been follow-up work to address this. However, the differential splicing of exons 4-6 suggests that these seven main isoforms of PML have an additional layer of complexity with internal variation that is poorly understood (Fagioli et al., 1992). All the PML isoforms have a nuclear localization sequence (NLS) encoded by exon 6 except for PML-VII which is cytoplasmic (Nisole et al., 2013). The isoforms differ in their allocation of the 8 potential SUMOylation sites, with 3 being found within the RBCC domain, 4 being around the NLS, and one site being only present on exon 8a (Nisole et al., 2013) (**Figure 1.3B**). The notable differences in the C-terminus sequences, localizations and SUMOylation sites all account to different functions for the various isoforms. The uncharacterized Exon 9 is only encoded by PML-I and not found in any other isoforms (**Figure 1.3A)**. These differences contribute to the isoforms having unique functions and play different contributing roles to PML NB formation, such as PML-I having the shortest resident time at bodies and PML-V having the longest (i.e., PML-V appears to contribute more to PML NB structural integrity than PML-I)(Weidtkamp-Peters et al., 2008).

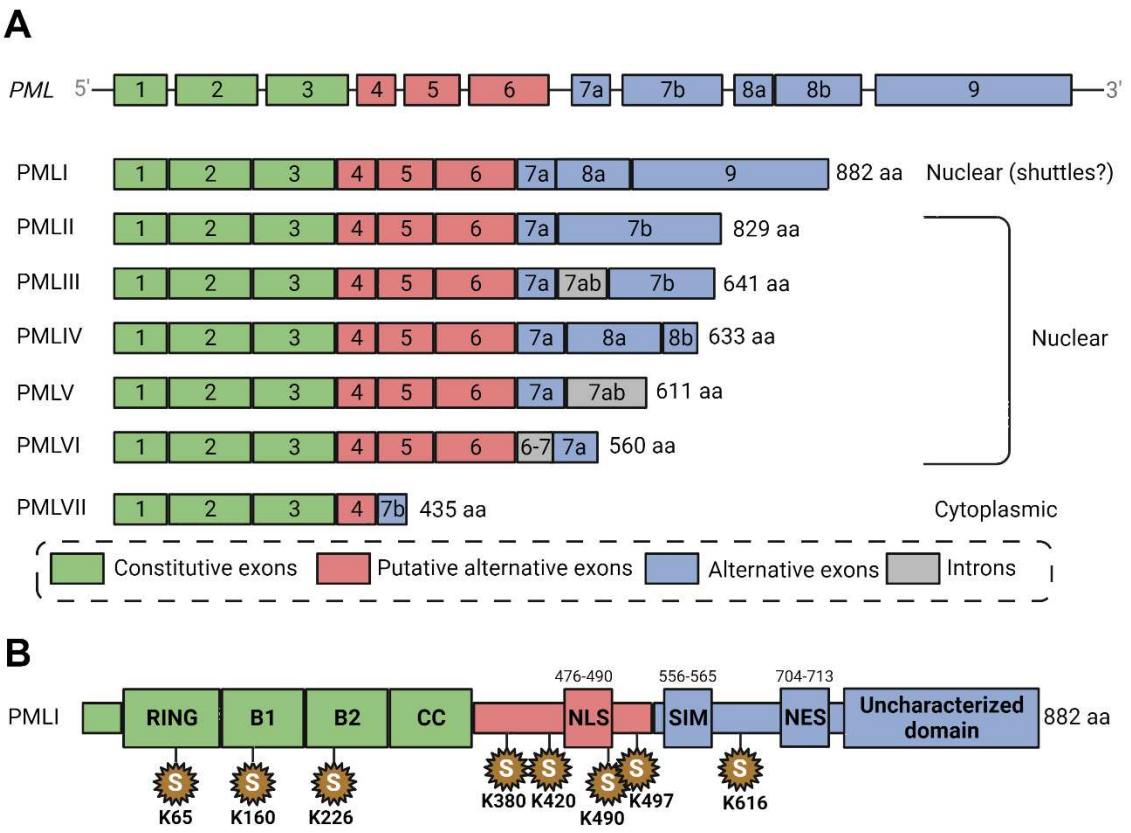

Figure 1.3. The different PML isoforms and domain architecture of PML-I. (A) The *PML* gene has 9 exons that can undergo alternative splicing, with 3 exons being conserved between the 7 main isoforms. There is potential for internal splicing of exons 4-6 but this is poorly understood. The C-terminal tails of the different isoforms differs due to extensive alternative splicing occurring between exons 7-9. The result is significant differences in amino acid length (882 aa – 435 aa), unique C-terminal tails, and differences in localization (PML-VII localizes to the cytoplasm). (B) PML-I is the most highly expressed isoform and represents the full-length protein. The following is a schematic of its major RBCC domain, NLS (nuclear localization sequence), NES (nuclear export sequence) and SUMOylation sites. PML-I also encodes the exon 9 region which is poorly understood in terms of function.

The different PML isoforms also seem to have unique interaction partners, which contributes to how they influence cellular processes in an isoform-specific manner. The most-well studied isoform is PML-IV. One function of PML-IV is in the regulation of p53 by inducing post-translational modifications such as acetylation, phosphorylation and SUMOylation on p53 (Bischof et al., 2022; Fogal et al., 2000; Ivanschitz et al., 2015). These modifications activate p53 to cause cellular senescence or cell death (Bischof et al., 2022; Fogal et al., 2000; Ivanschitz et al., 2015). However, PML-IV regulation of E2Fs and Rb is a contributing factor to cellular senescence (Vernier et al., 2011). A second mechanism by which PML-IV regulates p53 is through sequestration of E2F at nuclear bodies, to induce senescence (Vernier et al., 2011). The isoform also promotes the DNA damage (DDR) response by stabilizing histone modifier TIP60 when cells experience genotoxic stress (note; misannotated in the article but PML3 is referring to PML-IV not PML-III) (Wu et al., 2009). In addition, PML-IV also targets other key proteins involved in cancer progression such as through Myc destabilization and repression of nuclear EGFR activity (Buschbeck et al., 2007; Kuo et al., 2013). PML-IV overall, appears to promote tumour suppression functions by regulating apoptosis and senescence (via p53), the DDR (via TIP60), cell differentiation (via Myc), and cell proliferation (via EGFR).

PML-II is another isoform that has recently emerged as a PML isoform with specific functions that have not been linked to other isoforms. PML-II is linked to the formation of lipid associated PML bodies and senescence-associated threads, which I discuss in the next section (Jul-Larsen et al., 2010; Ohsaki et al., 2016). The isoform also has a novel role in immune signalling in multiple ways. Firstly, it promotes the

transcription of major histocompatibility complex (MHC) II genes by protecting the class II transactivator CIITA from degradation by the ubiquitin-proteasome system (UPS) (Ulbricht et al., 2012). The isoform also contributes to Interferon (IFN)-α mediated apoptosis by contributing to ERK and AKT signalling (Meng et al., 2021). In addition, PML-II promotes the recruitment of IRF3, NF-κB, and STAT1 to promoters of IFN-β responsive genes (Chen et al., 2015). As a result, PML-II can influence both antigen presentation and type I IFN signalling.

There are only a handful of studies looking specifically at the functions of other isoforms, aside from PML-IV and PML-II. PML-III has been linked to the global increase in SUMOylation in response to type I IFNs (Maroui et al., 2018). PML-III recruits Ubc9 to PML-NBs after IFN treatment, increasing the relative rates of SUMOylation occurring at NBs. PML-V on the other hand, seems to be involved in DNA repair, as it interacts with RAD51 (Boichuk et al., 2011). The PML-V and RAD51 interaction leads to enhanced homology directed repair of double-stranded breaks (Boichuk et al., 2011). Aside from these individual studies, there is not much else known in terms of isoform-specific functions for PML-III and PML-V.

Intriguingly, one of the most poorly understood isoforms is the longest sequence length isoform (882 residues) and the most abundant protein isoform within the cell, PML-I (Nisole et al., 2013). PML-I also encodes an exon 9 region that is unique and shares homology to an exonuclease-III domain but there has been no reported evidence of exonuclease activity for PML-I (Condemine, Takahashi, Le Bras, & de The, 2007). PML-I is also the only isoform with a nuclear export sequence (NES) (Nisole et al., 2013). However, the nucleocytoplasmic shuttling of PML-I has not been characterized and it is

unknown as to what biological functions cytoplasmic PML-I may have. However, PML-I has been shown to re-localize to nucleolar caps when cells undergo senescence (Condemine, Takahashi, Le Bras, & de The, 2007). Its localization to nucleolar caps seems to be tied to the exonuclease-like domain of PML-I (Condemine, Takahashi, Le Bras, & de The, 2007).

There have been two pathways, myeloid differentiation, and homology-directed DNA repair, linked specifically to PML-I based on its interactions with AML1 and RAD51, respectively (Boichuk et al., 2011; Nguyen et al., 2005). In both cases, PML-I binds to these proteins to promote AML1-transcription of myeloid differentiation factors and RAD51-mediated repair of double-stranded breaks (Boichuk et al., 2011; Nguyen et al., 2005). However, despite these reports, there has been no further characterization on how PML-I binding alters AML1 and RAD51 to promote their functions. In addition, as aforementioned, PML-V appears to be more involved with the regulation of RAD51 and has a greater influence on double-stranded break repair than PML-I. The key to understanding PML-I and its function appears to be tied to its unique and yet uncharacterized exon 9 sequence.

1.4 Different PML structures

1.4.1 ALT-associated bodies

Although the protein composition of PML NBs changes constantly, the PML NB themselves are stable structures that exist as hubs to mediate critical nuclear functions. However, PML NB are more dynamic in stressed cells and can shift in morphology, composition, and function in the context of cell cycle progression, stressful stimuli, and

virus infection. There are several non-canonical PML structures that only occur in abnormal cells (**Figure 1.4**). For example, in ~15% of all cancers, cells circumvent their rapid proliferation and eventual loss of telomeres through a pathway known as the alternative lengthening of telomeres (ALT) (Bryan et al., 1995).

Specifically in ALT-positive cells, PML co-localizes with the telomere marker TRF2 and promotes ALT processes at the telomere (Loe et al., 2020) (Figure 2). These novel PML structures, termed ALT-associated PML bodies, are essential for facilitating telomere lengthening by recruiting the BLM-TOPO3a-RMI (BTR) complex to telomeres (Chung et al., 2012). In the absence of PML, the BTR complex cannot be recruited to telomeres for lengthening via the ALT pathway (Loe et al., 2020). Since BLM is a canonical PML NB protein that interacts with PML through its own SUMO and tandem SIM motifs, this is likely the driving force behind BLM and eventual BTR complex localization at ALT-associated PML bodies (S. Liu et al., 2023; Stavropoulos et al., 2002; Zhu et al., 2008). Therefore, while APBs have novel functions and are specifically associated with ALT-associated PML bodies, mechanistically their roles are driven by SUMO-SIM interactions as with classical PML NB.

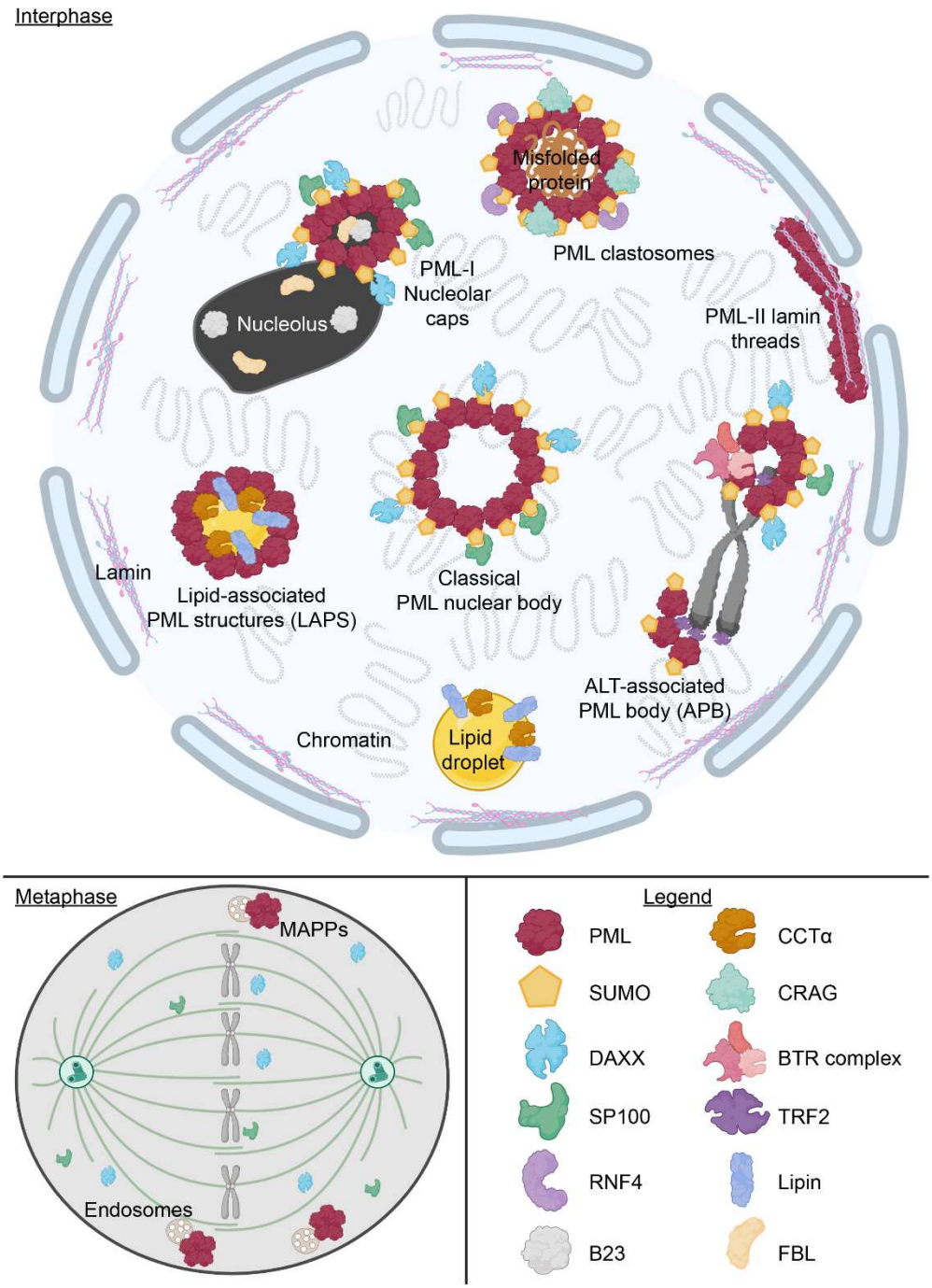

Figure 1.4. PML NBs exist as a multitude of unique structures with different regulatory roles. PML NBs form different structures to deal with various forms of cellular stress and contribute to different biological processes during interphase. These different structures have different protein compositions from one another and consequently, divergent roles in regulating cellular processes. In addition, PML NBs form another unique structure during mitosis, known as mitotic accumulations of PML protein (MAPPs) that differ in composition from their interphase PML NB counterparts.

1.4.2 PML-II threads in senescent cells

In senescent cells, PML can appear to form thread-like structures with the nuclear lamina and proteinaceous rings/caps around the nucleoli (Condemine, Takahashi, Le Bras, & de The, 2007; Jul-Larsen et al., 2010; Stixova et al., 2012) (**Figure 1.4**). While these PML NB structures are unique in terms of morphology, they appear to retain a similar composition to classical PML NB, harboring DAXX and SP100 (Condemine, Takahashi, Le Bras, & de The, 2007; Jul-Larsen et al., 2010). However, formation of these senescence associated PML structures are attributed to specific isoforms. PML-II is essential for the formation of senescence-associated PML-lamina threads (Jul-Larsen et al., 2010) whereas PML-I and PML-IV can both localize to the nucleolus, but PML-I is required for recruitment of PML-IV to nucleolar caps (Condemine, Takahashi, Le Bras, & de The, 2007). These PML structures have been implicated in Hutchinson-Gilford progeria syndrome, a premature aging syndrome resulting from disruption of nuclear lamina integrity (Wang et al., 2020). In patient fibroblasts, PML-II was not only a marker of late senescence but was a contributing factor to the accelerated senescence observed (Wang et al., 2020).

1.4.3 Mitotic accumulations of PML protein

Interphase cells primarily have PML NB that are SUMOylated and composed of canonical interactors such as DAXX and SP100. However, during mitosis, PML proteins form a unique SUMO-negative structure known as mitotic accumulations of PML protein (MAPP) (**Figure 1.4)** (Dellaire, Ching, et al., 2006). MAPPs also lack DAXX and SP100, which diffuse into the mitotic cytoplasm from prophase to metaphase (Chen et al., 2008;

Dellaire, Ching, et al., 2006; Everett et al., 1999). MAPPs form once PML NB are untethered from chromatin during mitosis, and they appear to be bound to early endosomes in dividing cells (Chen et al., 2008; Palibrk, Lang, et al., 2014). MAPPs remain in the cytoplasm until early G1 phase until PML protein within them is imported in the nucleus to re-establish PML NBs after the nuclear envelope reforms (Chen et al., 2008; Dellaire, Ching, et al., 2006).

1.4.4 PML clastosomes

PML NBs can also contain protein degradation machinery under stress conditions (Lafarga et al., 2002). These structures are referred to as PML clastosomes (**Figure 1.4**) and contain high concentrations of ubiquitin conjugates and components of the UPS (Lafarga et al., 2002). In addition to the protein degradation machinery, putative substrates such as short-lived transcription factors (c-Fos and c-Jun) also accumulate at these structures. The PML-IV isoform is important for the recruitment of the different subunits of the 19S regulatory complex and 20S catalytic core of the proteasome to the PML clastosome (Janer et al., 2006).

These structures are important anchors for preventing protein-misfolding diseases, as they are capable of degrading proteins misfolded in the nucleus from polyQ expansion and also non-polyQ proteins that are often misfolded in neurodegenerative disease such as TDP-43 (involved Amyotrophic Lateral Sclerosis and Frontotemporal lobar degeneration with ubiquitin-positive inclusions) (Guo et al., 2014). The polyQ expanded pathogenic misfolded proteins include ATXN1 in spinocerebellar ataxia type 1, ATXN1 in spinocerebellar ataxia type 7, and HTT in huntingtin's disease, that are degraded in

part through PML clastosomes after direct interaction (Guo et al., 2014; Janer et al., 2006). PML clastosomes selectively interact with misfolded proteins that are conjugated to SUMO2/3, with RNF4 mediating their ubiquitination and consequent degradation (Guo et al., 2014).

PML therefore appears to play an important role in neurodegenerative disease as a factor that mitigates nuclear accumulation of pathogenic misfolded proteins. However, PML NBs are also directly impacted in certain diseases. In neuronal intranuclear hyaline inclusion disease (NIHID), there are p62-positive and ubiquitin-positive nuclear aggregates at PML structures (Nakano et al., 2017). Importantly, the PML NBs found in NIHID cases did not form the typical shell and core structure that is typically observed and likely contributing to the observed inclusions (Nakano et al., 2017). However, it is not known as to whether the abnormalities to PML NB structure are causing the inclusions or if the inclusions are responsible for the abnormal NBs. Moreover, recently it was shown that in familial amyotrophic lateral sclerosis-frontotemporal dementia, PML NBs are strongly reduced, and this impairs the clearance of misfolded proteins (Antoniani et al., 2023). However, the mechanisms behind PML NB disruption in these disorders is still currently unknown.

1.4.5 Cajal-associated PML bodies

PML bodies also influence other subnuclear compartments such as Cajal bodies. Cajal bodies are associated with the nucleolus and contribute to the site of transcriptional activation, RNA metabolism, base modification, and the biogenesis of ribonucleoproteins (including snRNA (small nuclear ribonucleoproteins)) (Carmo-Fonseca et al., 1993;

Meier, 2017). A subset of Cajal bodies are also associated with PML (Cajal-associated PML bodies) in the nucleus of human cells (**Figure 1.4**) (Barcaroli et al., 2006; Berciano et al., 2007). PML bodies appears to promote Cajal bodies as their machinery interacts with Cajal body machinery at snRNA genomic loci (Sun et al., 2005). The SUMOylation associated E3-type ligase PIAS4 (PML NB localizing protein) interacts with coilin, a major constituent of Cajal bodies (Sun et al., 2005). When the sequence for the PIAS4 interaction region of coilin is removed, there is a significant reduction in the Cajal-associated PML bodies. However, the importance of PML-mediated SUMOylation of Cajal body machinery is still not well-understood.

1.4.6 Lipid-associated PML bodies (LAPs)

The lipid droplet (LD) is an organelle that is composed of proteins and monolayer of phospholipids at the surface, and a mixture of triacylglycerides, steryl esters, and/or retinyl esters within the neutral lipid core (Orban et al., 2011; Shen et al., 2016; Walther et al., 2017). Both nutrient stress and excess fatty acids result in the formation of lipid droplets (Henne et al., 2018). Some of these LDs also form in the nucleus (nuclear LDs) but are (1) unique in terms of their biogenesis, (2) differ in protein composition, and (3) ultimately the cellular processes they regulate/influence (Sołtysik et al., 2019). Lipid-associated PML bodies (LAPs) are PML nuclear bodies that associate with these nuclear LDs (**Figure 1.4**).

Most LAPs (~75%) resemble MAPPs in terms of composition, as they lack SUMO, DAXX and SP100 (Lee et al., 2020). However, unlike MAPPs that are amorphous, LAPs can form spheres that resemble typical PML NB morphology. Once

formed in the nucleus, LDs recruit PML along with other proteins such as CCTa and Lipin1 (McPhee et al., 2022). PML-II influences the formation of nuclear LDs (Ohsaki et al., 2016). The knockdown of PML-II results in a 30-50% reduction in the total number of nuclear LDs (Ohsaki et al., 2016). Similar results were seen in U2OS cells after CRISPR/Cas9 mediated knockout of *PML* (i.e., loss of total PML protein versus just the isoform) (Lee et al., 2020). While PML is emerging as an important factor involved in nuclear LD regulation, more work is required to better understand the functions it may have at these structures.

1.5 The role of *PML* in cancer

1.5.1 Acute promyelocytic leukemia

In Acute Promyelocytic Leukemia (APL), a distinct subtype of Acute Myeloid Leukemia, a recurrent chromosomal translocation can be found in more than 95% of patients (de The et al., 1990; Kakizuka et al., 1991; Longo et al., 1990; Rowley et al., 1977). The APL chromosome translocation t(15;17) event results in a fusion gene comprised of the *PML* gene (found on chromosome 15) and the Retinoic acid receptor alpha (*RAR*α) gene (found on chromosome 17) (Grignani et al., 1993; Mannan et al., 2020; Piazza et al., 2001). APL was first described in 1957 with rapid cancer progression where patients had an abundance of promyelocytes and severe bleeding (Hillestad, 1957). The chromosomal translocation involving the *RAR*α locus and *PML* locus results in a fusion transcript of *PML-RARα* (de The et al., 1990; Kakizuka et al., 1991). The transcript was shown to be detected in 100% of patients with t(15;17) (de The et al., 1990; Kakizuka et al., 1991). Transgenic mice revealed that the expression of *PML-RAR*α

in the myeloid lineage is critical for APL pathogenesis (He et al., 1998). The PML-RARα fusion protein forms homodimers that sequester RXR and PML proteins, and then repress the gene expression of key genes required for granulocyte differentiation by binding to retinoic acid response elements and recruiting corepressor proteins and DNA methylation enzymes (Kamashev et al., 2004; Wu et al., 2001). These fusion protein structures do not resemble typical PML NBs and lead to the formation of nuclear microspeckles, due to the loss of the SIM that is normally encoded on full length PML (Chelbi-Alix et al., 1995; Lallemand-Breitenbach & de The, 2010).

While initial chemotherapeutic approaches using daunorubicin in 1973 had some success against APL leukemic cells, the usage of all-trans retinoic acid (ATRA) in 1985 opened a new age for APL treatment (Bernard et al., 1973; Wang & Chen, 2008). The combination of chemotherapy with ATRA resulted in complete remission rates greater than 90% across patients. In addition, for cases with refractory or relapsed APL (as well as newly diagnosed), treatment with arsenic trioxide (ATO) further improved clinical outcomes (Wang & Chen, 2008). The combination of ATRA and ATO has led to synergistic therapy approaches and the development of new agents.

The PML-RARα fusion protein is targeted for degradation after all-trans retinoic acid treatment through the UPS. The treatment of ATRA causes SUG-1 binding to the AF-2 transactivation domain of RARα, which then promotes the degradation of the oncogenic fusion protein. In addition, the configuration change to PML-RARα post-treatment with ATRA, allowed for exchange of the corepressor proteins with coactivator proteins to initiate/promote granulocytic differentiation. Whereas with ATO treatment, there is degradation of wild type PML protein and PML-RARα but not RARα, suggesting

that PML is targeted by ATO (Chen et al., 1997; Chen et al., 1996). Arsenic binds directly to the cysteine residues of the zinc finger domain located within the RBCC domain of PML (X. W. Zhang et al., 2010). The arsenic bound PML interacts further with UBC9, a SUMO-conjugating enzyme, to enhance its degradation after polySUMOylation via the recruitment of RNF4 that ubiquitinates PML for degradation (Z. Chen et al., 2007; Geoffroy et al., 2010; V. Lallemand-Breitenbach et al., 2008; X. W. Zhang et al., 2010). Thus, by targeting both RARα and PML through ATRA and ATO leads to a synergistic attack on APL. These important findings revolving around APL and our understanding of PML-RARα have shaped the clinical success with treating the leukemia over the years.

1.5.2 PML and cancer

While APL is the first description of the *PML* gene, and the *PML-RAR*α fusion gene in particular, our understanding of PML NBs has expanded significantly over the last 30 years. I have discussed how PML NBs contribute to a multitude of cellular processes, form multiple structures in response to various stresses, and have different isoform-specific functions. As suspected, owing to the pleiotropy of PML functions, the relationship of *PML* is context-specific in different malignancies.

Tissue microarrays screening samples from a multitude of solid tumours of different histologic origins revealed that *PML* is downregulated in many types of cancer (Gurrieri et al., 2004). PML expression was lost or reduced in prostate adenocarcinomas, lymphomas, breast carcinomas, colon adenocarcinomas, lung carcinomas, CNS tumours and germ cell tumours (Gurrieri et al., 2004). The *PML* gene is typically not mutated but

these microarrays revealed that the PML protein is either lost or reduced in terms of expression across many different cancer types. In addition, the loss of PML expression was associated with tumour progression in prostate cancer, breast cancer and CNS tumours (Gurrieri et al., 2004). Moreover, other reports have shown that in prostate and lung cancer, the loss of PML promotes immune suppression and the likelihood of metastasis (Bernardi et al., 2006; Bezzi et al., 2018; Chen, Wan, et al., 2018; Y. T. Wang et al., 2017; Yuan et al., 2011).

PML was first described as a tumour suppressor based on the work in mouse models. Mouse models lacking *Pml* were more likely to develop tumours upon challenge with drugs that cause a two-stage/step skin carcinogenesis, dimethybenzanthracene (tumour initiating drug) and then 12-0-tetradecanoylphorbol-13-acetate (tumour promoting drug) (Wang, Delva, et al., 1998). There was a significant increase in the number of papillomas but the loss of *Pml* did not have a huge impact on metastasis. However, *Pml* complete inactivation or haplo-insufficiency did not affect the size, frequency or latency of breast tumors in a mammary tumor virus/neu murine model of mammary tumorigenesis (Rego et al., 2001). Therefore, how PML influences oncogenesis is largely dependent on the type of malignancy and likely subtypes dependent on molecular context.

In certain tumour types, *PML* appears to even function as an oncogene rather than as a tumour suppressor as previously discussed (Li et al., 2020; Mazza & Pelicci, 2013). *PML* is typically overexpressed in ovarian cancer and triple negative breast cancer (Carracedo et al., 2012; Liu et al., 2017). In these two malignancies, PML seems to shift the metabolic states of the cancer cells towards pro-tumour states by influencing

Peroxisome proliferator-activated receptor (PPAR) signalling (in breast cancer) and mitochondrial metabolism (in ovarian cancer) (Carracedo et al., 2012; Gentric et al., 2019). Whereas, in chronic myeloid leukemia, TNBC, and glioblastoma, oncogenic PML dramatically shifts cancer stem cell maintenance, cell migration and metastasis (Amodeo et al., 2017; Ito et al., 2008; Martin-Martin et al., 2016; Ponente et al., 2017; Zhou et al., 2015). Tissue-specific programming and how PML influences those pathways plays a critical role in dictating whether *PML* functions as an oncogene or tumour suppressor. This is best illustrated by comparing PML in prostate cancer where it inhibits metastasis by repressing the oncogenic lipogenesis pathway, whereas in glioblastoma, PML promotes cell migration and metastasis through differential regulation of the axon guidance pathway (Amodeo et al., 2017; Chen, Zhang, et al., 2018). Thus, PML can have an instrumental role in multiple malignancies as both a tumour suppressor or oncogene, depending on the tissue-specific gene networks.

1.6 The cGAS-STING pathway

A major pathway which is linked to PML in my thesis is the cGAS-STING pathway. Cyclic GMP-AMP synthase (cGAS) is a critical pattern recognition receptor that activates Stimulator of Interferon Genes (STING). cGAS senses cytosolic DNA which can from various forms of stress such as viral infection, genome instability, and mitochondrial dysfunction. Then, activation of STING induces type I IFN and nuclear factor kappa light chain enhancer of activated B cells (NF-κB) signalling pathways. As a result, it is an important player in relaying the DDR to innate immune signalling.

1.6.1 Sources of cytoplasmic DNA

DNA damage occurs within the nucleus, but the signalling associated with the inflammatory and type I IFN pathways occurs within the cytoplasm. The type I IFN signalling pathway likely evolved in the context of host-pathogen interactions and in response to DNA virus, bacteria, and RNA virus infection (Cai & Imler, 2021; Goubau et al., 2013; Liu et al., 2021; Patel et al., 2023). The relay which occurs between DDR and downstream type I IFN signalling relies on similar constituents that cells would encounter with pathogens, where the activation of downstream type I IFN signalling appears to be triggered by a handful of nucleic acids that accumulate in the cytoplasm (C. Liu et al., 2023). Cytoplasmic self-DNA is derived from different sources such as by products of DNA repair, mitochondrial DNA, micronuclei, and Long Interspersed Nuclear Element 1 (LINE-1/L1) retroelements (E. Erdal et al., 2017; Garcia Perez & Alarcon-Riquelme, 2017; Hancock-Cerutti et al., 2022; Harding et al., 2017; Hu et al., 2021; Sliter et al., 2018; Song et al., 2021; Thomas et al., 2017; Weindel et al., 2020; Xue et al., 2022). These different sources of cytoplasmic DNA are a result of cellular dysfunction and stress, which activates cGAS-STING signalling.

1.6.2 cGAS

The main factor involved in DNA-sensing within the cytoplasm is cGAS (cyclic GMP-AMP synthase) which senses dsDNA, retroelement DNA, micronuclei and more recently, chromatin bridges (Gao et al., 2015; C. Liu et al., 2023; Sun et al., 2013). Phase-separated cGAS binds to the sugar backbone of DNA and produces 2’3’-cyclic guanosine monophosphate–adenosine monophosphate (cGAMP) (Du & Chen, 2018; Zhou et al.,

2021a). cGAS can recognize self-DNA fragments that are as small as 40 bp, or guanosine-rich Y-form DNA larger than 12 bp, in a sequence-independent manner (Bartok & Hartmann, 2020; Herzner et al., 2015). In addition, cGAS can bind to heavily oxidized self-DNA which forms because of UV exposure and ROS (Gehrke et al., 2013). cGAS is activated more potently in response to larger DNA fragments indicating that the substrate length directly correlates with its activity (Luecke et al., 2017). This includes large L1 retroelement sequences that are expressed when heterochromatin loss is observed at their residing loci (Chuqian Liang et al., 2022). L1 can be directly bound by cGAS or cause the accumulation of other cytosolic DNA from DNA damage induced by L1, contributing to cGAS activation through multiple mechanisms (Gasior et al., 2006). cGAS is regulated by numerous proteins associated with the DDR that control its shuttling from the nucleus, the availability of cytoplasmic substrates, and its condensate formation (**Figure 1.5**) (Cho et al., 2022; Erkin Erdal et al., 2017; Lei et al., 2023; Singh et al., 2022; Tao et al., 2022). However, the main regulation of cGAS is through the actions of Three prime repair exonuclease 1 (TREX1), which is an exonuclease that clears numerous types of cytoplasmic DNA substrates (Mohr et al., 2021b; Simpson et al., 2020; Zhou et al., 2021b; W. Zhou et al., 2022).

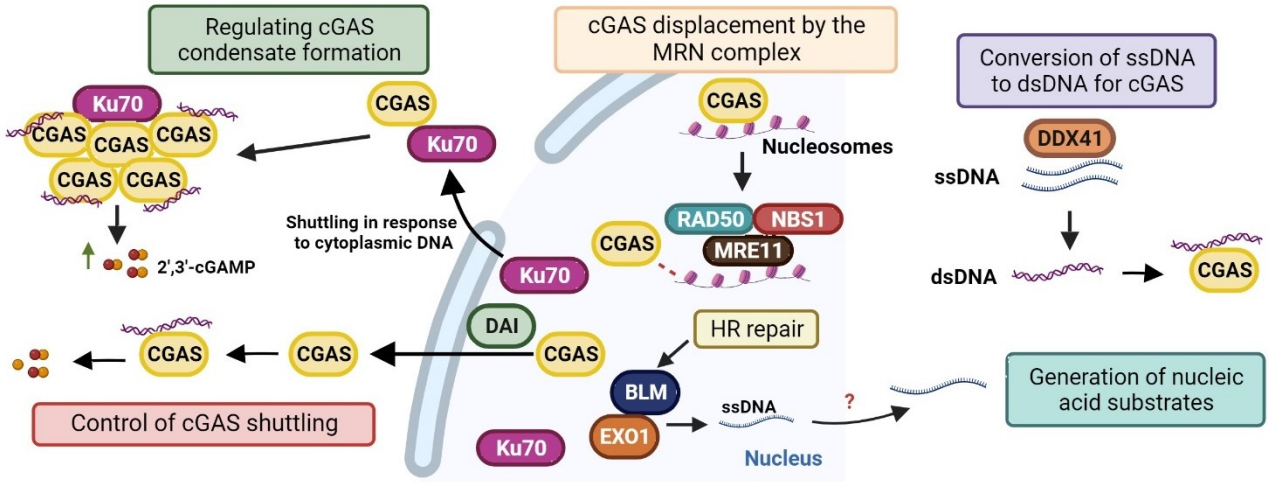

Figure 1.5. Regulation of cGAS activity. Different regulatory proteins exist that affect the ability of cGAS sensing of cytoplasmic DNA. These different proteins affect cGAS localization, the availability of recognizable cytoplasmic DNA substrate, and cGAS condensate formation. Many of these proteins are involved in the DDR and play dual roles in the relay between DNA damage and cGAS activation. Abbreviations: HR, Homologous Recombination; ssDNA, single-stranded DNA; dsDNA, double-stranded DNA, 2',3'-cGAMP, 2'3'-cyclic GMP-AMP; MRN complex, MRE11-Rad50-NBS1 complex.

1.6.3 STING

Upon cGAS sensing of cytosolic DNA, the signal is relayed to the major adaptor protein in the pathway, STING (**Figure 1.6**). Membrane protein STING resides in the endoplasmic reticulum (ER) in its inactive form as a homodimer, with a cytosol-facing binding domain (Ishikawa & Barber, 2008). The primary activator of STING is cGAS, which produces the cGAMP ligand, a secondary messenger that STING binds. Upon binding to cGAMP, a signalling ligand produced by cGAS, STING undergoes extensive conformation changes, and this leads to the assembly of STING dimers, which are further associated by disulfide bridges spanning separate dimers (Ablasser et al., 2013; Diner et al., 2013; Ishikawa & Barber, 2008; Wu et al., 2013; Zhang et al., 2013). The activated STING dimers then translocates rapidly to the ER-golgi intermediate compartment (ERGIC), where it recruits the TBK1 kinase to phosphorylate itself and IRF3 (Dobbs et al., 2015; Ishikawa & Barber, 2008; Ishikawa et al., 2009; Liu et al., 2015; Saitoh et al., 2009; Sharma et al., 2003; Tanaka & Chen, 2012).

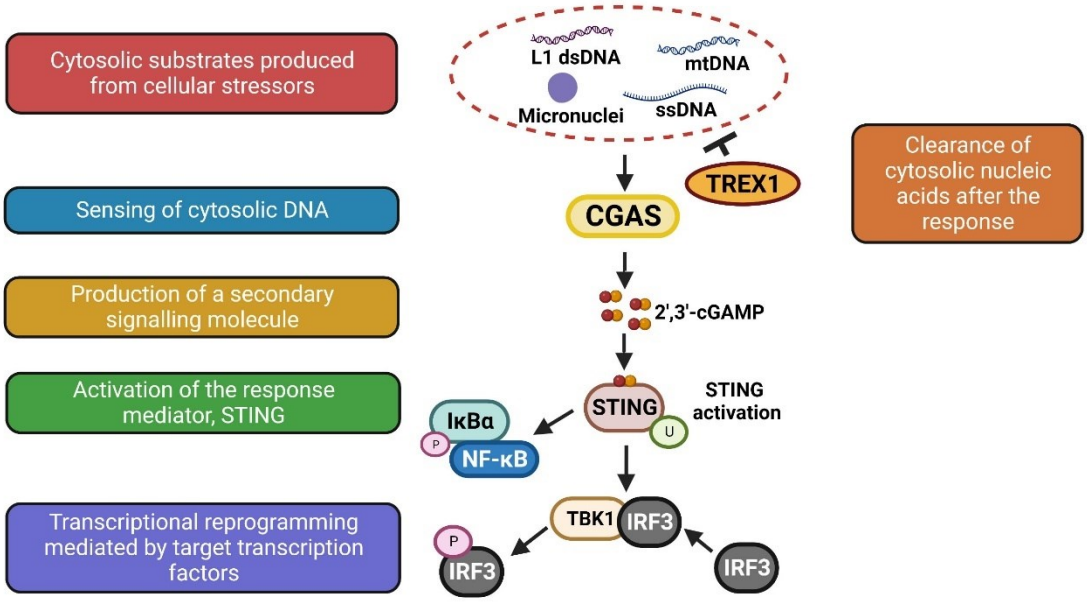

Figure 1.6. Overview of the cGAS-STING pathway. The cGAS-STING pathway senses cytosolic DNA to initiate a downstream immune signalling cascade to promote IRF3 and NF-kB mediated type I IFN signalling. cGAS senses cytosolic DNA in the form of L1 dsDNA, mitochondrial DNA (mtDNA), micronuclei and single stranded DNA (ssDNA). cGAS then produced cGAMP that activates STING to promote IRF3 and NF-kB translocation to the nucleus to activate NF-kB-mediated inflammatory signalling and IRF3-mediated innate immune signalling.

A series of ubiquitination events facilitate STING function, its interactions and degradation: (1) K63 ubiquitination to facilitate activation of STING, (2) K27 polyubiquitination then causes TBK1 recruitment and (3) K48 polyubiquitination sends STING for degradation by the proteasome system (Tsuchida et al., 2010; Wang et al., 2014; Wang et al., 2015; Zhang et al., 2012; Zhong et al., 2009). These post-translational modifications of STING and others help regulate its rapid activation and eventually required inactivation. The phosphorylated IRF3 dimerizes and then shuttles into the nucleus to induce the expression of various IFNs (such as IFNα and IFNβ) and Interferon-stimulated genes (ISGs). In addition, ERGIC localizing STING activates IKK, a kinase which phosphorylates the IκB family of inhibitors of NF-κB to cause their degradation (Ishikawa & Barber, 2008). Free NF-κB like IRF3, also shuttles to the nucleus and functions as a transcription factor to induce the expression of inflammatory cytokines and chemokines such as TNF, IL-1b and IL-6. As a result of STING adaptor activity, both IRF3 and NF-κB transcription factors are activated and capable of shifting the transcription of the cell towards type I IFN gene expression via ISGs. STING therefore is the essential "switch" that allows these transcription factors to dictate global changes in transcription.

1.6.4 Type I IFN signalling and NF-κB

The activation of IFN signalling in response to DNA damage was elegantly demonstrated over a decade ago by Brzostek-Racine et al., where they showed that agents which induced DSBs also activated ISGs, IFN-α and IFN-γ (Brzostek-Racine et al., 2011). However, the profile of ISGs differed between DDR and during infection,

suggesting that there were important differences in the activation and signalling of the type I IFN pathway in these two contexts. The activation of type I IFN signalling leads to the eventual expression of ISGs that carry out critical functions in the response. Extraordinarily, 10% of the genes in the human genome have the potential to be IFN-regulated (Shaw et al., 2017). Between birds, mammals and humans, there were a common core of 62 genes that were IFN-stimulated (Shaw et al., 2017). These genes are involved in a multitude of pathways including the antiviral response, antigen presentation, apoptosis, senescence, pattern recognition and sensing, and the suppression of IFN signalling (negative feedback loop genes) (Shaw et al., 2017). In addition to ISGs, the DDR pathway also activates the NF-κB (Nuclear factor kappa B) pathway which mediates the expression of the pro-inflammatory gene program. The NF-κB transcription factor induces the expression of cytokines and chemokines to facilitate the recruitment of immune cells to the cells experiencing severe DNA damage for clearance. Together, both ISGs and the NF-κB gene programs are key for how the DDR pathway utilizes innate immune signalling to carry out different cell fate decisions.

1.6.5 CGAS-STING in cancer

Loss of STING impairs the ability for cells to signal to the immune system when they experience severe DNA damage. Thus, the DDR cannot operate correctly to promote cell proliferation arrest by senescence or recruit immune cells to remove the genetically compromised cell, increasing the likelihood for oncogenesis. For these reasons, STING activity is often lost in or suppressed in many malignancies (Konno et al., 2018; Low et al., 2022; Qiu et al., 2022). The two primary mechanisms behind this are (1) loss-of-

function mutations and (2) epigenetic silencing of STING or CGAS promoter regions (Konno et al., 2018). When STING is suppressed in malignancies, this impedes the ability of the DDR to promote anti-tumour T-cell priming and tissue repair, effectively impairing the broader activation of immunosurveillance (Xia et al., 2016). Groups have successfully counteracted these epigenetic changes by treating glioblastoma tumours, that are often with silenced STING by the promoter being hypermethylated, with DNA methyltransferase inhibitor decitabine to reconstitute STING signalling (Low et al., 2022). The interaction between tumours and the immune system impacts patient prognosis. “Hot tumours” are associated with increased expression of IFNs, interleukins, and tumor necrosis factor (TNF), which help T-cell expansion and activation (Hegde et al., 2016). The activation of type I IFN signalling in this context allows for (1) tumour growth control by the immune system and (2) improved responses to therapeutic approaches (including immunotherapy and radiation therapy) (Benci et al., 2016; Burnette et al., 2011; Castiello et al., 2018; Dunn et al., 2005; Galon & Bruni, 2019; Herbst et al., 2014; Katlinski et al., 2017; Sistigu et al., 2014; X. Wang et al., 2017) . Whereas the suppression of type I IFN signalling leads to accelerated tumour development and poor clinical outcomes (Castiello et al., 2018; Katlinskaya et al., 2016; Katlinski et al., 2017). Immune cell recruitment appears to be a major dilemma in this context, since immune-excluded or “cold” tumours have cytotoxic CD8+ T lymphocytes restrained to the invasion margins with poor infiltration into the tumour microenvironment (Hegde & Chen, 2020). In striking contrast however, chronic activation of cGAS-STING can also be oncogenic as it promotes metastasis (Bakhoum et al., 2018).

1.7 Overview of Thesis Chapters

PML is a protein that forms nuclear bodies that act as important orchestrators of cellular processes through their regulation of numerous nuclear proteins. However, there are important questions remaining about the PML-I isoform, such as (1) the function of PML-I and its unique C-terminus, (2) the role of cytoplasmic PML and if it is relevant for its regulation of cellular processes and (3) how the PML-I isoform contributes to oncogenesis as either a tumour suppressor or oncoprotein. The difficulty with studying human PML arises from its complexity of various isoforms, pleiotropic functions, and its context-specific functions in different tissues. The objective of this thesis was to further our understanding of PML by taking into consideration its molecular evolution, to gather clues as to what the primary, conserved function of the PML protein is.

Chapter 2 explores the emergence of PML in jawed vertebrates and how its C-terminal domain gave rise to a novel family of DEDDh exonucleases (Plex9 proteins) in teleost fishes to regulate L1 retroelements and cGAS-STING signalling, akin to TREX1 in anamniote species. Then, Chapter 3 describes the conserved role of human PML-I in L1 suppression after nucleocytoplasmic shuttling. Furthermore, with a new understanding of PML, Plex9 and TREX1 ortholog functions, they are found to be downregulated during limb and fin regeneration and age-related senescence in vertebrates to promote cGAS-STING, which is the focus of Chapter 4. Finally, Chapter 5 provides a discussion on the chapters presented in the thesis, their implications, conclusions, and future directions.

1.8 Author Contributions

For sections previously published, Sabateeshan Mathavarajah prepared the manuscripts, Dr. Graham Dellaire (supervisor) provided editorial feedback.

Experimental data not performed by Sabateeshan Mathavarajah were for **Figure 2.8** (assistance from Roger lab)**, Figure 2.9** (assistance from Roger lab)**, Figures 2.10** (collected entirely by Langelaan lab), **Figure 3.5 (panels C, D)** (collected entirely by Langelaan lab), **Figure 4.7 (panel C)** (collected entirely by the Quinn lab) is indicated in the figure legends.

Chapter 2 – The Plex9 proteins, a novel family of DEDDh exonucleases

This chapter contains material (sections 2.2.3-2.2.6, 2.3, 2.4, 2.5; Figures 2.3-2.15) originally published in two manuscripts:

"Mathavarajah, S., Vergunst, K.L., Habib, E.B., Williams, S.K., He, R., Maliougina, M., Park, M., Salsman, J., Roy, S., Braasch, I. and Roger, A.J., 2023. PML and PML-like exonucleases restrict retrotransposons in jawed vertebrates. *Nucleic Acids Research*, *51*(7), pp.3185-3204."

"Mathavarajah, Sabateeshan, and Graham Dellaire. "LINE-1: an emerging initiator of cGAS-STING signalling and inflammation that is dysregulated in disease." *Biochemistry and Cell Biology* (2023). e-First."

2.1 Introduction

2.1.1 Teleost bony fish and the spotted gar

Bony vertebrates are comprised of two main lineages, the lobe-finned vertebrates (that include the tetrapods and lobe-finned fishes) and ray-finned fishes. Much of the biodiversity associated with the ray-finned fishes is found with teleost fish, that have more than 30,000 species. Teleost fish account for 98% of all ray-finned fish and account for half of all extant vertebrates (Ravi & Venkatesh, 2018). Teleost fish are also important biomedical models because of their basic body plan and developmental programs that resemble those of mammals. Moreover, there are many shared genes between mammals and teleost fishes that have conserved functions. Zebrafish (*Danio*

rerio) and medaka (*Oryzias latipes*) are some examples of key teleost species that have been used as genetic models due to their size, transparent embryos, and external development (Dooley & Zon, 2000; Kirchmaier et al., 2015). In addition, these species allow for efficient and easier breeding and maintenance in comparison to other vertebrate species (Dooley & Zon, 2000; Kirchmaier et al., 2015). These species have played a significant role in our understanding of human development, disease and more recently, in drug discovery (Hason & Bartůněk, 2019; Patton et al., 2021; Teame et al., 2019; Wang et al., 2021).

Comparative genomics in the 1990s revealed that teleost fishes had extra copies of genes that were normally found as single copies in tetrapod genomes. The analysis unveiled that teleost fishes had experienced an additional whole genome duplication event, also known as the teleost genome duplication event (Amores et al., 1998; Christoffels et al., 2004; Jaillon et al., 2004). These findings complicate our comparisons between teleost fishes and humans in terms of genetics, as the gene relationships were not 1:1 between homologs. Deciphering this problem helps with the translation of genetic data from zebrafish and other teleost fish genomes into more relevant information for biomedical research.

A solution was proposed in the form of the gars, which Darwin referred to as "Living fossils" in the *Origin of species* (1859) owing to their resemblance of fish observed in deep fossil records. Gars are an outgroup lineage of fish who did not undergo the Teleostei genome duplication event (**Figure 2.1**). They are more closely related to Teleostei (versus the 450 million years of separate genomic and morphological evolution between tetrapods and teleost fishes) as they belonged to the sister lineage Holostei.

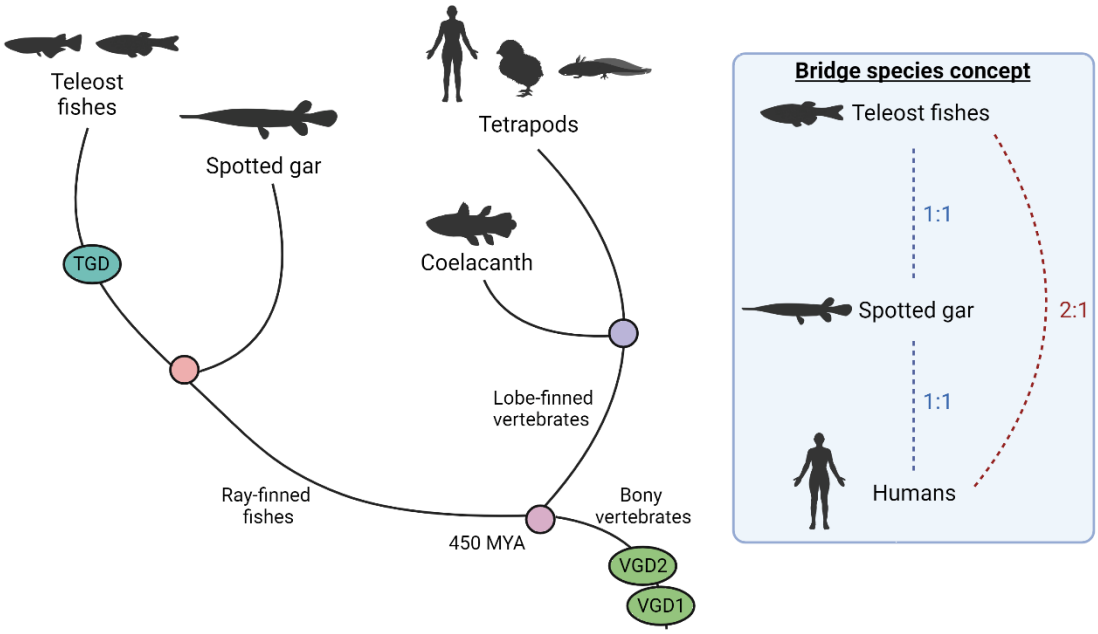

Figure 2.1. Bridge species concept when making comparisons between teleost fishes and humans. Zebrafish represent an important biomedical model for understanding human disease but there is a major difference between human genomes and teleost fish genomes, which are doubled from a Teleostei genome duplication (TGD) event. To make a 1:1 comparison between genomes, the spotted gar genome was sequenced, which is an outgroup species that did not undergo TGD. VGD1/2 refer to the two vertebrate genome duplication events that occurred earlier in vertebrate evolution.

Furthermore, their genome was not duplicated. The sequencing of the spotted gar (*Lepisosteus oculatus*) genome and eventual publication in 2016 now allows researchers to compare teleost fishes to the spotted gar before making comparisons to humans, acting as an important bridge species (Braasch et al., 2016). Since the publication on the spotted gar genome, the bridge species has helped reveal important revelations on tetrapod evolution including the origins of limb-fin development, evolution of enamel limb-fin regeneration, vertebrate transposable element diversification and the evolution of immune signalling (Bilal et al., 2021; Chalopin & Volff, 2017; Darnet et al., 2019; Nakamura et al., 2016; Simmer et al., 2021).

2.1.2 DEDDh exonucleases

The DEDDh family of exonucleases, also known as the RNase T or DnaQ-like family constitute more than 70,000 proteins encoded in the genomes of prokaryotes and eukaryotes (Yang, 2011; Zuo & Deutscher, 2001). The family is marked by a DEDDh domain that consists of a similar mixed αβ fold and four conserved acidic amino acids (DEDD, aspartate-glutamate-aspartate-aspartate) (Yang, 2011). The residues allow them to bind two cations (such as magnesium) in the active site with a nearby histidine or tyrosine residue (the general base in the chemical reaction). The DEDDh exonucleases have exonuclease activity in the 3'-to-5' direction, with nucleic acid substrates including different forms of RNA and DNA. They remove a single nucleotide at the 3' end of the substrate through each catalytic action and when done so repeatedly, can cleave apart the entire nucleic acid.

Different DEDDh exonucleases have varied substrate preferences for binding and digestion despite potentially being capable of digesting multiple substrates. This is best illustrated by the CRN-4 and NP exonucleases that prefer to digest double-stranded DNA or RNA, versus ExoI and ISG20 that prefer single-stranded DNA or RNA (Hastie et al., 2012; Horio et al., 2004; Hsiao et al., 2009; Korada et al., 2013). Then, there are DEDDh exonucleases that target the overhangs of nucleic acids such RNase T, Snp and 3′hExo (Hsiao et al., 2012; Kupsco et al., 2006). While the DEDDh exonucleases are similar in terms of their αβ fold and conserved acidic amino acids, minor differences in protein composition are sufficient for the variation in substrate recognition and other factors such as length of digestion and sequence preference. RNAse T substrate recognition is mediated by several active site hydrophobic residues that can shift its conformation from active to inactive upon substrate binding (Hsiao et al., 2012).

The diversity of exonucleases and their distinct biochemical activity allows them to play important roles in a multitude of biochemical pathways including RNA maturation, RNA turnover, DNA replication and DNA repair (Yang, 2011; Zuo & Deutscher, 2001). These are essential processes for the wellbeing of the cell and thus why the dysfunction of human DEDDh exonucleases is deleterious and attributed to multiple human diseases. A classic example is with the WRN DEDDh exonuclease where mutations to the exonuclease domain are linked to Werner syndrome, a premature aging disease (Perry et al., 2006; Zhao et al., 2008). WRN typically removes secondary structures that form at replication forks and its absence results in stalled replication forks that can lead to fork collapse or breakage (Rossi et al., 2010). While WRN is one

example, the different DEDDh exonucleases play key surveillance, processing, and regulatory roles to mediate normal cell progression without abnormalities.

Several human and viral DEDDh exonucleases are involved in host-pathogen dynamics as they are involved in virus infection and gene replication (Crow et al., 2006; Lee-Kirsch et al., 2007). An example is with the Three prime repair exonuclease 1 (TREX1) exonuclease that is hijacked during Human immunodeficiency virus (HIV) infection. TREX1 is utilized by HIV to digest any nonproductive viral transcripts that would otherwise accumulate, and trigger innate immune responses (Hasan & Yan, 2014). Thus, TREX1 hides HIV from pattern recognition receptors that would normally sense the virus and activate downstream immune signalling. Intriguingly, one function of TREX1 in cells is to attenuate type I IFN signalling and prevent overactive signalling, indicating that viruses try to exploit this normal regulatory function of TREX1. While TREX1 is one example, DEDDh exonucleases collectively contribute to maintaining cellular homeostasis, with an emerging role in innate immune signalling.

2.2.3 TREX1

The cGAS-STING axis is stimulated by various cytosolic nucleic acids in the form of cytoplasmic ssDNA, dsDNA, and micronuclei. Despite so many substrates, there is one major exonuclease, TREX1, that primarily clears cytosolic DNA in the form of ssDNA, dsDNA, and micronuclei to limit the type I IFN response through cGAS-STING (**Figure 2.2**) (Li et al., 2017a; Mohr et al., 2021a; Zhang et al., 2020).

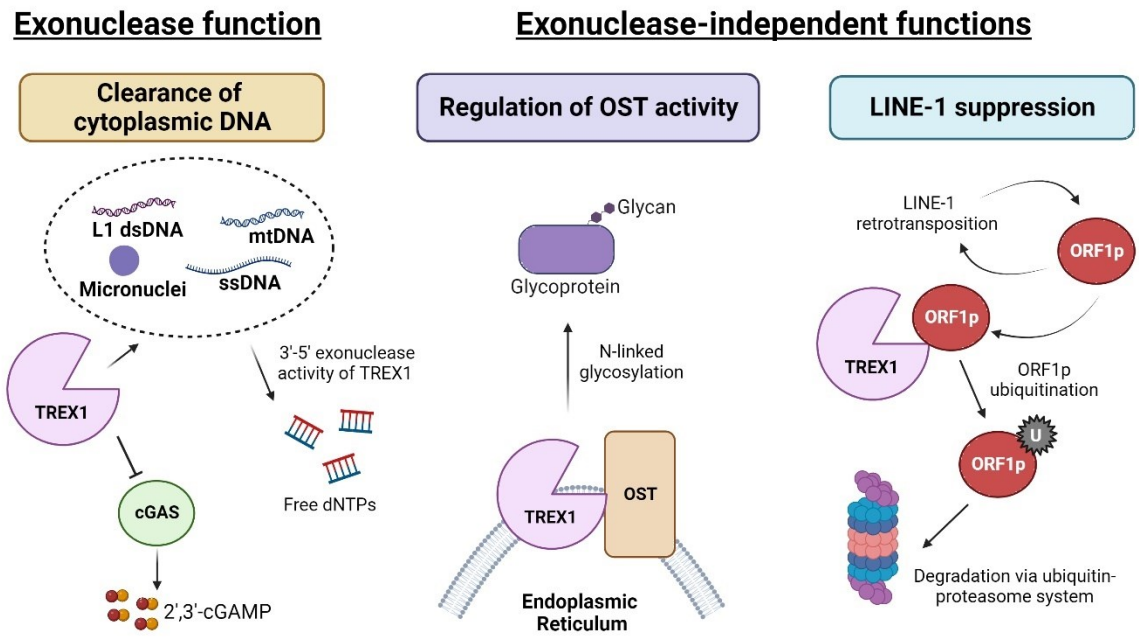

Figure 2.2. Cellular processes regulated by TREX1. TREX1 has exonuclease-dependent/independent functions in regulating different biological pathways. Its 3'-5' exonuclease activity clears cytosolic DNA to prevent activation of cGAS. Whereas, it interacts with Oligosaccharyltransferase (OST) to promote N-linked glycosylation of proteins. The loss of TREX1 leads to abnormal OST activity and the build up free glycans. TREX1 also prevents cGAS activation in an exonuclease-independent way by preventing LINE-1 propagation by interacting with LINE-1 ORF1p and promoting its degradation via the ubiquitin-proteasome system.

The TREX1 protein is 314 residues in length and characterized by two main domains, the N-terminal DEDDh catalytic domain (1-242 aa) and a C-terminal polyproline helix that is required for its localization to the ER (de Silva et al., 2007; Orebaugh et al., 2013; Perrino et al., 1994). TREX1 forms a stable homodimer for catalytic activity, where the protomers are connected by a stable network of hydrogen bonds, hydrophobic interactions, and an extended β-sheet core (Orebaugh et al., 2011). Unlike other exonucleases, TREX1 must form the dimeric structure for catalytic activity (Orebaugh et al., 2011). TREX1 was first isolated from human myeloblast extracts as the major exonuclease with 3'-5'-exonuclease activity (Perrino et al., 1994). TREX1 primarily targets DNA as its endogenous nucleic acid substrate, as TREX1 activity is 1000-fold less with RNA and RNA-DNA duplexes (Belyakova et al., 1993; Mazur & Perrino, 1999, 2001; Perrino et al., 1994; Yuan et al., 2015).

The loss of TREX1 leads to an autoimmune disease known as Aicardi-Goutières syndrome (AGS), where type I IFN signalling is upregulated and unchecked to the point where tissues are damaged, after DNA damage occurs (Crow et al., 2006). The primary molecular dysregulation in AGS is from cGAS hyperactivation as cytosolic DNA builds up from the absence of TREX1, that typically digests the DNA (Berndt et al., 2022; Gray et al., 2015; Xiao et al., 2019). However, mutations to the TREX1 C-terminus also prevent its association with Oligosaccharyltransferase (OST), a protein involved in catalyzing protein N-linked glycosylation events at the ER (Hasan et al., 2015) (**Figure 2.2**). The loss of TREX1 leads to dysregulated catalytic activity by OST and the build up free glycans that trigger type I IFN signalling through a TBK1-dependent (which is downstream of STING signalling) but not cGAS-dependent mechanism (Hasan et al.,

2015). The interaction between OST and TREX1 is regulated by cell cycle coordinated phosphorylation of the TREX1 C-terminus domain that is responsible for its localization (Kucej et al., 2017).

In addition to OST regulation, TREX1 is also involved in L1 regulation in a exonuclease-independent manner (**Figure 2.2**). The loss of Trex1 in AGS mice models results in reduced survival from inflammatory myocarditis (Morita et al., 2004). These Trex1-deficient hearts also had elevated levels of cytosolic DNA, with L1 retroelements being enriched in the accumulating cytosolic DNA and driving the inflammation observed (Stetson et al., 2008). In a TREX1-deficient human stem cell model, it was shown that L1 accumulation and elevated cGAS-STING signalling could be suppressed by treating cells with a reverse transcriptase inhibitor (Thomas et al., 2017). The results indicate that L1 cytosolic DNA was driving overactive type I IFN signalling in the absence of TREX1.

It was then shown that mutations associated with TREX1 in Aicardi-Goutières syndrome where exonuclease function is retained, still result in the disease. These mutations that do not affect exonuclease function rather impair the ability of TREX1 to suppress L1 (Li et al., 2017a). TREX1 suppresses L1 by interacting with ORF1p and promoting its degradation by the UPS (Li et al., 2017a). TREX1 suppresses L1 through an exonuclease-independent mechanism and the absence of this function results in overactive cGAS-STING signalling through the accumulation of L1. The regulation of L1 by suppressors such as TREX1 and other proteins is critical for preventing tonic type I IFN signalling because of L1 accumulation, which can contribute to inflammation in disease.

2.2.4 LINE-1 and genome instability

Endogenous retroelements pose a threat to our genome as relics that continue to drive our evolution. Retroelements are self-replicating sequences of DNA that spread sporadically throughout the genome as a mutagen. There are several different types of retroelements that exist in eukaryotes and that are still actively expressed. One of the most common sequences of retroelements in the human genome, comprising ~17% of our DNA, is the LINE-1/L1 class of non-LTR transposons that represent a family of AT-rich elements (Ardeljan et al., 2017; Eric S. Lander et al., 2001). L1 elements, like other retroelements, use an RNA intermediate expressed from genome loci to reverse transcribe a copy of their DNA to re-insert back into the genome. The L1 element is approximately 6 kilobases in sequence length and encodes two ORFs essential for its retrotransposition, ORF1p and ORF2p (Ostertag & Kazazian, 2001). Primate L1 sequences also encode an ORF0p sequence that promotes L1 mobility to promote its retrotransposition (Denli et al., 2015). L1 elements are the only active retroelements in the human genome that are autonomous (i.e., do not require external factors) in their retrotransposition.

When L1 elements are expressed, ORF1p forms a homotrimer that complexes with L1 RNA as a critical chaperone which is required for target-site-primed reverse transcription that mediates the insertion of new L1 DNA at a genomic loci (Hohjoh & Singer, 1996; Luan et al., 1993; Martin & Bushman, 2001; Martin et al., 2005). At the insertion site, ORF2p first acts as the endonuclease to provide the initial single-stranded nick at the site for invasion and annealing of the L1 RNA to the cleaved region. Then, ORF2p functions as the reverse transcriptase to generate the new L1 DNA. The result of the actions of ORF1p and ORF2p is the integration of newly replicated L1 sequence at a

new genomic locus, effectively propagating the sequence. The L1 sequences are effectively drivers of genetic evolution and variation that have a long history in shaping vertebrate genomes (Beck et al., 2010; E. S. Lander et al., 2001). However, they pose a dilemma as active mutagens that are harbingers of genome instability as they can potentially disrupt the function of coding genes, generating aberrant fusion genes, promoting chromosomal breaks and translocations (Gasior et al., 2006; B. Rodriguez-Martin et al., 2020) (McKerrow et al., 2022). In addition, in cancer, LINE-1 expression is linked to massive chromosome rearrangements, p53 mutations and activation of the ATM-RAD50/SMC1 axis (McKerrow et al., 2022). Therefore, a role for LINE-1 in genome instability is well-established as a mutagen that can cause genomic catastrophes.

An emerging theme in genome instability is that DNA damage reflects downstream innate immune signalling. There is a significant degree of crosstalk between the DDR machinery and innate immune signalling to initiate cell fate responses to unresolved DNA breaks and damage. There is a relay occurring between both the DDR in the nucleus and downstream type I IFN signalling in the cytoplasm. Interestingly, when mice neurons incur DNA damage or DNA repair was inhibited (by the loss of ATM), there is rapid export of AT-rich repetitive DNA into the cytoplasm (Song et al., 2021; Thomas et al., 2017). These AT-rich elements were later shown to be L1 DNA (Garcia Perez & Alarcon-Riquelme, 2017; Thomas et al., 2017). LINE-1 retroelements appear to be involved in this relay between the DNA damage response pathway and type I IFN pathway, where they play an important role in activating the cGAS-STING pathway.

2.1.5 Mechanism behind LINE-1 propagation

The full-length LINE-1 retroelement includes a 5'-untranslated region (UTR), two open reading frames that encode machinery required for retrotransposition (ORF1 and ORF2), as well as a 3'-UTR with polyadenine tracts for delivery to the cytoplasm (**Figure 2.3**). A third open reading frame situated antisense on the 5'-UTR of the LINE-1 transcript, ORF0, is also encoded. Although ORF0 localizes to PML nuclear bodies and ultimately contributes to LINE-1 mobility in primates, its cellular function remains to be fully characterized. ORF1p acts as an RNA-binding chaperone that forms a trimeric complex with L1 mRNA. ORF1p contributes to the formation of L1 RNPs but is dispensable for target primed reverse transcription (TPRT) (**Figure 2.3**)(Cost et al., 2002). An important function for ORF1p is facilitating the condensation of L1 RNPs, a process that minimize off-target transposition and mediates the cycle of L1 propagation (Sil et al., 2023).

While ORF1p performs structural and stability roles in the L1 RNP, the ORF2p enzyme acts the endonuclease and reverse transcriptase that facilitates the re-integration of L1 elements. The N-terminus of ORF2p targets a specific sequence, 3−′AA/TTTT−5′, to produce a single strand nick with its endonuclease activity that relies on a single Mg^{2+} ion for catalysis (Clements & Singer, 1998; Mathias et al., 1991; Weichenrieder et al., 2004). Following nicking of DNA, a distinct domain in the ORF2p C-terminus is then required for RNA binding and reverse transcription of the L1 mRNA to complete the integration of new L1 DNA into the host genome (Christian et al., 2017; Piskareva et al., 2013; Piskareva & Schmatchenko, 2006).

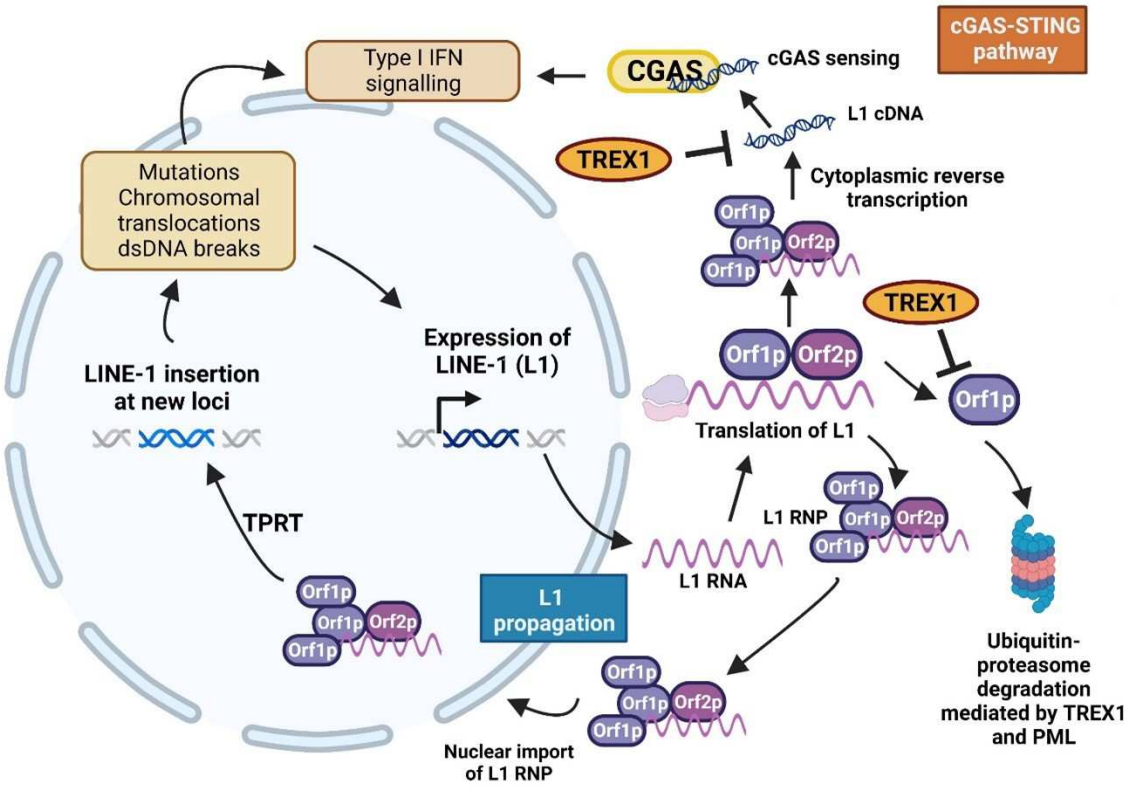

Figure 2.3. LINE-1 (L1) retrotransposition can result in the activation of cGAS-STING. When L1 elements are expressed and translated, they can be imported as L1 ribonucleoproteins (RNPs) to the nucleus. Once in the nucleus, L1 RNPs facilitate the insertion of LINE-1 through target primed reverse transcription (TPRT) at a new genomic locus, which can result in mutations, chromosomal translocation, or dsDNA breaks. The genome instability and DNA damage caused by L1 insertion at a new genome locus can induce type I IFN signalling. L1 RNA can also be reverse transcribed in the cytoplasm to generate L1 cDNA that is sensed by cGAS to initiate type I IFN signalling through STING.

The current TPRT model for L1 retrotransposition, describes a cycle of shuttling events involving the L1 element constituents. Retrotransposition is initiated by RNA polymerase II binding to the 5′-UTR promoter regions of LINE-1 to mediate the transcription of LINE-1 (Lavie et al., 2004). Once L1 mRNA is synthesized, it is exported to the cytoplasm for the translation of ORF1p and ORF2p to form the L1 RNP. The resultant L1 RNP is then trafficked to the nucleus through an unknown mechanism. Then, the ORF2p endonuclease recognizes and cuts specific sequences (consensus site 3−′AA/TTTT−5′) on the bottom DNA strand. The result of cutting is a free 3' hydroxyl of the nicked DNA that is utilized by the ORF2p to produce complementary DNA using the L1 mRNA as a template for reverse transcription (Hancks & Kazazian, 2016; Wang & Jordan, 2018; Wei et al., 2001). L1 distribution throughout the human genome reveals that ORF2p endonuclease activity and DNA replication determine L1 integration site preferences (Flasch et al., 2019). Although the mammalian genome encodes more than 100,000 copies of the L1 element, very few are full length and active, with only 80-100 L1 elements being retrotransposition-competent in humans (Brouha et al., 2003).

The localization of ORF1p and ORF2p have been reported in various compartments across different tissues. However, a recent study looking at endogenously tagged ORF1p and ORF2p revealed that they localize both to the nucleus and cytoplasm, with the localization differing significantly between cells in a population with active L1 retroelements (Mita et al., 2018). L1 retrotransposition peaks during S-phase, when the required dNTP pools for reverse transcription are also elevated (Mita et al., 2018). While ORF1p is nuclear in the G1-phase, it shuttles to be exclusively cytoplasmic in G2/S/M, indicating that ORF1p-depleted L1 RNPs drive TPRT. These results further highlight the

dispensable nature of ORF1p for TPRT and how the dynamics of ORF1p and ORF2p localization contribute to L1 retrotransposition. The cells being in G1 or S/G2/M will result in vastly different scenarios for how L1 retroelements propagate through ORF1p and ORF2p actions.

2.1.6 L1-mediated dysregulation of cGAS-STING in disease and aging

Several diseases characterized by elevated inflammatory cytokines are associated with loss of function of suppressors of L1 activity and cGAS-STING activation, which is summarized below.

3.1.4.1 Fanconi Anemia

Fanconi Anemia (FA) is a rare hereditary disorder with its pathology being characterized by increased susceptibility to cancer and elevated levels of pro-inflammatory cytokine production (Bagby & Alter, 2006). The disease results from mutations to any 1 of the 23 known FA genes, which also encode proteins that form a complex (FA complex) that mediates interstrand crosslink (ICL) repair in a cell-cycle dependent manner (Kim et al., 2008; Rio & Bueren, 2008). The loss of FA complex function results in an accumulation of DNA breaks and genome instability.

While the role of the FA complex in DNA repair and genome stability is well-established, how the loss of the complex results in a pro-inflammation state was not well-understood. FA-deficient macrophages were found to overproduce cytokines in response TLR4 and TLR7/8 agonists (Garbati et al., 2016). However, unexpectedly, the occurrence

of DNA strand breaks and large chromosome breaks were neither necessary nor sufficient to account for the overproduction of inflammatory cytokines (Garbati et al., 2016). Brégnard et al., later found that FA-deficient cells (SLX4 deficiency model) accumulate cytoplasmic DNA, which triggers cGAS-STING signalling (Bregnard et al., 2016). Interestingly, the cytoplasmic DNA was enriched for L1-derived sequences, which was causing overactive cGAS activity (Bregnard et al., 2016). cGAS activity could be suppressed in this model by treatment with a reverse transcriptase inhibitor, further highlighting that L1 accumulation in the cytoplasm resulted in elevated type I IFN signalling in FA-deficient cells (Bregnard et al., 2016). Therefore, L1 and cGAS-STING appear to be key in explaining how FA-patients have elevated levels of cytokine production.

In addition, a high-throughput retrotransposition assay screen later identified that FA factors and DSB repair machinery active during S/G2 phase as critical suppressors of LINE-1 retrotransposition (Mita et al., 2020). Nearly all the FA factors behaved as restrictive factors for L1 aside from FANCJ, with possibly unique mechanisms of L1 inhibition existing for the different proteins (i.e., parallel pathways for L1 suppression) (Mita et al., 2020). While not all the FA factors were not specifically examined mechanistically, how BRCA1 restricts L1 was determined. BRCA1 interacted with L1 machinery to reduce L1 ORF2p translation by binding to L1 mRNA (Mita et al., 2020). The study conceptualizes the idea of replication forks and sites of replication being preferred sites for L1 activity in mammalian cells, with BRCA1 and other HR and FA factors acting to inhibit L1. However, it also suggests that L1 dysregulation is a common hallmark in the different forms of FA, considering that they all play a role in suppressing L1.

3.1.4.2 Aicardi-Goutières syndrome

While I have discussed how TREX1 loss results in AGS through dysregulation of the cGAS-STING pathway, there are six other genes that when mutated, also cause AGS. These include SAMHD1, ADAR1, IFIH1/MAVS and three subunits of the ribonuclease H2 endonuclease complex (RNASEH2A, RNASEH2B, RNASEH2C). A common hallmark of all these forms of AGS is overactive type I IFN signalling, which results in autoimmune disease (Rice et al., 2007). The tonic type I IFN signalling has been suggested to occur through cGAS-STING for loss of function mutations associated with the RNASEH2 complex and SAMHD1 (Schumann et al., 2023). In the case of

SAMHD1, this occurred through the IFIH1 pathway, a parallel cytosolic RNA sensing pathway that was then primed by cGAS-STING (Schumann et al., 2023). In contrast, loss of function of the RNASEH2 complex phenocopied TREX1, where mice models showed elevated levels of LINE-1 that fed caused overactive cGAS-STING signalling (Mackenzie et al., 2016; Pokatayev et al., 2016).

Intriguingly, all these different enzymes have also been linked to LINE-1, as suppressors through various mechanisms. IFIH1 appears to suppress LINE-1 retroelements upstream of all the other enzymes. The N-terminal 2CARD domain of IFIH1 interacts with the L1 5'-UTR to suppress the L1 promoter and its expression (Yan et al., 2022). SAMHD1 also suppresses L1 in the nucleus similar to IFIH1. Phosphorylated SAMHD1 interacts with L1 RNPs and inhibits retrotransposition by then depleting local dNTPs surrounding the L1 RNP to limit synthesis of new L1 elements in the nucleus (Herrmann et al., 2018). The function of RNASEH2A also appears to be in the nucleus for restricting L1, where it binds to L1 RNA to prevent formation of the L1-derived RNA-DNA hybrids (Choi et al., 2018). The RNASEH2 complex requires the MOV10 helicase to jointly suppress L1 retrotransposition (Arjan-Odedra et al., 2012; Choi et al., 2018; Li et al., 2013). ADAR1 also binds to L1 RNA but how it contributes to L1 suppression is unknown since L1 RNA is not edited by ADAR1 (Orecchini et al., 2017). All these different AGS-associated proteins contribute to L1 regulation through unique mechanisms within the nucleus, whereas TREX1 limits L1 as a last resort in the cytoplasm.

3.1.4.3 Dermatomyositis

LINE-1 accumulation and resultant cGAS-STING dysregulation has also been linked to autoimmune diseases that are not considered genetic disorders such as Dermatomyositis (DM). DM affects both the skin and muscle and is caused by chronic inflammation to these tissues (Callen & Wortmann, 2006). However, the molecular changes that facilitate these changes or the genetic factors involved are currently unknown for the disease. A group recently found that the muscle specimens of DM patients have elevated levels of type I IFN associated cytokines and proteins such as TBK1, p-IRF3, and p-TBK1, that are all downstream of STING signalling (M. Zhou et al., 2022). In addition, the muscles also have elevated transcripts of cGAS and STING, indicating that the cGAS-STING axis is directly upregulated (M. Zhou et al., 2022). Overactive cGAS-STING signalling was contributing to the inflammation observed in the muscles of DM patients.

The transcriptional changes indicate that DM patients have elevated levels of cGAS-STING components but the mechanism behind this was unknown. In another study, the levels of LINE-1 retroelements was elevated in DM patient samples and this correlated well to higher levels of type I IFN signalling (Kuriyama et al., 2021). The upregulation in LINE-1 was a result of reduced L1 promoter methylation in DM patient samples, indicating that the transcriptional changes was in part a result of histone methylation changes that favoured the expression of LINE-1 retroelements and potentially cGAS and STING (Kuriyama et al., 2021). Therefore, L1 retroelements and cGAS-STING appear to also be dysregulated in DM.

In this chapter, I characterize the molecular evolution of PML and identify a novel family of genes which I describe as the PML-like exon 9-like (Plex9) genes. I demonstrate through phylogenetic analyses that the *PML* gene first emerged in jawed vertebrates and was lost from the genomes of teleost fishes and salamanders. While PML is lost, teleost fishes have retained Plex9 genes that are homologous to the DEDDh exonuclease C-terminus of spotted gar PML. These Plex9 exonucleases are active and capable of degrading DNA. In addition, the Plex9 proteins have an exonuclease-independent function in supressing L1 retroelements to maintain genome stability. In an example of convergent evolution, the Plex9 proteins regulate the cGAS-STING pathway akin to TREX1, as their ectopic expression complements TREX1 loss in human cells. Taken together, these results describe a new family of DEDDh exonucleases that are related to PML in teleost fish which help us better understand how vertebrates prevent retroelement propagation and regulate cGAS-STING.

2.2 Materials and Methods

2.2.1 Phylogenetic analyses

Two rounds of searches on the protein and transcriptome sequences were carried out to detect homologs to the human PML sequence in sequenced eukaryote species. A phylogenetic dataset of PML proteins was constructed by collecting 72 protein sequences from NCBI via a PSI-BLASTp or tBLASTn search followed by reverse BLASTP. For searches, in the first round I targeted both the full length PML (sequence for isoform PML-I) and the C-terminus of PML (an amino acid stretch from positions 600-882; the C-terminal DEDDh exonuclease domain (CDE)) in the second round. The logic behind

this stems from the RBCC motif being highly conserved and associated with TRIM19 proteins. The C-terminus is unique to PML. The *E-value* threshold (-e) was set as 0.001, the *E-value* threshold for inclusion in the multipass model (-h) as 0.002 (default value), and the maximum running iterations (-j) as 5. For transcriptome sequences, tBLASTn was used and the *E-value* threshold (-e) was set as 0.001. For species with fully sequenced genomes available, PML orthology was confirmed by synteny to the human *PML* loci.

A separate dataset of the Plex and TREX exonucleases was constructed through a similar approach but searching for both the C-terminus of PML, zebrafish Plex9.1 and Plex9.2 and TREX1. resulting in a dataset of 104 proteins. Previously identified homolog PML-CDE sequences that had homologous sequence and synteny were added to the Plex and TREX dataset. Both datasets were aligned using mafft einsi with default settings (Katoh et al., 2002). The Exonuclease III (ExoIII) dataset was trimmed so that only the ExoIII, and ExoIII-like, domains remained, while the C-terminal exonuclease domain was removed from the PML alignment. Both datasets were further trimmed using trimal v1.4.rev15 with the -gappyout setting (Capella-Gutierrez et al., 2009), resulting in a PML data set containing 545 sites and a ExoIII dataset containing 242 sites. These datasets were used to estimate maximum-likelihood phylogenies using IQTree v1.5.5 (Nguyen et al., 2015) using the LG+C60+gamma model of evolution. **These analyses were done with the help of the Roger lab.**

2.2.2 PML RBCC domain phylogeny

The resulting PML phylogeny (**Figure 2.8**), created using the RBCC domains of the protein, shows the expected relatedness between major groups of metazoans, with moderate support. This analysis identifies the ancestral PML originating from within Chondrichthyes (the sharks & rays). This phylogeny highlights the divergence of the PML ortholog found in *Lepisosteus oculatus,* an Actinopterygii fish identified as possessing a full-length PML sequence, which, as expected, is sister to Sarcopterygii. To assess domain architectures, InterPro 88.0 (https://www.ebi.ac.uk/interpro/) was utilized. Orthologs used in the analysis include ones from the following species (corresponds to silhouettes in Figure 2.7): *Amblyraja radiata*, *Scyliorhinus canicular*, *Lepisosteus oculatus*, *Tachyglossus aculeatus*, *Sarcophilus harrisii*, *Mus musculus, Pteropus vampyrus*, *Capra hircus*, *Ursus maritimus*, *Homo sapiens*, *Alligator sinensis*, *Pogona vitticeps*, *Chelonia mydas* and *Coturnix japonica*.

2.2.3 ExoIII domain phylogeny

The phylogenetic analysis of TREX, Plex9, and PML-CDE domains (**Figure 2.9**) shows that within metazoans, TREX and Plex proteins are distantly related and diverged before the last common ancestor of this group. Furthermore, this phylogeny shows that the ExoIII domains of PML are more closely related to Plex exonucleases. Syntenic analysis from the sequenced genomes revealed that TREX1 first appears in tetrapods due to its presence in amphibian genomes and that it likely arose from a gene duplication of TREX2. In contrast, genes encoding Plex9 sequences share synteny to the PML locus. Overall, this analysis is well supported by bootstrap values, highlighting the robust nature

of the relationships uncovered, both between and within these two distinct exonuclease families.

2.2.4 Plasmid construction

RNA isolated from the tissue of each species was used for cloning the axolotl *TREX*, spotted gar *pml*, and zebrafish *plex9.1* and *plex9.2*. RNA for downstream cloning was derived from axolotl limbs that were dissected and stored in Trizol. In the case of zebrafish, the RNA is derived from 24 hpf zebrafish embryos. The RNeasy (Qiagen) kit was used for all extractions, according to the manufacturer's instructions. The cDNAs were prepared using the SuperScript™ IV One-Step RT-PCR System (Invitrogen) and sequenced prior to subcloning into indicated vectors.

Synthetic genes coding for zebrafish Plex9.1 (Ile44-Leu244; Ensembl:ENSDARG00000092584; NCBI: XP_005174272.1) was purchased (BioBasic Inc) and ligated into a modified pET21 expression vector that contained upstream sequences coding for a hexahistidine tag (H), maltose binding protein (M), and tobacco etch virus protease recognition (T) sequence to create pHMT-zfPlex9. Site directed mutagenesis was used to create pHMT-zfPlex9.1 (D61N) using pHMT-zfPlex9.1 as a template. The fidelity of all plasmids was verified by sanger sequencing (Eurofins Genomics).

In addition, along with *zfplex9.1*, another zebrafish gene coding for *plex9.2* (Ensembl ID: ENSDARG00000093773; NCBI: XP_002666829.1) was utilized in the study. In addition, axolotl TREX1/2/3 sequences (AMEXTC_0340000192613,

AMEXTC_0340000056847, AMEXTC_0340000061536) from the axolotl transcriptome Am_3.4 available on Axolotl-omics (https://www.axolotl-omics.org). These coding gene sequences were all cloned into CMV-based FLAG-tagging and Clover-tagging vectors (CMV-FLAG-J1 and CMV-Clover-J1; derived from commercially available vectors pEGFP-C1 and pEGFP-N1; Clontech) for ectopic expression in human cells.

2.2.5 Protein expression and purification of zfPlex9.1 and zfPlex9.1 (D61N)

BL21(DE3) *E. coli* (New England BioLabs Inc.) were transformed with pHMT-zfPlex9.1 and pHMT-zfPlex9.1 (D61N). Transformed cells were grown in LB media to an OD_{600} of ~0.6, after which protein expression was induced with 0.5 mM IPTG. After overnight expression at 20 °C (16 °C for pHMT-zfPlex9.1 (D16N)), cells were resuspended in lysis buffer (HMT-ZfPLEX9.1: 20 mM Tris pH 7.5, 100 mM NaCl, 5 mM β-mercaptoethanol (BME); HMT-ZfPLEX9.1 (D61N): 20 mM CHES pH 9, 100 mM NaCl, 5 mM BME, 5 mM $MgCl_2$, lysed by sonication, and clarified by centrifugation (25,000 × g for 20 min at 4 °C). The supernatant was loaded onto an amylose chromatography column (New England BioLabs Inc.), washed with lysis buffer, and eluted with lysis buffer containing 10 mM maltose. The proteins were then incubated with TEV protease overnight in elution buffer (HMT-ZfPLEX9.1) or with concurrent overnight dialysis at 4 °C against dialysis buffer (HMT-ZfPLEX9.1 (D61N): 20 mM CHES pH 9, 100 mM NaCl, 5 mM BME, 5 mM $MgCl_2$). After cleavage, exonuclease domains were isolated using Ni^{2+} affinity chromatography and then purified by size exclusion chromatography (HiLoadTM 16/600 SuperdexTM 75 pg) using 20 mM Tris pH 7.5, 100 mM NaCl, 5 mM BME (HMT-ZfPLEX9.1 and HMT-ZfPLEX9.1 (D61N)).

Purifications were monitored by SDS-PAGE and UV/Vis absorbance (using predicted extinction coefficients at 280 nm of 20970 and 20970 $M^{-1}cm^{-1}$ for ZfPLEX9.1 and ZfPLEX9.1 (D61N), respectively). **These purifications were done by the Langelaan lab.**

2.2.6 In vitro exonuclease assays

Exonuclease reactions (40 µL) contained 500 nM 5'-6-FAM labeled oligonucleotide (ssDNA: 5'-ATACGACGGTGACAGTGTTGTCAGACAGGT-3'or dsDNA pseudo-palindrome: 5'-TCACGTGCTGAC/GTCAGCACGACG-3'), 20 mM Tris pH 7.5, 2 mM dithiothreitol, and 100 µg/mL BSA. For metal specificity assays the reactions contained 625 nM of zfPlex9.1 and 2 mM metal ($MgCl_2$, $MnCl_2$, $ZnSO_4$, or $CaCl_2$) or 10 mM EDTA. Exonuclease titration assays contained 4.9–625 nM of zfPlex9.1 or zfPlex9.1 (D61N) and 5 mM $MgCl_2$. Reactions were allowed to proceed for 20 min at room temperature and then quenched with 3 volumes of 100% ethanol, dried via speed vac, resuspended in 10 µL formamide, resolved by urea PAGE (19% 29:1 acrylamide and 7 M urea in TBE), and visualized using a fluorescence imager (VersaDoc). **These exonuclease assays were done by the Langelaan lab.**

2.2.6 Generation of a CRISPR/Cas9 KO lines and cell culture

I generated U2OS cells lacking *TREX1* expression, by designing a strategy to knock-in a puromycin resistance cassette into exon 2 of *TREX1*, thereby disrupting *TREX1* gene expression but not overlapping with the *ATRIP* protein encoding region.

U2OS was used a cell line since they have impaired cGAS-STING signalling and allow for us to focus on L1-retrotransposition in an interferon-independent manner(Deschamps & Kalamvoki, 2017).

Two guide RNAs targeting the Cas9(D10A) nuclease to the *TREX1* locus were designed utilizing the CHOPCHOP v3 webtool for designing guide RNAs(Labun et al., 2019). I selected the top two guide RNAs, g1 (5'-CCCAACCATGGGCTCGCAGGCCCTGCCCCCGGGGCCCATGCAGACCCTCATCTTTTTCGACATGG-3') and g2 (5'-CCATGTATGGGGTCACAGCCTCTGCTAGGACCAAGCCAAGACCATCTGCTGTCACAACCACTGCACACCTGG-3') and cloned these guides into the All-in-one (AIO)-PURO vector encoding the Cas9D10A nickase (Addgene #74630). U2OS cells were treated with 2 µg/mL of puromycin (Invitrogen) and resultant clones were isolated. Resultant clones were screened by both western blotting and immunofluorescence to confirm that TREX1 expression was absent (**Figure 2.4**)

ATRIP expression in the *TREX1* KO lines was also examined, which was previously ignored in other reports of a human *TREX1* KO line, despite *TREX1* being nested in the locus of *ATRIP* (Kucej et al., 2017; Mohr et al., 2021a). I was unable to get a positive clone with guide 2 (g2) and this appears to be a result of ATRIP levels being altered, where two prominent bands are present (data not shown). Therefore, the clone generated from guide 1 (which still shows a faint secondary ATRIP protein band that is not present in WT cells) was utilized. This clone was used as TREX KO#1 for experiments involving L1 suppression, a previously established function for TREX1 (both via KO models in mice and overexpression studies) (Li et al., 2017a; Thomas et al.,

2017). Our addback of TREX1 restored L1 suppression, supporting the notion that elevated L1 retrotransposition was a result of TREX1 loss and not ATRIP being altered (**Figure 2.4**). U2OS WT and TREX1 KO cells were cultured in Dulbecco's modified Eagle's medium (Life Technologies) supplemented with 10% fetal calf serum, at 37°C with 5% CO_2.

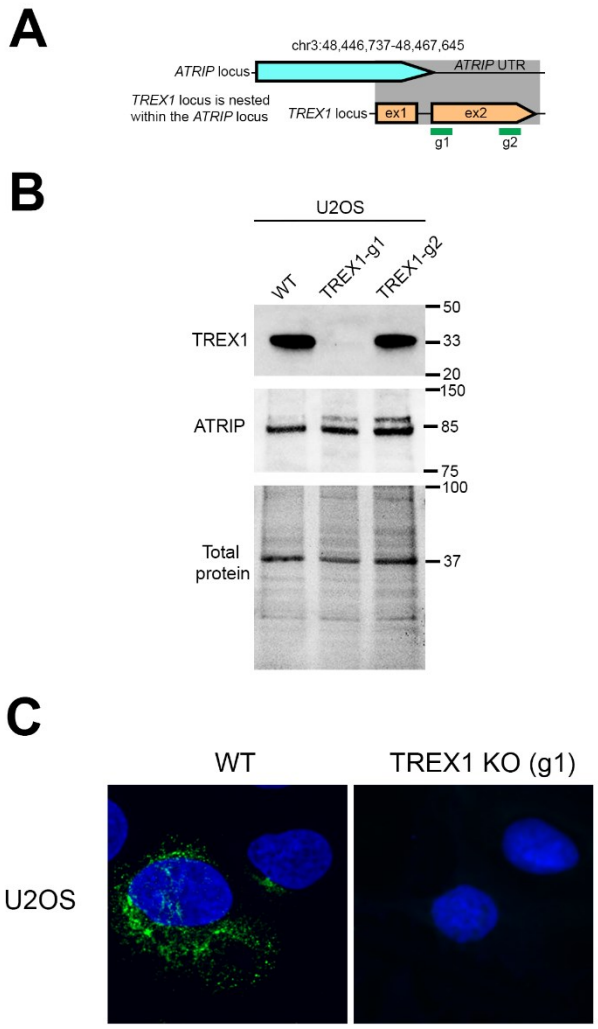

Figure 2.4. Generation of a *TREX1* knockout using CRISPR/Cas9 in U2OS cells. (**A**) Scheme for targeting human *TREX1*. A single guide RNA (sgRNA) targeting *TREX1* exon 2 (g1) was used to generate a TREX1 knockout cell line, which lacked TREX1 protein. (**B**) Editing at the *TREX1* locus presents difficulty due to the *TREX1* gene is nested within the ATRIP UTR region and therefore probed for any changes in ATRIP levels. A detailed description of the CRISPR/Cas9 targeting of *TREX1* is described in the Materials and Methods. (**C**) Immunostaining for TREX1 in WT and *TREX1* knockout cells. Scale bar represents 20 μm.

2.2.7 LINE retrotransposition assays

To assess the effect of proteins on retrotransposition, I utilized methods for previously characterized plasmids encoding a LINE retroelement (human L1, zfL2-1, zfL2-2 or UnaL1) that encode a neomycin cassette that when transfected into cells, is only successfully re-integrated upon retrotransposition (**Figure 2.5**) (Benitez-Guijarro et al., 2018; Bogerd, Wiegand, Doehle, et al., 2006; Bogerd, Wiegand, Hulme, et al., 2006; Choi et al., 2018; Moran et al., 1996; Muckenfuss et al., 2006). Upon G418 (Thermo Fisher) selection, it is possible to quantify the number of positive clones that survived which will be proportional to the LINE activity occurring. Co-expression of the proteins of interest with the LINE encoding plasmid, will determine which proteins enhance, suppress, or have no impact on cell LINE retrotransposition. HeLa and U2OS cells were utilized for LINE retrotransposition since they are susceptible to high levels of LINE retrotransposition in culture (Benitez-Guijarro et al., 2018; Moran et al., 1996).

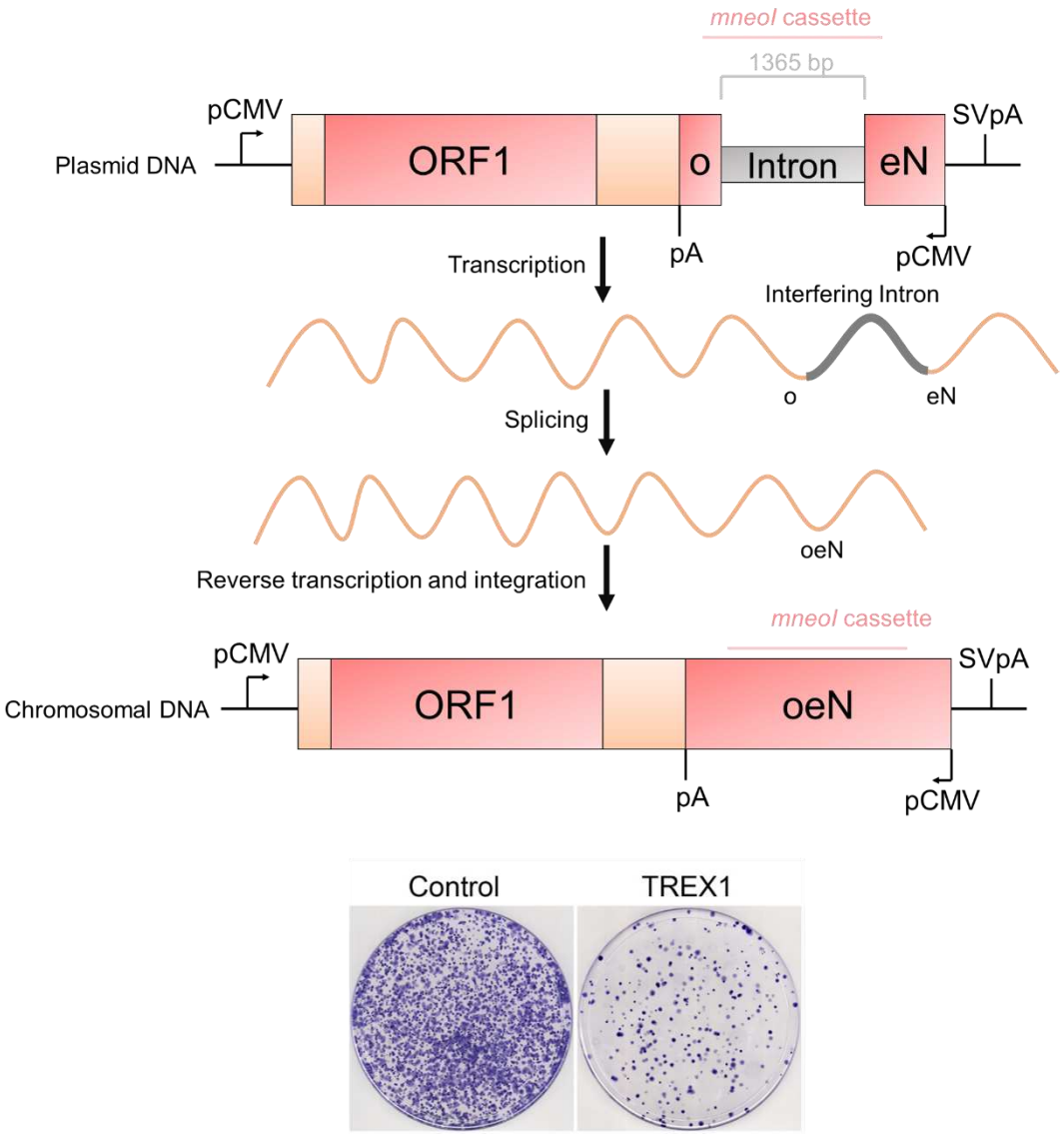

Figure 2.5. LINE-1 reporter assay. The LINE-1 reporter assay takes advantage of a LINE-1 retroelement that encodes a *neo* gene that has an intervening intron. After transfection of the reporter plasmid with a protein expression vector of interest, the reporter L1 element is transcribed, the intron is spliced, and a *neo* gene is integrated to the genome of the transfected cell if there is successful L1 retrotransposition. If the co-transfected protein enhances or suppresses L1 retrotransposition, this will result in more or fewer colonies that are neomycin resistant. Below is an example of the readout from the assay where TREX1, a suppressor of L1 retroelement, is co-transfected and the result is fewer colonies at the end of the experiment.

Cells (HeLa or U2OS) were seeded in a 6-well at densities of 2 x 10^5 per well, left to attach for 24 hours and co-transfected using Lipofectamine 3000 (Roche) with (1) 1 ug of a retrotransposon encoding plasmid (2.5ug for the zfL2-1 retrotransposon) and (2) with 500 ng of a FLAG-tagged protein of interest. The only exception was the GFP-TREX1(D18N) plasmid which was obtained from Addgene (27220). No difference was observed between cell toxicity or transfection efficiencies between GFP-TREX1(D18N) and the other plasmids (data not shown). The relative cytotoxic effects and transfection efficiencies were tested for all plasmids utilized in the LINE-1 experiments (**Figure 2.6** and **Figure 2.7**) but did not observe significant differences.

After 2 days post-transfection, the cells were reseeded on a 10 cm plate, allowed to adhere for 24 hours, and then incubated with G418 (500 ug/mL for HeLa; 400 ug/mL for U2OS) for a total of 10 days for HeLa and 14 days for U2OS. Then post-selection, the resistant colonies were fixed with 1 mL of methanol for 20 minutes. The colonies were then washed with PBS and stained with 0.5% crystal violet (stained for 30 minutes in 5% acetic acid and 2.5% isopropanol) for 30 minutes. The entire fixation and staining procedure were completed at room temperature. Colonies were then counted and retrotransposition activity was determined.

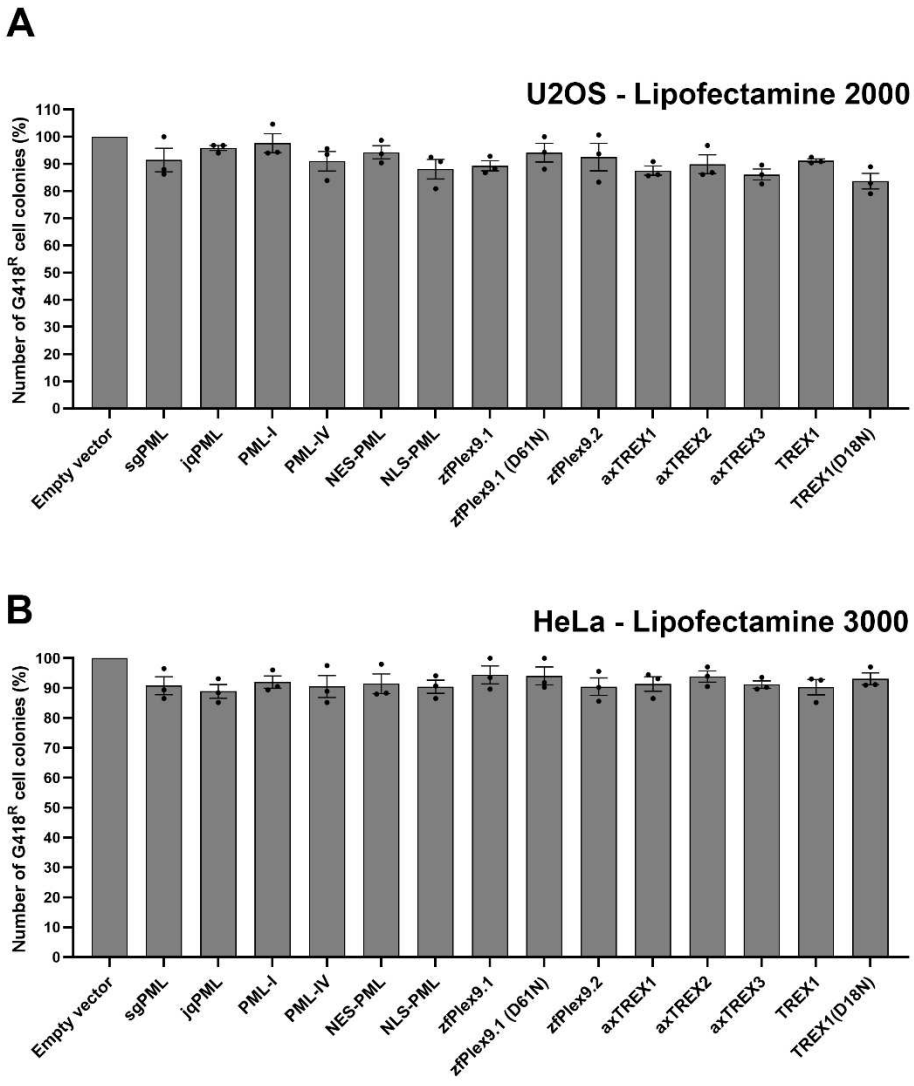

Figure 2.6. Assessing cytotoxic effects of the tested PML, Plex9 and TREX1 proteins. Cells were transfected using (**A**) Lipofectamine 2000 (U2OS cells) or (**B**) Lipofectamine 3000 (HeLa cells). To determine the cytotoxic effects of overexpressing the plasmids of interest, cells were co-transfected with 1 µg of *neo*-resistance encoding pcDNA3.1 plasmid and 1 µg of FLAG-tagged protein encoding plasmid or an empty FLAG encoding plasmid as control. After 12 days of G418 selection, neomycin resistant colonies (i.e., $G418^R$) were fixed with methanol, stained for crystal violet, and counted. Cytotoxicity is shown relative to the empty FLAG vector, which is shown as 100%.

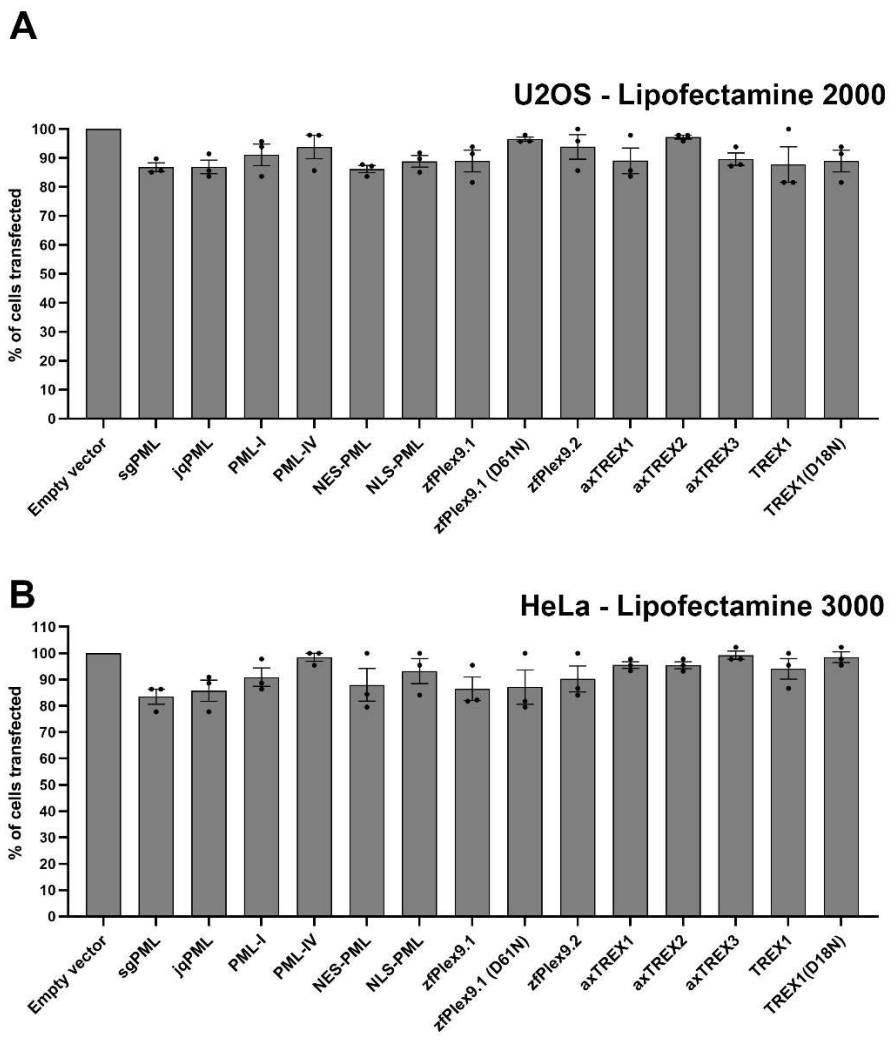

Figure 2.7. Determining transfection efficiencies for the LINE-1 assay. Cells were transfected using (**A**) Lipofectamine 2000 (U2OS cells) or (**B**) Lipofectamine 3000 (HeLa cells). To determine the transfection efficiency during co-transfections with the L1-encoding plasmid, cells were co-transfected with 1 µg of L1 plasmid, 0.5 µg of FLAG-tagged protein and 0.5 µg of a Clover expression vector. After 24 hours, cells were fixed and the percentage of Clover expressing cell (i.e., transfected cells) was determined. There was no significant difference in terms of efficiency between the different vectors used for transfection. ****P<0.0001, ***P < 0.001, **P < 0.01, *P < 0.05, one-way ANOVA; Holm-Šídák for multiple-comparison.

2.2.8 2',3'-cGAMP quantification

4×10^6 cells (for WT and TREX1 KO) were seeded into 15-cm dishes, and 24 hours later cells were transfected with the Bluescript vector (empty vector control) and Human L1 plasmid (used in L1 retrotransposition assay) using Lipofectamine 2000 reagent (Invitrogen). Cells were harvested 36 hours after transfection, washed with 2x with PBS and pelleted before lysis. Samples were resuspended in 500 µL M-PER (mammalian protein extraction reagent) lysis buffer (Thermo Scientific). Lysates were incubated on ice for 30 minutes with gentle agitation every 10 minutes, before being spun down at 16,000 x g, 4° C for 10 min. Samples were quantified using the 2′3′cGAMP ELISA Kit (Cayman Chemical) according to the manufacturer's instructions.

2.2.9 Immunofluorescence microscopy

For micronuclei counting (**Figure 2.12**), cells were transfected with protein expression vectors (e.g., zfPlex9.1, axTREX1 and human TREX1) and treated for 48 hours post-transfection with 5 µM reversine (MPS1 inhibitor used to induce micronuclei formation) (Adell et al., 2023; Toufektchan & Maciejowski, 2021; Tucker et al., 2023). The percentage of transfected cells with micronuclei were counted after overexpression of zfPlex9.1, axTREX1, and human TREX1. Multinucleated cells and cells lacking intact nuclear envelopes (i.e., signs of rupture) were not included in the quantification. For experiments, >100 cells were counted across three independent biological replicates.

For transfections, cells were seeded into wells containing coverslips in 6-well dishes, then transfected the next day with expression vectors. One day after transfection, coverslips were washed briefly with PBS and the cells were fixed in 2% PFA,

permeabilized with 0.5% Triton X-100 in PBS and blocked with 4% BSA in PBS. Cells were then immunolabeled with primary antibodies specific for FLAG (mouse anti-FLAG M2, Sigma, F3165, 1:200) and TREX1 (rabbit anti-TREX1, Abcam, ab185228, 1:400). Then for secondary staining, coverslips were washed with PBS and incubated with Alexa-Fluor 647 donkey anti-rabbit, Alexa-Fluor 555 donkey anti-rabbit, and Alexa-Fluor 488 donkey anti-mouse (Thermo Fisher Scientific) secondary antibodies. Finally, the cells were washed several times in PBS and incubated with 1 µg/mL of 4',6-diamidino-2-phenylindole (DAPI) (Sigma) to visualize the nuclei.

For transfections, the ER was marked using plasmids obtained from Addgene and individuals. The ER was marked using a Cytochrome p450 (CytERM) tagged to mScarlet (Addgene #85066), which was utilized as an ER marker. Plasmids for flag-tagging of proteins of interest are described above under plasmid construction, aside from FLAG-TREX1 (Addgene #27218), GFP-TREX1 (Addgene #27219) and GFP-TREX1 (D18N) (Addgene #27220) which were obtained from Addgene. U2OS cells were transfected using Lipofectamine 2000 (Invitrogen) and HeLa cells using Lipofectamine 3000 (Invitrogen), according to the manufacturer instructions.

Fluorescent micrographs were captured with a Prime95 scientific complementary metal-oxide-semiconductor (sCMOS) camera (Photometrics) using a custom-built spinning-disk confocal laser Zeiss Cell Observer Microscope (Intelligent Imaging Innovations, 3i) equipped with a 1.4 NA 63X immersion oil objective lens and both laser (3i) and LED illumination via a Spectra light engine (Lumencor). Images were captured and processed using Slidebook 6.1 (3i) and assembled into figures using Adobe Photoshop CS5.

2.2.9 Western blotting

For western blot analysis, cells were recovered from confluent 10 cm culture dishes and washed with PBS. The cells were lysed on ice for 20 minutes in RIPA buffer (Sigma) with protease inhibitors (P8340, Sigma). Lysates were cleared (10 min, 15 000 × g, 4°C) and protein extracts were analyzed by SDS-PAGE and western blotting using 5% milk powder with 0.1% Tween 20 in PBS as a blocking solution. Protein was transferred to Nitrocellulose membrane (BioRad). Total protein was determined directly on the membrane using the 4-15% Mini-PROTEAN TGX-Stain Free Protein Gel system (BioRad). Antibodies used for Western blotting analysis were: rabbit anti-TREX1 (Abcam, ab185228, 1:1000) and anti-ATRIP (Sigma, PLA1030, 1:1000).

2.2.10 Statistical analysis

All statistical analyses were performed using GraphPad Prism 9.0.1. The sample size and error bars for each experiment are defined in the figure legends. Comparisons between groups for LINE1 retrotransposition and the 2’3’-cGAMP assay were analysed by a repeated measures one-way ANOVA, with the Geisser-Greenhouse correction and then a Tukey's multiple comparisons test between groups.

2.2.11 Animal ethics

For axolotl work, Axolotl Université de Montreal animal ethics committee authorization was: 20-103. The Université de Montral animal ethics committee is

recognized by the CCAC. The use of zebrafish embryos for generation of RNA was approved by Dalhousie University Committee on Laboratory Animals (Protocol Number 20-130)

2.3 Results

2.3.1. The PML gene emerges in jawed vertebrate species

To elucidate the evolutionary history of *PML*, putative orthologs were identified from publicly available databases of eukaryote genomes and transcriptomes (**Figure 2.8**). PML-I orthologs were identified in jawed vertebrates (Gnathostomata) including extant cartilaginous fishes (Chondrichthyes) and bony vertebrates (Euteleostomi) (Brazeau & Friedman, 2015). I could not identify orthologs of PML in agnathan cyclostome (lamprey and hagfish) genomes (**Figure 2.8**). In addition, there is divergence of the *PML* gene in amniotes (**Figure 2.8**).

Among Chondrichthyes, PML ortholog architecture can be stratified into three groups, those with genomes encoding full length PML-I, those encoding putative orthologs with only a conserved RBCC domain, and those with a C-terminal transmembrane domain (**Figure 2.8**). While the RBCC domain is common among TRIM family proteins (Meroni, 2012), the C-terminal domain of PML-I encoded by exon 9 uniquely shares homology with DEDDh exonucleases, which was originally annotated as a putative exonuclease III domain (Condemine, Takahashi, Le Bras, & de The, 2007). This C-terminal DEDDh exonuclease (CDE) domain is conserved in bird, reptile, and mammalian PML orthologs as a predicted enzyme fold; however, the predicted catalytic residues are mutated in tetrapod orthologs of PML-I (**Figure 2.8**). Uniquely in ray-finned fish (such as paddlefish, spotted gar and sturgeon) and in cartilaginous fishes such as sharks and rays, PML orthologs have a CDE with intact catalytic residues, suggesting that they could be functional exonucleases (**Figure 2.8**).

During vertebrate evolution, the *PML* gene appears to have been lost several times in major extant euteleostome lineages, including amphibians and teleost fishes (**Figure 2.8**). A PML ortholog could also not be identified in the coelacanth genome, the most basally diverging lineage of extant Sarcopterygii (lobe-finned fishes). Similarly, a *PML* gene was not identified in the lungfish genome. Within reptiles, turtles show conservation of the CDE, whereas lizard genomes encode a truncated PML ortholog lacking the CDE (**Figure 2.8**). Birds similarly have PML homologs that resemble full-length PML. Since turtles are thought to be more closely related to archosaurs than lepidosaurs, our analyses suggest that bird and turtle ancestral lineages retained an ortholog resembling full-length PML (Nisole et al., 2013).

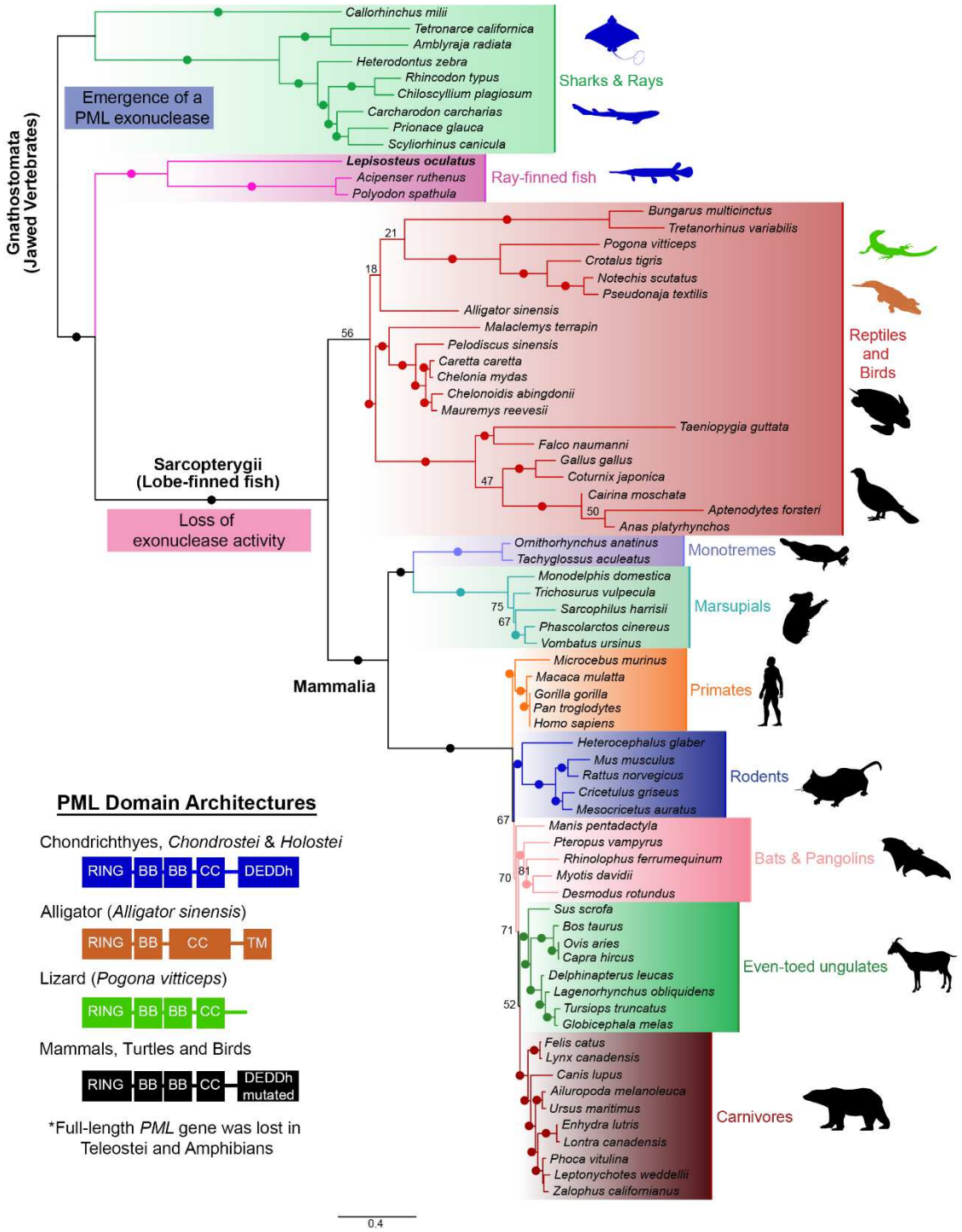

Figure 2.8. Domain architecture and Maximum Likelihood phylogenetic tree showing the relationships of PML homologs. 70+ protein sequences encoded in genomes from representative vertebrates were identified and utilized to construct the phylogenetic tree. PML emerged as an exonuclease in jawed vertebrates and eventually

lost the catalytic residues for activity in amniote species. Teleost fishes and amphibians lack full-length PML-I. Ultrafast bootstrap values are shown as numbers if <85% and indicated with solid dots on branches if >85%. Branch lengths indicate the expected number of amino acids substitution per site. Domains for homologs were determined using InterPro (https://www.ebi.ac.uk/interpro/) and 4 different domain architectures (left) were seen across analyzed sequences. Domain abbreviations refer to RBCC (Ring-B-box-Coiled Coil), BB (B-box), CC (Coiled coil), and DEDDh (3'-5' DEDDh exonuclease). Potential orthologs with ambiguity in sequence were omitted (e.g., tropical clawed frog). Sequences from species that were analyzed are shown in silhouettes and coloured according to the corresponding domain architecture on the left. Blue silhouettes indicate representative species with a PML ortholog encoding a predicted exonuclease domain. Silhouettes for species were obtained from PhyloPic (http://phylopic.org). ***Data presented in this figure was collected with the help of the Roger lab.***

2.3.2. A novel family of exonucleases, PML-like exon 9 (Plex9)

Most ray-finned fish species (99.8%) are teleost fish that underwent a genome duplication event accompanied by subsequent gene order rearrangements (Davesne et al., 2021). During this event, it appears that the full length *PML* gene was lost in teleost fishes. However, a pair of genes in zebrafish share a high degree of percent identity to the CDE of spotted gar *PML* (sgPML). The spotted gar species is an outgroup species that did not undergo a Teleost genome duplication event. I describe these novel genes as Pml-like exon 9 genes (*Plex9.1* and *Plex9.2*), which like the PML-CDE, share sequence similarity with TREX1 and TREX2, the two major DEDDh exonucleases in mammals (Hemphill & Perrino, 2019; Huang et al., 2018). A closer examination of the spotted gar *pml* locus also revealed the presence of two adjacent upstream genes that appear to have duplicated from the PML-CDE (**Figure 2.9A**). Phylogenetic analyses also indicated that Teleostei Plex9 shares the highest similarity to the PML-CDE, and across genera, TREX1 orthologs consistently cluster independently from Plex9 orthologs (**Figure 2.9B**). Thus, *plex9* genes in Telostei are DEDDh exonucleases closely related to the CDE of PML-I and are not evolutionarily related to *TREX1/2*.

Plex9 orthologs can be identified in other ray-finned fishes and in the elasmobranch sub-class of cartilaginous fish, whereas the TREX1 gene first appears in the tetrapod ancestor since it is found in amphibian species and amniotes (**Figure 2.9**). Neither *plex9.1* or *plex9.2* orthologs can be identified in lobe-finned fish (**Figure 2.9**). TREX2 predates TREX1 and can be found conserved in cephalochordates such as *Branchiostoma floridae*. *TREX1* was likely derived from a duplication of the *TREX2* gene (**Figure 2.9**). Thus, while tetrapods lost the *Plex9* genes, they retained the newly emerged

TREX1 gene and the *PML* gene encoding a CDE domain. In amphibians, a putative ortholog of *TREX1* can be identified but not genes resembling *PML* or the *plex9* orthologs. The axolotl genome encodes a TREX1 ortholog and there is expression of three transcripts for TREX1-like proteins (*axTREX1*, *axTREX2*, *axTREX3*). Previously, it was thought that *TREX1* was exclusive to mammals (Lindahl et al., 2009), however it appears that the progenitor *TREX1* gene encoding a DEDDh exonuclease is more generally present in tetrapod genomes.

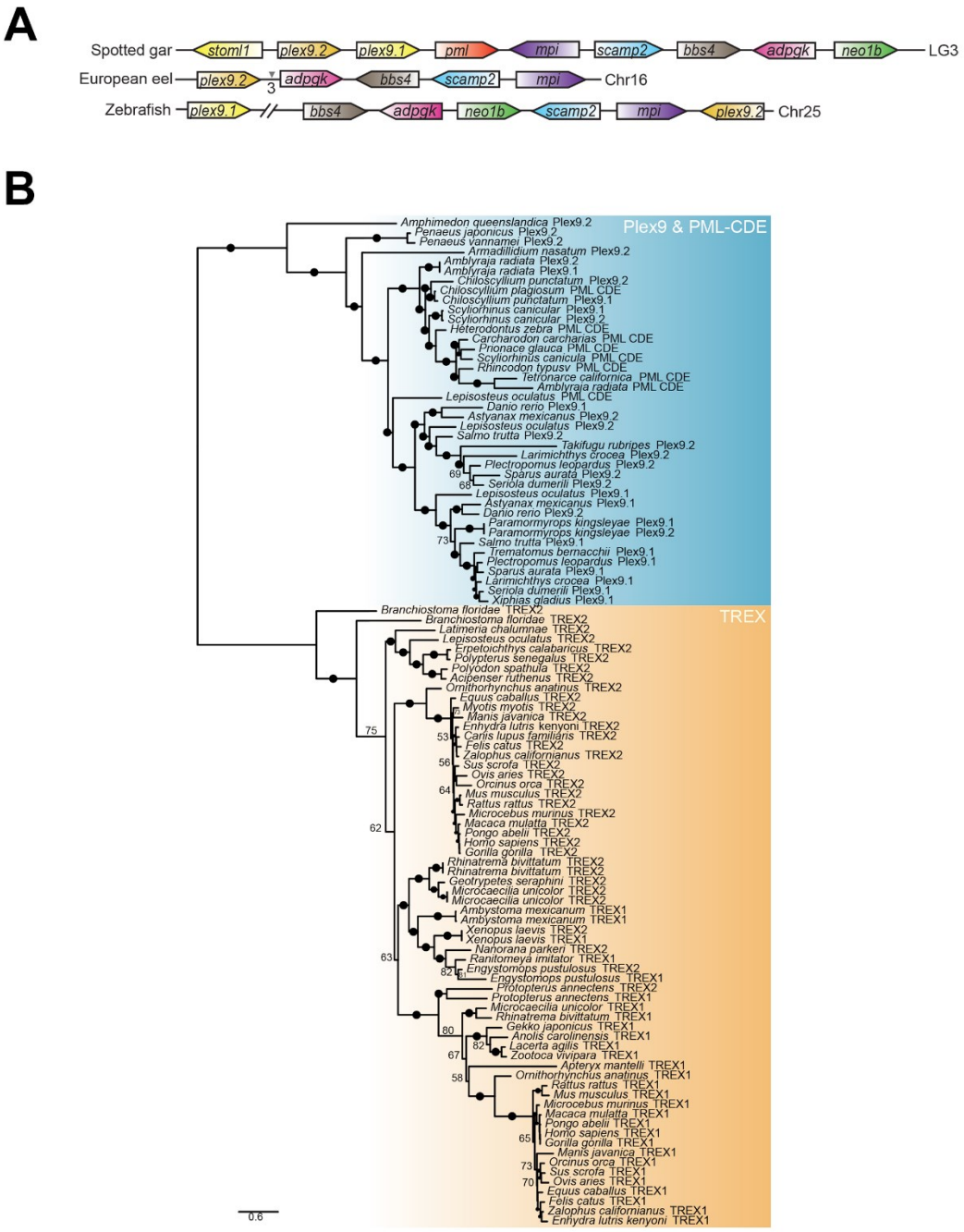

Figure 2.9. Origins of PML-like exon 9 (*Plex9*) and *TREX1* genes. (A) Teleost *plex9* genes show synteny to the spotted gar *pml* locus. Similarly coloured genes represent homologs between species. The chromosome where the *pml* locus is found in each species is indicated on the right. The intervening arrows with numbers indicate the number of intervening adjacent genes that exist between the homologous genes not found in the syntenic region. **(B)** Plex9 homologs resemble both TREX1/2 and PML exonucleases but are related to PML exonucleases. A maximum likelihood tree was constructed using Plex9, PML CDE and TREX1/2 protein sequences. While the TREX1 proteins cluster with TREX2, sequences for Plex9 cluster with PML CDE sequences.

Bootstrap values are indicated beside each node. Ultrafast bootstrap values are shown as numbers if <85% and indicated with solid dots on branches if >85%. Branch lengths indicate the expected number of amino acid substitutions per site. ***Data presented in this figure was collected with the help of the Roger lab.***

2.3.4. zfPlex9.1 is an active DNA exonuclease

TREX1 is a DEDDh exonuclease capable of degrading both ssDNA and dsDNA in the presence of divalent cations (Brucet et al., 2008; W. Zhou et al., 2022). Owing to the similarity between TREX1 and zfPlex9.1, we tested performed exonuclease assays in parallel to assess their exonuclease activity in the presence of different metal ions: Zn^{2+}, Ca^{2+}, Mg^{2+} and Mn^{2+} (**Figure 2.10A** and **Figure 2.10B)**. We found that recombinant zfPlex9.1 (aa 44-244) could degrade ssDNA and dsDNA in the presence of Mg^{2+} and Mn^{2+} (**Figure 2.10A** and **Figure 2.10B**). Thus, zfPlex9.1 (aa 44-244) can cleave ssDNA and dsDNA in the presence of specific cations. A comparison between Mouse Trex1 (1-242 aa) and zfPlex9.1 activity at different recombinant protein concentrations indicates that Trex1 (1-242 aa) cleaves ssDNA and dsDNA at a higher efficiency than zfPlex9.1 (**Figure 2.10C-F**). However, there appears to be slight differences in substrate specificity as zfPlex9.1 cuts ssDNA (versus dsDNA) at a higher rate and Trex1 cuts dsDNA (versus ssDNA) at a higher rate (**Figure 2.10C-F**). An alignment of zfPlex9.1, zfPlex9.2 and Trex1 revealed a conservation of the DEDDh catalytic residues that allowed us to phenocopy the exonuclease deficient D18N TREX1 mutation by mutating the cognate residue in zfPlex9.1 (i.e., D61N). The D61N mutation completely impaired zfPlex9.1 catalytic activity (**Figure 2.10E** and **Figure 2.10F**). Thus, zfPlex9.1 can digest ssDNA and dsDNA through catalytic residues found in the conserved DEDDh domain.

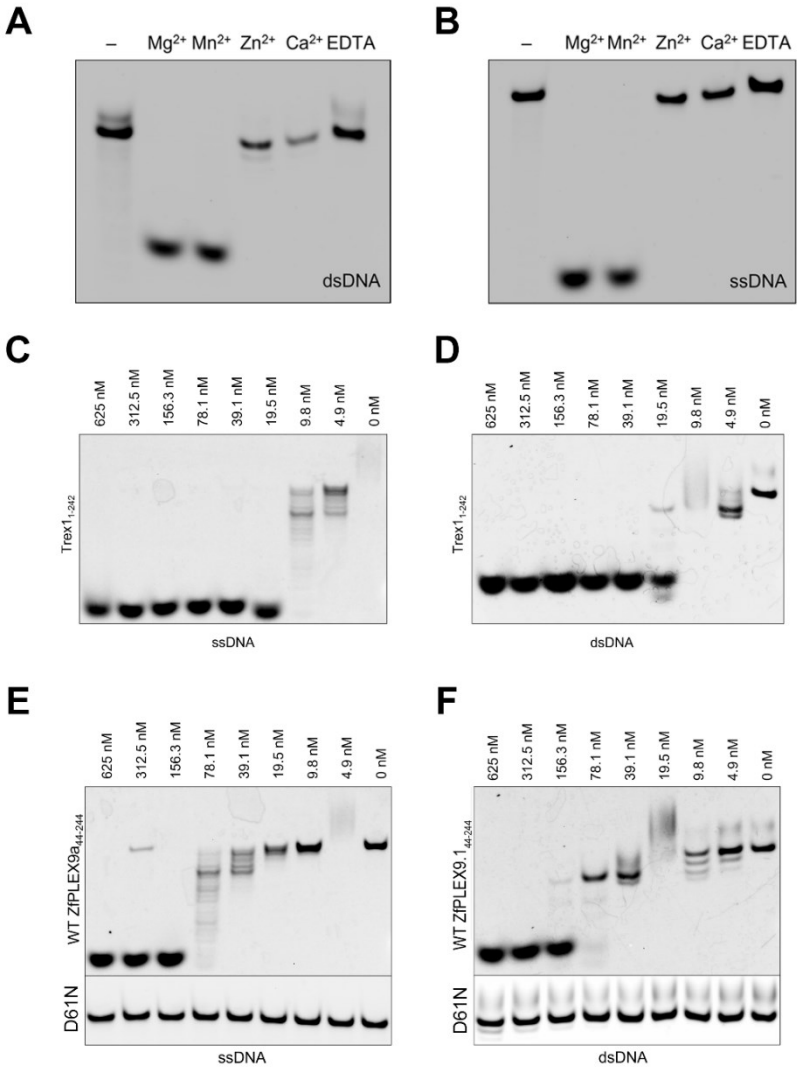

Figure 2.10. Plex9 proteins represent a novel class of DEDDh DNA exonucleases. (**A**) and (**B**) zfPlex9.1 requires Mg2+ or Mn2+ for activity. Fluorescent oligonucleotides were incubated with zfPlex9 and the indicated metal. Samples were resolved by UREA-PAGE and visualized via fluorescence imaging. "-" refers to input without the addition of cations. (**C**) and (**D**) Mouse Trex1 was purified akin to zfPlex9.1 and enzymatic activity was assessed for comparison of activity to zfPlex9.1. Both ssDNA (**C**) and dsDNA (**D**) were utilized as substrates at different concentrations. (**E**) and (**F**) zfPlex9 (D61N) lacks catalytic activity towards DNA. Substrates of ssDNA (**E**) and dsDNA (**F**) were utilized. Fluorescent oligonucleotides were also incubated with zfPlex9.1 (D61N). Samples were resolved by UREA-PAGE and visualized via fluorescence imaging. ***Data presented in this figure was collected by the Langelaan lab.***

2.3.3. zfPlex9.1 and axTREX1 localize to the ER and micronuclei with ectopic expression

To better understand the function of the Plex9 and non-mammalian TREX1 proteins, I cloned the zebrafish *plex9* genes (*zfplex9.1* and *zfplex9.2*), as well as the TREX1 ortholog isoforms from the axolotl genome (*axTREX1*, *axTREX2*, *axTREX3*) to assess their cellular roles and localization in mammalian cell assays (**Figure 2.11**). In addition, cells were co-transfected with a fluorescent marker for the ER (CytERM), an ER-localization domain from rabbit cytochrome p450 (Costantini et al., 2012). As previously shown, TREX1 localizes primarily to the ER, which contributes to its recognition of micronuclei and interaction with OST (Kucej et al., 2017; Mohr et al., 2021a). The expression of these orthologs in U2OS cells revealed that zfPlex9.1 localized to the ER primarily, whereas zfPlex9.2 primarily to the cytoplasm (**Figure 2.11**). Orthologs of TREX1 from axolotl, axTREX1 and the axTREX2 isoform, localized to the ER and cytoplasm in a similar manner as TREX1 (**Figure 2.11**). Thus, these different DEDDh exonucleases from zebrafish and axolotl localize similarly to human TREX1.

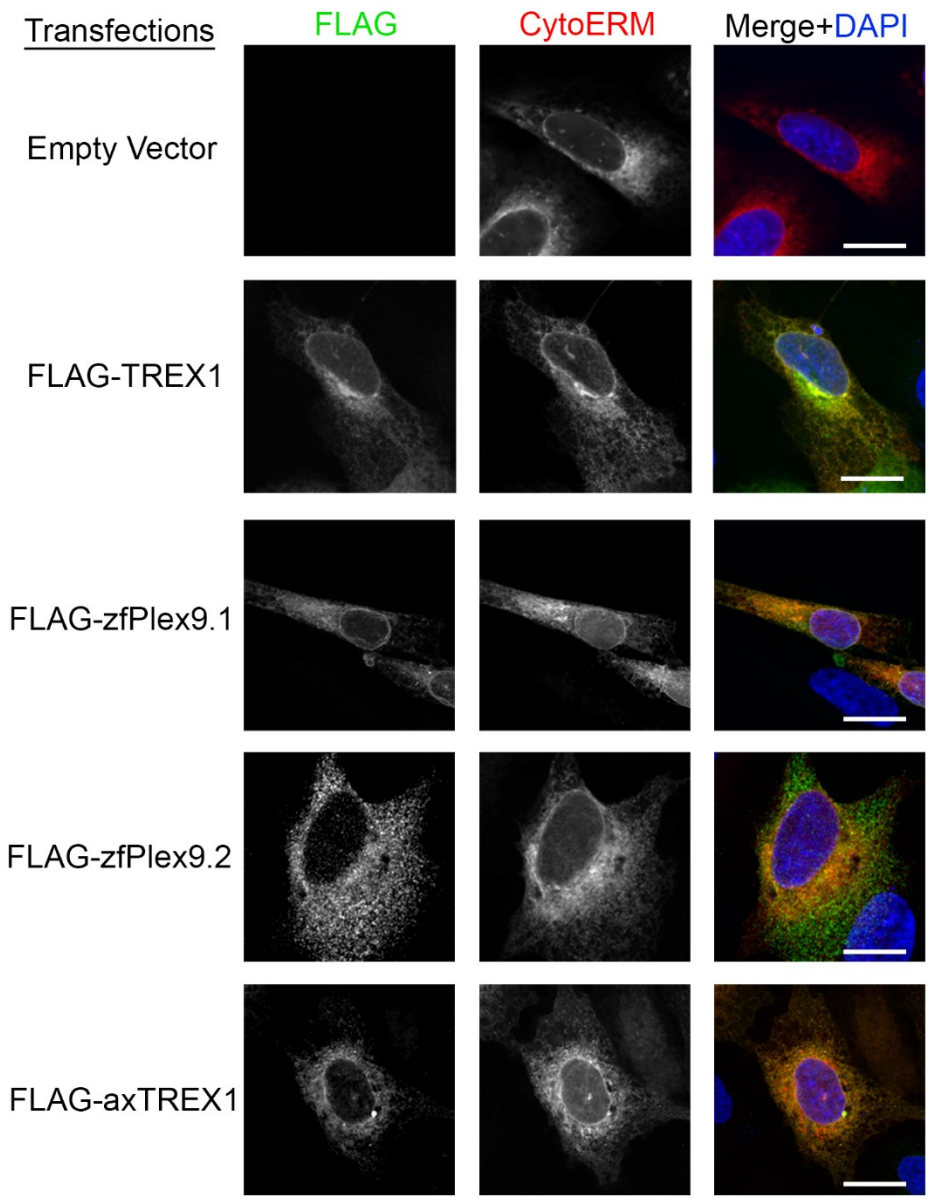

Figure 2.11. zfPlex9.1 and axTREX1 localize to the ER and cytoplasm. Ectopic expression of zebrafish Plex9.1/.2 (zfPlex9.1/.2) and axTREX1/2 reveals that these proteins localize to the ER and cytoplasm. Proteins were FLAG-tagged and expressed in U2OS cells to assess localization. A domain of Cytochrome p450 (CytERM) tagged to mScarlet (addgene #85066) was utilized as an ER marker. An empty vector (BlueScript) was used as a control. Scale bars represent 10 μM.

An important role for DNA exonuclease function for TREX1 is the clearance of micronuclei (Stetson et al., 2008). To determine whether zfPlex9.1 and axTREX1 proteins were degrading micronuclei akin to TREX1, U2OS cells were treated with reversine, which induces micronuclei by causing the mis-segregation of chromosomes (Li et al., 2017a). Just like TREX1, zfPlex9.1 and axTREX1 also accumulated at micronuclei (**Figure 2.12A**). In addition, cells overexpressing TREX1, zfPlex9.1 and axTREX1, had less micronuclei after 48 hours of 5 μM reversine treatment (**Figure 2.12B**). Cells expressing catalytically inactive mutants TREX1 (D18N) and zfPlex9.1 (D61N) showed no change relative to the empty vector control in terms of micronuclei counts (**Figure 2.12B**). Thus, the exonuclease activity of zfPlex9.1 allows it to function in micronuclei clearance akin to TREX1.

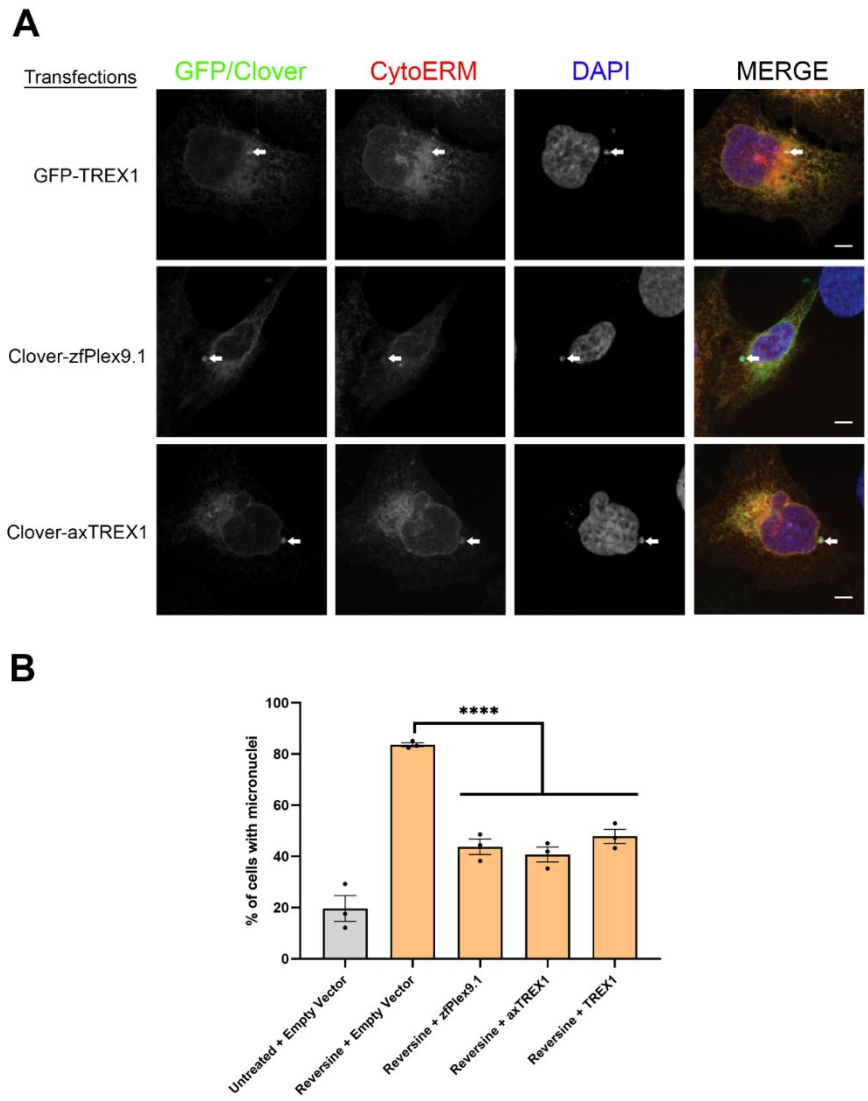

Figure 2.12. zfPlex9.1, axTREX1 and human TREX1 localize to micronuclei and promote micronuclei clearance. (**A**) Zebrafish zfPlex9.1 and axolotl axTREX1 accumulate at micronuclei like human TREX1. U2OS WT cells were transfected with GFP and Clover tagged human TREX1, zfPlex9.1 and axTREX1. domain of Cytochrome p450 (CytERM) tagged to mScarlet (Addgene #85066) was utilized as an ER marker to visualize ER-tubule invasion into the micronuclei. U2OS cells were treated 24 hours post-transfection with 5 µM reversine and were then fixed for immunostaining. Arrows indicate where micronuclei are present. Scale bars represent 5 µm for images (**B**) Cells were transfected and treated for 48 hours post-transfection with 5 µM reversine and a reduction in the number of cells with micronuclei was observed upon overexpression of zfPlex9.1, axTREX1, and human TREX1. For statistics, a one-way ANOVA was used, with Tukey's multiple comparison test (n=3). ****P<0.0001

2.3.5. sgPML, zfPlex9.1 and axTREX1 proteins restrict vertebrate LINE retroelements

TREX1 is the essential brake of the cGAS-STING pathway in mammals and has been shown to prevent genome instability by degrading cytosolic DNA and micronuclei, in addition to repressing endogenous L1 retrotransposons (Li et al., 2017a; Stetson et al., 2008; Thomas et al., 2017). The cGAS-STING pathway is highly conserved in metazoans (Wu et al., 2014). Despite lacking a *TREX1* gene homolog, teleost fishes have a functional cGAS-STING pathway (de Oliveira Mann et al., 2019a; Liu et al., 2020), raising the possibility that another DEDDh exonuclease may exist that functionally replaces TREX1. Given that teleost *plex9.1* and *plex9.2* genes encode active DEDDh exonucleases capable of degrading ssDNA and dsDNA that may be involved in micronuclei clearance, I hypothesized that these proteins may have functionally converged with TREX1 to compensate for its absence in the teleost lineage.

The role of TREX1 in L1 suppression is independent of catalytic exonuclease function (Li et al., 2017a). Similarly, the related SAMHD1 restriction factor, also suppresses L1 in a catalytically independent manner (Seamon et al., 2015). Both TREX1 and SAMHD1 appear to restrict L1 through their nucleic acid binding functions (Li et al., 2017a; Seamon et al., 2015). The Plex9 proteins bind nucleic acids and are active exonucleases. Given their mutual exclusivity with TREX1 in the fish genomes in which they are found, I next assessed if they functionally replace TREX1 in L1 suppression.

To accomplish this, a neomycin-resistance based clonogenic L1 assay was utilized, which was previously used to demonstrate the role of TREX1 in regulating L1 (Stetson et al., 2008), to determine if these zfPlex9 exonucleases, axTREX1/2/3, could also suppress L1 retrotransposition. I also tested the PML ortholog from the spotted gar

(sgPml), to assess if the function in LINE-1 suppression was conserved between the Plex9 enzymes and the related PML protein. As reported previously, TREX1 and exonuclease deficient TREX1 (D18N) both significantly suppressed human L1 activity significantly ($p<0.0001$, Figure 5A). Consistent with a convergent role in the suppression of L1 retrotransposition, zfPlex9.1 and zfPlex9.2, axTREX1 and axTREX2, all potently suppressed L1 activity (**Figure 2.13**). The axTREX3 isoform which encodes a truncated DEDDh domain was unable to suppress L1 retrotransposition, indicating that a full DEDDh domain was required for the repression. However, when the requirement for catalytic activity was examined, like TREX1 (D18N), exonuclease-deficient zfPlex9.1 (D61N) also suppressed L1 retrotransposition (**Figure 2.13**). Moreover, the related sgPml, was also capable of suppressing L1 retroelements similar to TREX1, axolotl TREX1 orthologs and zebrafish Plex9 proteins.

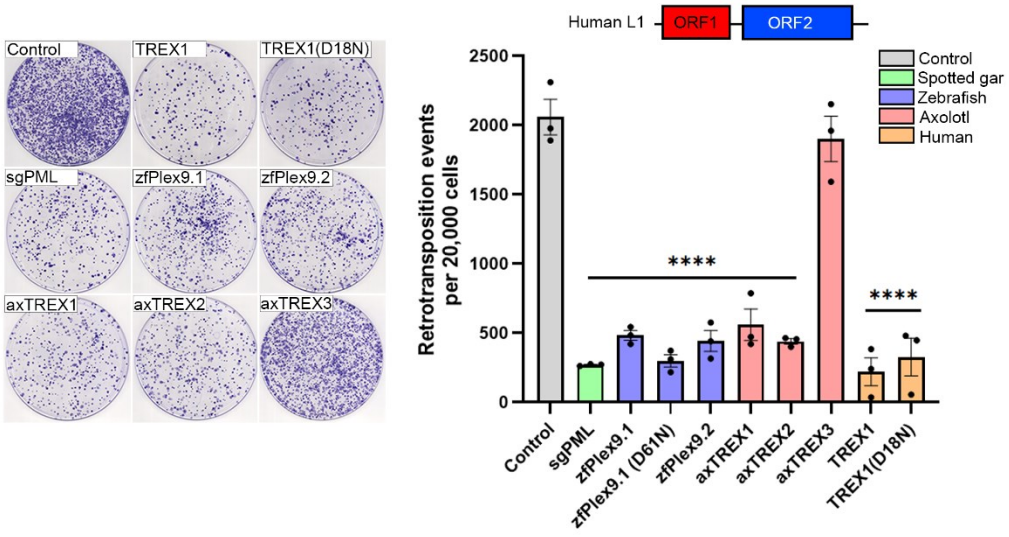

Figure 2.13. sgPml, Plex9 and axTREX1 proteins suppress human L1 activity in an exonuclease-independent manner. (right) Retrotransposition of human L1 was assessed with the co-expression of the FLAG-tagged versions of indicated proteins. Both catalytically dead versions of TREX1 and zfPlex9a (D18N and D61N, respectively) were also examined. Resultant plates from the assay (left) were stained with 0.5% crystal violet and quantified. Except for GFP-TREX1(D18N) which was previously obtained from Addgene, the other proteins were FLAG-tagged. Controls represent empty vector (FLAG-tag backbone) used in the co-transfection with the L1 plasmid. For statistics, a one-way ANOVA was used, with Tukey's multiple comparison test (n=3). ****P<0.0001

While L1 is active in mammals, related endogenous retroelements exist in other metazoan lineages. For example, the related LINE-2 (L2) elements are active in echinoderms and teleost fishes, but not mammals (Lindič et al., 2013; Lovšin et al., 2001; Shao et al., 2019). Several teleost LINE elements have been characterized (Shen et al., 2006). I wanted to determine if zfPlex9 and sgPml proteins could suppress these active L2 elements. Neomycin-based retrotransposon reporters encoding teleost L2s were used for this purpose (zfL2-1, zfL2-2 and UnaL2) (Lindic et al., 2013). Ray-finned zfPlex9.1, zfPlex9.2, and sgPml potently suppressed the retrotransposition of both zfL2-1 and zfL2-2 (**Figure 2.14A** and **Figure 2.14B**). Amphibian axTREX1 and axTREX2, also suppressed the teleost L2 elements like the Plex9 proteins (**Figure 2.14A** and **Figure 2.14B**). However, again, the truncated axTREX3 protein had no effect on L2 suppression (**Figure 2.14A** and **Figure 2.14B**). Human TREX1, although capable of suppressing zfL2-1 and zfL2-2, was not as efficient at suppressing these L2 elements compared to the teleost Plex9 proteins, suggesting a degree of species tropism between DEDDh exonucleases and their target retroelements. Therefore, it appears that Plex9 and TREX1 orthologs broadly inhibit LINE retroelements, including L2 elements found in other vertebrate species.

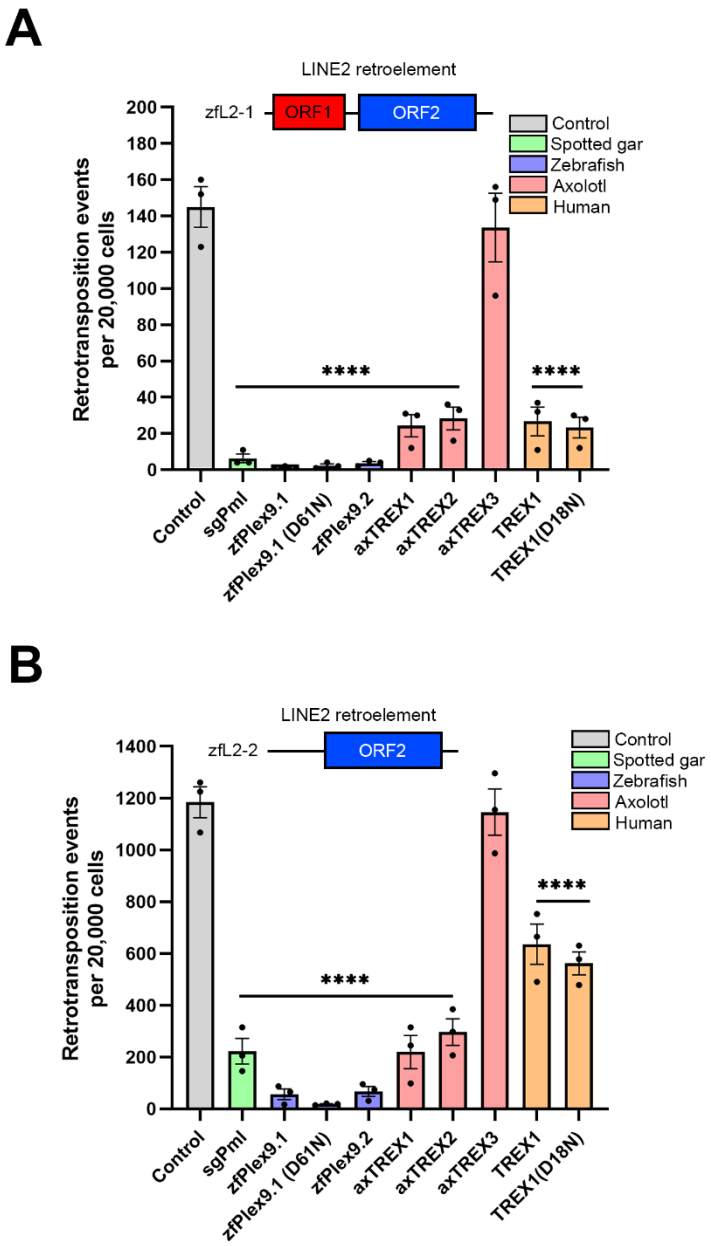

Figure 2.14. Plex9, TREX1 and sgPml also restrict zebrafish LINE-2 retrotransposition. Retrotransposition activity of zebrafish L2 elements were also assessed in (**A**) zfL2-1 and (**B**) zfL2-2 as described in Figure 2.13. Retrotransposition of the different zebrafish L2 reporter plasmids was assessed with the co-expression of the FLAG-tagged versions of indicated proteins. Except for GFP-TREX1(D18N) which was previously obtained from Addgene, the other proteins were FLAG-tagged. Controls represent empty vector (FLAG-tag backbone) used in the co-transfection with the L1 plasmid. For statistics, a one-way ANOVA was used, with Tukey's multiple comparison test (n=3). ****P<0.0001

2.3.6. zfPlex9.1 and axTREX1 complement human TREX1 KO cells and suppress cGAS-STING

I next sought to determine if the Plex9 proteins could functionally complement the increase in L1 activity previously demonstrated for TREX1 loss in human cells (Li et al., 2017a; Stetson et al., 2008). Thus, I generated a TREX1 knockout (KO) U2OS line for these experiments (**Figure 2.4**). As expected, TREX1 KO led to a significant increase in human L1 retrotransposition, which was reversed by the overexpression of FLAG-TREX1 or GFP-TREX1(D18N) (**Figure 2.15A**). Consistent with being true TREX1 orthologs in axolotl, the axTREX1 and axTREX2 proteins encoding full-length DEDDh domains also successfully inhibited L1 retrotransposition when over expressed in TREX1 KO U2OS cells (**Figure 2.15A**). The ectopic expression of zfPlex9.1 and zfPlex9.2 also significantly reduced human L1 retrotransposition in the TREX1 KO cell line (**Figure 2.15A**). Thus, zfPlex9.1 and zfPlex9.2 have a similar convergent function to TREX1 with respect to suppression of LINE retroelements.

TREX1 inhibits the production of 2',3'-cGAMP by CGAS after L1 activity occurs (Gao et al., 2015). There was a significant increase in 2',3'-cGAMP caused by TREX1 loss with the transfection of the L1 plasmid (**Figure 2.15B**). The observed increase in 2',3'-cGAMP in TREX1 KO cells could be reversed by the addback of zfPlex9.1 and axTREX1 (**Figure 2.15B**). Together, these results are consistent with an early role for TREX1 in the suppression of L1 activity in amniotes, and that in species that lack TREX1 such as zebrafish and other ray-finned fish, Plex9 proteins converged in function to similarly suppress L1 retroelements and downstream cGAS-STING signalling.

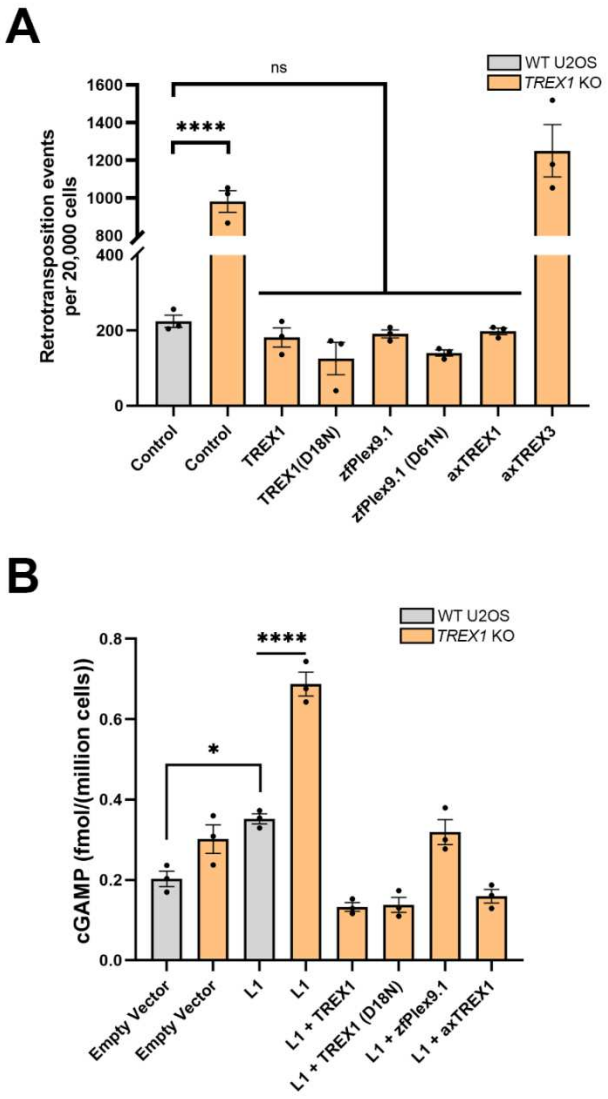

Figure 2.15. Plex9 proteins can compensate for *TREX1* loss to suppress L1 and cGAS activity. (**A**) Retrotransposition activity was elevated in *TREX1* knockout cells and addback of the zfPlex9.1 and zfPlex9.2, as well as axTREX1 and axTREX2, reversed this phenotype (n=3). (**B**) 2',3'-cGAMP levels in U2OS WT and *TREX1* knockout cells after the transfection of an empty vector and the human L1 vector (n=3). 2',3'-cGAMP concentrations were normalized to cell number for each experiment. Except for GFP-TREX1(D18N) which was previously obtained from Addgene, the other proteins were FLAG-tagged. Empty vector represents the empty FLAG-tag vector used in the co-transfection with the L1 plasmid. For statistics, a one-way ANOVA was used, with Tukey's multiple comparison test. ****P<0.0001, *P<0.05

2.4 Discussion

The widely distributed DEDDh exonucleases play important roles in DNA replication, DNA repair, RNA maturation, and RNA turnover (Cheng et al., 2018; Hsiao et al., 2012; Yang, 2011; Zuo & Deutscher, 2001). Here, I describe and characterize the teleost Plex9 proteins as a novel subfamily of DEDDh exonucleases that have converged on a similar function in L1 suppression and micronuclei clearance to TREX1 (**Figure 2.12** and **Figure 2.15)**. While amniote PML orthologs do not encode a DEDDh exonuclease, that fish Pml orthologs are predicted to be active exonucleases. Importantly, the Plex9 proteins are not evolutionarily related to the emergence of TREX1 orthologs in amniotes, rather they are most likely derived from a separate progenitor PML-like exonuclease. The Plex9 proteins, however, fill an important gap in what is known regarding cGAS-STING evolution as they seem to play the role of TREX1 as suppressors of cGAS-STING in Teleost fish cells. In addition, they can perform other known mammalian TREX1 functions such as micronuclei clearance and L1 suppression (**Figure 2.12** and **Figure 2.14)**. Considering that the Plex9 proteins have a different origin from TREX1, they appear to be a convergently evolved solution to regulating the conserved cGAS-STING pathway in fish. The evolution of suppression machinery in host cell immune signalling pathways is critical for the prevention of sustained immune signalling and damaged inflammation.

In addition to characterizing the Plex9 enzymes, orthologs of PML in fish were identified that are predicted to be DEDDh exonucleases. Previously, it was suggested that human PML-I encodes an exonuclease-fold in its C-terminus (exon 9) but there has been no demonstration of enzymatic activity and catalytic residues appear to be mutated

(Condemine, Takahashi, Le Bras, & de Thé, 2007). However, sgPML functions in the suppression of LINE-1 retroelements akin to Plex9 enzymes that were characterized (**Figure 2.14**). It appears that sgPML and Plex9 enzymes share functions owing to their similar DEDDh domains. Thus, our work describes two new related DEDDh exonucleases, PML and Plex9 enzymes, in fish, that warrant further investigation.

In mammals, L2 retroelements are no longer active but they are still present and active in the genomes of other vertebrate species, including the zebrafish. Two known zebrafish L2 retroelements, zfL2-1 and zfL2-2 have been well-characterized and differ in terms of their mechanisms behind retrotransposition. However, a unique difference between zfL2-1 and zfL2-2 is that the shorter zfL2-2 sequence only encodes ORF2p and not ORF1p (Hayashi et al., 2014; Sugano et al., 2006). Zebrafish Plex9.1 and human TREX1 were both capable of suppressing these zfL2-2 (**Figure 2.14**). Such cross-species restriction of retroelement has been shown before using the reptilian APOBEC protein (Lindič et al., 2013). Currently, the mechanism behind how TREX1 restricts LINE-1 retrotransposition is reliant on its targeting of ORF1p for degradation through the ubiquitin-proteasome system, which occurs in an exonuclease-independent manner (Li et al., 2017a). However, considering that zfL2-2 only encodes ORF2p for retrotransposition, it suggests that TREX1 and the Plex9.1 DEDDh exonucleases have a secondary mechanism that allows them to suppress retrotransposition in a ORF1p-independent manner. It is possible that these DEDDh exonucleases also interact with ORF2p from these LINE retroelements or target the L1 mRNA for inhibition. Supporting the latter possibility is the notion that the TREX1-ORF1p interaction was contingent on binding to RNA (possibly L1 mRNA) (Li et al., 2017a). The broad and constantly evolving nature

of the self-propagating retroelements supports the notion of these DEDDh exonucleases having multiple mechanisms for suppressing retrotransposition.

The clearance of ruptured micronuclei by TREX1 relies on its localization to the ER, where ER tubules invade the ruptured micronuclei to promote TREX1 digestion and prevent cGAS activation (Mohr et al., 2021a). The hydrophobic C-terminus domain of TREX1 is 72 amino acids and required for its localization to the ER (Orebaugh et al., 2013). It is commonly mutated in AGS, where mislocalization of TREX1 prevents its regulation of cGAS (Mohr et al., 2021b; Orebaugh et al., 2013). However, the ER-resident zfPlex9.1 lacks a similar C-terminal domain for localization to the ER (**Figure 2.11**). It will be intriguing to uncover the unique trafficking of zfPlex9.1 to the ER, which likely contributes to how it clears micronuclei akin to TREX1.

While this work establishes Plex9 as a regulator of cGAS-STING and LINE retrotransposition, it did not explore the role of the protein in DNA repair. TREX1 has recently been shown to be involved in both nucleotide excision repair and base excision repair. TREX1 can clear intermediates formed during base excision repair or the small, excised damage-containing nucleotides in nucleotide excision repair (Kim et al., 2022; Wei et al., 2022; Yang et al., 2022). Nucleotide excision repair and base excision repair are highly conserved pathways in vertebrate species (Krokan & Bjørås, 2013; Schärer, 2013). It is possible that the Plex9 proteins also contribute to these two repair pathways in zebrafish considering their ability to degrade ssDNA and dsDNA (Kim et al., 2022; Wei et al., 2022; Yang et al., 2022). Future examination of Plex9 enzymes may reveal that they contribute to DNA repair processes in fish, as another way to contribute to genome stability.

Chapter 3 – PML emerged as a cytoplasmic regulator of LINE-1

This chapter contains material (sections 3.2, 3.3, 3.4, Figures 3.4-3.12) originally published in one manuscript:

"Mathavarajah, S., Vergunst, K.L., Habib, E.B., Williams, S.K., He, R., Maliougina, M., Park, M., Salsman, J., Roy, S., Braasch, I., Roger, A.J., and Dellaire, G. 2023. PML and PML-like exonucleases restrict retrotransposons in jawed vertebrates. *Nucleic Acids Research*, *51*(7), pp.3185-3204."

3.1 Introduction

3.1.1 SUMOylation pathway and PML

PML NB biology is intertwined with SUMOylation and is often considered a nuclear hub for SUMO modification and interactions. SUMOylation is a post-translation modification where there is covalent attachment of SUMO, of which there are 5 paralogs in primates (SUMO1-5) (Celen & Sahin, 2020; Flotho & Melchior, 2013; Y. C. Liang et al., 2016; Varejao et al., 2020). SUMO proteins are part of the Ubiquitin-like protein family and have similar structures but share little sequence identity (~20%) to ubiquitin (Celen & Sahin, 2020). SUMO-2/3 are 95% identical and often described together since they cannot be identified separately (Varejao et al., 2020). In contrast to SUMO1 and SUMO2/3 that are ubiquitously expressed in cells, the expression of SUMO4 and SUMO5 is restricted to specific tissues (SUMO4, liver; SUMO5, lung and spleen) (Bohren et al., 2004; Y. C. Liang et al., 2016; Varejao et al., 2020). SUMO conjugates are added to target proteins at lysine residues, typically at the following consensus motif

characterized by a hydrophobic residue, target lysine and an acidic residue (ψKxE/D) (Zhao et al., 2014). However, numerous non-canonical motifs also exist for SUMO conjugation. The SUMOylation pathway resembles the NEDDylation and Ubiquitination cycles, where there are E1 (UBA2), E2 (UBC9) and E3 enzymes (e.g., PIAS1) that process the SUMO peptide and transfer it for conjugation to a desired protein (Kim et al., 2002). Similarly, there are deSUMOylation pathways in place to remove the SUMO moiety from a target protein.

The differences between SUMO1 and SUMO2/3 allow for diversity between SUMOylated targets that extends past merely different SUMO-conjugations occurring via paralogs. SUMO2/3 have the capacity for polymeric branching as they have internal lysine residues (K7, K21 and K33) that can serve as attachment sites (akin to ubiquitin) (Hendriks et al., 2014) (Tatham et al., 2001). Whereas SUMO1 lacks internal attachment sites and typically serves as the termination residue or for mono-SUMOylation of targets (Sahin et al., 2022). However, in some stress responses, SUMO1 branching has been observed but the mechanisms and functions of poly-SUMO1 branching is unknown (Hendriks et al., 2018; Matic et al., 2010). Thus, these paralogs allow for complex SUMO branching patterns that can entirely shift target protein conformations and their accessibility to substrates and/or interactors.

PML NBs are formed through SUMOylation, with monomers being SUMO-modified and interacting with SIMs of other monomers (as reviewed in Section 1.2). The full-length PML-I and PML-IV monomer has the potential for SUMOylation at 8 sites (K65, K160, K226, K380, K400, K490, K497, K616) and a SIM (Nisole et al., 2013). The SIM is only present on isoforms PML-I to PML-IV, as the SIM hydrophobic core

"VVVI" is encoded by exon 7a (residues 556-559) (Nisole et al., 2013). One SUMOylation site, K616 is only present on PML-I and PML-IV (Schilling et al., 2017). Three major SUMOylation sites (K65, K160, and K490) have canonical SUMOylation motifs (ψKxE/D; or the inverted E/DKxψ) and are located within the RING-finger, B1 box, and Nuclear Localization Sequence (NLS) (Da Silva-Ferrada et al., 2012; Kamitani et al., 1998). SUMOylation of PML can either regulate its assembly or degradation based on the residue modified (**Figure 3.1**).

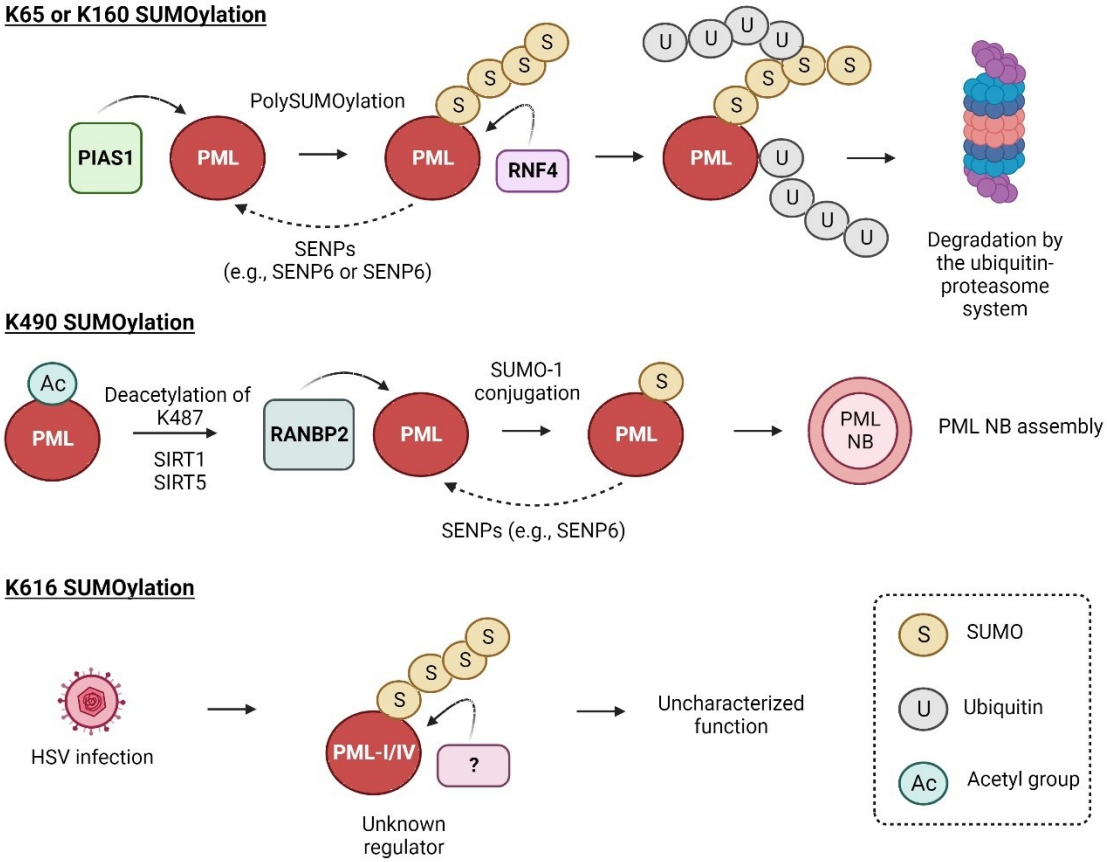

Figure 3.1. Regulation of PML by SUMOylation at different lysine residues. PML can be regulated by SUMOylation at different residues. K65 and K160 are normally polySUMOylated and this triggers ubiquitination by RNF4 to consequently send PML for degradation by the ubiquitin-proteasome system. In contrast, the mono-SUMOylation of K490 (SUMO-1 conjugation) promotes the assembly of NBs. Finally, there is another validated site, K616, that is polySUMOylated but its functions and regulation is unknown.

SUMOylation of K490 is regulated by RanBP2 and promotes PML NB assembly and consequent maintenance (Cheng & Kao, 2012; Zhong et al., 2000). The SUMOylation at site K490 has an additional layer of regulation as it is mutually exclusive with acetylation at K487 and requires the actions of deacetylases SIRT1 and SIRT5 prior to SUMOylation (Guan et al., 2014). In contrast, SUMOylation at K65 and K160 by PIAS1 promotes PML degradation (El McHichi et al., 2010). The degradation of polySUMO-modified PML, which can occur after ATO treatment or in response to TGF-β (discussed in Section 1.5.1), occurs via poly-SUMO-specific E3 ubiquitin ligase RNF4 that ubiquitinates PML for degradation via the UPS (El-Asmi et al., 2019; Valérie Lallemand-Breitenbach et al., 2008; Sun et al., 2007; Michael H Tatham et al., 2008). Intriguingly, ATO treatment causes SUMO switching where K65, which is usually conjugated to SUMO2 (capable of branching), is first deconjugated and then conjugated to SUMO1, and K160 preferentially becomes polySUMOylated for RNF4-binding and consequent degradation (Fasci et al., 2015). Another regulatory layer to the degradation of PML is that CK2 mediates direct phosphorylation of PML at Ser517, which further promotes the degradation of SUMO-modified PML (Scaglioni et al., 2006). Depending on the PML isoform and its length, different SUMOylation sites are present for conjugation, and then can affect how the different isoforms are regulated or contribute to PML NB assembly or degradation. In addition to these SUMOylation sites, there are 5 other sites (K226, K380, K400, K497, K616) that were identified by SUMO-targeted proteomics, but they are poorly understood in terms of their regulation and function (Galisson et al., 2011; Vertegaal et al., 2006). However, K380, K400 and K497 (as well as K160 and K490) can be conjugated to the recently identified SUMO5 isoform which

promotes NB assembly (Y.-C. Liang et al., 2016). However, PML K616 was validated as a unique modification that occurs in PML-I and PML-IV isoforms during herpes simplex virus type 1 infection but how it contributes to isoform-specific function is unknown (Cuchet-Lourenço et al., 2011).

The SUMO-PML mesh formed from SUMOylation begins to act as a hub for other proteins that are (1) already modified proteins that interact via their SUMO conjugate with the PML-SIM and (2) unmodified proteins that interact via their own SIM. Once recruited to PML NBs, other regulatory factors may modify target proteins for post-translational modifications or to facilitate interactions. The SUMOylated PML-SIM interaction is best illustrated with Death Domain Associated protein (DAXX), that has been well-studied as a PML NB localizing factor that has a SIM. DAXX first is recruited to PML bodies through its SIM, which is regulated by phosphorylation by CK2 (residues Ser737 and Ser739) (Chang et al., 2011). The negatively charged SIM results in a higher affinity for DAXX towards SUMO1 versus SUMO2/3, resulting in an interaction between SUMO1 conjugated PML and DAXX (Chang et al., 2011). Then, at bodies, DAXX is also conjugated to SUMO1, and the modified form is then capable of interacting with new proteins (such as the SUMOylated glucocorticoid receptor) (Drane et al., 2010; Ishov et al., 1999). In addition, DAXX can then contribute to H3.3 deposition and ultimately chromatin assembly (which occurs with ATRX, another PML NB component) at the correct stage of the cell cycle and at heterochromatin (dictated by PML NBs) (Drane et al., 2010; Salomoni, 2013; Shastrula et al., 2019). The dynamics between DAXX and PML NB illustrate how different nuclear proteins can be regulated by PML NBs via the SUMOylation pathway. Thus, PML NBs through their orchestration

of nuclear SUMOylation events dictate protein–protein interactions, change protein intracellular localization, or directly modify activities resulting in changes in transcription, replication, chromatin assembly, and DNA repair.

3.1.2 Genome stability, the DNA damage response, and the role of PML NBs

3.1.2.1 Mechanisms maintaining genome stability

Genome stability refers to the error-free preservation of genetic material by organisms by both germline and somatic cells (Dion-Cote & Barbash, 2017). Organisms constantly experience stress from the external environment in the form of exogenous genotoxic agents such as ultraviolet light, oxidative stress, radiation, and chemical mutagens. Then, internal kinks in their own genetics can manifest itself in disease and aging through various molecular events such as mitochondria dysfunction or dysregulated retroelement expression. DNA damage events are not rare and in fact, each of the ~10^{13} cells in a human body receives tens of thousands of DNA lesions per day (Jackson & Bartek, 2009). After DNA damage, there are several important decisions that the cell can make which includes halting cell cycle progression, attempting DNA repair, and initiating senescence or cell death (apoptosis, pyroptosis, and necroptosis) pathways (Rodier et al., 2009; Roos & Kaina, 2006; von Zglinicki et al., 2005; X. P. Zhang et al., 2010; Zhou & Elledge, 2000).

If DNA repair is chosen, a network of proteins assembles to maintain homeostasis in response to DNA damage, and this is collectively referred to as the DNA damage response (DDR) pathway. The main steps of the DDR involve (1) the initiation signal and

the sensing of damage, (2) recruiting repair factors for the specific type of damage and (3) carrying out repair (Chatterjee & Walker, 2017; Hakem, 2008; Jackson & Bartek, 2009; Ranjha et al., 2018). Different errors are repaired using the major repair pathways such as non-homologous end joining (NHEJ), mismatch repair (MMR), homologous recombination (HR), base-excision repair (BER), and nucleotide excision repair (NER) (Hakem, 2008). These pathways are extensive and require a vast number of known and unknown proteins, with the DDR involving at least 450 proteins, to carefully orchestrate the repair of DNA damage and maintain a stable genome (Jackson & Bartek, 2009; Pearl et al., 2015). Impairment in the DDR causes numerous forms of cancer, autoimmune disease, and neurodegenerative disease (Jackson & Bartek, 2009).

3.1.2.2 DNA damage response (DDR)

DNA damage is sensed with specificity towards the type of damage that occurred. One catastrophic result of damage is a double-stranded break (DSB), and this is sensed by the MRN complex (MRE11-RAD50-NBS1) (Bian et al., 2019; Iijima et al., 2008; Lavin et al., 2015; Syed & Tainer, 2018). The MRN complex also detects collapsed replication forks and the dysfunction of telomeres (Bian et al., 2019; Iijima et al., 2008; Lavin et al., 2015; Syed & Tainer, 2018). The complex recruits ATM (ataxia-telangiectasia mutated), a serine/threonine kinase, to phosphorylate γH2A.X (a variant histone) at Ser-139 (Collins et al., 2020). The phosphorylation of γH2A.X serves as a landmark for repair factors and indicates where the DSB occurred (Collins et al., 2020; Palla et al., 2017; Podhorecka et al., 2010; Sharma et al., 2012). Subsequently, a “repair

foci" will form, where numerous proteins are recruited to facilitate DNA repair at the site of damage.

Similar sensors and recruitment strategies exist for other forms of DNA damage, such as ATRIP (Single-stranded DNA bound to RPA at damage sites; recruitment of ATR), Ku70/Ku80 (DSB), SOSS1/2 (Single-stranded DNA at breaks), DDB1/2 (bulky lesion) and DNA glycosylase (non-bulky lesion) (Jin & Weaver, 1997; Mullins et al., 2015; Nam & Cortez, 2009; Scrima et al., 2008; Zou & Elledge, 2003). While these descriptions delineate the sensors, there is overlap in terms of their sensing and functions within different repair pathways. The transduction of the DDR pathway is driven by phosphorylation cascades, where the three central serine/threonine kinases ATM, ATR and DNA-PKcs (belonging to phosphatidylinositol-3-kinase-like kinase family) coordinate these events (Blackford & Jackson, 2017; Burger et al., 2019; Lempiainen & Halazonetis, 2009; Lovejoy & Cortez, 2009; Marechal & Zou, 2013; Menolfi & Zha, 2020).

ATM and ATR are highly conserved in eukaryotes and have distinct roles: (1) ATM primarily senses DSBs and (2) ATR senses DNA cross-links, base modifications, and stalled replication forks (Marechal & Zou, 2013). However, it is important to note that there is overlap between the kinases in terms of their associated pathways, such as both kinases regulating cell cycle checkpoint associated proteins (Marechal & Zou, 2013). ATM and ATR are master regulators that phosphorylate hundreds of target repair-associated proteins (Beli et al., 2012; Bensimon et al., 2010; Matsuoka et al., 2007; Smolka et al., 2007; Stokes et al., 2007). Whereas, DNA-PKcs specifically phosphorylate machinery associated with NHEJ (Yue et al., 2020). All these transducers are activated in

response to both DNA breaks and various genotoxic stresses to maintain genome integrity by initiating DNA repair. Then, in a second wave of phosphorylation, ATM and ATR target cell fate regulators such as p53, Chk1, Chk2 and MK2 protein kinases to enact apoptosis, cell cycle arrest, and the suppression of DNA replication (Marechal & Zou, 2013; Ronco et al., 2017). Therefore, the functions of ATM, ATR and DNA-PKcs connect the DNA repair pathways to numerous cell fate decisions.

3.1.2.3 PML NBs coordinate the DNA damage response

PML NBs contribute to the DDR as both a sensing factor and by helping orchestrate the repair response. Dellaire et al., showed that PML NBs are more than just passive accumulations of SUMO-modified nuclear proteins (Dellaire, Ching, et al., 2006). During both the early phases of S-phase (where chromatin topology changes) and when DNA breaks are introduced, PML NBs lose their radial symmetry and integrity and become fragmented microbodies via a fission mechanism (**Figure 3.2**) (Dellaire, Ching, et al., 2006). Electron microscopy studies have shown that PML NBs make extensive contact with chromatin and respond to changes in chromatin tensegrity (a factor of compression and tension) after DNA damage result in changes to NB integrity (Aranda-Anzaldo, 2016; Eskiw et al., 2004). Intriguingly, the formation of microbodies does not occur when repair factors are inhibited, such as NBS1 or the checkpoint kinases ATM, CHK2, and ATR (Dellaire, Ching, et al., 2006).

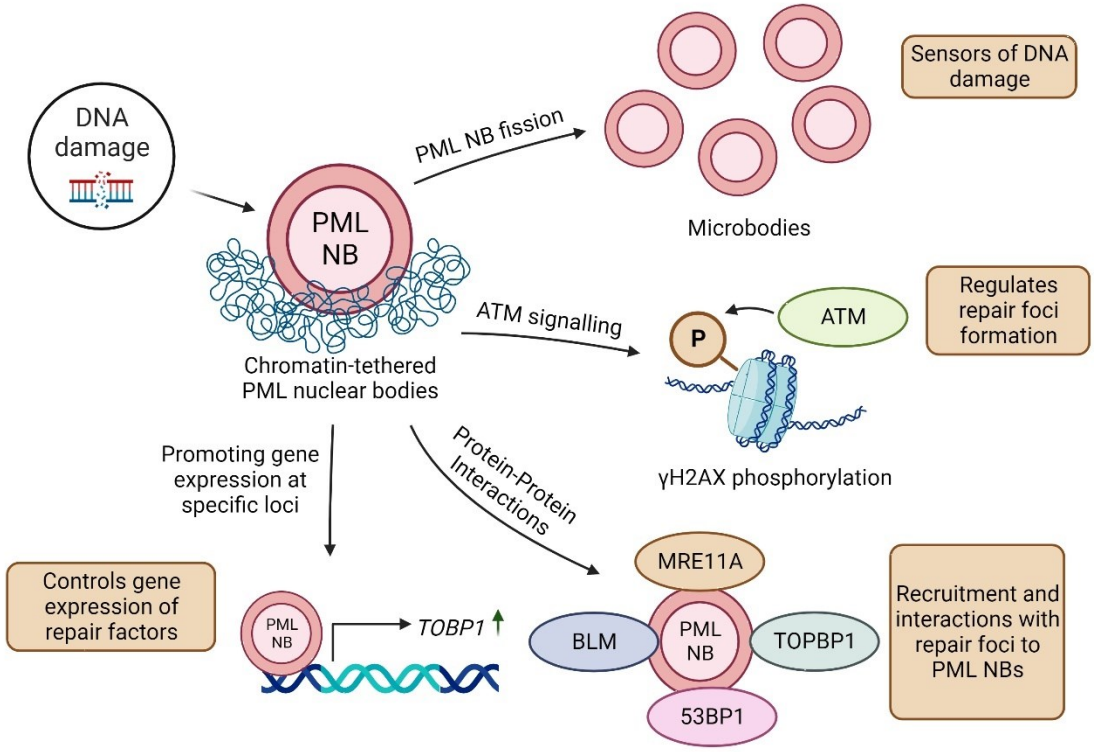

Figure 3.2. PML NBs maintain genome stability by contributing to the DNA damage response. PML NBs respond to DNA damage by forming microbodies in response and increasing in number within the nucleus. These damage-responsive foci promote repair foci formation, the recruitment of repair factors and control the gene expression of repair factors such as *TOBP1*. These different roles for PML NBs contribute to how they regulate the DNA damage response.

In most reports and with work done in the Dellaire lab, PML NBs are typically juxtaposed to repair foci versus directly co-localizing – except for with persistent damage foci formed from ionizing radiation (Vancurova et al., 2019). However, these repair-foci adjacent PML NBs are important for efficient DNA repair. The disruption of PML NBs delays the DDR, with the timing of γ-H2AX phosphorylation and activation of ATM being slowed (di Masi et al., 2016). PML NB proximity to DNA breaks directly affects HR efficiency and the loss of NBs results in impaired HR (Attwood et al., 2020). These PML microbodies formed from DNA damage colocalize with different factors associated with the DDR such as the DSB sensor MRE11A (part of the MRN complex), the SUMO-modified 53BP1, a topoisomerase IIβ-binding protein TOPBP1 and BLM (Bøe et al., 2006; Galanty et al., 2009; Patel et al., 2017; Vancurova et al., 2019; Xu et al., 2003; Zhong et al., 1999). In addition, there are feedback loops existing between PML NBs and localizing repair factors that regulate their gene expression, such as TOPBP1, as its expression is PML-dependent (Xu et al., 2003). Typically, PML NBs are proteinaceous and lack nucleic acids, but the ones associated with repair are active with DNA metabolism occurring as they accumulate ssDNA in response to DNA damage (Bøe et al., 2006; Boisvert et al., 2000). When PML NBs are lost, cells experiencing DNA damage are halted from S-phase or sensitized for apoptosis (Bøe et al., 2006).

PML NBs therefore contribute to the expression, subcellular localization, and function of these different repair factors. It is likely that PML contributes to the efficiency and regulation of DNA repair events by modulating the recruitment and removal of various proteins at foci by facilitating different post-translation modifications. Thus, PML NBs are important contributing factors to how cells respond to DNA damage

as an accessory subnuclear compartment, which creates a local spatiotemporal niche for the required factors to contribute to repair.

3.1.3 Cytoplasmic PML

"Nuclear" PML bodies have been well-studied and attributed numerous cellular functions, but the PML protein has also been reported in the cytoplasm. The concept of PML in the cytoplasm is debated as it has been difficult to reproduce results and characterize the mechanisms behind its shuttling from the nucleus. However, there is a nuclear export sequence (NES) encoded uniquely in the PML-I isoform sequence (amino acids 704–713 encoded by exon 9) (Nisole et al., 2013). The identified NES is a Chromosome region maintenance 1 (CRM1) recognition site, a protein that functions as the most general and prevalently used receptor for nucleocytoplasmic shuttling (Fung & Chook, 2014). PML was shown to be a CRM1-interacting protein from mass spectrometry studies but additional evidence validating the interaction or the requirements for PML shuttling has not been demonstrated (Buczek et al., 2016b).

The strongest evidence for the presence of cytoplasmic PML is during viral infection, where HIV infection results in PML redistribution to the cytoplasm (**Figure 3.3**) (Turelli et al., 2001). The shuttling event observed during HIV infection could be blocked by treatment with a CRM1 inhibitor, Leptomycin B (Turelli et al., 2001). The shuttling response directly relates to the cell's capacity to fight the virus as the PML knockdown has been shown to increase HIV infectivity in cells (Kahle et al., 2015).

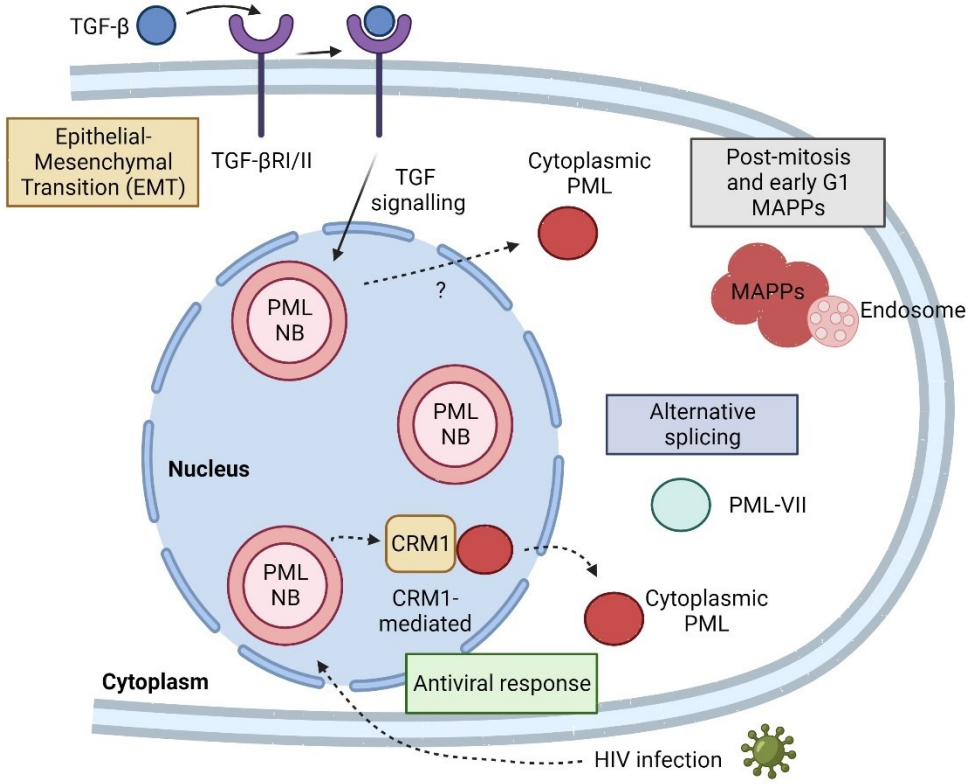

Figure 3.3. Evidence behind cytoplasmic PML and the associated pathways. The presence of PML in the cytoplasm is a controversial topic with difficulty in reproducing results and the mechanism behind shuttling being unknown. However, there are certain stimuli that trigger PML shuttling to the cytoplasm such as EMT and the antiviral response. There are also PML structures known as MAPPs that persist in the cytoplasm in early G1 after mitosis that can be considered "cytoplasmic" PML. Finally, there is a PML isoform, PML-VII that also is found in the cytoplasm and a product of alternative splicing as it does not encode the required NLS for nuclear localization.

Intriguingly, a PML isoform has been suggested as a cytoplasmic localizing protein, PML-VII, that lacks exons 5 & 6. PML-VII is only 435 amino acids in length and lacks an NLS (encoded on exon 6). The isoform has shown to repress HSV-1 infection by sequestering the viral protein ICP0 in the cytoplasm (McNally et al., 2008). Intriguingly, ICP0 targets PML-I for degradation, another isoform with putative cytoplasmic localization with unknown function (Cuchet-Lourenço et al., 2012). It is possible that the evolution of some PML isoforms by host cells was a consequence of different isoforms being able to curb virus infection. However, it is currently unknown if PML-VII contributes to PML-I stability during HSV-1 infection by preventing ICP0 degradation.

There have also been reports on cytoplasmic PML contributing to Transforming growth factor Beta (TGF-β) signalling. TGF-β signalling regulates multiple distinct cellular processes such as apoptosis, cell proliferation, cell plasticity, and migration (Massague, 2012). The effects of TGF-β signalling differ depending on the cellular context. The binding of TGF-β to target receptors leads to the activation of Suppressor of Mothers against Decapentaplegic transcription factors (SMADs) that induce the gene expression of target genes (Derynck & Zhang, 2003). Importantly, the signalling pathway is essential for the transdifferentiation of epithelial cells to mesenchymal cells (EMT, epithelial to mesenchymal transition) that promote tumour cell metastasis in cancer (Kubiczkova et al., 2012; Valcourt et al., 2005). Groups have reported that TGF-β treatment also induces the expression of cytoplasmic PML, which is required for SMAD activation and translocation to the nucleus (Lin et al., 2004). Interestingly, the PML protein was shown to interact with SMAD2/3 and SARA (Smad anchor for receptor

activation) (Lin et al., 2004). However, the pool of cytoplasmic PML involved in this TGF-β response localize to the early endosome, which has also been observed in untreated early G1 phase cells prior to the reformation of the nuclear envelope, the MAPPs (Dellaire, Eskiw, et al., 2006; Palibrk, Lång, et al., 2014). It is likely that the cytoplasmic PML protein contributes to SMAD regulation are not shuttled protein but rather MAPPs (discussed in Section 1.4.3) that occur during mitosis and persist to the early G1 phase. However, further examination is required to determine the origins of cytoplasmic PML regulating SMADs.

In addition, follow-up work has shown that in prostate cancer cells, PML can be identified in the cytoplasm, and this contributes to EMT (Buczek et al., 2016b). However, the Dellaire lab has been unable to replicate these results in the same prostate cancer lines using multiple validated antibodies and fluorescently tagged PML protein (unpublished). Groups have also had success studying cytoplasmic PML as a regulator of cell death, where it contributes to death-induced calcium flux as an ER-localizing protein (Bellodi et al., 2006; Giorgi et al., 2010; Wang, Ruggero, et al., 1998). However, this work was facilitated by fusion PML protein designed to localize to the ER (i.e., with an ER-localizing sequence that is not present in the PML sequence). Without endogenous PML studies in this context, it is hard to weigh the contribution of cytoplasmic ER-localizing PML to cell death versus the overarching function of PML NBs (via p53 and other target proteins). Therefore, despite all the work on PML and its function in the cytoplasm, aside from a clear role established during viral infection, its (i) nucleocytoplasmic shuttling, (ii) function in the cytoplasm and (iii) contribution to pathway regulation all remain an enigma.

3.2 Materials and Methods

3.2.1 Plasmid construction

RNA isolated from the tissue of each species was used for cloning the spotted gar *pml*. Two gar individuals were raised as described in Darnet et al. (2019) to a total length of ~30cm, euthanized with a lethal dose of MS-222 (Sigma); then tissues (muscle, gills, intestine, liver, brain, spleen, heart, gas bladder) were dissected, and stored in RNAlater (Ambion) (Darnet et al., 2019). A caudal fin clip was stored in 95% ethanol. From the available tissue, expression of *sgpml* was highest in the spleen and thus this was utilized for downstream cloning. Synthetic genes coding for spotted gar PML-CDE (Ala497–Glu766; Ensembl: ENSLOCG00000014935; NCBI: XP_015199146.1) was purchased (BioBasic Inc) and ligated into a modified pET21 expression vector that contained upstream sequences coding for a hexahistidine tag (H), maltose binding protein (M), and tobacco etch virus protease recognition sequence (T) to create pHMT-sgPml-CDE, respectively.The fidelity of all plasmids was verified by sanger sequencing (Eurofins Genomics).

Quail RNA for quail PML cDNA was isolated from a pellet of QM5 cells (quail muscle 5 cells). The RNeasy (Qiagen) kit was used for all extractions, according to the manufacturer's instructions. The cDNAs were prepared using the SuperScript™ IV One-Step RT-PCR System (Invitrogen) and sequenced prior to subcloning into indicated vectors. These coding gene sequences were all cloned into CMV-based FLAG-tagging and Clover-tagging vectors (CMV-FLAG-J1 and CMV-Clover-J1; derived from commercially available vectors pEGFP-C1 and pEGFP-N1; Clontech).

For *Polyodon spathula* (NCBI: XP_041075354) and *Terrapene carolina triunguis* (Ensembl ID: ENSTMTG00000003177, NCBI: XP_024070906.1) *PML* coding gene sequence DNA was synthesized through gBlocks™ Gene Fragments in two parts (Integrated DNA Technologies). Overlap extension PCR was utilized to generate the full sequence, which was then cloned into the CMV driven FLAG-tag vectors used for the other coding sequences.

Human PML-I K616A was generated using the Q5® Site-Directed Mutagenesis Kit (E0554S) and cloned with the CMV driven FLAG-tag vector. Template PML-I cDNA was sequence verified and previously published on (Attwood et al., 2020). The same sequence was used to generate the PML mutants lacking (N-terminal RBCC sequence only) or encompassing the CDE (aa positions 596-882) and tagged with both an SV40 NLS and the PML-I NES at the N-terminus. The localizations of these different mutants were assessed and confirmed prior to the usage of the sequences for the LINE-1 assay (**Figure 3.4**).

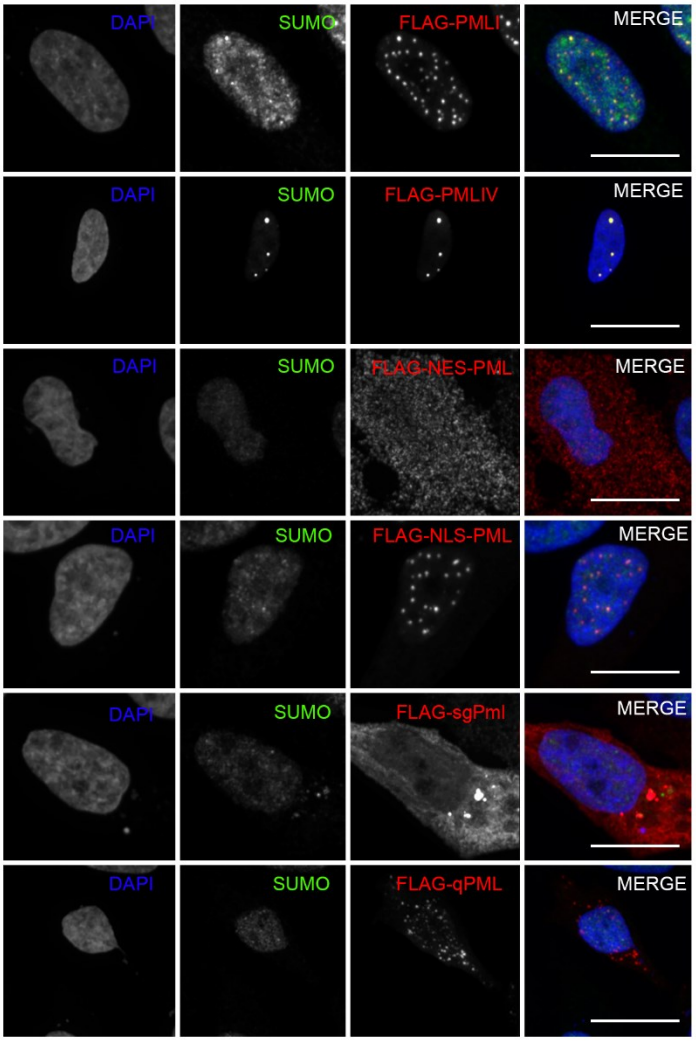

Figure 3.4. Subcellular localizations of human PML, mutants and orthologs utilized in LINE-1 assay. Localizations of FLAG-tagged PML isoforms, mutants and orthologs in U2OS cells. Cells were transfected with the different vectors encoding FLAG-tagged proteins. Scale bars represent 10 μm.

3.2.2 Protein expression and purification of sgPml-CDE

BL21(DE3) *E. coli* (New England BioLabs Inc.) were transformed with pHMT-sgPml-CDE. Transformed cells were grown in LB media to an OD_{600} of ~0.6, after which protein expression was induced with 0.5 mM IPTG. After overnight expression at 20 °C, cells were resuspended in lysis buffer: 20 mM Tris pH 8, 500 mM NaCl, 5 mM BME, lysed by sonication, and clarified by centrifugation (25,000 × g for 20 min at 4 °C). The supernatant was loaded onto an amylose chromatography column (New England BioLabs Inc.), washed with lysis buffer, and eluted with lysis buffer containing 10 mM maltose. The protein was then incubated with TEV protease overnight with concurrent overnight dialysis at 4 °C against dialysis buffer: 20 mM Tris pH 8, 250 mM NaCl, 5 mM BME. After cleavage, exonuclease domains were isolated using Ni^{2+} affinity chromatography and then purified after being diluted 5-fold with 20 mM MES (2-(N-morpholino) ethanesulfonic acid) pH 6, 5 mM BME and purified by cation exchange chromatography (HiTrap™ SP HP, cytiva). Purifications were monitored by SDS-PAGE and UV/Vis absorbance using a predicted extinction coefficient at 280 nm of 18450 $M^{-1}cm^{-1}$. **These purifications were done by the Langelaan lab.**

3.2.3 In vitro exonuclease assays

Exonuclease reactions (40 µL) contained 500 nM 5'-6-FAM labeled oligonucleotide (ssDNA: 5'-ATACGACGGTGACAGTGTTGTCAGACAGGT-3'or dsDNA pseudo-palindrome: 5'-TCACGTGCTGAC/GTCAGCACGACG-3'), 20 mM Tris pH 7.5, 2 mM dithiothreitol, and 100 µg/mL BSA. For metal specificity assays the reactions contained 625 nM of sgPml-CDE and 2 mM metal ($MgCl_2$, $MnCl_2$, $ZnSO_4$, or

$CaCl_2$) or 10 mM EDTA. Exonuclease titration assays contained 4.9–625 nM of zfPlex9.1 or zfPlex9.1 (D61N) and 5 mM $MgCl_2$. Reactions were allowed to proceed for 20 min at room temperature and then quenched with 3 volumes of 100% ethanol, dried via speed vac, resuspended in 10 μL formamide, resolved by urea PAGE (19% 29:1 acrylamide and 7 M urea in TBE), and visualized using a fluorescence imager (VersaDoc). **These exonuclease assays were done by the Langelaan lab.**

3.2.4 Cell culture

PML CRISPR/Cas9 KO lines, both immortalized NHDF and U2OS, were previously generated and characterized (Attwood et al., 2020). U2OS osteosarcoma cell lines (parental U2OS, $U2OS^{Clover–PML}$ (Pinder et al., 2015), $U2OS^{GFP–PML-I}$, U2OS PML KO cells (Attwood et al., 2020)) were cultured in Dulbecco's modified Eagle's medium (Life Technologies) supplemented with 10% fetal calf serum, at 37°C with 5% CO_2. QM5 (Quail Muscle clone 5) cells were a gift from the Roy Duncan lab (Dalhousie University) and grown like U2OS. NHDF (WT and PML KO cells) were cultured in alpha-modified Minimum Essential Medium (Life Technologies) supplemented with 15% fetal calf serum and GlutaMAX (Thermo Fisher) at 37°C with 5% CO_2.

3.2.5 2',3'-cGAMP quantification

6×10^6 U2OS cells (for PML KO and WT experiments) were seeded into 15-cm dishes, and 24 hours later cells were transfected with the Bluescript vector (empty vector control) and Human L1 plasmid (used in L1 retrotransposition assay) using Lipofectamine 2000 reagent (Invitrogen). Cells were harvested 36 hours after

transfection, washed with 2x with PBS and pelleted before lysis. Samples were resuspended in 500 µL M-PER (mammalian protein extraction reagent) lysis buffer (Thermo Scientific). Lysates were incubated on ice for 30 minutes with gentle agitation every 10 minutes, before being spun down at 16,000 x g, 4° C for 10 min. Samples were quantified using the 2′3′cGAMP ELISA Kit (Cayman Chemical) according to the manufacturer's instructions.

3.2.6 LINE retrotransposition assays

To assess the effect of proteins on retrotransposition, I utilized methods for previously characterized plasmids encoding a human L1 retroelement that encodes a neomycin cassette that when transfected into HeLa or U2OS cells, is only successfully re-integrated upon retrotransposition. The method for the L1 assay is described in detailed within section 2.2.7.

To determine protein levels of T7-tagged ORF1p after ubiquitin-proteasome inhibition. Cells on a 10cm^2 plate were transfected with 5µg of the L1 plasmid encoding T7-ORF1p or an empty vector using Lipofectamine 2000. For addback experiments, cells were transfected with an additional 5µg of FLAG-PML-I, FLAG-PML-IV, or FLAG empty vectors ("-" control). Then, after 24 hours, I treated U2OS cells with MG132 (Sigma; M7449) at varying concentrations (1µM, 2.5µM, 5µM) for 8 hours as described previously (Haller et al., 2014). Cells were then washed with PBS twice and samples were handled for western blotting (described below).

3.2.7 Immunofluorescence microscopy

For transfections, cells were seeded into wells containing coverslips in 6-well dishes, then transfected the next day with expression vectors. One day after transfection, coverslips were washed briefly with PBS and the cells were fixed in 2% PFA, permeabilized with 0.5% Triton X-100 in PBS and blocked with 4% BSA in PBS. Cells were then immunolabeled with primary antibodies specific for FLAG (mouse anti-FLAG M2, Sigma, F3165, 1:200), T7 (rabbit anti-T7, Millipore/Sigma, AB3790, 1:200), PML (two antibodies used; sheep anti-PML, Diagnostics Scotland, PML2A, 1:500; rabbit anti-PML, Bethyl Laboratories, A301-167A, 1:1000), SUMO (two antibodies used; mouse anti-SUMO-1, clone 21C7, Zymed, #33-2400, 1:200; rabbit anti-SUMO-1, Abcam, ab32058, 1:200), rabbit anti-DAXX (polyclonal D7810; Sigma-Aldrich, 1:500), rabbit anti-SP100 (Chemicon, 1380) and TREX1 (rabbit anti-TREX1, Abcam, ab185228, 1:400).

Then for secondary staining, coverslips were washed with PBS and incubated with Alexa-Fluor 647 donkey anti-rabbit, Alexa-Fluor 488 donkey anti-sheep, Alexa-Fluor 488 donkey anti-rabbit, and Alexa-Fluor 555 donkey anti-mouse (Thermo Fisher Scientific) secondary antibodies. Finally, the cells were washed several times in PBS and incubated with 1 μg/mL of 4',6-diamidino-2-phenylindole (DAPI) (Sigma) to visualize the nuclei.

For transfections, I marked L1 RNP structures using plasmids obtained from colleagues. T7-tagged ORF1p was previously used to mark L1 RNPs and encoded in the pES2TE1 vector. U2OS cells were transfected using Lipofectamine 2000 (Invitrogen)

and HeLa cells using Lipofectamine 3000 (Invitrogen), according to the manufacturer instructions.

Fluorescent micrographs were captured with a Prime95 scientific complementary metal-oxide-semiconductor (sCMOS) camera (Photometrics) using a custom-built spinning-disk confocal laser Zeiss Cell Observer Microscope (Intelligent Imaging Innovations, 3i) equipped with a 1.4 NA 63X immersion oil objective lens and both laser (3i) and LED illumination via a Spectra light engine (Lumencor). Images were captured and processed using Slidebook 6.1 (3i) and assembled into figures using Adobe Photoshop CS5.

3.2.8 Western blotting

For western blot analysis of SUMOylation status, cells were recovered from confluent 10 cm culture dishes and washed with PBS. U2OS cells were treated for 24 hours with 1 μM ML-792 (Selleckchem), a SUMO E1 inhibitor (targets SAE1) to inhibit total SUMOylation within cells (He et al., 2017). After treatment, cells were then washed twice with PBS and either harvested for western blotting or fixed for immunofluorescence staining. Cells were lysed on ice for 20 minutes in 6 mM Urea lysis buffer with protease inhibitors (P8340, Sigma) and sonicated, before further processing. For all other samples, the cells were lysed on ice for 20 minutes in RIPA buffer (Sigma) with protease inhibitors (P8340, Sigma).

Lysates were cleared (10 min, 15 000 × g, 4°C) and protein extracts were analyzed by SDS-PAGE and western blotting using 5% milk powder with 0.1% Tween

20 in PBS as a blocking solution. Protein was transferred to Nitrocellulose membrane (BioRad). Total protein was determined directly on the membrane using the 4-15% Mini-PROTEAN TGX-Stain Free Protein Gel system (BioRad). For homemade gels, actin was used as a loading control. Antibodies used for Western blotting analysis were: rabbit anti-SUMO1 (Abcam, ab32058, 1:2000), rabbit anti-ubiquitin (linkage K48) (Abcam, ab140601, 1:4000), mouse anti-T7 (Millipore, AB3790, 1:2000), mouse anti-FLAG (Millipore, F1804, 1:2000), mouse anti-actin (Sigma, A2228, 1:5000).

3.2.9 Statistical analysis

All statistical analyses were performed using GraphPad Prism 9.0.1. The sample size and error bars for each experiment are defined in the figure legends. Comparisons between groups for LINE1 retrotransposition and the 2'3'-cGAMP assay were analysed by a repeated measures one-way ANOVA, with the Geisser-Greenhouse correction and then a Tukey's multiple comparisons test between groups.

3.2.10 Animal ethics

Spotted gar work was approved by the Institutional Animal Care and Use Committee at Michigan State University (protocol no. AUF 10/16-179-00).

3.3 Results

3.3.1. Spotted gar PML is an active exonuclease

The discovery of full length PML-I orthologs in ray-finned fish, sharks and rays encoding putatively active CDE domains was intriguing (Chapter 2). The spotted gar genome was used to further explore PML-I from ray-finned fish (Braasch et al., 2016). The spotted gar lineage diverged ~350 million years ago from the teleost lineage before the teleost genome duplication event and has a slowly evolving genome (Braasch et al., 2016). These features make the spotted gar an excellent representative species for studying the *PML* gene in fish. At the locus encoding the spotted gar *pml* ortholog (referred to as *sgpml*), there is strong synteny to the human *PML* locus on human chromosome 15, with flanking genes *STOML1, ISLR, CCDCC33* being conserved within the syntenic region (**Figure 3.5A**). In addition, a bridging amniote species was also utilized; *Coturnix japonica* (Japanese quail) encodes a *PML* locus (referred to as *qPML*) with synteny to both the spotted gar and human loci (**Figure 3.5A**).

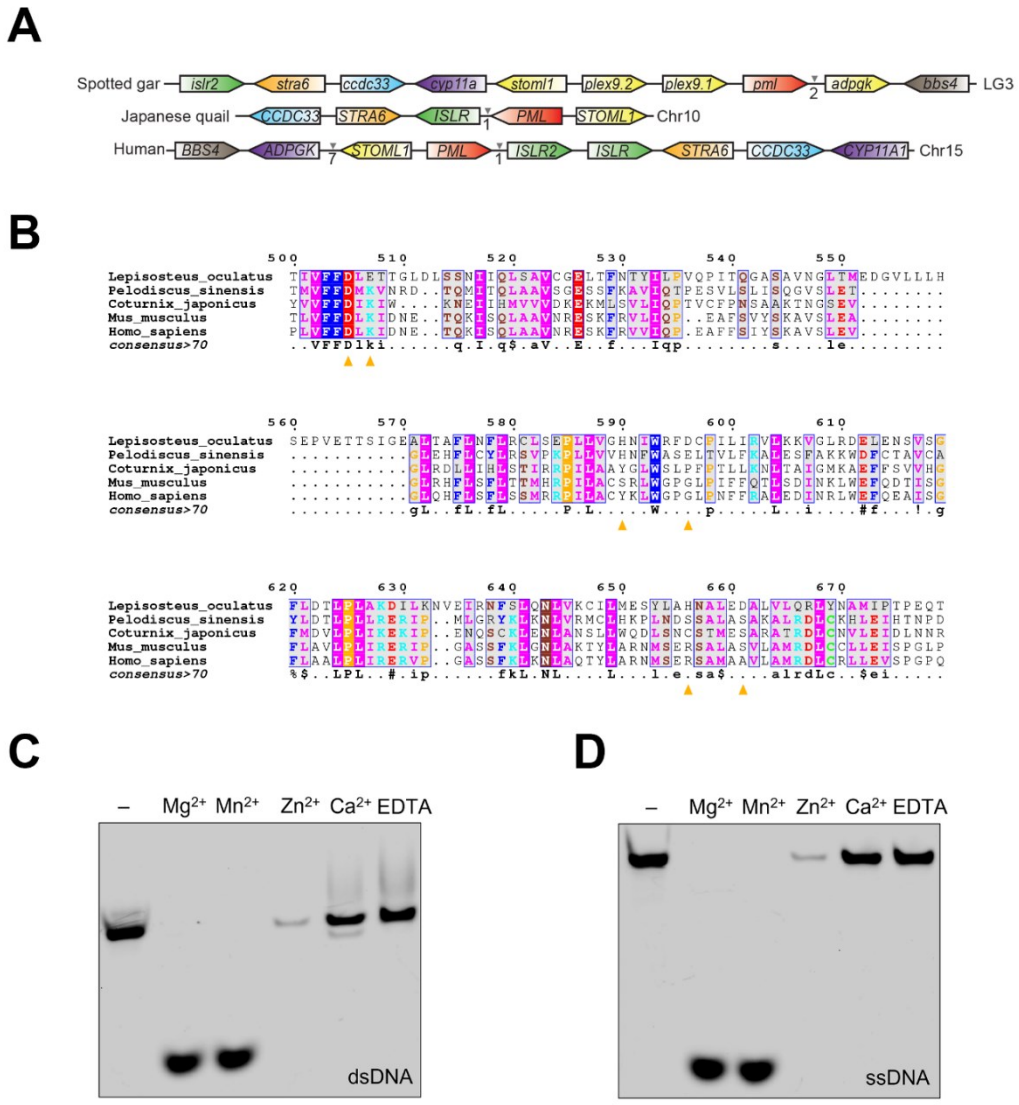

Figure 3.5. Spotted gar Pml is an active cytoplasmic DNA exonuclease. (**A**) Synteny of *pml* locus between the genomes of the Spotted gar, Japanese quail and Humans. Similarly coloured genes represent homologs between species. The chromosome where the *pml* locus is found in each species is indicated on the right. The intervening arrows with numbers indicate the number of intervening adjacent genes that exist between the homologous genes not found in the syntenic region. (**B**) MUSCLE alignment of the C-terminal DEDDh exonuclease domain identified in the spotted gar PML (sgPml) protein with other vertebrate PMLs. The consensus sequence is displayed below the sequences for residues with over 70% conservation across species. Yellow arrows indicate predicated catalytic residues for sgPml (**C, D**) Exonuclease activity of purified sgPml-CDE requires Mg^{2+} or Mn^{2+}. Fluorescent oligonucleotides were incubated with sgPml-CDE in the presence of the indicated divalent cation or EDTA. "-" refers to input without the addition of cations. ***Data presented in this figure (C, D) was collected by the Langelaan lab.***

Given that the sgPml protein encodes a potentially active CDE (**Figure 3.5B)**, I cloned the full length *sgPml* gene from gar splenic tissue for further characterization. We also expressed the codon optimized putative DEDDh exonuclease of sgPml (residues 497-766) and purified it to homogeneity (**Figure 3.5C** and **Figure 3.5D**). The sgPml-CDE encodes an active exonuclease capable of degrading ssDNA and dsDNA when incubated with Mg^{2+} and Mn^{2+} (**Figure 3.5C** and **Figure 3.5D**). Thus, akin to other DEDDh family exonucleases (Huang et al., 2018), and like zfPlex9.1 and TREX1, it appears that sgPml can degrade DNA in the presence of divalent cations.

3.3.2. PML localization transitioned to the nucleus from the cytoplasm

Next, I characterized the cellular localization of sgPml by expressing it in human wild type (WT) and PML KO U2OS osteosarcoma cells. Strikingly, in contrast to the mammalian PML protein, sgPml did not form nuclear bodies and localized diffusely in the cytoplasm, forming ~1-3 cytoplasmic body-like puncta (**Figure 3.6**). When the American Paddlefish PML ortholog (another predicted PML exonuclease) was expressed, it localized to the cytoplasm like sgPml (**Figure 3.7A**). Both PML orthologs in fish localize to the cytoplasm, indicating that exonuclease-active PML is a cytoplasmic protein.

Since mammalian PML NBs are associated with post-translation modifications of nuclear body proteins by the small ubiquitin like modifier (SUMO) (Nisole et al., 2013), we also examined SUMO1 localization relative to these cytoplasmic sgPml puncta. These sgPml puncta were negative for SUMO1 immuno-staining, unlike mammalian PML nuclear bodies that accumulate SUMO1 (**Figure 3.6)**.

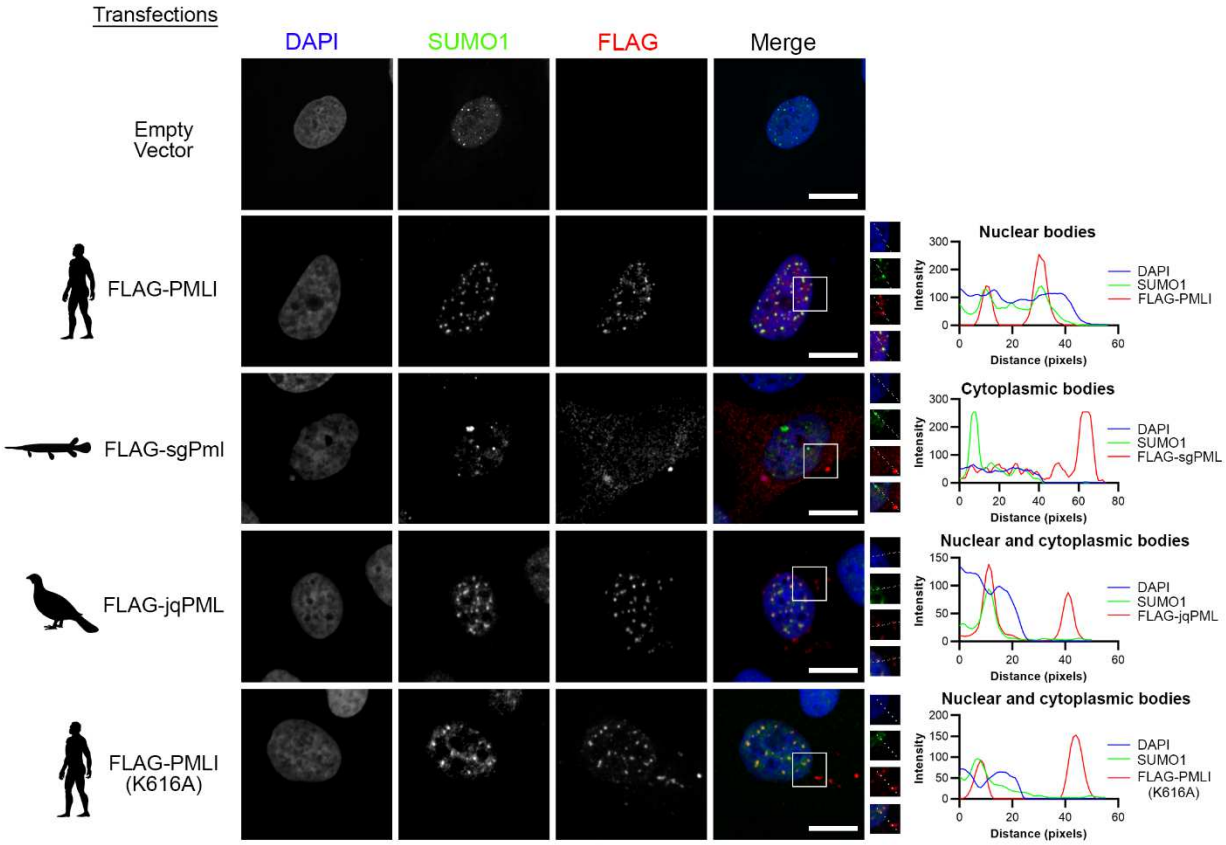

Figure 3.6. Gar PML localizes to the cytoplasm. Subcellular localizations of FLAG-tagged PML-I, sgPml, quail PML (jqPML) and PML-I (K616A). Cells were transfected with the various FLAG-tagged proteins and stained for SUMO1. Scale bars represent 10 μM for

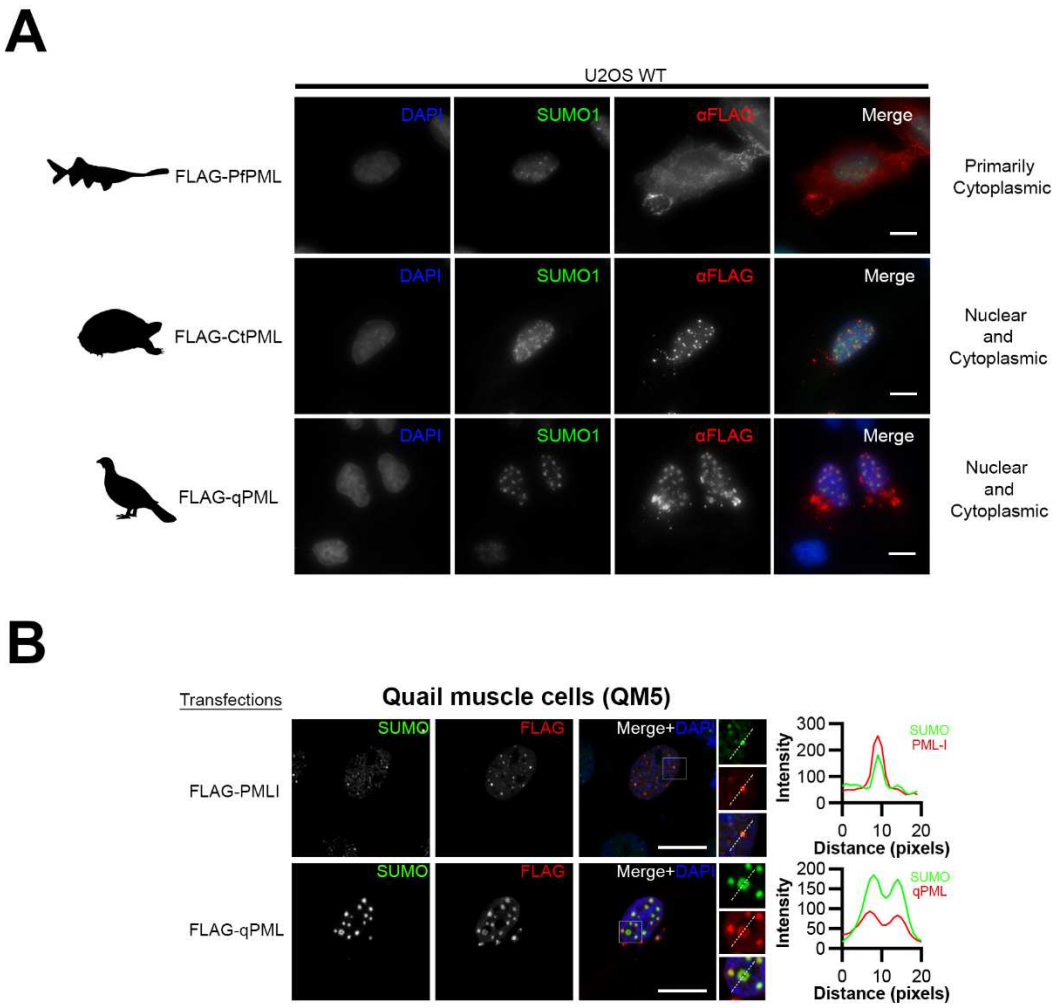

Figure 3.7. PML NBs are present in amniote species. (**A**) Subcellular localizations of FLAG-tagged PML orthologs from American paddlefish (*Polyodon spathula*; pfPML), Common box turtle (*Terrapene Carolina*; CtPML) and Japanese quail (*Coturnix japonica;*qPML). Proteins were ectopically expressed in U2OS cells. (**B**) Localizations of FLAG-tagged human PML-I and quail PML in quail cells. Quail cells (QM5) were transfected with both FLAG-tagged Quail PML (qPML) and human PML-I. qPML is found forming nuclear bodies accumulating SUMO akin to human PML but also localize to the cytoplasm. Silhouettes for species were obtained from PhyloPic. Scale bars represent 10 µm. Subcellular

Sequence comparisons revealed that the target lysines involved in human PML SUMOylation, which first appear in amniote species according to our evolutionary reconstruction, align partly to the CDE and its catalytic residues (**Figure 3.5B**). This could suggest that a shift in PML cellular function and localization may have occurred concurrently with the acquisition of SUMOylation. To assess the possibility that SUMO site evolution drove the nuclear localization and function of PML, I cloned qPML (from Japanese quail). The expression of jqPML and human PML-I in quail cells all led to the formation of SUMO1 colocalizing nuclear bodies (**Figure 3.7B**). Similarly, expression of jqPML in human cells also led to SUMO1 accumulating at jqPML nuclear bodies (**Figure 3.7B**). However, like sgPml, jqPML also formed cytoplasmic bodies lacking SUMO1 (**Figure 3.7B**). The expression of a PML ortholog from a turtle species mirrored the localization of jqPML (**Figure 3.7B**). These results indicate that PML orthologs from amniote species can form nuclear bodies and are likely SUMOylated, as they co-localize with SUMO1.

To assess whether sgPml formed nuclear bodies in the absence of SUMOylation, cells were treated with ML-792, a SUMO E1 inhibitor that blocks total SUMOylation within the cell (**Figure 3.8A**). sgPml was still capable of forming cytoplasmic puncta even after SAE1 inhibitor treatment, consistent with these cytoplasmic sgPml bodies forming in a SUMO-independent manner (**Figure 3.8A**).

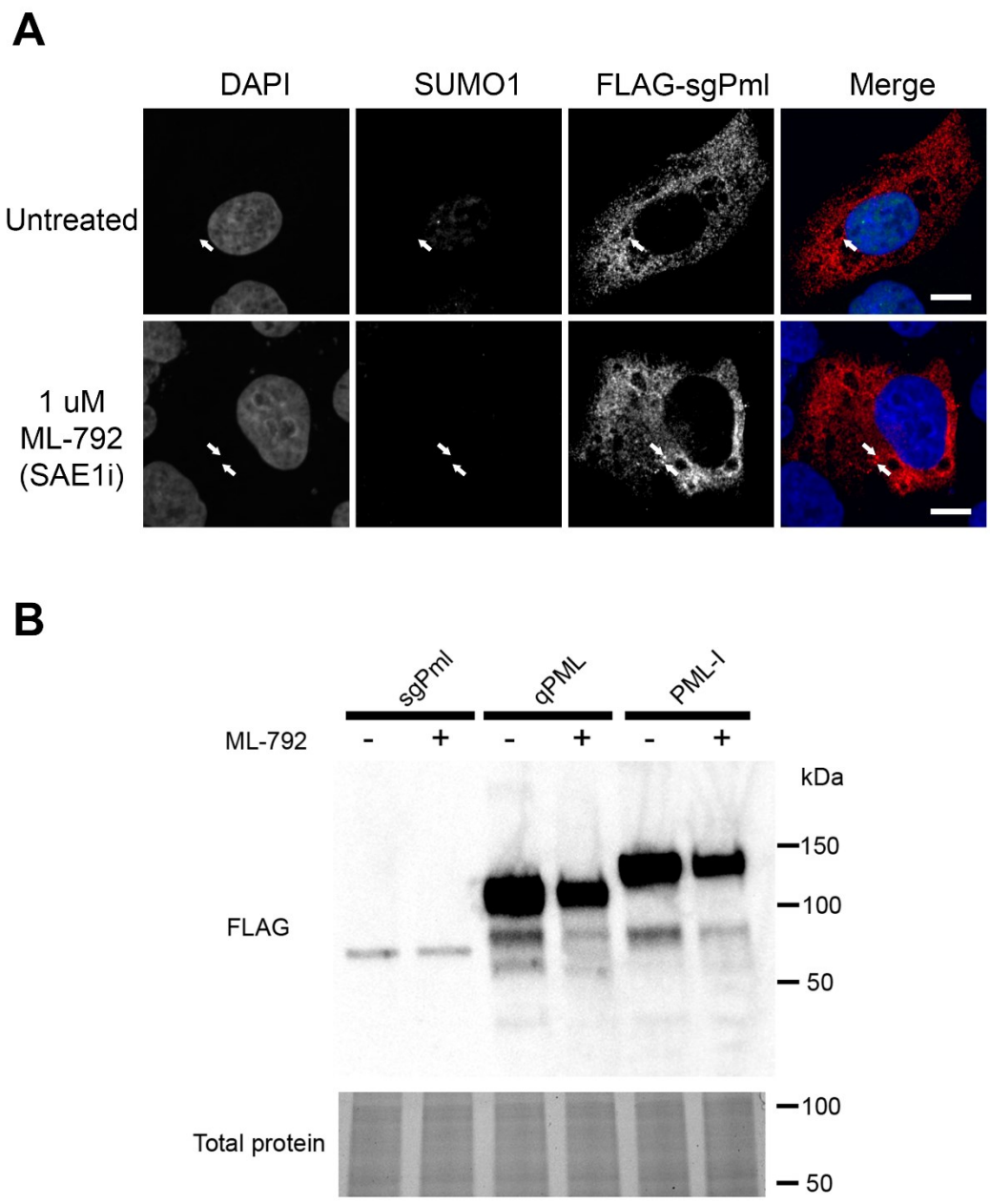

Figure 3.8. sgPml forms SUMO-independent cytoplasmic bodies whereas qPML is likely SUMOylated to form nuclear bodies. (**A**) Subcellular localization of sgPml after ML-792 treatment (SAE1 inhibitor) in U2OS cells. sgPml forms cytoplasmic bodies even in the absence of SUMOylation occurring in the cells. (**B**) Western blot showing the expression of FLAG-tagged sgPml, jqPML, and PML-I proteins in U2OS cells. U2OS cells were transfected and then treated with DMSO or ML-792 overnight. Cells were then lysed in 6 M urea to maintain SUMO-conjugated proteins. Multiple bands are observed for jqPML and PML-I that are reduced with ML-792 treatment, indicating that it is likely modified by SUMO. Whereas, the sgPml band is observed at a single MW, indicating that it is likely not modified.

Human PML K616 is one of the lysine residues with the potential to be poly-SUMOylated (Cuchet-Lourenco et al., 2011). Intriguingly, the residue also aligns to a catalytic residue of the sgPml CDE (**Figure 3.5B**). The conserved lysine also appears to have been one of the first potential SUMOylation sites appearing in amniote orthologs of PML, suggesting that it may have contributed to the shift in PML localization from cytoplasm to nucleus (**Figure 3.5B** and **Figure 3.7**). I generated a PML-I K616A mutant and found that its localization shifted to the cytoplasm, where it formed numerous cytoplasmic puncta that were negative for SUMO1 (**Figure 3.6**). Human PML-I K616A is likely able to still maintain some protein at nuclear bodies owing to its other SUMOylation sites. The localization resembled that of jqPML, which both formed nuclear bodies and cytoplasmic puncta (**Figure 3.6**). Thus, the PML-I K616 SUMOylation site appears to play an important and conserved role across species in dictating the nuclear localization of PML.

When the ectopic expression of orthologs was examined by western blotting, FLAG-jqPML appeared as multiple bands like human PML-I (**Figure 3.8B**). However, FLAG-sgPml appeared as a single band indicating that it is not likely modified by SUMO as suggested by the immuno-staining (**Figure 3.8B**). The jqPML higher molecular weight band migrated approximately ~12 kDa higher, which would be the predicted molecular weight of jqPML conjugated to SUMO1 (a single moiety). Treatment of cells with the SAE1 inhibitor ML-792, thus blocking global SUMOylation, resulted in a reduction in the higher molecular weight jqPML and human PML bands (**Figure 3.8B**). These results support the importance of PML SUMOylation for nuclear body formation, and indicates

that avian and turtle PML orthologs, with the acquisition of SUMO-target lysine residues, can localize to both the cytoplasm and the nucleus to form PML NBs.

3.3.3. Human PML shuttles to the cytoplasm to suppress LINE-1 retroelements

While human PML retained the DEDDh exonuclease fold, the catalytic residues are changed relative to sgPml, and there is no evidence to suggest it is an active exonuclease (**Figure 3.5B**). To date no cellular function has been ascribed to the human PML-I CDE (**Figure 3.9A)**. Since I and others have shown that L1-suppression is an exonuclease-independent function for TREX1 and the Plex9 proteins (Chapter 2), and that sgPML also represses L1 retrotransposition (Chapter 2), I hypothesized that human PML may have retained a role in suppressing L1 activity via the CDE.

To test this hypothesis, HeLa cells were co-transfected with the human L1 reporter with FLAG-tagged human PML-I, PML-IV or jqPML; the latter to demonstrate conserved PML function in L1 suppression in other amniotes. PML-IV is almost identical to PML-I but lacks the CDE domain encoded by exon 9 (aa positions 596-882) (**Figure 3.9A**). PML-I, but not PML-IV, significantly suppressed L1 activity ($p<0.05$) (**Figure 3.9B**). Then, to determine if the loss of endogenous PML influenced L1 retrotransposition in PML KO U2OS cells, we conducted the L1 assay in these cells (Attwood et al., 2020). KO of PML in U2OS cells increased L1 activity nearly 2-fold ($p<0.01$) compared to WT cells, which was reversed by expression of PML-I, jqPML or sgPml (**Figure 3.9B**).

Next, I wanted to examine if the increase in L1 retrotransposition also resulted in elevated levels of cGAS activity. Like in the absence of TREX1 (Chapter 2), 2',3'-

cGAMP levels were elevated significantly ($p<0.01$) in the absence of PML after L1 transfection (**Figure 3.9C**). The increase in 2',3'-cGAMP could be suppressed by the addback of PML-I into the PML KO cells (**Figure 3.9C**). Collectively these data indicate that PML orthologs from 3 distinct vertebrate species, quail, human, and gar, are capable of robustly suppressing human L1 activity. In addition, PML contributes to the regulation of cGAS by suppressing L1 retrotransposition.

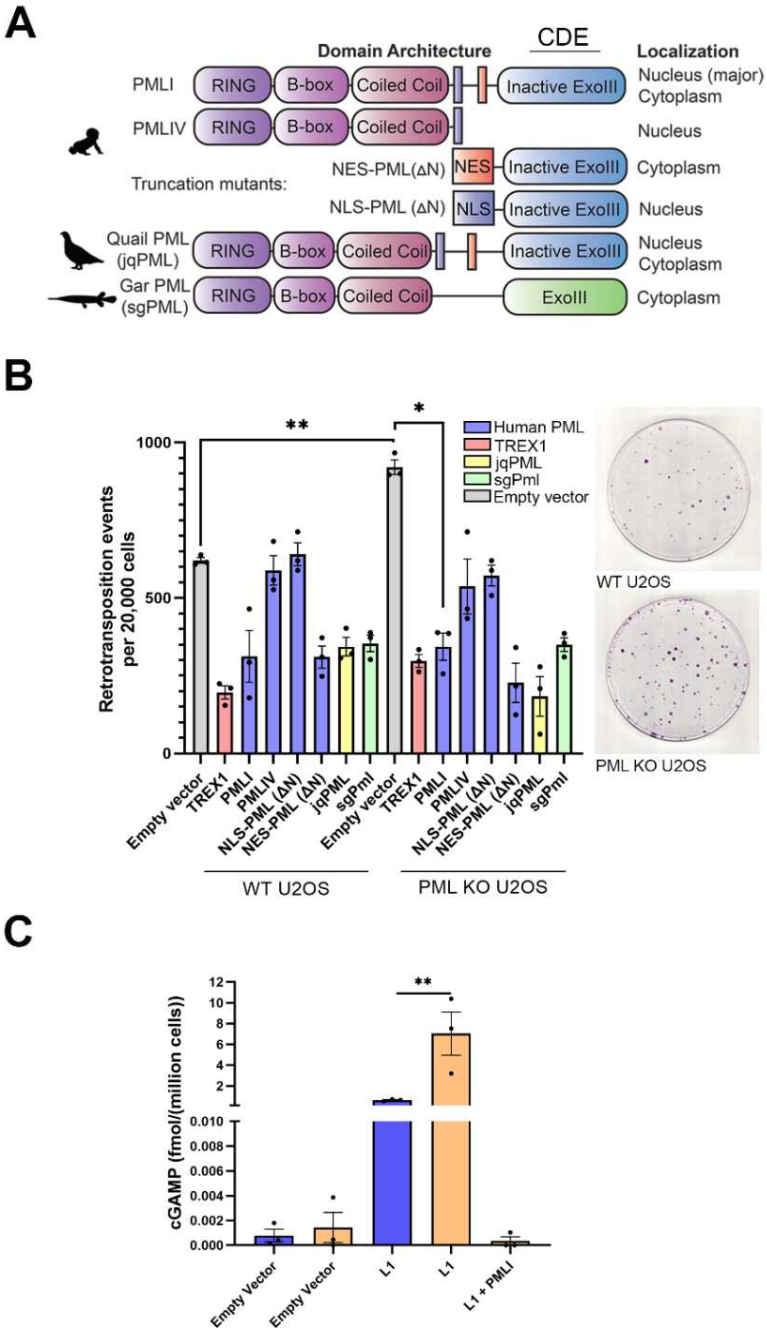

Figure 3.9. PML-I restricts L1 retrotransposition and cGAS activity through its CDE. (**A**) PML mutants were generated encompassing the CDE (aa positions 596-882) and tagged with both an SV40 NLS and the PML-I NES at the N-terminus. The mutants lack the C-terminal RBCC domain of PML. (**B**) Loss of *PML* elevates L1 activity which can be reversed with the addback of PML-I and the NES-PML mutant (n=3). Resultant plates from the assay were stained with 0.5% crystal violet and quantified. (**C**) 2',3'-cGAMP levels in U2OS WT and *PML* knockout cells after the transfection of an empty vector and the human L1 vector (n=3). 2',3'-cGAMP concentrations were normalized to cell number for each experiment.

In addition to encoding a C-terminal DEDDh exonuclease-like domain, PML-I also uniquely encodes a nuclear export signal (NES) for which no known stimulus has been identified to trigger nucleocytoplasmic shuttling (Condemine et al., 2006). Considering that zfPlex9.1, sgPml and TREX1 are cytoplasmic/ER localizing proteins (Chapter 2) unlike human PML, I suspected that PML may localize to the cytoplasm to restrict L1 retrotransposition via its CDE. Therefore, to determine if PML nucleocytoplasmic shuttling occurs directly in response to the stress of L1 retrotransposition, we transfected cells with the L1 reporter plasmid and examined PML localization (**Figure 3.10**). Indeed, in cells transfected with the active human L1 retroelement, endogenous PML shuttled robustly to the cytoplasm (**Figure 3.10A**). In the cytoplasm, PML formed large SUMO-negative puncta that resembled cytoplasmic sgPml bodies, which also co-localized with TREX1 puncta (**Figure 3.10A**).

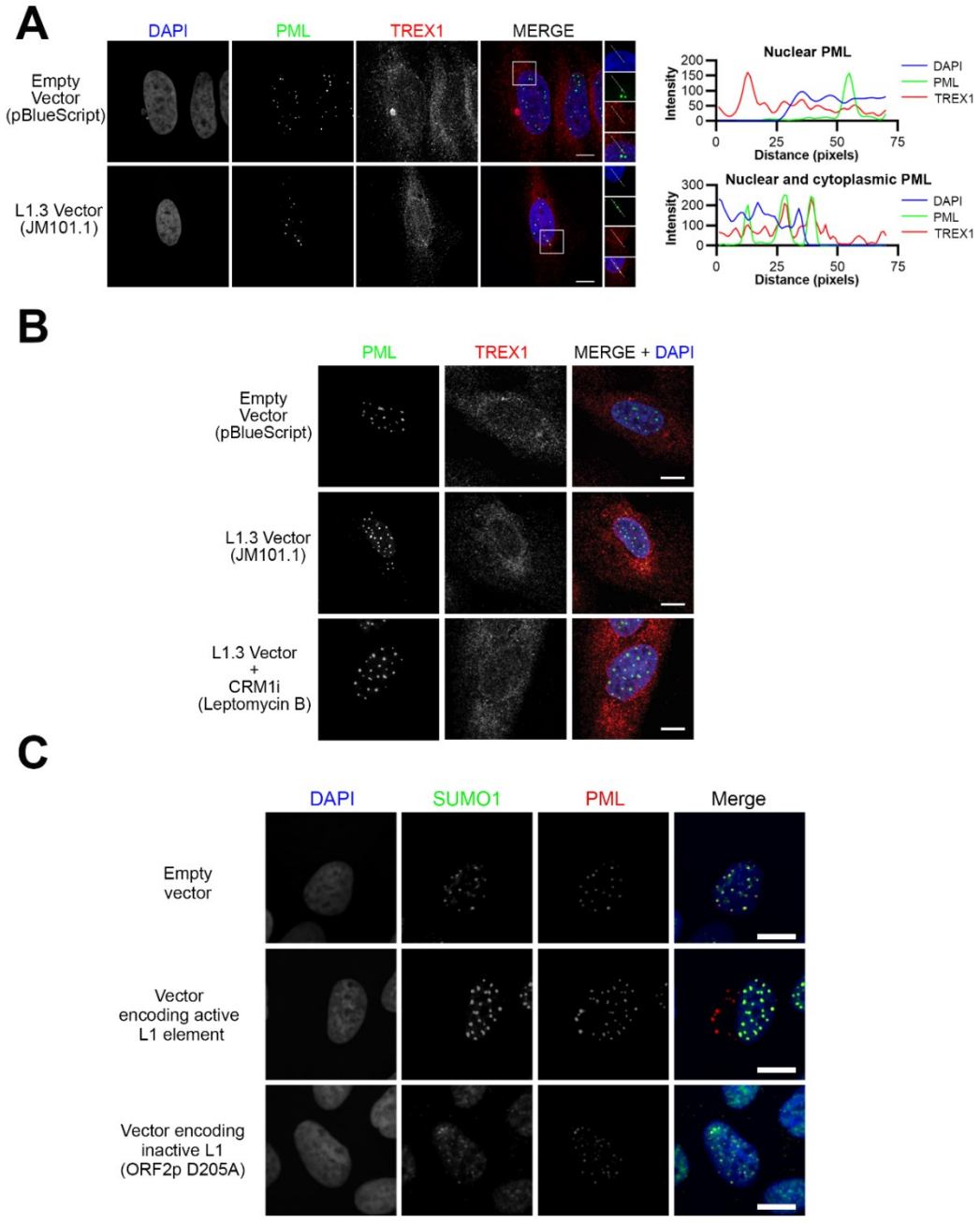

Figure 3.10. PML-I shuttles to the cytoplasm to suppress L1 by promoting the degradation of ORF1p. (**A**) Transfection of the human L1 retrotransposition vector led to cytoplasmic PML puncta forming. PML co-localized partly with TREX1 in the cytoplasm after L1 retroelements were active. (**B**) The nucleocytoplasmic shuttling of PML-I is CRM1-dependent. Treatment of U2OS cells overexpressing GFP-PML-I for 3 hours with 10 ng/mL of Leptomycin B, a potent inhibitor of CRM1, a nuclear export protein, led to retention of GFP-PML-I in the cytoplasm. (**C**) PML-I does not shuttle when cells are transfected with a L1 element not capable of retrotransposition (ORF2p D205A mutation). Scale bars represent 10 μm for images.

Since PML-I encodes a putative NES (positions 704–713) and has been identified as an interactor of CRM1 (Buczek et al., 2016a; Nisole et al., 2013), I next examined if PML shuttling required CRM1/XPO1, a major nuclear export protein involved in NES-dependent shuttling. To determine if PML-I shuttling was dependent on CRM1, the CRM1-inhibitor leptomycin B was utilized (Kudo et al., 1999). In the presence of leptomycin B, PML-I shuttling to the cytoplasm did not occur (**Figure 3.10B**). In addition, in cells transfected with a mutated L1 element not capable of retrotransposition (ORF2p D205A mutation), PML-I to the cytoplasm was not observed (**Figure 3.10C**). Together, these data indicate that PML nucleocytoplasmic shuttling occurs in a CRM1-dependent manner in response to active L1 retrotransposition.

Substantial PML protein is still retained in the nucleus even under conditions of high L1 activity, raising the possibility of a nuclear function for the DEDDh domain of PML in suppressing L1 retrotransposition (**Figure 3.10**). To determine if this is the case, N-terminus truncation mutants of PML were generated that encoded the PML-I C-terminus (aa 597-882) with either the upstream putative NES or a nuclear localization signal from SV40 (SV40-NLS) (**Figure 3.9A**). The NES-PML mutant potently suppressed L1 activity, in a manner comparable to jqPML and sgPml (**Figure 3.9B**). In contrast, the constitutively nuclear NLS-PML-I C-terminus had no significant effect on L1 retrotransposition (**Figure 3.9B**). These results collectively indicate an evolutionary conserved role for PML in suppressing L1 elements, which it accomplishes by CRM1-dependent nucleocytoplasmic shuttling of PML-I and requires its NES and C-terminal DEDDh domain.

3.3.5. PML-I has a conserved role in suppressing L1 by promoting ORF1p degradation

Previous work on TREX1 revealed that it suppresses L1 by depleting ORF1p through the ubiquitin-proteasome system (Li et al., 2017a). Consistent with PML playing a role in ORF1p degradation, after L1 transfection, there was a higher expression of T7-tagged ORF1p in PML KO compared to PML WT U2OS cells (**Figure 3.11A**). Then, to assess if this is due to impaired ORF1p degradation through the proteasome, L1 transfected cells were treated with the proteasome inhibitor MG132 (**Figure 3.11A**). MG132 treatment of WT cells resulted in the accumulation of T7-ORF1p as concentrations of MG132 increased, as expected. In the PML KO cells, T7-ORF1p protein levels did not change with increasing concentrations of MG132 (**Figure 3.11A**). Further, addback of PML-I but not PML-IV to PML KO cells reduced the accumulation of T7-ORF1p (**Figure 3.11B**). The data suggests that PML-I promotes the proteasome-mediated degradation of ORF1p to suppress L1. These results collectively indicate an evolutionary conserved role for PML in suppressing L1 elements, which it accomplishes by CRM1-dependent nucleocytoplasmic shuttling of PML-I to then enhance the degradation of L1 ORF1p in the cytoplasm. Taken together, a role exists for the Plex9, PML and TREX1 DEDDh exonucleases in the suppression of L1 retroelements in vertebrate species to maintain genome stability (**Figure 3.12**).

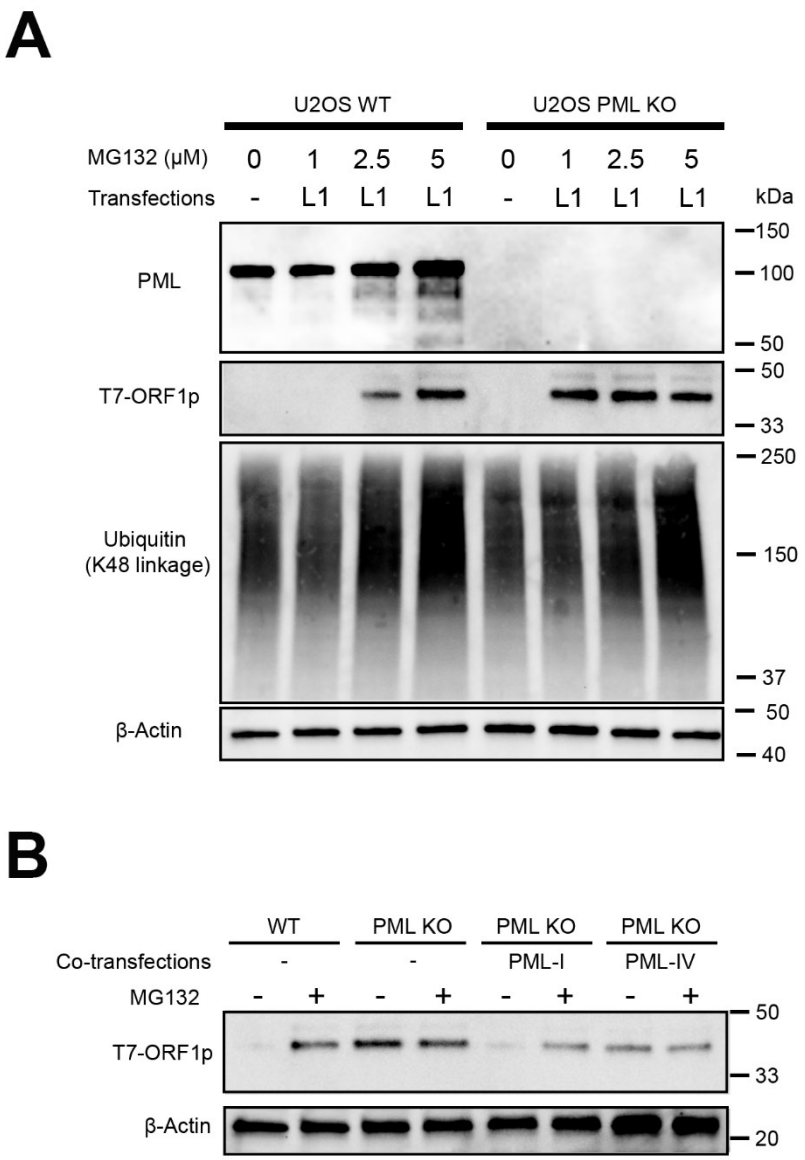

Figure 3.11. PML-I promotes the degradation of L1 ORF1p through the ubiquitin-proteasome system. (A) U2OS cells (WT and PML KO) were transfected with an empty vector (-) or the L1 element with T7-tagged ORF1p. Cells were then treated with different concentrations of MG132 (inhibitor of ubiquitin-proteasome mediated degradation) for 10 hours and T7-ORF1p protein levels were examined. (**B**) The addback of PML-I reverses the accumulation of T7-ORF1p in the PML KO cells but not PML-IV.

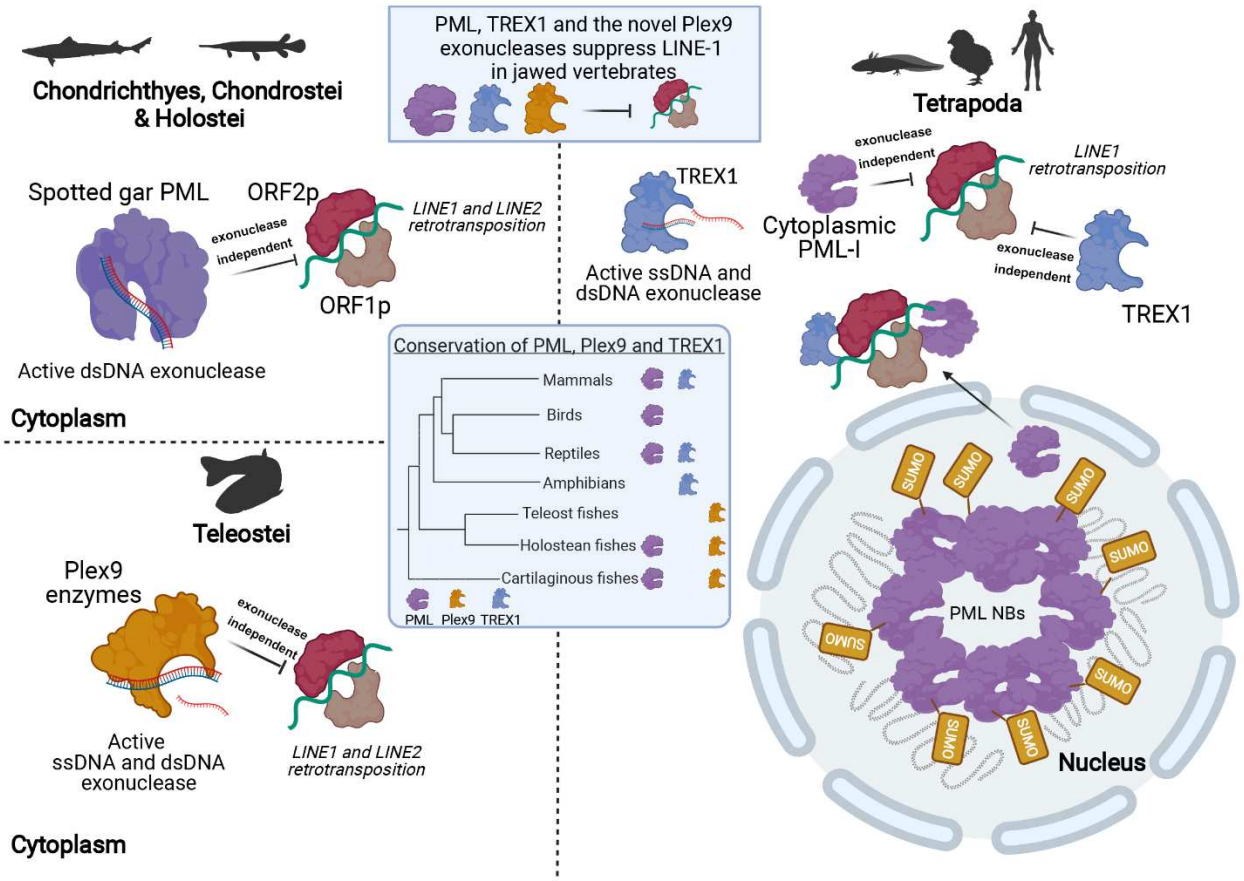

Figure 3.12. Overview of the suppression of LINE-1 retrotransposition in jawed vertebrates through the collective functions of PML, Plex9 and TREX1 enzymes. In fish, PML and novel Plex9 enzymes play a major role in suppressing both LINE-1 and LINE-2 elements. Despite the loss of *PML* in Teleost fish genomes, they have retained *Plex9* genes for the purpose of restricting LINE retrotransposition. *TREX1* appears later in tetrapods, where *Plex9* genes are lost. In addition, enzymatic PML function is lost and the protein forms nuclear bodies rather than localizing to the cytoplasm. However, PML has a retained an exonuclease-independent role for the surveillance of LINEs by shuttling to the cytoplasm to suppress the LINE1 retrotransposition. The three families of protein (PML, Plex9 and TREX) share an important function in maintaining genome integrity in jawed vertebrates as "brakes" preventing LINE-1 propagation.

3.4 Discussion

This study of PML gene evolution highlights how the availability of newly sequenced genomes from diverse taxa can help illuminate the complex molecular evolution of vertebrate genes and the functions they encode. Here, I determined that PML-I encodes a vestigial DEDDh exonuclease domain that has a novel evolutionarily conserved function in L1 suppression in humans and other amniotes (**Figure 3.5**). The PML protein has changed significantly over the course of jawed vertebrate evolution, both in cellular localization and function, which seems to be intricately tied to its SUMOylation. For example, human PML-I is primarily a nuclear protein acting as a scaffold for PML NB formation, while gar and paddlefish PML localize to the cytoplasm (**Figure 3.6** and **Figure 3.7**). Nonetheless, human PML-I can still facilitate L1 suppression through the acquired ability to shuttle to the cytoplasm via its nuclear export signal (**Figure 3.9** and **Figure 3.10**). This feature represents a remarkable compensation mechanism that allows PML to retain its key role in surveillance and suppression of L1 retroelement activity despite its divergence during amniote evolution, which is consistent with the broader role of PML in antiviral innate immune pathways (Geoffroy & Chelbi-Alix, 2011; Scherer & Stamminger, 2016).

The cellular roles of cytoplasmic PML have been relatively understudied, particularly PML-I whose role in the cytoplasm has remained a mystery for over a decade since its first observation by Condemine and colleagues (Condemine, Takahashi, Le Bras, & de The, 2007). L1 retroelement activation results in reproducible shuttling of PML-I to the cytoplasm in a manner that requires the NES of PML and is CRM1-dependent. Furthermore, ray-finned fish, turtle, and avian PML orthologs which localize primarily

and partially to the cytoplasm (respectively), can robustly inhibit L1 activity, indicating that this cytoplasmic function of PML was conserved over the course of amniote evolution. PML has also been reported to localize to the cytoplasm in response to HIV-1 infection and during epithelial-mesenchymal transition (EMT) (Buczek et al., 2016a; Turelli et al., 2001). It will be of interest to determine if in these contexts PML nucleocytoplasmic shuttling is also CRM1-dependent and/or related to L1 activity.

PML SUMOylation is a key part of its biology, where it contributes to how it forms nuclear bodies and how it is also targeted for degradation (Gärtner & Muller, 2014). PML-I K616 was described as a residue that can be polySUMOylated during HSV-1 infection but how it contributes to the isoform's function was unknown (Cuchet-Lourenço et al., 2011). When PML K616 is mutated to a residue unable to conjugate SUMO, PML-I is retained significantly in the cytoplasm rather than in the nucleus (**Figure 3.6**). Under normal growth conditions, PML is primarily nuclear, but it appears that SUMOylation at K616 contributes to the nuclear retention of PML and prevents shuttling. It is important to note that while the SUMOylation site is nearly 100 amino acids upstream of the PML-I NES, it is possible that polySUMOylation or proximity from folding could impede the PML-I interaction with CRM1. The result also suggests that there are likely SENPs that exist that respond to L1 and promote the deSUMOylation of PML K616 for shuttling. Uncovering the SENPs involved in this process will provide new insights into how PML shuttling is regulated. Since cytoplasmic PML lacks any SUMO signal, it is likely that the entire PML-I isoform undergoes deSUMOylation by SENPs before shuttling can occur, hence why this is also not a common event observed with PML aside from when L1 retroelements are expressed (**Figure 3.10**).

PML has been well-studied as a protein involved in antiviral defence by host cells, where it responds to numerous types of viruses, with some choosing to target PML to promote their infection (Scherer & Stamminger, 2016). During HIV infection, PML shuttles to the cytoplasm and this supposedly interferes with early viral events in its life cycle (Turelli et al., 2001). PML shuttling during HIV infection occurs in part due to retroviral reverse transcription (Dutrieux et al., 2015). Intriguingly, suppressors of L1 also have dual roles in limiting HIV infection but the connection between L1 and HIV is complex and still ambiguous (Zhao et al., 2021). However, reports indicate that during HIV infection, there is elevated levels of L1 retrotransposition occurring, which could be a reason for why PML shuttles to the cytoplasm during infection. More work is required to determine the connection between HIV infection, PML and L1 retrotransposition.

While PML and TREX1 are both well-studied, their dynamic subcellular localization is less understood, and our study raises the question of why amniote PML retains the ability to suppress L1 elements. TREX1 and PML co-localize in the cytoplasm when L1 elements are overexpressed (**Figure 3.10**). This leads us to conjecture that PML and TREX1 are mechanistically connected and contribute cooperatively to genome stability by suppressing retroelements, potentially via common SUMO-dependent protein interactions. Importantly, the two proteins can regulate L1 ORF1p in a similar way to promote its degradation. It will be intriguing to determine if PML and TREX1 function independently at these structures or synergistically to promote ORF1p degradation (**Figure 3.11**). Overall, our study has uncovered the convergent evolution of the Plex9 exonucleases in the teleost fish lineage that lacks TREX1 and PML orthologs, and a

primordial role for PML in the suppression of L1 retrotransposition that is conserved across 350 million years of evolution.

Our work also has implications for our understanding of the coevolution of retrotransposons and host restriction factors that restrict them in vertebrate species. While L1s contribute to genetic variation, this is juxtaposed to their negative impact on genome integrity (Gasior et al., 2006; Goodier, 2016). As a result, several mechanisms have evolved to safeguard genome stability by preventing L1 propagation, including their suppression by TREX1 (Stetson et al., 2008; Thomas et al., 2017). In lobe-finned vertebrates, including humans, TREX1 appears to be a major suppressor of L1s. However, prior to the emergence of TREX1, PML and Plex9 proteins have been important contributors to safeguard genomes from L1 propagation in fish. The regulation of the highly conserved cGAS-STING pathway appears to be tied to how host factors restrict or enhance L1, which has implications for innate immune signalling and senescence (Bregnard et al., 2016; C. Liang et al., 2022; Stetson et al., 2008). Thus, DEDDh exonucleases have a unifying role in suppressing L1 retrotransposition that, surprisingly, is also independent of their exonuclease function.

Chapter 4 – PML, Plex9 and TREX1 are involved in vertebrate regeneration and aging

This chapter contains material (sections 4.2, 4.3, 4.4, Figures 4.2-4.8) originally submitted and under revision at JEZ-B, Journal of Experimental Zoology, Part B:

Mathavarajah, S. Thompson, A.W., Stoyek, M.R., Quinn T.A., Roy, S., Braasch, I., and Dellaire, G. 2023. Suppressors of cGAS-STING are downregulated during fin-limb regeneration and aging in aquatic vertebrates. *Journal of Experimental Zoology Part B: Molecular and developmental evolution*, accepted.

4.1 Introduction

4.1.1 Wound healing in mammals: an emerging role for cGAS-STING

Wound healing is an essential process for how animals respond to injury and it occurs through a sequence of molecular and cellular events that are well-characterized. This is best illustrated with cutaneous wound healing, where in the early stages of wound healing post-injury, there is hemostasis and the activation of both keratinocytes and inflammatory cells (Gonzalez et al., 2016). Then, there is an intermediate stage that involves the proliferation and migration of keratinocytes, fibroblast proliferation, then matrix deposition and the development of new vasculature (angiogenesis) (Eming et al., 2014). At the later stages of wound healing, there is remodelling of the ECM that is required for scar formation and the restoration of a barrier (Eming et al., 2014). The whole process is spatiotemporal, involving multiple cell types that secrete cytokines, chemokines (for immune cell recruitment and activation), and growth factors (Diller &

Tabor, 2022; Eming et al., 2014). Immune signalling pathways are important for facilitating the pro-inflammatory signalling required for orchestrating wound healing. There is balance between scar formation (which can reduce the function of the tissue or organ) and tissue regeneration (complete healing) depending on the injury, the tissue in question, and the ability for appropriate remodelling of the tissue microenvironment. Thus, there are multiple pathways involved in tissue regeneration including growth factor signalling, immune cell recruitment and activation, senescence signalling, and angiogenesis (**Figure 4.1)**.

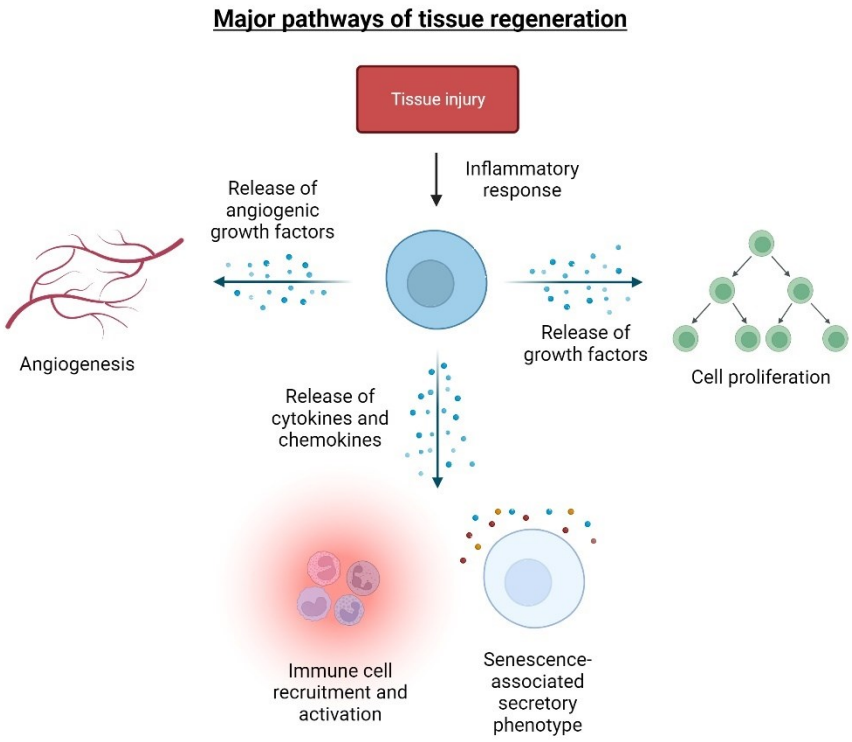

Figure 4.1. Major pathways involved in tissue regeneration. Cells at the site of injury secrete numerous factors to promote pathways that are involved in tissue regeneration, including angiogenesis, immune cell recruitment and activation, senescence signalling and cell proliferation.

4.1.2 Tissue regeneration in mammals and role of cGAS-STING

In contrast to wound healing that is a ubiquitous process across human tissues, regeneration only occurs in a limited capacity in mammalian organs (**Figure 4.2**) (S. E. Iismaa et al., 2018). In adult humans, there is very slow turnover of epithelial cells (e.g., <0.005% of hepatocytes are actively mitotic), whereas cells in the intestinal crypt and skin are replaced quickly (5 days and 12-30 days, respectively). Thus, there is a three-part spectrum to human tissues and their regenerative ability: tissues (i) showing minimal or no self-renewal (heart and central nervous system), (ii) slow cell turnover (pancreas and liver), or (iii) active renewal (skin and intestines) (Leblond, 1964).

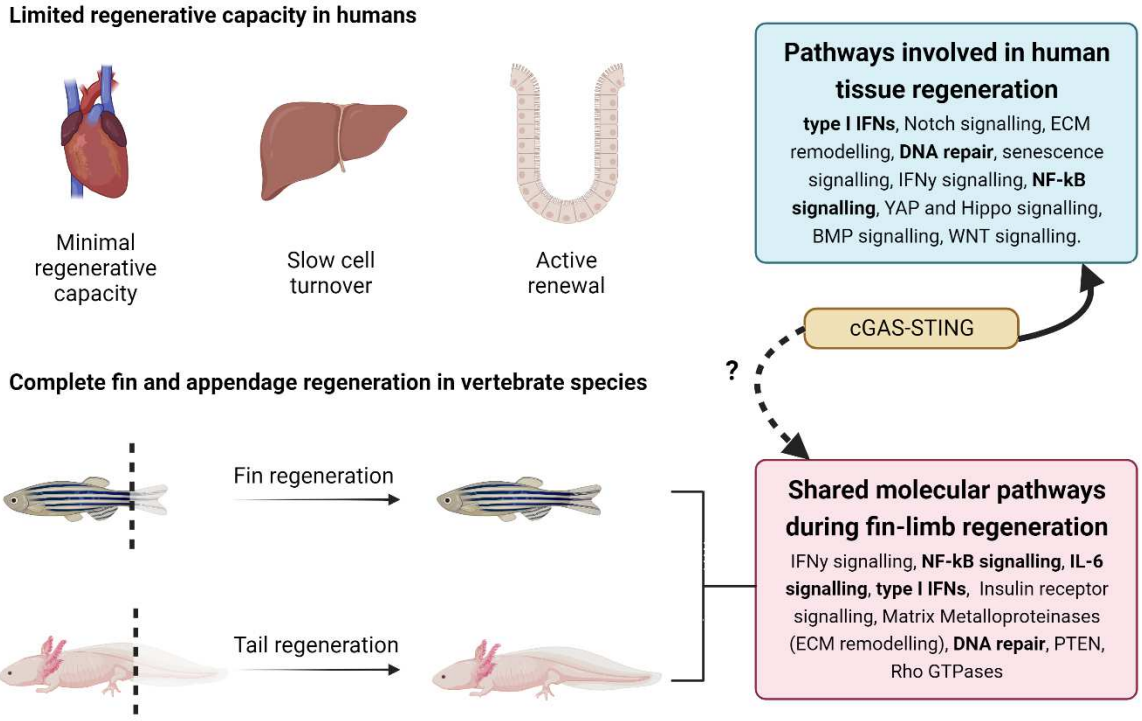

Figure 4.2. Comparison between tissue regeneration in humans and other vertebrate species. The capacity for tissue regeneration differs across organs in humans. There are many developmental, immune signalling, and repair pathways involved in tissue regeneration (listed on the right are the key pathways) (Gawriluk et al., 2020; Godwin, 2014; Siiri E. Iismaa et al., 2018; Zhao et al., 2016). In contrast to humans, other vertebrate species, such as anamniote vertebrate species (amphibians and fish) can regenerate complete appendages and fins. There are similar molecular pathways activated to progress limb-fin regeneration, which are also involved in human tissue regeneration (shown on the right) (Darnet et al., 2019). In humans, cGAS-STING regulates these pathways and connects DNA damage signalling to innate immune signalling. However, it is unknown if the pathway also contributes to regeneration in aquatic vertebrate species.

The intestinal epithelium is complex as it carries out functions in absorption and secretion while acting as an important barrier, while facing constant physical and mechanical loads. Intestinal stem cells located at the crypt bottom play an important part in the high regenerative capacity of this tissue as they drive homeostatic renewal and regeneration in response to injury (Barker et al., 2012; Bjerknes & Cheng, 2005; Gehart & Clevers, 2019). The immediate molecular pathways involved in acute intestinal regeneration include STING and its induction of downstream type I IFN signalling (Leibowitz et al., 2021). In response to radiation, it was shown that STING-deficient mice had nearly an 80% reduction in crypt regeneration (in comparison to wild type mice), indicating that the adaptor was important for normal intestinal regeneration (Leibowitz et al., 2021). Similarly impaired regeneration was observed in the absence of cGAS (Leibowitz et al., 2021). STING-dependent secretion of type I IFNs by epithelial cells after injury induces the expression of genes associated with innate mucosal immunity, macrophage chemotaxis, and IFN-γ (Leibowitz et al., 2021). However, IFN-β also seems to be the key factor that signals intestinal stem cells to proliferate and therefore it is fundamental for the initial events of regeneration (Leibowitz et al., 2021). Intriguingly, other cytosolic sensing pathways are involved in intestinal regeneration in response to radiation. RIG-I, which senses cytoplasmic RNA, and then activates MAVS, is also required for intestinal regeneration (Fischer et al., 2017). Considering that there is crosstalk between the RIG-I and STING signalling pathways, it appears that there is a collective role for the different innate immune signalling pathways in tissue regeneration (Zevini et al., 2017).

4.1.3 Expression changes to cGAS-STING machinery regulate wound healing

In mammals, the type I IFN and NF-κB signalling regulating cGAS-STING pathway is also involved in the early stages of wound healing and regeneration of the peripheral nervous system, liver and intestinal wall in mammals, where it contributes to the inflammation and the recruitment of macrophages to the site of injury (**Figure 4.3**) (Leibowitz et al., 2021; Morozzi et al., 2021; X. Wang et al., 2023). During nerve regeneration, multiple reports have shown that injury to the peripheral nerve of mice results in the upregulation of *CGAS* gene expression and elevated production of cGAMP to promote downstream STING activation (Morozzi et al., 2021; X. Wang et al., 2023). IFNγ causes *CGAS* upregulation after there is local translation of IFNγ in the injured axons (X. Wang et al., 2023). Multiple cell types seem to be involved including the injured axons themselves, as IFNγ-stimulated Schwann cells and infiltrating blood cells produce cGAMP as well (X. Wang et al., 2023). However, if STING is lost in these mice, there is poor recruitment of macrophages and reduced microglial activation after injury (Morozzi et al., 2021).

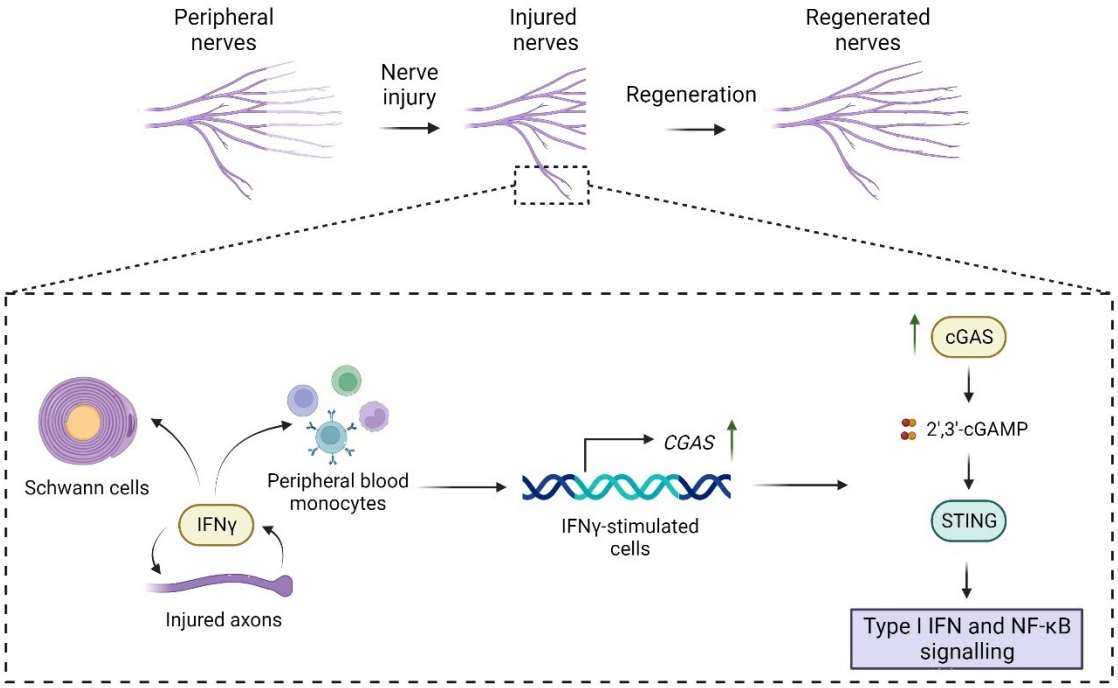

Figure 4.3. cGAS is upregulated during peripheral nerve regeneration. In response to injury, injured axons secrete IFNγ that alter gene expression profile for the axon, neighboring axons and other cell types in the vicinity (Peripheral blood monocytes and Schwann cells). *CGAS* expression is upregulated, and this activates type I IFN and NF-κB signalling to promote peripheral nerve regeneration.

STING-independent functions for cGAS in wound healing, as it has also been shown be involved in the liver wound healing response (STING is weakly expressed in liver tissue) (Lei et al., 2018). In livers, cGAS induces autophagy in response to injury which attenuates apoptosis signalling by the clearance of damaged mitochondria (Lei et al., 2018). However, there is limited work on the mechanisms behind how cGAS activation causes a downstream autophagy response in the absence of STING (which has been shown to induce autophagy) (D. Liu et al., 2019). Collectively, these findings indicate that the regulation of cGAS-STING machinery gene expression is critical for how injured tissues promote inflammatory signalling.

4.1.4. Tissue regeneration in aquatic vertebrate species

Tissue regeneration occurs in many different animal species, with the capacity for regeneration varying significantly among even highly related animals (Alibardi, 2017; Brockes & Gates, 2014; Dwaraka & Voss, 2021; Goss & Holt, 1992; McLaughlin et al., 1983; Nogueira et al., 2016; Simon & Tanaka, 2013; Tomlinson et al., 1985). Anamniote vertebrate species display a robust capacity for regeneration, with the ability to regenerate entire limbs or fins after injury to the endoskeleton. Not only do these different vertebrate species share an ability to regenerate but there is an overlap in the molecular pathways involved in regeneration between the early blastema of ray-finned fish and lobe-finned vertebrates (Darnet et al., 2019). For example, the transcriptional changes are remarkably similar during the early stages of tetrapod limb and actinopterygian fin regeneration (between bichir (*Polypterus senegalus)* and axolotl) (Darnet et al., 2019) in pathways that control inflammatory responses and innate immune signalling (e.g., IFNα-

like signalling). In addition to inflammation, numerous cellular pathways are involved in facilitating the wound healing response, such as the proliferation of progenitor cells, the maintenance of their genome integrity, cell differentiation with positional memory, extracellular matrix remodelling, and the prevention of apoptosis (McCusker et al., 2015). Key signalling proteins and their respective pathways such as fibroblast growth factors, bone morphogenetic proteins, and Wnt, all contribute to the process (**Figure 4.2**) (McCusker et al., 2015). Intriguingly, DNA damage response associated genes are also activated in response to regeneration in these model systems (Darnet et al., 2019). The DNA damage response is critical for early blastema proliferation during vertebrate regeneration, presumably as a contributor to downstream immune signalling during wound healing (Garcia-Lepe, Cruz-Ramirez, & Bermudez-Cruz, 2021; Garcia-Lepe, Torres-Dimas, Espinal-Centeno, Cruz-Ramirez, & Bermudez-Cruz, 2022; Sousounis et al., 2020). Inflammatory pathways are critical for the recruitment of macrophages and other immune cells to the wound (Brockes & Gates, 2014; Darnet et al., 2019; Godwin et al., 2013; Nogueira et al., 2016). Intriguingly, DNA damage response associated genes are also activated in response to regeneration in these model systems (Darnet et al., 2019). The DNA damage response is critical for early blastema proliferation during vertebrate regeneration, presumably as a contributor to downstream immune signalling during wound healing (Garcia-Lepe et al., 2021; Garcia-Lepe et al., 2022; Sousounis et al., 2020).

cGAS-STING is a highly conserved pathway, and the axis can be found conserved in the genomes of all vertebrate species (Wu et al., 2014). Several additional observations from aquatic models suggest that cGAS-STING has an evolutionarily

conserved role in animal wound healing and regeneration: During axolotl regeneration, progenitor limb blastema cells secrete IL-8 (Tsai et al., 2019) and STING-dependent IL-6 signalling (C. Wang et al., 2023) is one of the most enriched overlapping pathways between fin and limb regeneration (Darnet et al., 2019).

Despite the known role of cGAS-STING in wound healing and tissue regeneration discussed above, it remains unclear the extent to which the exonuclease suppressors of this pathway, such as TREX1 are involved. It will be intriguing to examine if they play a deeply conserved role in tissue regeneration in other vertebrate species, or if the pathway is an evolutionary innovation of the mammalian lineage. Considering that *cGAS* expression is regulated during wound healing, there is a possibility that TREX1 and other DEDDh exonucleases are differentially regulated as well.

4.1.5 Cellular senescence

In vertebrate species, biological aging is associated with a gradual functional decline of organs, and this is caused by cells transitioning into a "senescent" state over time (Herbig et al., 2006). However, aside from organismal aging, the pathway is also essential as a controlled signalling cascade in other instances, such as in embryonic development where it plays an important role in the early remodelling and tissue patterning (Storer et al., 2013). The senescence program therefore is a double-edged sword that can be both beneficial and detrimental at different stages in an animal's life (a classic example of evolutionary antagonistic pleiotropy) (Campisi, 2003; Giaimo & d'Adda di Fagagna, 2012; Kirkwood & Austad, 2000; Ohtani et al., 2012; Williams,

1957). Cellular senescence occurs in response to the accumulation of stress (both endogenous and exogenous) in the form of telomere dysfunction, impaired mitochondria function, persistent DNA damage, oncogene-driven transcriptional rewiring in cancer, and also chemotherapeutic drugs (J. H. Chen et al., 2007; Di Micco et al., 2021). There are hallmark features to senescent cells which are both cell intrinsic and cell extrinsic (Kumari & Jat, 2021). The cell intrinsic changes include a halt to cell proliferation and irreversible arrest from the cell cycle. Tumour suppressor proteins mediate cell cycle arrest for senescence and these major factors such as p53/p21 and p16/Rb axes (**Figure 4.4**) (Kuilman et al., 2010).

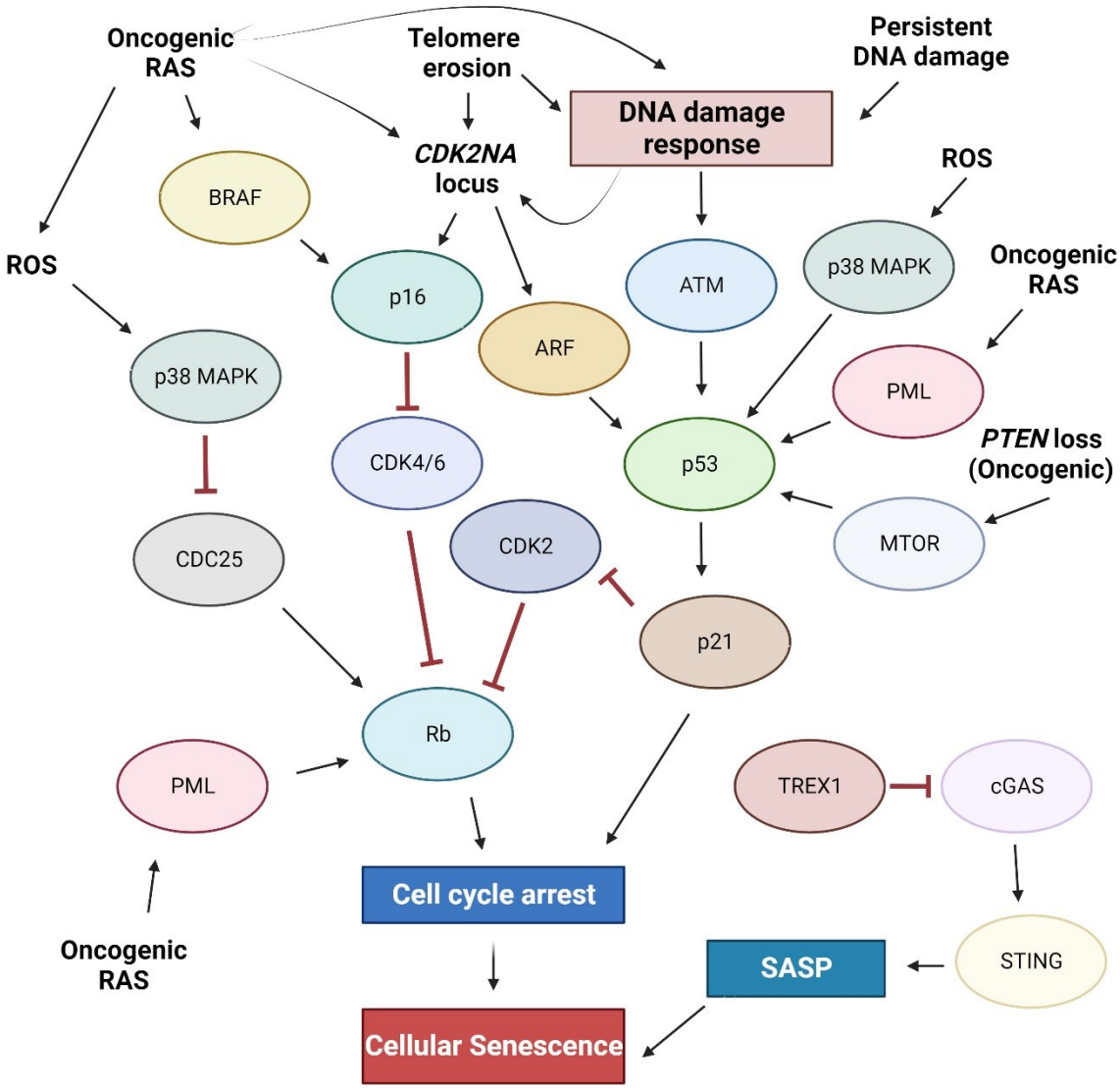

Figure 4.4. Overview of molecular pathways involved in cellular signalling, including p53, p16 and cGAS-STING. There are multiple pathways involved in senescence signalling but to initiate cell cycle arrest, the regulatory factors primarily function through p53 and Rb signalling pathways (Mijit et al., 2020; Ohtani et al., 2004; Salama et al., 2014). However, there is also crosstalk between p53 and Rb (via CDK2/p21). cGAS-STING is then involved in Senescence-associated secretory phenotype (SASP) that is required for cellular senescence (Schmitz, Maurmann, Guma, Bauer, & Barbé-Tuana, 2023).

PML NBs are important modulators of both cell-intrinsic senescence axes involved in senescence. In response to both *ras* signalling and replicative senescence, there is an increase in PML NB number and size, which promotes the activation of the co-localizing p53 and Rb proteins (Ferbeyre et al., 2000). The increased PML NB size and quantity are in part a result of increases in cellular zinc levels within senescent cells, that promote PML NB formation and function by enhancing SUMO-SIM interactions (as discussed in Section 1.2) (M. Lussier-Price et al., 2022). PML NBs also promote the expression of regulatory factors such as SOCS1 that regulates p53 function (Saint-Germain et al., 2017). A report has also shown that isoform-specific functions exist in senescence, where PML-IV isoform induces senescence (in a *ras*-independent manner) through the activation of p53 by promoting its phosphorylation at Ser46 and acetylation at Lys382 (Bischof et al., 2002). However, it appears that in general, PML NB induce senescence predominantly through the p16/Rb axis versus p53 (Mallette et al., 2004). Thus, PML NBs play an important role as a modulator of the senescence program.

The cell extrinsic element to cellular senescence is described as the Senescence associated secretory phenotype (SASP). While senescent cells are arrested from further proliferation, they are still metabolically active. SASP is a complex process where senescent cells secrete numerous proteins to alter the tissue microenvironment in a cell type dependent manner (Coppe et al., 2008; Maciel-Baron et al., 2016). The secreted material includes growth regulating modulators, angiogenic proteins, bioactive lipids, extracellular matrix components, matrix metalloproteinases, pro-inflammatory cytokines, chemokines. These secreted factors mediate an important cascade of reinforcing cell cycle arrest and recruiting immune cells for the clearance of senescent cells. Two

important secreted factors are NF-κB-dependent interleukin 6 (IL6) and interleukin 8 (IL8) that are key pro-inflammatory proteins capable of reinforcing senescence or inducing senescence in neighboring cells (i.e., both autocrine and paracrine) (Davalos et al., 2010; Freund et al., 2010; Hardy et al., 2005; Hopfner & Hornung, 2020; Soto-Gamez & Demaria, 2017; Hui Yang et al., 2017).

4.1.6 cGAS-STING function in senescence

An essential molecular axis that initiates SASP is the cGAS-STING pathway. Cytoplasmic DNA results from different stimuli in senescent cells that then activates cGAS-STING signalling. In age-related senescence, the expression of previously dormant L1 retroelements results in STING activation and senescence signalling (De Cecco, Ito, Petrashen, Elias, Skvir, Criscione, Caligiana, Brocculi, Adney, Boeke, Le, Beausejour, et al., 2019). This phenomenon has been termed “inflammaging”, and the age-related activation of endogenous retroelements such as LINE-1 in senescent cells can promote further aging by inducing additional IFN and inflammatory cytokine production through the cGAS-STING pathway (Andrade et al., 2022; Schmitz, Maurmann, Guma, Bauer, & Barbe-Tuana, 2023). In addition, in senescent cells, there can be dysfunction of mitochondria and consequent accumulation of reactive oxygen species that then induce cytoplasmic chromatin fragments that activate cGAS (Vizioli et al., 2020). A final known contributing stimulus to aging cells related to cGAS-STING is the disruption of nuclear integrity, where alterations to nuclear shape and the fragility of the nuclear envelope result in STING activation (Sladitschek-Martens et al., 2022). As cells senescence,

retroelements, mitochondria dysfunction, and disrupted nuclear integrity feeds result in cytoplasmic DNA that cGAS senses and responds to.

cGAS plays an essential role in relaying the cytoplasmic DNA and its absence in human cells prevents the expression of pro-inflammatory cytokines during senescence (H. Yang et al., 2017). Similarly, blocking STING activity in senescent cells abolishes the SASP and consequent inflammation from the absence of pro-inflammatory factors (Gulen et al., 2023; Takahashi et al., 2018). The STING-dependent activation of the NF-κB pathway and IRF3-dependent IFN signalling feeds into SASP as it generates the required factors for secretion. The secretion of IFNs through STING not only amplifies the immune response to promote the clearance of senescent cells in tissue but also reinforces senescence signalling (Frisch & MacFawn, 2020). Thus, cGAS senses the accumulating cytoplasmic DNA in senescent cells to activate STING, which induces IFN and pro-inflammatory signalling in these cells for SASP.

Typically, cytoplasmic DNA is removed by TREX1 (and additional exonucleases such as DNASE2) but in senescent cells, these clearance exonucleases are downregulated to promote STING-induced SASP (Takahashi et al., 2018). The downregulation of TREX1 in senescent cells occurs in response to the actions of E2Fs (E2F1 and E2F3) and oncogenic Ras signalling (Takahashi et al., 2018). *TREX1* knockout mice have been shown to have an extreme response to senescence-inducing stimuli, such as ionizing radiation, where they accumulate a significantly higher number of senescent cells. In addition, *TREX1* knockout mice have high expression levels of SASP factors, such as IL-6, IL-8, p16, matrix metalloproteinases, and IL-1β (Takahashi et al., 2018). In senescent cells, the accumulation of cytoplasmic DNA occurs by: (i) stimuli in the form of L1,

aberrant mitochondria, or disrupted nuclear morphology and then (ii) downregulation of the exonucleases that remove cytoplasmic DNA, to finally (iii) activate cGAS-STING signalling to induce SASP. The three-step process is critical for the SASP through cGAS-STING. When these steps are dysregulated, it results in aging-related inflammation, neurodegeneration, and multiple disorders (e.g., Diabetic retinopathy and Huntington's disease) where the pathway promotes premature senescence (Gulen et al., 2023; Jauhari et al., 2020; H. Liu et al., 2023).

Similar changes in inflammatory gene expression have also been observed in zebrafish, where immune cells accumulate in elderly animals in response to STING, with numerous chemokines being upregulated (Reuter et al., 2022). Zebrafish hearts appear to accumulate senescent cells and have gene signatures reminiscent of SASP. Intriguingly, while senescent cells that occur from aging reduce regenerative capacity, this is not the case after the on-set of regeneration (Reuter et al., 2022).. In axolotl, it was shown that senescence signalling and the formation of senescent cells after injury helps promote limb regeneration by inducing progenitor cell proliferation (Yu et al., 2023). It is possible that this is similar to what occurs in the mammalian gut where STING-induction and IFN signalling promotes intestinal progenitor cell proliferation (Leibowitz et al., 2021). However, the mechanisms behind STING activation in these fish during age-related senescence is unknown. It is possible that there are similar changes to Plex9.1 gene expression, the teleost fish equivalent of TREX1, to facilitate these changes in cGAS-STING activity.

In this chapter, I survey the expression of inflammatory genes in three different anamniote species, including fin and limb regeneration in the non-teleost fish spotted gar (*Lepisosteus oculatus*) and the amphibian axolotl (*Ambystoma mexicanum*), and during zebrafish (*Danio rerio*) cardiac aging. In aquatic vertebrates, the promyelocytic leukemia (Pml) protein and newly discovered DEDDh exonucleases known as PML-like exon 9 (Plex9) proteins can suppress the cGAS-STING pathway through their exonuclease function and through the suppression of LINE-1, akin to mammalian TREX1. Our results indicate that Pml, Plex9.1, and Trex1 share strikingly similar gene regulation in these aquatic vertebrate species during regeneration and aging, where they are downregulated to promote cGAS-STING activity and downstream pro-inflammatory signalling. This suggests an evolutionary old function of cGAS-STING program that evolved in a fish ancestor of living jawed vertebrates, if not earlier.

4.2 Materials and Methods

4.2.1 Cell Lines and 2'3'-cGAMP treatment

Previously derived cell lines from the longnose gar, *Lepisosteus osseus* (GARL, liver derived fibroblasts (Fuguo Liu, Niels C Bols, et al., 2019), axolotl (AL-1 limb dermal fibroblast derived cell line (Denis et al., 2015)) and zebrafish (ZKS, zebrafish kidney stromal cells (Stachura et al., 2009)) were used. Gar-L cells were maintained in Leibovitz L15 (L-15) medium supplemented with 10% newborn bovine calf serum (NCBS, New Zealand origin, ThermoFisher), and 1% Pen/Strep (100 U/ml penicillin and 100 μg/mL streptomycin) in CO2-independent and dark conditions. AL-1 cells were grown in a mixed media (62.5% MEM (Gibco) and 25% water) with 10% fetal bovine serum (ThermoFisher) supplemented with 100 U penicillin-streptomycin, glutamine, and insulin within a humidified incubator at 25°C with 2% CO2. ZKS cells were maintained in culture media consisting of 10% fetal bovine serum (FBS; ThermoFisher), 55% L-15, 32.5% Dulbecco modified Eagle medium (DMEM) (Gibco) and 12.5% Ham F-12 (Gibco). ZKS media was supplemented with 150 mg/L sodium bicarbonate, 2% penicillin/streptomycin (10 U/mL stock), 1.5% N-2-hydroxyethylpiperazine-N′-2-ethanesulfonic acid (HEPES), 1% l-glutamine and 0.1 mg/mL gentamycin. ZKS cells were grown at 32°C and 5% CO2. 2′3′-cGAMP (InvivoGen) was transfected into cells using Lipofectamine 2000 (Invitrogen) or JetPRIME (PolyPlus) at 100ng or 2 μg. Untreated cells received the Lipofectamine 2000 or JetPRIME lacking 2′3′-cGAMP. All cell lines were passaged at a 1:2 split when cells reached 80-90% confluency. For conditioned media experiments, cells were transfected, and then media was collected 48

hours later. The conditioned media was added to fresh media at a ratio of 1:1 and the naïve cells were incubated for 24 hours, after which, RNA was collected.

4.2.2 Regeneration experiments

Spotted Gar (n-12, 19-25cm standard length) were anesthetized in 160mg/L MS-222 (Sigma) and caudal fins were amputated via a vertical cut using the ventral apex as a landmark to begin the cut. This amputated, posterior part of the caudal fin from 0dpa was put in RNA later and stored at -80C. Gar with amputated fins were monitored until a time of secondary sampling at 7dpa (n=4), 16dpa (n=4), and 32dpa (n=4) upon which time the regenerating caudal fin was sampled under anesthesia by via another vertical cut anterior to the initial 0dpa cut site. This resulted in a thin strip of fin tissue (up to ~1cm in width) that contained original caudal fin tissue as well as all regenerated tissue up to that time point. All 7dpa, 16dpa, and 32dpa tissues was put in RNA later and stored at -80C. All gars were euthanized at the end of the experiment in 300mg/L MS-222. Day 0 samples were collected for all animals and then matched to the animals for each timepoint when regenerating tissue was later collected. Thus, we refer to day 0 as Amputated Fin (AF) for each individual animal and the re-sampled regenerative blastema as Regenerative Blastema (RB) throughout the thesis.

The axolotl limbs were amputated at the level of the zeugopod (forearm, through the radius and ulna bones) under anesthesia using buffered MS222 0.1X dissolved in 40% Holtfreter's solution. Blastema from the regenerating limb were then isolated at different

stages of the regenerating bud (early - ~6 days post amputation; medium – 8-9 days post amputation; late - 10-12 days post amputation)(Stocum, 1979).

4.2.3 RNA extractions from isolated tissue

Dissected tissues were lysed and homogenized using Trizol reagent (Thermo) according to the manufacturer's directions and frozen at -80°C for further analysis. Blastema RNA from gar and axolotl were isolated from single tissue samples. Hearts were pooled from 3 animals for zebrafish samples. Zebrafish included young adult (6-10 months post fertilization) and aged (20-24 months post fertilization) cohorts. The samples were then processed for RNA using the Ambion PureLink RNA Mini Kit (Thermo) according to the manufacturer's protocol and an on-column DNase I digestion. Quality and quantity of RNA was measured using a Nanodrop 2000 spectrophotometer (Thermo). Absorbance measurements A260/A280 and A260/A230 with ratios ~2.0 were accepted for downstream analysis by RT-qPCR.

4.2.4 RT-qPCR

cDNA was generated from 1 µg of RNA (for axolotl) or 500 ng of RNA (for zebrafish and spotted gar) using the BioRad 5X iScript RT supermix kit (BioRad Laboratories Canada; Mississauga, ON, CA) for RT-qPCR, after which samples were diluted 1:1 with nuclease-free water. Control samples lacking reverse transcriptase were included to confirm no genomic DNA contamination. Quantitative PCR (qPCR) was performed on cDNA samples using the 2X SsoAdvanced Universal SYBR Green

Supermix (BioRad). The reactions were performed using BioRad CFX Connect and all experiments were done in triplicate. Primers were designed using NCBI Primer Blast (**https://www.ncbi.nlm.nih.gov/tools/primer-blast/**). Gene expression data were normalized to at least two reference genes from each species (spotted gar –*actb* and *gapdh*; axolol – *gapdh* and *rpl4*; zebrafish - *rplp0* and *actb1*) and analyzed using the BioRad CFX Maestro Software. Data were collected and analyzed as per the MIQE guidelines (Bustin et al., 2009).

4.2.5 2'3'- cGAMP quantification

Gar blastema and axolotl blastema were weighed, washed 3x with PBS and then lysed using M-PER (Thermo Scientific). Individual zebrafish hearts were washed 3x with PBS, homogenized using a grinder and then lysed using M-PER. Lysates were incubated on ice for 30 minutes with gentle agitation every 10 minutes, before being spun down with 16,000 x g at 4° C for 10 min. Samples were quantified using a 2′3′-cGAMP ELISA kit (Cayman Chemical) according to the manufacturer's instructions.

4.2.6 Immunohistochemistry

For immunofluorescence assessment of the presence and distribution of γ-H2AX in the zebrafish heart, ventricles were isolated from zebrafish expressing eGFP under the myocyte-specific *myl7* promoter (*tg(myl7:eGFP)*) for visualisation of the cardiac musculature. As previously described (Stoyek et al., 2018), the hearts were fixed overnight in 4% paraformaldehyde (Electron Microscopy Sciences) with 1% DMSO

(Sigma-Aldrich) in phosphate-buffered saline (Sigma-Aldrich). The hearts were then rinsed three times for 15 min each in PBS and transferred to a solution containing 0.1% Triton X-100 (PBS-T; T9284, Sigma-Aldrich) in PBS with mouse monoclonal anti-H2a.x (1:100; JBW301; Millipore) and incubated for 3 days with agitation at 4ºC. Tissues were rinsed three times for 15 min each in PBS-T and transferred to PBS-T containing the appropriate secondary antibody (1:300, AlexaFluor555; A-21429, Fisher Scientific) for 2 days with agitation at 4ºC. Final rinsing was done in PBS and specimens were placed in Scale CUBIC-R1 clearing solution (Susaki et al., 2014) overnight at room temperature with gentle agitation. Ventricles were sectioned roughly in half with midline cut on the axial plane and hearts were then mounted on glass slides in CUBIC-R1 for confocal microscopy. Processed specimens were examined as whole-mounts using an LSM 710 confocal microscope using Zeiss Zen software (Carl Zeiss, Toronto, Canada). **These immunostainings were done by the Quinn lab.**

4.2.7 Animal ethics

Spotted gar work was approved by the Institutional Animal Care and Use Committee at Michigan State University (protocol no. PROTO201900309). All the experiments done with axolotls were approved by the Université de Montréal institutional animal care committee in accordance with the Canadian Council on Animal Care. All experimental procedures with zebrafish were approved by the Dalhousie University Committee for Laboratory Animals (protocol number 20-074) and followed the guidelines of the Canadian Council on Animal Care.

4.2.8 Statistical analyses

For statistical analyses between groups of 3 or more (for gar, axolotl and cell line experiments), significance was determined using a One-way ANOVA, with Tukey's post-hoc analysis used for comparison. For zebrafish aging experiments where comparison was made between 2 cohorts, significance was determined using a Student's t-test (two-tailed). All statistical analyses were completed using GraphPad Prism 9.

4.3 Results

4.3.1 Immune signalling is upregulated in the early stages of gar caudal fin regeneration

The spotted gar is capable of fin regeneration, where it is able to completely regenerate a functional, innervated fin even after the injury to the endoskeleton (**Figure 4.5A**) (Darnet et al., 2019). However, it is unknown as to what role innate immune signalling plays a role in promoting fin regeneration in the organism. The spotted gar genome encodes IFN genes which are stimulated in response to stimuli mimicking an antiviral response such as poly(I:C) (F. Liu et al., 2019). I therefore assessed during spotted gar fin regeneration if the gar IFN related genes were upregulated and if this corresponded to changes in cGAS-STING expression. Regenerative blastema isolated from spotted gar at various stages of caudal fin regeneration were examined and assessed for innate immune signalling associated genes in terms of expression (**Figure 4.5A**). There were changes to Ifn genes such as *ifnb* and *ifnc1*, which were upregulated ~98-fold and ~96-fold respectively at the earliest stage of 7 days post-amputation (7 dpa) (**Figure 4.5B**). In addition, orthologs of inflammatory interleukins Il6 and Il8, were also found to be significantly upregulated 7 dpa in the regenerative blastema. By 16 dpa, *ifnb, ifnc1*, *il6* and *il8* returned to baseline levels. Both IFN and inflammatory signalling pathways are upregulated initially during spotted gar fin regeneration but eventually return to baseline expression levels over the course of regeneration. Thus, in gar, regeneration occurs in phases, and the early phase relies on gene expression changes to the innate immune signalling pathway.

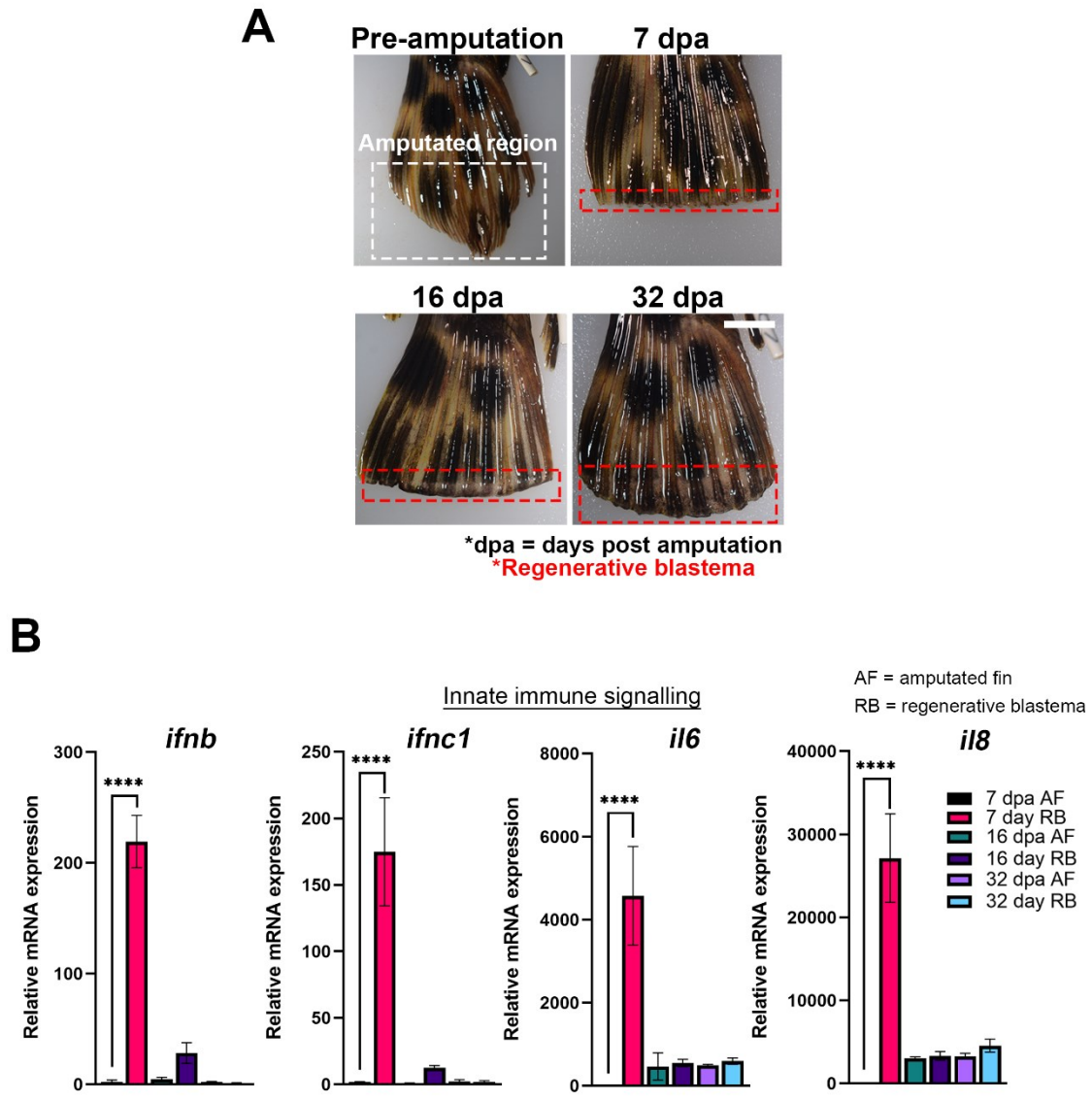

Figure 4.5. Early-stage gar regenerative blastema transition into a pro-inflammatory state. (A) Spotted gar caudal fins were amputated, and regeneration was observed over a 32-day period, with regenerative blastema being collected at the indicated timepoints for molecular analysis. Scale bar indicates 1 cm **(B)** Interferons and Interleukins are upregulated in blastema at 7dpa before returning to baseline levels (n=3). Gene expression of *ifnb, ifnc1, il6* (Interleukin 6), and *il8* (Interleukin 8-like) was assessed and significantly different from the original amputated fin (AF) only a 7 dpa. Variation between groups was assessed with a one-way ANOVA, with Tukey's post-hoc analysis for pairwise comparison between groups. ****$p < 0.0001$

cGAS-STING is a conserved regulator of type I IFNs and interleukins such as IL6 and IL8 in mammals (Chernyavskaya et al., 2017; Ge et al., 2015; Glück et al., 2017). cGAS-STING predates IFN evolution, as IFNs emerged in jawed vertebrates in contrast to cGAS-STING genes that are present in invertebrate genomes and involved in NF-κB signalling (Martin et al., 2018; Secombes & Zou, 2017). The cGAS-STING pathway is conserved, and the involved machinery can be identified in the gar genome (**Figure 4.6A**). Then, cGAS activity was measured in the gar model by measuring the levels of 2′3′-cGAMP, the product of cGAS. Consistent with cGAS-STING activation, the 7 dpa blastema had significantly elevated amounts of 2′3′-cGAMP (**Figure 4.6B**). However, the expression of cGAS and STING orthologs in the gar fin regenerative blastema did not significantly change. The gar Plex9.1 or PML proteins likely function as the suppressor of the cGAS-STING pathway based on our previous work (Chapter 2 and Chapter 3) (Mathavarajah et al., 2023). The expression of suppressor proteins of cGAS activity in gar, Plex9.1 and Pml was also surveyed. There were no changes to *plex9.1* expression, there was a ~8-fold reduction in *pml* gene expression at 7 dpa (**Figure 4.6C)**. Thus, it appears that *pml* expression is reduced to facilitate cGAS activity in gar blastema during the early stages of regeneration.

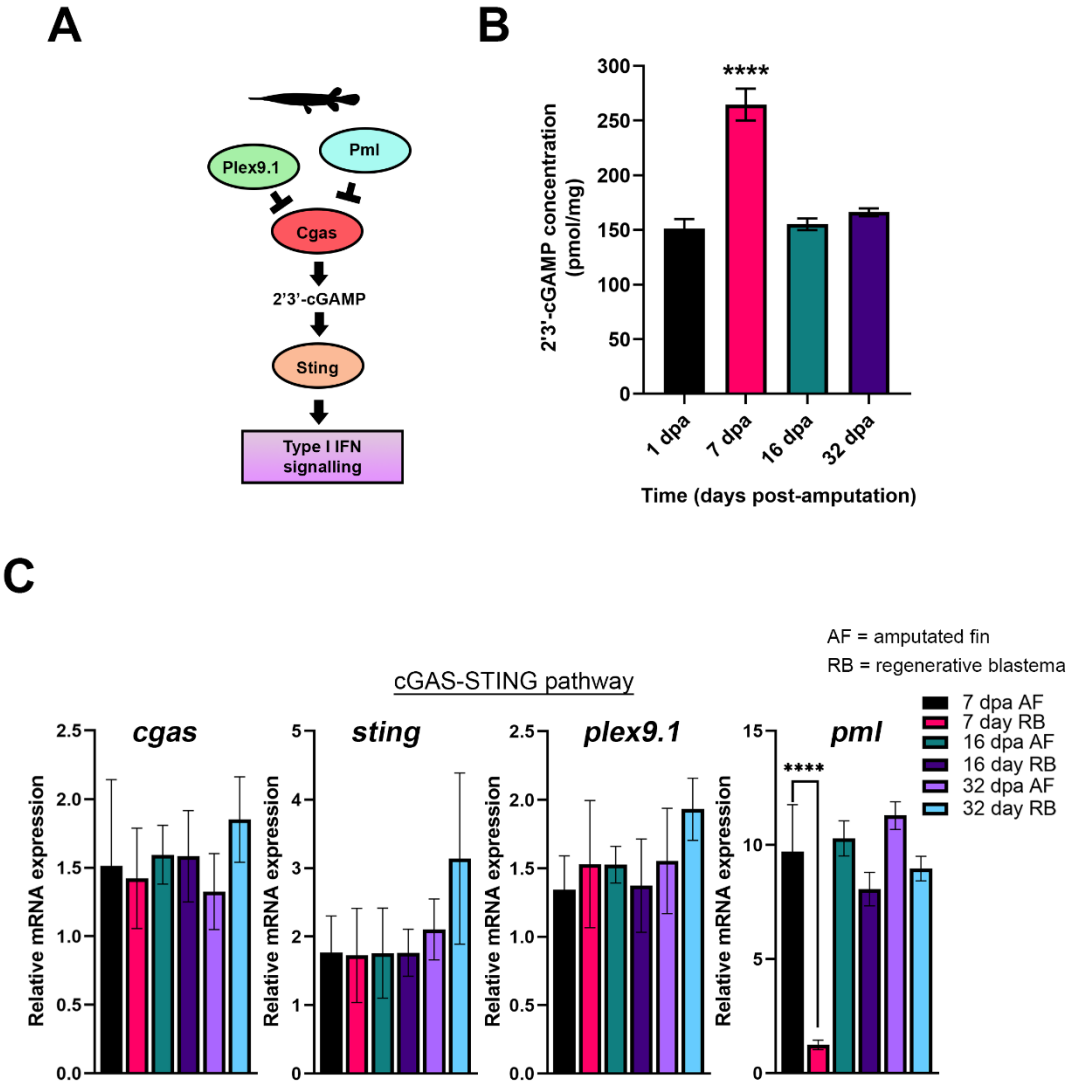

Figure 4.6. cGAS activity is upregulated in the early stages of gar regenerative blastema. (A) Overview of the cGAS-STING pathway in the spotted gar. **(B)** 2'3'-cGAMP levels are elevated specifically at 7dpa in regenerative blastema. 2'3'-cGAMP concentrations were determined from the same caudal fins used for RNA isolation. **(C)** Gene expression analysis of cGAS-STING pathway orthologs in gar indicate that *pml* is downregulated to facilitate immune signalling via the cGAS-STING axis. Variation between groups was assessed with a one-way ANOVA, with Tukey's post-hoc analysis for pairwise comparison between groups. ****$p < 0.0001$

4.3.2 Cross-species conservation of cGAS-STING activation in early stages of regeneration

I next examined inflammatory gene expression, cGAS-STING activity, and the expression of cGAS suppressors during axolotl limb regeneration. First, the gene expression of axolotl *il6* and *il8* was measured in tissue isolated from regenerating axolotl (**Figure 4.7A**) at the early stages of regeneration (timepoints of 0h, 6h, 24h, 48h, 96h) and at three major stages of limb regeneration (i.e. the early, medium and late bud stage) (**Figure 4.7B**). Intriguingly, *il8* was significantly upregulated within the first 48 hours of regeneration and remained elevated throughout the medium and late bud stage **Figure 4.7B**). In contrast, *il6* was upregulated within 96 hours (**Figure 4.7B**) and remained elevated only through the early bud stage. Axolotl have a similar cGAS-STING axis as the spotted gar but differ in the suppressor involved, where the axolotl genome does not encode *plex9.1* or *pml* orthologs and *Trex1* plays this role. Next, cGAS activity was assessed and there were elevated levels of 2′3′-cGAMP strictly during the early bud stage of limb regeneration (**Figure 4.8B**). Like the gar regenerative blastema, there were no significant changes in the expression of axolotl *cgas* or *sting* during the 4 days of wound healing or at the different limb bud stages (**Figure 4.8C**). The gene expression of axolotl Trex1 was also examined, as axolotl TREX1 suppresses axolotl cGAS-STING, like in mammals (**Figure 4.8C**). There was a significant and immediate ~48-fold decrease in *Trex1* gene expression in the blastema within 6 hours of limb removal, with *Trex1* expression only restored at the late bud stage (**Figure 4.8C**). Collectively, these data indicate that during limb-fin regeneration, Trex1 and Pml, appear to be downregulated to promote type I IFN signalling during regeneration in axolotl and gar, respectively.

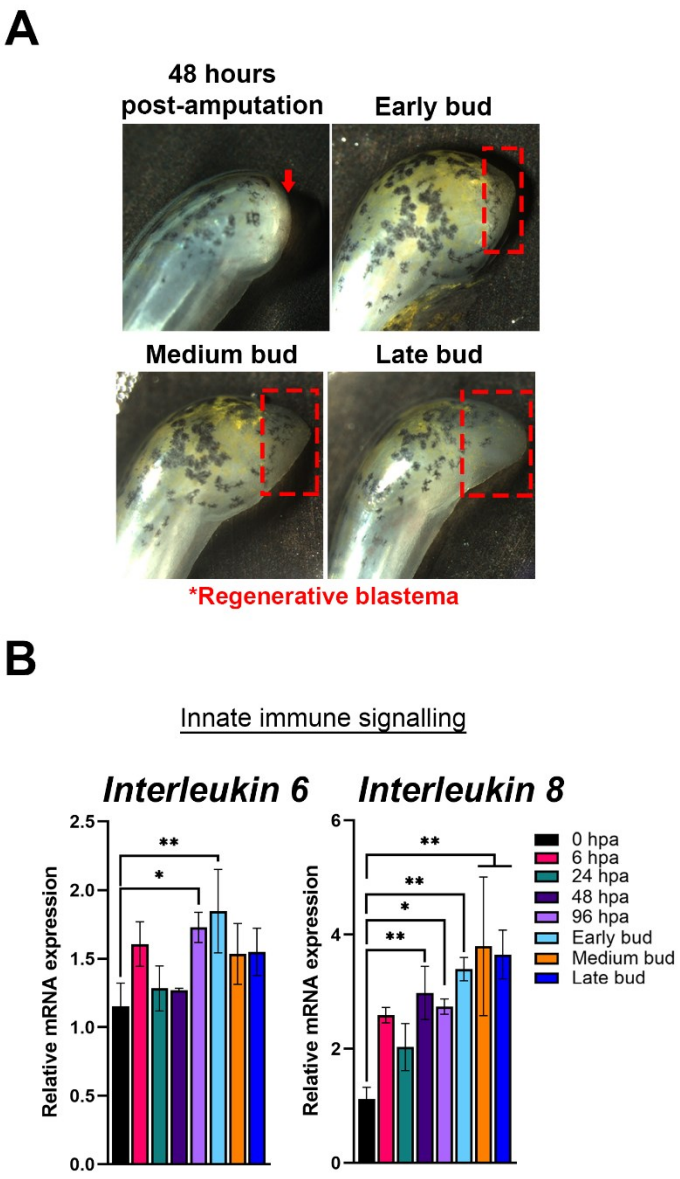

Figure 4.7. *Il6* and *Il8* are upregulated during axolotl limb regeneration. (A) Axolotl limbs were amputated at the level of zeugopod and regeneration was observed at different stages of limb regeneration. **(B)** An increase in the expression of interleukin 6 (*Il6*) and interleukin 8 (*Il8*) was observed in the early stages of axolotl limb regeneration. Blastema from the regenerating limb was isolated within the first 96 hours and then at three different stages of limb regeneration (early, medium, and late bud). Variation between groups was assessed with a one-way ANOVA, with Tukey's post-hoc analysis for pairwise comparison between groups. *$p < 0.05$, **$p < 0.01$

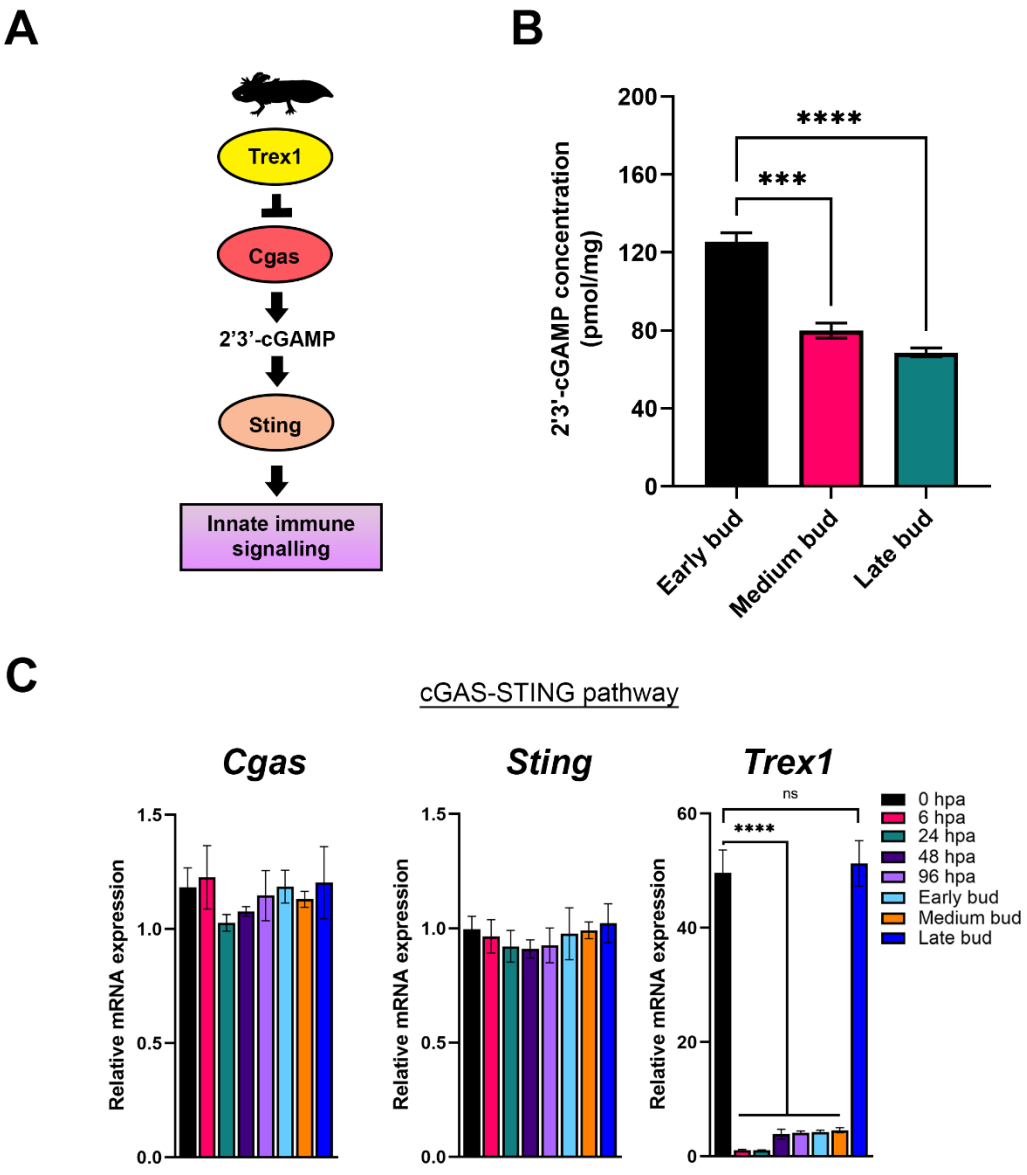

Figure 4.8. Trex1 is downregulated in the limb regenerative blastema of axolotl. (A) Overview of the cGAS-STING pathway in the axolotl. **(B)** 2'3'- cGAMP levels are elevated in the early bud of the regenerating axolotl limb. 2'3'-cGAMP concentrations were determined from the same axolotl regenerative blastema used for RNA isolation. **(C)** Gene expression analysis of the cGAS-STING pathway orthologs in axolotl indicate that *Trex1* is downregulated during the stages of regeneration where cGAS activity is elevated. Variation between groups was assessed with a one-way ANOVA, with Tukey's post-hoc analysis for pairwise comparison between groups. ***$p < 0.001$, ****$p < 0.0001$

4.3.3 Plex9 enzymes have elevated expression in the cardiac tissue of aged fish

The Plex9.1 enzyme is also capable of suppressing cGAS-STING (Mathavarajah et al., 2023); however, there was no significant changes in Plex9.1 expression during gar regeneration. Therefore, I sought to determine if Plex9.1 may be differentially regulated to influence cGAS-STING signalling in another biological process, such as aging. During aging, the cGAS-STING pathway promotes SASP and inflammatory cytokine expression that underlies cellular senescence (Hui Yang et al., 2017). However, since the spotted gar is collected from wild spawns, we used the laboratory spawned and maintained zebrafish model for comparing young versus elderly fish. Another experimental advantage of the zebrafish and other teleost fishes is a lack of orthologs for either Pml and Trex1 (Mathavarajah et al., 2023), making it an ideal model to observe *plex9.1* gene expression and its impact on cGAS-STING activity without overlapping contributions of Pml and Trex1 to cGAS suppression.

Zebrafish Plex9.1 expression is highest in the adult heart (data not shown) and for that reason, I used hearts from young and elderly zebrafish as our model for studying cGAS-STING in senescence. When hearts of aged zebrafish were examined for STING-dependent immune signalling genes, there were elevated levels of *ifnphi1*, *il8* and *isg15* (**Figure 4.9A**). Similarly, markers of senescence such as *p21* and *p53* were also upregulated in the hearts of elderly fish (**Figure 4.9B**). In addition, γH2AX, a cellular senescence marker, is upregulated in the elderly fish cardiomyocytes (**Figure 4.9C**).

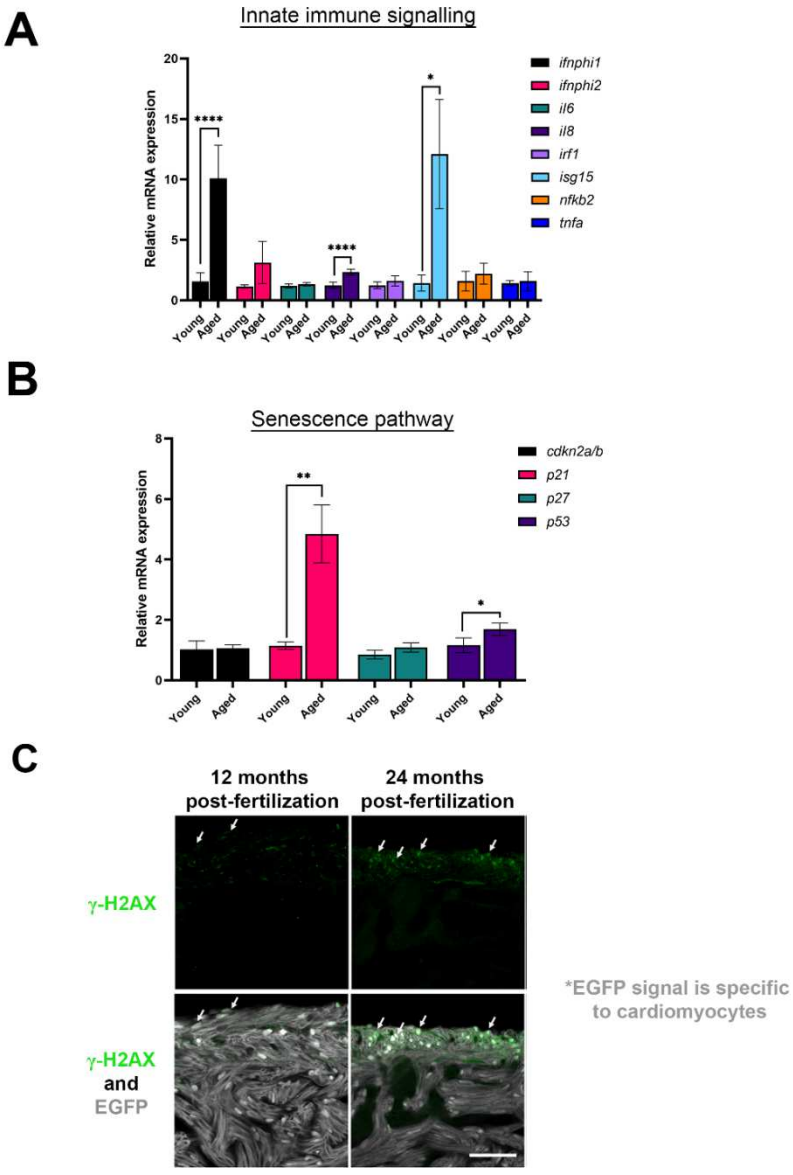

Figure 4.9. Hearts from elderly zebrafish have elevated gene expression associated with innate immunity and senescence. (A, B) Gene expression analysis of zebrafish hearts from young and aged cohorts shows differences in innate immune signalling markers **(A)** and senescence markers **(B)**. **(C)** γ-H2AX foci, a marker of senescence are present in a greater abundance of cells in the hearts of elderly zebrafish. Myocytes were visualized using a *tg(myl7:eGFP)* reporter that the transgenic animals express. Scale bar is 50 µm. Variations between animal cohorts was assessed with a one-way ANOVA, with Tukey's post-hoc analysis for pairwise comparisons between groups. *$p < 0.05$, **$p < 0.01$, ****$p < 0.0001$. ***Data presented in panel C was collected by the Quinn lab.***

cGAS-STING has been shown to contribute to the antiviral response in zebrafish to prevent HSV infection by promoting type I IFN activation (Ge et al., 2015). I wanted to determine if the pathway is also involved in fish age-related senescence by promoting IFN gene expression and senescence signalling (i.e., through *il8*). When cGAS activity was examined in hearts from young versus aged zebrafish, there was significantly increased levels of 2′3′-cGAMP in the hearts from aged animals (**Figure 4.10A**). However, like with limb-fin regeneration in the gar and axolotl, there were no significant changes in either *cgasa* or *sting1* expression relative to age (**Figure 4.10B**), and *cgasb* expression was not detected in cardiac tissue (data not shown). I previously showed that Plex9.1 suppresses cGAS activity akin to TREX1 (Chapter 2). In contrast to *cgasa* and *sting1*, there was a ~68-fold drop in *plex9.1* expression between the young and aged zebrafish hearts (**Figure 4.10B**). These results indicate that cGAS activity increases in the hearts of elderly zebrafish, in part due to the downregulation of Plex9.1 expression.

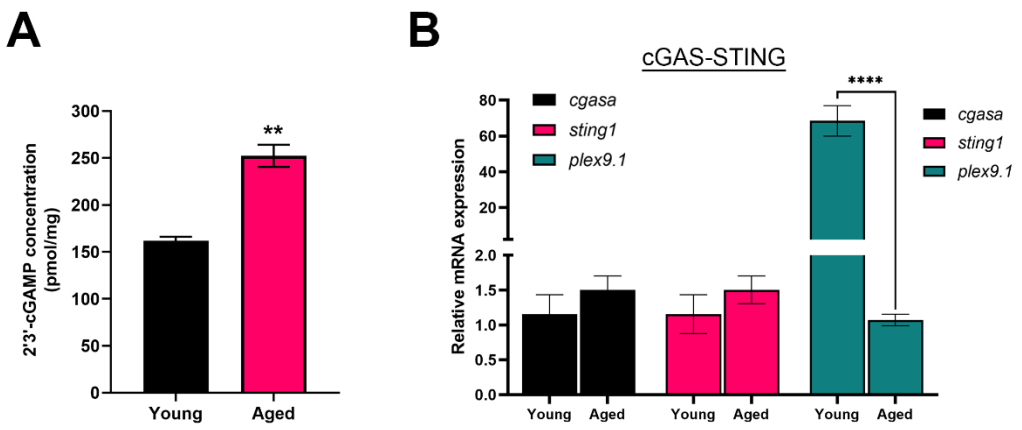

Figure 4.10. cGAMP is elevated in hearts from elderly zebrafish and regulates the expression of *pml, Trex1,* and *plex9.1*. (A) cGAS activity is elevated in the elderly zebrafish. 2'3'-cGAMP concentrations were determined from individual hearts isolated from young and aged zebrafish. **(B)** Gene expression analysis of the cGAS-STING pathway orthologs in axolotl indicate that *plex9.1* expression is reduced in hearts from aged zebrafish. *cgasb* expression could not be detected in the zebrafish heart samples. **(f)** Treating cell lines derived from gar (GARL), axolotl (AL1) and zebrafish (ZKS) with cGAMP altered expression of the different cGAS suppressors. Gene expression in zebrafish hearts was compared with an unpaired, two-tailed Student's t-test (two-tailed). Variations between animal cohorts was assessed with a one-way ANOVA, with Tukey's post-hoc analysis for pairwise comparisons between groups. **$p < 0.01$, ****$p < 0.0001$

4.3.4 Pml, Plex9.1 and Trex1 are downregulated in response to 2′3′-cGAMP

Since spotted gar *pml* and axolotl *Trex1* expression is reduced during the early stages of fin and limb regeneration, and zebrafish *plex9.1* expression is reduced in the cardiac tissue of aged zebrafish, I hypothesized that 2′3′-cGAMP may play a feedback role in controlling the expression of these suppressors of cGAS-STING. To address this hypothesis, cell culture models derived from gar, axolotl, and zebrafish (GARL, AL-1 and ZKS cells, respectively) were employed to decipher which stimuli alter *pml*, *Trex1* and *plex9.1* expression. Cells were transfected with 2′3′-cGAMP at low (100 ng) and high (2 µg) concentrations to activate the cGAS-STING pathway and examined gene expression of the exonucleases. The two concentrations of cGAMP provide an idea of how different levels of the molecules on the spectrum (like during different stages of regeneration), influence gene expression. However, it is not a direct corollary for STING activation. In gar, axolotl, and zebrafish cells, *pml*, *Trex1* and *plex9.1* gene expression (respectively) decreased in response to low 2′3′-cGAMP levels (**Figure 4.11**). However, at higher concentration of 2′3′-cGAMP, the expression of all three enzymes significant increased (**Figure 4.11)**. Thus, 2′3′-cGAMP levels and therefore resulting activity of cGAS, directly impacts the gene expression of *pml, Trex1* and *plex9.1*.

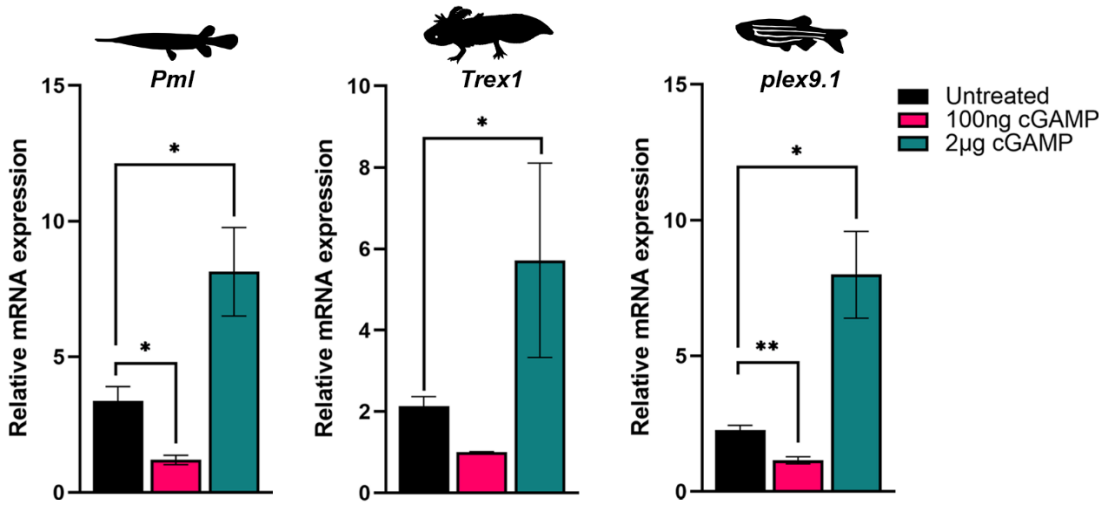

Figure 4.11. cGAMP can regulate the expression of *Pml*, *Trex1* and *plex9.1*. Treating cell lines derived from gar (GARL), axolotl (AL1) and zebrafish (ZKS) with cGAMP altered expression of the different cGAS suppressors. Gene expression in zebrafish hearts was compared with an unpaired, two-tailed Student's t-test (two-tailed). Variations between treatment groups was assessed with a one-way ANOVA, with Tukey's post-hoc analysis for pairwise comparisons between treatments. *$p < 0.05$, **$p < 0.01$

I also further examined if the cGAMP response was cell intrinsic or had a paracrine signalling component in the three species. For these experiments, *interleukin 8* (*Il8*) expression was utilized as it was significantly upregulated in response to aging and regeneration across the three species, and in response to low dose 2′3′-cGAMP treatment (**Figure 4.12**). Consistent with a paracrine component to the cGAMP response, conditioned media from transfected cells when applied to naïve untreated cells, induced a significant increase in *Il8* expression in the gar, zebrafish and axolotl cells (**Figure 4.12**). There was no significant difference between incubation with conditioned media and transfection with 2′3′-cGAMP for zebrafish and axolotl (**Figure 4.12**). However, while there was a ~15-fold increase in *il8* expression in response to cGAMP treatment in gar cells, conditioned media elicited an attenuated but significant increase of only ~5 fold (**Figure 4.12**). Although the reason for the reduced *il8* induction in gar cells treated with conditioned media is unclear, it is worth noting that gar cells are grown at room temperature, which could affect the secretion of paracrine factors.

The observation of cGAS activity in the different species indicate: (1) during regeneration and age-related senescence there is a robust upregulation of gene expression programs that promote inflammation and interferon signalling, (2) cGAS is active during tissue regeneration and age-related senescence, (3) the increase in cGAS activity is likely a consequence of DEDDh exonucleases such as Pml, Plex9.1 and Trex1 being downregulated during limb-fin regeneration and aging (**Figure 4.13**). Thus, there exists a role for these DEDDh exonucleases in the regulation of limb-fin regeneration and aging via cGAS-STING.

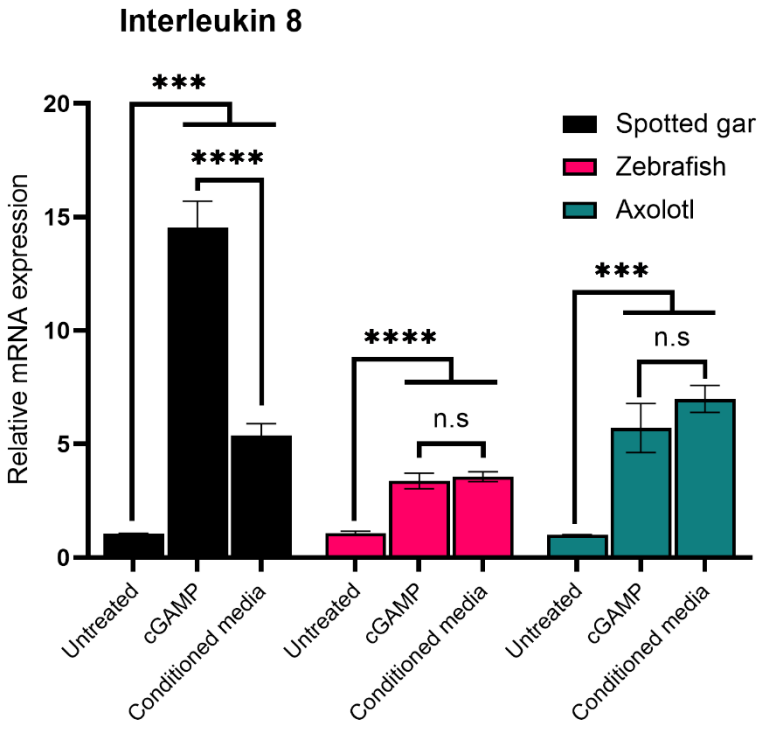

Figure 4.12. Conditioned media from cGAMP treated cells induces the upregulation of interleukin 8. Gene expression analysis of interleukin 8 orthologs in gar, axolotl, and zebrafish cell lines after transfection with 2'3'-cGAMP (100 ng) or with conditioned media. The conditioned media was obtained from each cell line 48 hours after 2'3'-cGAMP transfection and added to naïve cells with fresh media (1:1 ratio), then expression was analyzed 24 hours post-treatment. Variation between groups was assessed with a one-way ANOVA, with Tukey's post-hoc analysis for pairwise comparison between groups. ****$p < 0.0001$, ***$p < 0.001$

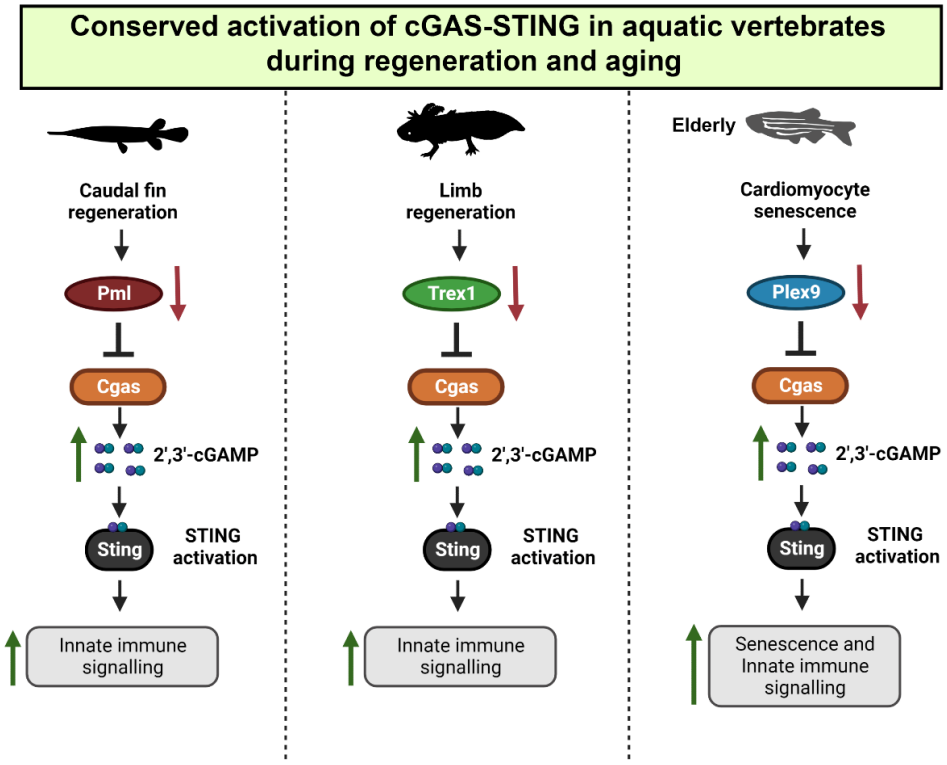

Figure 4.13. Summary of how cGAS-STING is regulated during limb-fin regeneration and senescence in aquatic vertebrates. Innate immune signalling is important for facilitating regeneration and age-related senescence in aquatic vertebrates. cGAS activity is upregulated to promote these pathways in the three different vertebrate species during these biological processes. To facilitate the upregulation of cGAS activity, DEDDh exonucleases such as Pml, Trex1 and Plex9, that typically suppress cGAS, are downregulated.

4.4 Discussion

The spotted gar was recently shown to be capable of regenerating its caudal fin after amputation to the endoskeleton (Darnet et al., 2019). In axolotl, a similar regenerative blastema is associated with activation of innate immune signalling (Darnet et al., 2019), however, it is unclear whether activation of innate immune signalling in regenerative blastema is conserved across species. During the early stages, regenerative blastema in the spotted gar and axolotl share similarities in the transcriptional changes that promote STING-dependent immune signalling during regeneration. Specifically, Il6 and Il8, two key cytokines expressed in response to STING activation are upregulated in both gar and axolotl regenerative blastema. IL-8 was recently shown to be essential for axolotl limb regeneration (Tsai et al., 2019), and IL-6 is a well-established factor involved in mammalian liver regeneration, which has been shown to also be involved fin regeneration in axolotl and bichir (Streetz et al., 2000). The similar upregulation of both in early gar fin regeneration seen in the current study suggests that STING activity is increased by cells at the site of injury in a conserved program across bony vertebrates, which corresponds to an increase in 2′3′-cGAMP in gar blastema. Therefore, there is conserved reprogramming of regenerative blastema towards a highly active innate immune signalling state in the early stages of spotted gar fin regeneration, similar to what has been observed in other species capable of regeneration.

IFN genes likely arose in the earliest jawed vertebrates, as these genes are present in extant cartilaginous and bony fish (Redmond et al., 2019). Paralogous genes representing all three IFN subgroups (I-III) can be found in the spotted gar genome (Braasch et al., 2016) In a gar cell line, IFNc1 but not IFNb paralogs are upregulated in

response to viral mimicry using poly (I:C) treatment that activates IFN gene expression *via* the retinoic acid inducible gene I (RIG-I) pattern recognition receptor and the mitochondrial antiviral signalling protein (MAVS) (Fuguo Liu, Niels C. Bols, et al., 2019). However, here, both IFNc1 and IFNb are expressed in the regenerative blastema, which is regulated by cGAS activation. Thus, in gar it appears that IFNc1 responds to both viral mimicry and fin damage, whereas IFNb expression is specific to wound healing and cGAS activation. In the future, it will be of interest to determine if these differences in IFN gene regulation can be exploited to further explore the evolutionary conservation of specialized innate immune responses to different cell stresses (viral infection, DNA damage, wound healing) and their corresponding pattern recognition receptors in early jawed vertebrates.

In fishes, the cGAS-STING pathway has been shown to play an important role in their antiviral and antibacterial immune responses (de Oliveira Mann et al., 2019a; Liu et al., 2020; Sellaththurai et al., 2023). Our results extend these observations to the conservation of cGAS-STING function in tissue regeneration and aging. Moreover, this work provides the first data regarding the regulation of key suppressors of cGAS (Pml, Trex1 and Plex9.1) in jawed vertebrates during wound healing and aging. Specifically, during ray-finned fish and amphibian fin and limb regeneration, the expression of *pml*, *Trex1* and *plex9.1* is tied to the activity of cGAS, providing a potential feedback mechanism to potentiate or dampen downstream IFN gene regulation (Figure 3). Importantly, how bony vertebrate cells respond to stress in the form of a wound or aging appears to rely on the initial downregulation of these suppressor exonucleases, to promote cGAS-STING signalling.

Key cytokines involved in inflammaging (i.e. IL6 and IL8) are upregulated in our aquatic vertebrate models during both tissue regeneration and aging. This is consistent with the fact that a significant number of cells at the site of injury senesce (Li et al., 2021). These cells are then cleared by macrophages after their recruitment (Li et al., 2021). In addition, recent work on axolotl limb regeneration has revealed that senescent cells create a pro-proliferative niche for progenitor cell expansion and blastema outgrowth (Yu et al., 2022). Thus, cGAS-STING activation and cGAS suppressor downregulation during regeneration promotes cell senescence while simultaneously creating an environment primed for immune cell recruitment and tissue remodelling.

Previous work identified *plex9.1* among the downregulated genes during cardiomyocyte regeneration akin to *pml* during gar caudal fin regeneration (Wu et al., 2015). Ray-finned fish *plex9.1*, which functions akin to tetrapod Trex1 (Mathavarajah et al., 2023) is also downregulated in the hearts of aged zebrafish, which correlates to elevated cGAS activity. This is consistent with Plex9.1 playing a potentially important role in maintaining cardiac function in teleost fish during aging, as previous work found that mice lacking Trex1 exhibit severe inflammatory myocarditis, cardiomyopathy and eventually circulatory failure (Morita et al., 2004; Stetson et al., 2008). Thus, the reduced expression of cGAS suppressor enzymes likely contributes to normal biological aging and senescence across different bony vertebrate species (De Cecco, Ito, Petrashen, Elias, Skvir, Criscione, Caligiana, Brocculi, Adney, Boeke, Le, Beausejour, et al., 2019; H. Yang et al., 2017).

The de-repression of retroelements also occurs during aging and can activate cGAS (De Cecco, Ito, Petrashen, Elias, Skvir, Criscione, Caligiana, Brocculi, Adney,

Boeke, Le, Beausejour, et al., 2019). For example, LINE-1 retroelements were recently shown to promote the senescence associated secretory phenotype through the activation of cGAS-STING (De Cecco, Ito, Petrashen, Elias, Skvir, Criscione, Caligiana, Brocculi, Adney, Boeke, Le, Beausejour, et al., 2019). Previously, we have demonstrated that Pml, Trex1 and Plex9.1 collectively suppress LINE retroelements as an exonuclease-independent function to limit cGAS activation (Chapter 2) (Mathavarajah et al., 2023). Considering that cardiac tissue from older zebrafish had higher levels of 2′3′-cGAMP, coupled with a decrease in cGAS-suppressor *plex9.1* expression, the activation of cGAS-STING in senescing cells seems to be a conserved pathologic process in vertebrates.

In the future, the comparative biomedical investigation of aquatic vertebrate model systems such as the gar, zebrafish and axolotl will provide a useful experimental paradigm for studying the co-evolution of endogenous retroelements and the genes that suppress their pathological consequences during development, regenerative wound healing, and aging.

Chapter 5 – Conclusion

5.1 Preface

PML is an important, highly conserved gene in vertebrates that encodes an arsenal of isoforms that help regulate cellular functions, with many of these proteins contributing to tumour suppression. The work presented in this thesis expands our understanding of how the *PML* and *Plex9* genes have evolved in different vertebrate species to play important functions in wound healing and aging, while contributing to genome stability, a retained fundamental cellular function in mammals. This chapter will discuss some of these main findings and how future biomedical work can build on the novel Plex9 genes and the newly found direct role for cytoplasmic PML in genome stability. Finally, conclusions drawn from this thesis will expand on the current roles of PML in both oncogenesis and wound healing to be exploited in the future as both a biomarker and in therapeutic approaches.

5.2 Plex9 enzymes, convergently evolved regulators of cGAS-STING

cGAS and *STING* encoding orthologs appeared more than 600 million years ago (can be identified in choanoflagellate genomes) and is found highly conserved in vertebrate species as a key pattern recognition receptor sensing pathway in vertebrates (Margolis et al., 2017; Yu & Liu, 2021). The cGAS-STING pathway has been shown to function in the innate immune response predating the evolution of interferons, such as in *Drosophila* where it is required for NF-κB signalling (via the NF-kB transcription factor Relish) in response to bacterial infection (Martin et al., 2018; Slavik et al., 2021). In IFN-

secreting vertebrates such as fish, there is a conserved role for the cGAS-STING pathway in the antiviral response that utilizes a similar molecular pathway as mammals, where downstream modules of NF-κB and IRF3 are activated via the actions of TBK1 (Chen et al., 2020; de Oliveira Mann et al., 2019b; Ge et al., 2015). However, despite the emerging work illustrating the conserved functions of cGAS-STING, an important part of the axis, TREX1 is not well-described in other species. An important aspect of TREX1 is that it prevents sustained STING activation and damaging inflammation, functioning as an important brake for the pathway.

In this thesis, I described the molecular evolution of TREX1, which first emerges in the genomes of tetrapods such as salamanders (Chapter 2). However, this poses a significant conundrum in fish, as there is conserved cGAS-STING signalling but a missing factor to "turn off" or suppresses the pathway, akin to TREX1. The novel Plex9 DEDDh DNA exonucleases (related to the C-terminus of the *PML* gene) play this important role of suppressing cGAS-STING signalling in teleost fishes (Chapter 2). These cytoplasm and ER-localizing enzymes are capable of micronuclei degradation and suppressing L1 retroelements, two important functions for TREX1 (Li et al., 2017b; Mohr et al., 2021b). Moreover, these Plex9 enzymes can compensate for the loss of TREX1 when ectopically expressed in *TREX1* KO human cells, to suppress cGAS activation (Chapter 2). Intriguingly, these Plex9 exonucleases are lost in species where TREX1 is present (tetrapods). Thus, in an example of convergent evolution, two DEDDh exonucleases of different gene origins function as suppressors of the cGAS-STING pathway in fish and tetrapod species.

Currently, a fish model for studying type I interferonopathies (e.g., Aicardi–Goutières) does not exist (Crow & Stetson, 2022). There are differences between the IFNs in teleost fish and mammals, but the critical upstream signalling components are highly conserved (Hamming et al., 2011). Targeting the *Plex9* genes that regulate the cGAS-STING pathway in zebrafish (or other teleost fishes) could be a potential way to generate a model for studying type I interferonopathies. The zebrafish model has been used to study all sorts of human diseases and been a powerful model for new insights (Choi et al., 2021). The innovation of such a model will be beneficial for gathering new insights into the dysregulated pathways associated with type I interferonopathies. Moreover, it will also provide a strong screening model to identify potential small molecule therapeutics to treat type I interferonopathies. Therefore, future work examining *Plex9* genes using morpholino (a tool for gene silencing) or via CRISPR/Cas9 knockout in zebrafish and other fish models could generate an innovative model for studying autoimmune disease and the highly conserved cGAS-STING pathway.

5.3 PML NBs, an amniote innovation

In studying the evolution of the PML gene, our work has implication for our understanding of how non-membrane bound organelles may have evolved in eukaryotic cells (Chapter 3). The origins of eukaryote organelles are largely understood from the perspective of endosymbiosis. However, there are organelles that are likely derived from autogenous organellogenesis (i.e., recycling machinery and digestive vacuoles) (Dacks et al., 2008). The nucleus is a complex organelle that includes a variety of subnuclear organelles within it, including PML NBs, Cajal bodies, paraspeckles and splicing

speckles, that contribute to its architecture and function (Handwerger & Gall, 2006; Liu et al., 2018). Nuclear bodies are an important aspect to nuclear architecture as they create an environment that is spatially compartmentalized to create distinct regions within a confined volume, and consequently concentrating proteins and their substrates or interactors, to potentially facilitate more efficient reactions within the cell (Mao et al., 2011). PML orthologs in fish lacked the known lysine residues for SUMOylation and localized to the cytoplasm as active exonucleases. This suggests that amniote species have uniquely evolved a subnuclear organelle/compartment, which contributes to their cellular complexity.

PML NBs are membrane-less and represent molecular condensates that self-organize into organelles, in a process regulated by SUMOylation and likely occurring by phase separation (Banani et al., 2016; Corpet et al., 2020; Shen et al., 2006). PML NBs emerged in amniote species coincident with the appearance of TREX1. I was able to identify that unlike non-teleost fish orthologs of PML, the orthologs of PML from turtle and quail genomes localize to the nucleus and form SUMOylated bodies (Chapter 3). Intriguingly, SUMOylation sites for PML orthologs can be identified first in amniote species and one of these sites, K616, aligns to an acidic residue responsible for catalytic activity for the catalytically active PML exonuclease in fish. Therefore, it appears that PML neofunctionalization appears to have occurred from the loss of exonuclease function and gain of new self-organization function primed by SUMOylation and its localization in the nucleus.

PML NBs represent an extreme form of SUMO-SIM interactions facilitating phase separation in eukaryote cells. The noncovalent interactions between SUMO

modified proteins and the SIMs of other proteins can drive liquid-liquid phase separation (Lin et al., 2006; Matunis et al., 2006; Shen et al., 2006). In addition, studies have shown using an engineered recombinant protein pairing of a protein with multiple repeats of a SIM (from PIASx) and multiple repeats of human SUMO3, when mixed, can assemble into phase-separated droplets (Banani et al., 2016). The PML protein evolving SUMOylation sites while already having a SIM likely led to the scaffold protein being able to self-oligomerize and form membraneless organelles within the nucleus. Our work highlights how membrane-less organelles not derived from endosymbiosis could originate from a single gene encoding a protein with the capacity for self-organization such as PML, which has led to the amniote innovation of the PML NB.

5.4 PML-I, a dynamic tumour-suppressive isoform that maintains genome stability

The PML-I isoform is the most conserved *PML* isoform in vertebrate species and the most highly expressed in human cells (Nisole et al., 2013). In addition, PML-I encodes a unique exon 9 region that has yet to be characterized. However, our understanding of PML-I function has been limited aside from the protein being known to uniquely interact with a handful of proteins. We showed that the exon 9 region of PML-I is an active exonuclease domain in fish orthologs of PML, while amniote orthologs of PML have lost this function (Chapter 2 and Chapter 3). These findings indicate that PML was once an active DEDDh exonuclease capable of degrading DNA (Chapter 3). However, another function for the exon 9 region is its role in suppressing L1 activity, which is a conserved function in humans (Chapter 3). Furthermore, PML-I promotes the

degradation of L1 ORF1p by the UPS to restrict L1 retrotransposition (Chapter 3). PML-I acts as an important sensor that mitigates the effects of L1 retrotransposition, which is a major perturbant for genome stability.

In many malignancies, I have discussed how PML expression is reduced. Our findings indicate that in these different types of cancer such as prostate adenocarcinomas, lymphomas, breast carcinomas; an important tumour suppression function of PML-I is lost where it prevents mutagenesis by L1 retrotransposition (Gurrieri et al., 2004). PML NBs are capable of sensing DNA damage and responding in a manner to promote the recruitment of required factors to repair foci. However, in the context of L1, the PML protein can directly play a role in preventing L1 propagation and further mutagenesis (Chapter 3). In addition, PML can be considered a regulator of cGAS-STING signalling alongside TREX1 to prevent sustained signalling of type I IFN signalling in response to L1. PML appears to therefore be involved in multiple steps towards maintaining genome stability, including (i) facilitating DNA repair and cell fate decisions as NBs, (ii) directly suppressing L1 retrotransposition and (iii) regulating downstream cGAS-STING signalling in response to persistent damage (via L1 propagation). Thus, a staple role for the PML protein both directly and indirectly via NBs is its contribution to genome stability, which is lost in cancer when PML expression is lost.

In APL, there is a fusion event between *PML* and *RARα* that leads to the loss of exon 9 that encodes the PML C-terminus domain (Ibáñez et al., 2016; Lehmann-Che et al., 2018; Ronchini et al., 2017). The C-terminus of PML-I is involved in L1 retroelement suppression. This suggests that in APL, there is a possibility that L1 retroelements are dysregulated in the absence of PML-I. However, there has been no work examining L1

retroelements in APL, thus it is currently unknown as to whether loss of PML-I influences L1 retroelement dynamics in APL. It is important to note that in relapse patients with the PML/RARα fusion gene, an elevated degree of somatic mutations is observed and this could possibly occur in response to L1-mutagenesis (Ibáñez et al., 2016; Lehmann-Che et al., 2018; Ley et al., 2013; Riva et al., 2013; Ronchini et al., 2017). An examination of L1-induced mutagenesis in APL patient tumour cells lacking PML-I function warrants an investigation.

5.5 Cytoplasmic PML in cancer

PML shuttling and function in the cytoplasm has been a debated topic, with there being many issues replicating results or artificial systems being generated to study cytoplasmic PML (rather than examining endogenous protein). However, I've shown that the shuttling of PML is a regulated response that occurs in response to the expression of L1 retroelements (Chapter 3). In addition, the nucleocytoplasmic shuttling occurs through CRM1, as Leptomycin B treatment prevented PML shuttling with L1 (Chapter 3). These findings have implications for PML in the context of cancer. Currently, it is difficult to assess LINE-1 expression in tumours due to the heterogeneity of L1 sequences with retrotransposition-competency, which amounts to approximately 80-100 different elements (Brouha et al., 2003). This is still a relatively small pool of elements considering that over 99% of L1 elements are inactive. Yet, in cancer, the active elements have been shown to delete large regions on chromosomes (spanning megabases, leading to the loss of tumour suppressor genes), large scale duplications and complex translocations (Bernardo Rodriguez-Martin et al., 2020). The most affected malignancies

from L1 expression are esophageal adenocarcinomas, head-and-neck cancer, and colorectal cancers. However, there are limited antibodies available to histologically follow L1 activity in cancer cells (Sharma et al., 2016).

The presence of PML in the cytoplasm can serve as a biomarker for highly mutagenic tumour cells in patient samples. If PML localizes to the cytoplasm in these tumour cells, it indicates that shuttling occurred in response to LINE-1 retrotransposition. In addition, this information could be overlayed with genetic info on the background of the tumour to inform therapeutic decisions (especially those involving DNA repair inhibitors). For example, if it is (1) known that a tumour sample has cells with cytoplasmic PML and (2) that it is HR-deficient, this would suggest the following: Cytoplasmic PML indicative of high L1 expression means that the cells experience high rates of L1-derived mutagenesis and with HR-deficiency, this potentially indicates a high success for PARP inhibitor therapy (i.e., synthetic lethality) (Slade, 2020). However, there needs to be additional work testing the sensitivity of PML to shuttling at different levels of L1 activity. This could be done by transfecting different amounts of L1 elements and testing PML shuttling. In addition, the current PML antibody used for screening in histological samples requires fine-tuning and new protocols to accurately detect between NBs and cytoplasmic signal. After these initial studies, cytoplasmic PML could serve as an early diagnostic tool to predict the highly mutagenic cancers that are more aggressive and have poorer outcomes.

5.6 Conserved regulation of cGAS-STING in limb-fin regeneration and aging in vertebrates

The cGAS-STING pathway is highly conserved in vertebrate species and contributes to host immunity in different species, where the pathway is critical for pathogen sensing and responding via interferons and inflammatory signalling (Cai & Imler, 2021; Margolis et al., 2017). However, it was unknown how cGAS-STING signalling contributes to other major biological processes in animals and what factors regulate the pathway. I've examined the role of the highly conserved cGAS-STING pathway in aquatic vertebrates and found that it contributes to both tissue regeneration and aging (Chapter 4). In addition, the downregulation of the Plex9, Pml and Trex1 exonucleases in these different species is a critical regulatory step to control the activity of cGAS and downstream signalling during limb-fin regeneration and aging (Chapter 4).

PML has been linked to wound healing in the past where it was involved in endothelial cell migration and potentially the reformation of vasculature (Cheng et al., 2012). Intriguingly, in this context, mammalian PML is upregulated in response to type I IFN signalling via the IFNα/β stimulated response element (ISRE) located in its promoter region (Stadler et al., 1995). However, spotted gar *PML* expression is inversely related to high levels of cGAS activity during fin regeneration, likely because of its role in regulating cGAMP levels (Chapter 4). A similar mechanism of gene regulation has been observed with TREX1 to promote cGAS activity during senescence (Takahashi et al., 2018). Intriguingly, the downregulation of *Pml*, *Plex9*, and *Trex1* occurs across all three different species examined, the spotted gar, zebrafish and axolotl, in response to cGAMP. However, it is unknown as to whether cGAMP can elicit the downregulation through

STING-independent mechanisms, such as a novel set of transcription factors instead of IRF3 and NF-κB in these organisms. There have been reports of cGAS regulating autophagy via STING-independent mechanisms, so it is possible that other cGAMP-targets exist (D. Liu et al., 2019). This will be intriguing to explore in the future, as to whether cGAMP induces transcriptional rewiring via STING-independent mechanisms.

Moreover, our work suggests that during teleost fish aging, there is downregulation of *plex9.1* akin to the downregulation of *Trex1* in aged mice (Chapter 4) (Du et al., 2023). Considering that L1 retroelements have recently been shown to be a driving factor of inflammatory signalling during aging, it is tempting to speculate that the dysregulation of *TREX1* in mammals and *plex9.1* in teleost fish contributes to senescent signalling (De Cecco, Ito, Petrashen, Elias, Skvir, Criscione, Caligiana, Brocculi, Adney, Boeke, Le, Beauséjour, et al., 2019). At the least, there are likely similar changes in the regulation of these exonucleases across species, possibly through epigenetic changes that occur with aging. Alternatively, it could be a consequence of cGAMP-regulation of gene expression, which is also occurring. However, it is still unclear as to what stimuli or changes in aged-related senescence can trigger the downregulation of the exonucleases.

In contrast to how they prevent senescence signalling in aging, these exonucleases are desirable targets for therapeutic intervention in wound healing. It is possible that targeting TREX1 and other DEDDh exonucleases therapeutically using newly available small molecule inhibitors can be a mechanism to kickstart regeneration pathways via type I IFN signalling in mammals. In particular, the sustained type I IFN activation with TREX1 inhibition could promote the recruitment of immune cells and remodelling at the site of injury (Francica et al., 2022; Hemphill et al., 2021). These experiments could be

done in the axolotl model, which has a TREX1 ortholog that regulates cGAS-STING, and the model is amenable for such tissue regeneration studies.

Bibliography

1. Ablasser, A., Goldeck, M., Cavlar, T., Deimling, T., Witte, G., Rohl, I., Hopfner, K. P., Ludwig, J., & Hornung, V. (2013). cGAS produces a 2'-5'-linked cyclic dinucleotide second messenger that activates STING. *Nature*, *498*(7454), 380-384. https://doi.org/10.1038/nature12306

2. Adell, M. A. Y., Klockner, T. C., Höfler, R., Wallner, L., Schmid, J., Markovic, A., Martyniak, A., & Campbell, C. S. (2023). Adaptation to spindle assembly checkpoint inhibition through the selection of specific aneuploidies. *Genes Dev*, *37*(5-6), 171-190. https://doi.org/10.1101/gad.350182.122

3. Alibardi, L. (2017). Hyaluronic acid in the tail and limb of amphibians and lizards recreates permissive embryonic conditions for regeneration due to its hygroscopic and immunosuppressive properties. *Journal of Experimental Zoology Part B: Molecular and Developmental Evolution*, *328*(8), 760-771. https://doi.org/https://doi.org/10.1002/jez.b.22771

4. Amodeo, V., A, D., Betts, J., Bartesaghi, S., Zhang, Y., Richard-Londt, A., Ellis, M., Roshani, R., Vouri, M., Galavotti, S., Oberndorfer, S., Leite, A. P., Mackay, A., Lampada, A., Stratford, E. W., Li, N., Dinsdale, D., Grimwade, D., Jones, C., . . . Salomoni, P. (2017). A PML/Slit Axis Controls Physiological Cell Migration and Cancer Invasion in the CNS. *Cell Rep*, *20*(2), 411-426. https://doi.org/10.1016/j.celrep.2017.06.047

5. Amores, A., Force, A., Yan, Y. L., Joly, L., Amemiya, C., Fritz, A., Ho, R. K., Langeland, J., Prince, V., Wang, Y. L., Westerfield, M., Ekker, M., & Postlethwait, J. H. (1998). Zebrafish hox clusters and vertebrate genome evolution. *Science*, *282*(5394), 1711-1714. https://doi.org/10.1126/science.282.5394.1711

6. Andrade, B., Jara-Gutierrez, C., Paz-Araos, M., Vazquez, M. C., Diaz, P., & Murgas, P. (2022). The Relationship between Reactive Oxygen Species and the cGAS/STING Signaling Pathway in the Inflammaging Process. *Int J Mol Sci*, *23*(23). https://doi.org/10.3390/ijms232315182

7. Antolini, F., Lo Bello, M., & Sette, M. (2003). Purified promyelocytic leukemia coiled-coil aggregates as a tetramer displaying low alpha-helical content. *Protein Expr Purif*, *29*(1), 94-102. https://doi.org/10.1016/s1046-5928(03)00004-4

8. Antoniani, F., Cimino, M., Mediani, L., Vinet, J., Verde, E. M., Secco, V., Yamoah, A., Tripathi, P., Aronica, E., Cicardi, M. E., Trotti, D., Sterneckert, J., Goswami, A., & Carra, S. (2023). Loss of PML nuclear bodies in familial amyotrophic lateral sclerosis-frontotemporal dementia. *Cell Death Discovery*, *9*(1), 248. https://doi.org/10.1038/s41420-023-01547-2

9. Aranda-Anzaldo, A. (2016). The interphase mammalian chromosome as a structural system based on tensegrity. *J Theor Biol*, *393*, 51-59. https://doi.org/10.1016/j.jtbi.2016.01.005

10. Ardeljan, D., Taylor, M. S., Ting, D. T., & Burns, K. H. (2017). The Human Long Interspersed Element-1 Retrotransposon: An Emerging Biomarker of Neoplasia. *Clin Chem*, *63*(4), 816-822. https://doi.org/10.1373/clinchem.2016.257444

11. Arjan-Odedra, S., Swanson, C. M., Sherer, N. M., Wolinsky, S. M., & Malim, M. H. (2012). Endogenous MOV10 inhibits the retrotransposition of endogenous retroelements but not the replication of exogenous retroviruses. *Retrovirology*, *9*, 53. https://doi.org/10.1186/1742-4690-9-53

12. Attwood, K. M., Salsman, J., Chung, D., Mathavarajah, S., Van Iderstine, C., & Dellaire, G. (2020). PML isoform expression and DNA break location relative to PML nuclear bodies impacts the efficiency of homologous recombination. *Biochem Cell Biol*, *98*(3), 314-326. https://doi.org/10.1139/bcb-2019-0115

13. Bagby, G. C., & Alter, B. P. (2006). Fanconi anemia. *Semin Hematol*, *43*(3), 147-156. https://doi.org/10.1053/j.seminhematol.2006.04.005

14. Bakhoum, S. F., Ngo, B., Laughney, A. M., Cavallo, J. A., Murphy, C. J., Ly, P., Shah, P., Sriram, R. K., Watkins, T. B. K., Taunk, N. K., Duran, M., Pauli, C., Shaw, C., Chadalavada, K., Rajasekhar, V. K., Genovese, G., Venkatesan, S., Birkbak, N. J., McGranahan, N., Lundquist, M., … Cantley, L. C. (2018). Chromosomal instability drives metastasis through a cytosolic DNA response. Nature, 553(7689), 467–472. https://doi.org/10.1038/nature25432

15. Banani, S. F., Rice, A. M., Peeples, W. B., Lin, Y., Jain, S., Parker, R., & Rosen, M. K. (2016). Compositional Control of Phase-Separated Cellular Bodies. *Cell*, *166*(3), 651-663. https://doi.org/10.1016/j.cell.2016.06.010

16. Barcaroli, D., Dinsdale, D., Neale, M. H., Bongiorno-Borbone, L., Ranalli, M., Munarriz, E., Sayan, A. E., McWilliam, J. M., Smith, T. M., Fava, E., Knight, R. A., Melino, G., & De Laurenzi, V. (2006). FLASH is an essential component of Cajal bodies. *Proc Natl Acad Sci U S A*, *103*(40), 14802-14807. https://doi.org/10.1073/pnas.0604225103

17. Barker, N., van Oudenaarden, A., & Clevers, H. (2012). Identifying the stem cell of the intestinal crypt: strategies and pitfalls. *Cell Stem Cell*, *11*(4), 452-460. https://doi.org/10.1016/j.stem.2012.09.009

18. Barroso-Gomila, O., Trulsson, F., Muratore, V., Canosa, I., Merino-Cacho, L., Cortazar, A. R., Perez, C., Azkargorta, M., Iloro, I., Carracedo, A., Aransay, A. M., Elortza, F., Mayor, U., Vertegaal, A. C. O., Barrio, R., & Sutherland, J. D. (2021). Identification of proximal SUMO-dependent interactors using SUMO-ID. *Nat Commun*, *12*(1), 6671. https://doi.org/10.1038/s41467-021-26807-6

19. Bartok, E., & Hartmann, G. (2020). Immune Sensing Mechanisms that Discriminate Self from Altered Self and Foreign Nucleic Acids. *Immunity*, *53*(1), 54-77. https://doi.org/10.1016/j.immuni.2020.06.014

20. Beck, C. R., Collier, P., Macfarlane, C., Malig, M., Kidd, J. M., Eichler, E. E., Badge, R. M., & Moran, J. V. (2010). LINE-1 retrotransposition activity in human genomes. *Cell*, *141*(7), 1159-1170. https://doi.org/10.1016/j.cell.2010.05.021

21. Beli, P., Lukashchuk, N., Wagner, S. A., Weinert, B. T., Olsen, J. V., Baskcomb, L., Mann, M., Jackson, S. P., & Choudhary, C. (2012). Proteomic investigations reveal a role for RNA processing factor THRAP3 in the DNA damage response. *Mol Cell*, *46*(2), 212-225. https://doi.org/10.1016/j.molcel.2012.01.026

22. Bellodi, C., Kindle, K., Bernassola, F., Dinsdale, D., Cossarizza, A., Melino, G., Heery, D., & Salomoni, P. (2006). Cytoplasmic function of mutant promyelocytic leukemia (PML) and PML-retinoic acid receptor-alpha. *J Biol Chem*, *281*(20), 14465-14473. https://doi.org/10.1074/jbc.M600457200

23. Belyakova, N. V., Kleiner, N. E., Kravetskaya, T. P., Legina, O. K., Naryzhny, S. N., Perrino, F. W., Shevelev, I. V., & Krutyakov, V. M. (1993). Proof-reading 3'-->5' exonucleases isolated from rat liver nuclei. *Eur J Biochem*, *217*(2), 493-500. https://doi.org/10.1111/j.1432-1033.1993.tb18269.x

24. Benci, J. L., Xu, B., Qiu, Y., Wu, T. J., Dada, H., Twyman-Saint Victor, C., Cucolo, L., Lee, D. S. M., Pauken, K. E., Huang, A. C., Gangadhar, T. C., Amaravadi, R. K., Schuchter, L. M., Feldman, M. D., Ishwaran, H., Vonderheide, R. H., Maity, A., Wherry, E. J., & Minn, A. J. (2016). Tumor Interferon Signaling Regulates a Multigenic Resistance Program to Immune Checkpoint Blockade. *Cell*, *167*(6), 1540-1554 e1512. https://doi.org/10.1016/j.cell.2016.11.022

25. Benitez-Guijarro, M., Lopez-Ruiz, C., Tarnauskaite, Z., Murina, O., Mian Mohammad, M., Williams, T. C., Fluteau, A., Sanchez, L., Vilar-Astasio, R., Garcia-Canadas, M., Cano, D., Kempen, M. H., Sanchez-Pozo, A., Heras, S. R., Jackson, A. P., Reijns, M. A., & Garcia-Perez, J. L. (2018). RNase H2, mutated in Aicardi-Goutieres syndrome, promotes LINE-1 retrotransposition. *EMBO J*, *37*(15). https://doi.org/10.15252/embj.201798506

26. Bensimon, A., Schmidt, A., Ziv, Y., Elkon, R., Wang, S. Y., Chen, D. J., Aebersold, R., & Shiloh, Y. (2010). ATM-dependent and -independent dynamics of the nuclear phosphoproteome after DNA damage. *Sci Signal*, *3*(151), rs3. https://doi.org/10.1126/scisignal.2001034

27. Berciano, M. T., Novell, M., Villagra, N. T., Casafont, I., Bengoechea, R., Val-Bernal, J. F., & Lafarga, M. (2007). Cajal body number and nucleolar size correlate with the cell body mass in human sensory ganglia neurons. *J Struct Biol*, *158*(3), 410-420. https://doi.org/10.1016/j.jsb.2006.12.008

28. Bernard, J., Weil, M., Boiron, M., Jacquillat, C., Flandrin, G., & Gemon, M. F. (1973). Acute promyelocytic leukemia: results of treatment by daunorubicin. *Blood*, *41*(4), 489-496. https://www.ncbi.nlm.nih.gov/pubmed/4510926

29. Bernardi, R., Guernah, I., Jin, D., Grisendi, S., Alimonti, A., Teruya-Feldstein, J., Cordon-Cardo, C., Simon, M. C., Rafii, S., & Pandolfi, P. P. (2006). PML inhibits HIF-1alpha translation and neoangiogenesis through repression of mTOR. *Nature*, *442*(7104), 779-785. https://doi.org/10.1038/nature05029

30. Bernardi, R., Papa, A., & Pandolfi, P. P. (2008). Regulation of apoptosis by PML and the PML-NBs. *Oncogene*, *27*(48), 6299-6312. https://doi.org/10.1038/onc.2008.305

31. Berndt, N., Wolf, C., Fischer, K., Costa, E. C., Knuschke, P., Zimmermann, N., Schmidt, F., Merkel, M., Chara, O., & Lee-Kirsch, M. A. (2022). Photosensitivity and cGAS-dependent IFN-1 activation in patients with lupus and TREX1 deficiency. *Journal of Investigative Dermatology*, *142*(3), 633-640. e636.

32. Bezzi, M., Seitzer, N., Ishikawa, T., Reschke, M., Chen, M., Wang, G., Mitchell, C., Ng, C., Katon, J., Lunardi, A., Signoretti, S., Clohessy, J. G., Zhang, J., & Pandolfi, P. P. (2018). Diverse genetic-driven immune landscapes dictate tumor progression through distinct mechanisms. *Nat Med*, *24*(2), 165-175. https://doi.org/10.1038/nm.4463

33. Bian, L., Meng, Y., Zhang, M., & Li, D. (2019). MRE11-RAD50-NBS1 complex alterations and DNA damage response: implications for cancer treatment. *Mol Cancer*, *18*(1), 169. https://doi.org/10.1186/s12943-019-1100-5

34. Bilal, S., Etayo, A., & Hordvik, I. (2021). Immunoglobulins in teleosts. *Immunogenetics*, *73*(1), 65-77. https://doi.org/10.1007/s00251-020-01195-1

35. Bischof, O., Kirsh, O., Pearson, M., Itahana, K., Pelicci, P. G., & Dejean, A. (2002). Deconstructing PML-induced premature senescence. *EMBO J*, *21*(13), 3358-3369. https://doi.org/10.1093/emboj/cdf341

36. Bjerknes, M., & Cheng, H. (2005). Gastrointestinal stem cells. II. Intestinal stem cells. *Am J Physiol Gastrointest Liver Physiol*, *289*(3), G381-387. https://doi.org/10.1152/ajpgi.00160.2005

37. Blackford, A. N., & Jackson, S. P. (2017). ATM, ATR, and DNA-PK: The Trinity at the Heart of the DNA Damage Response. *Mol Cell*, *66*(6), 801-817. https://doi.org/10.1016/j.molcel.2017.05.015

38. Bøe, S. O., Haave, M., Jul-Larsen, A. s., Grudic, A., Bjerkvig, R., & Lønning, P. E. (2006). Promyelocytic leukemia nuclear bodies are predetermined processing sites for damaged DNA. *Journal of Cell Science*, *119*(16), 3284-3295. https://doi.org/10.1242/jcs.03068

39. Bogerd, H. P., Wiegand, H. L., Doehle, B. P., Lueders, K. K., & Cullen, B. R. (2006). APOBEC3A and APOBEC3B are potent inhibitors of LTR-retrotransposon function in human cells. *Nucleic Acids Res*, *34*(1), 89-95. https://doi.org/10.1093/nar/gkj416

40. Bogerd, H. P., Wiegand, H. L., Hulme, A. E., Garcia-Perez, J. L., O'Shea, K. S., Moran, J. V., & Cullen, B. R. (2006). Cellular inhibitors of long interspersed element 1 and Alu retrotransposition. *Proc Natl Acad Sci U S A*, *103*(23), 8780-8785. https://doi.org/10.1073/pnas.0603313103

41. Bohren, K. M., Nadkarni, V., Song, J. H., Gabbay, K. H., & Owerbach, D. (2004). A M55V polymorphism in a novel SUMO gene (SUMO-4) differentially activates heat shock transcription factors and is associated with susceptibility to type I diabetes mellitus. *J Biol Chem*, *279*(26), 27233-27238. https://doi.org/10.1074/jbc.M402273200

42. Boichuk, S., Hu, L., Makielski, K., Pandolfi, P. P., & Gjoerup, O. V. (2011). Functional connection between Rad51 and PML in homology-directed repair. *PLoS One*, *6*(10), e25814. https://doi.org/10.1371/journal.pone.0025814

43. Boisvert, F. M., Hendzel, M. J., & Bazett-Jones, D. P. (2000). Promyelocytic leukemia (PML) nuclear bodies are protein structures that do not accumulate RNA. *J Cell Biol*, *148*(2), 283-292. https://doi.org/10.1083/jcb.148.2.283

44. Borden, K. L., Boddy, M. N., Lally, J., O'Reilly, N. J., Martin, S., Howe, K., Solomon, E., & Freemont, P. S. (1995). The solution structure of the RING finger domain from the acute promyelocytic leukaemia proto-oncoprotein PML. *EMBO J*, *14*(7), 1532-1541. https://doi.org/10.1002/j.1460-2075.1995.tb07139.x

45. Borden, K. L., Lally, J. M., Martin, S. R., O'Reilly, N. J., Solomon, E., & Freemont, P. S. (1996). In vivo and in vitro characterization of the B1 and B2 zinc-binding domains from the acute promyelocytic leukemia protooncoprotein PML. *Proc Natl Acad Sci U S A*, *93*(4), 1601-1606. https://doi.org/10.1073/pnas.93.4.1601

46. Braasch, I., Gehrke, A. R., Smith, J. J., Kawasaki, K., Manousaki, T., Pasquier, J., Amores, A., Desvignes, T., Batzel, P., Catchen, J., Berlin, A. M., Campbell, M. S., Barrell, D., Martin, K. J., Mulley, J. F., Ravi, V., Lee, A. P., Nakamura, T., Chalopin, D., . . . Postlethwait, J. H. (2016). The spotted gar genome illuminates vertebrate evolution and facilitates human-teleost comparisons. *Nat Genet*, *48*(4), 427-437. https://doi.org/10.1038/ng.3526

47. Brangwynne, C. P., Mitchison, T. J., & Hyman, A. A. (2011). Active liquid-like behavior of nucleoli determines their size and shape in Xenopus laevis oocytes. *Proc Natl Acad Sci U S A*, *108*(11), 4334-4339. https://doi.org/10.1073/pnas.1017150108

48. Brazeau, M. D., & Friedman, M. (2015). The origin and early phylogenetic history of jawed vertebrates. *Nature*, *520*(7548), 490-497. https://doi.org/10.1038/nature14438

49. Bregnard, C., Guerra, J., Dejardin, S., Passalacqua, F., Benkirane, M., & Laguette, N. (2016). Upregulated LINE-1 Activity in the Fanconi Anemia Cancer Susceptibility Syndrome Leads to Spontaneous Pro-inflammatory Cytokine Production. *EBioMedicine*, *8*, 184-194. https://doi.org/10.1016/j.ebiom.2016.05.005

50. Bregnard, T., Ahmed, A., Semenova, I. V., Weller, S. K., & Bezsonova, I. (2022). The B-box1 domain of PML mediates SUMO E2-E3 complex formation through an atypical interaction with UBC9. *Biophys Chem*, *287*, 106827. https://doi.org/10.1016/j.bpc.2022.106827

51. Brockes, J. P., & Gates, P. B. (2014). Mechanisms underlying vertebrate limb regeneration: lessons from the salamander. *Biochem Soc Trans*, *42*(3), 625-630. https://doi.org/10.1042/BST20140002

52. Brouha, B., Schustak, J., Badge, R. M., Lutz-Prigge, S., Farley, A. H., Moran, J. V., & Kazazian, H. H., Jr (2003). Hot L1s account for the bulk of retrotransposition in the human population. Proceedings of the National Academy of Sciences of the United States of America, 100(9), 5280–5285. https://doi.org/10.1073/pnas.0831042100

53. Brown, J. R., Conn, K. L., Wasson, P., Charman, M., Tong, L., Grant, K., McFarlane, S., & Boutell, C. (2016). SUMO Ligase Protein Inhibitor of Activated STAT1 (PIAS1) Is a Constituent Promyelocytic Leukemia Nuclear Body Protein That Contributes to the Intrinsic Antiviral Immune Response to Herpes Simplex Virus 1. *J Virol*, *90*(13), 5939-5952. https://doi.org/10.1128/JVI.00426-16

54. Brucet, M., Querol-Audí, J., Bertlik, K., Lloberas, J., Fita, I., & Celada, A. (2008). Structural and biochemical studies of TREX1 inhibition by metals. Identification of a new active histidine conserved in DEDDh exonucleases. *Protein Sci*, *17*(12), 2059-2069. https://doi.org/10.1110/ps.036426.108

55. Bryan, T. M., Englezou, A., Gupta, J., Bacchetti, S., & Reddel, R. R. (1995). Telomere elongation in immortal human cells without detectable telomerase activity. *EMBO J*, *14*(17), 4240-4248. https://www.ncbi.nlm.nih.gov/pubmed/7556065

56. Brzostek-Racine, S., Gordon, C., Van Scoy, S., & Reich, N. C. (2011). The DNA damage response induces IFN. *J Immunol*, *187*(10), 5336-5345. https://doi.org/10.4049/jimmunol.1100040

57. Buczek, M. E., Miles, A. K., Green, W., Johnson, C., Boocock, D. J., Pockley, A. G., Rees, R. C., Hulman, G., van Schalkwyk, G., Parkinson, R., Hulman, J., Powe, D. G., & Regad, T. (2016a). Cytoplasmic PML promotes TGF-beta-

associated epithelial-mesenchymal transition and invasion in prostate cancer. *Oncogene*, *35*(26), 3465-3475. https://doi.org/10.1038/onc.2015.409

58. Burger, K., Ketley, R. F., & Gullerova, M. (2019). Beyond the Trinity of ATM, ATR, and DNA-PK: Multiple Kinases Shape the DNA Damage Response in Concert With RNA Metabolism. *Front Mol Biosci*, *6*, 61. https://doi.org/10.3389/fmolb.2019.00061

59. Burnette, B. C., Liang, H., Lee, Y., Chlewicki, L., Khodarev, N. N., Weichselbaum, R. R., Fu, Y. X., & Auh, S. L. (2011). The efficacy of radiotherapy relies upon induction of type i interferon-dependent innate and adaptive immunity. *Cancer Res*, *71*(7), 2488-2496. https://doi.org/10.1158/0008-5472.CAN-10-2820

60. Buschbeck, M., Uribesalgo, I., Ledl, A., Gutierrez, A., Minucci, S., Muller, S., & Di Croce, L. (2007). PML4 induces differentiation by Myc destabilization. *Oncogene*, *26*(23), 3415-3422. https://doi.org/10.1038/sj.onc.1210128

61. Bustin, S. A., Benes, V., Garson, J. A., Hellemans, J., Huggett, J., Kubista, M., Mueller, R., Nolan, T., Pfaffl, M. W., Shipley, G. L., Vandesompele, J., & Wittwer, C. T. (2009). The MIQE guidelines: minimum information for publication of quantitative real-time PCR experiments. *Clin Chem*, *55*(4), 611-622. https://doi.org/10.1373/clinchem.2008.112797

62. Cai, H., & Imler, J. L. (2021). cGAS-STING: insight on the evolution of a primordial antiviral signaling cassette. *Fac Rev*, *10*, 54. https://doi.org/10.12703/r/10-54

63. Callen, J. P., & Wortmann, R. L. (2006). Dermatomyositis. *Clin Dermatol*, *24*(5), 363-373. https://doi.org/10.1016/j.clindermatol.2006.07.001

64. Campisi, J. (2003). Cancer and ageing: rival demons? *Nat Rev Cancer*, *3*(5), 339-349. https://doi.org/10.1038/nrc1073

65. Capella-Gutierrez, S., Silla-Martinez, J. M., & Gabaldon, T. (2009). trimAl: a tool for automated alignment trimming in large-scale phylogenetic analyses. *Bioinformatics*, *25*(15), 1972-1973. https://doi.org/10.1093/bioinformatics/btp348

66. Cappadocia, L., Mascle, X. H., Bourdeau, V., Tremblay-Belzile, S., Chaker-Margot, M., Lussier-Price, M., Wada, J., Sakaguchi, K., Aubry, M., Ferbeyre, G., & Omichinski, J. G. (2015). Structural and functional characterization of the phosphorylation-dependent interaction between PML and SUMO1. *Structure*, *23*(1), 126-138. https://doi.org/10.1016/j.str.2014.10.015

67. Carmo-Fonseca, M., Ferreira, J., & Lamond, A. I. (1993). Assembly of snRNP-containing coiled bodies is regulated in interphase and mitosis--evidence that the coiled body is a kinetic nuclear structure. *J Cell Biol*, *120*(4), 841-852. https://doi.org/10.1083/jcb.120.4.841

68. Carracedo, A., Weiss, D., Leliaert, A. K., Bhasin, M., de Boer, V. C., Laurent, G., Adams, A. C., Sundvall, M., Song, S. J., Ito, K., Finley, L. S., Egia, A., Libermann, T., Gerhart-Hines, Z., Puigserver, P., Haigis, M. C., Maratos-Flier, E., Richardson, A. L., Schafer, Z. T., & Pandolfi, P. P. (2012). A metabolic prosurvival role for PML in breast cancer. *J Clin Invest*, *122*(9), 3088-3100. https://doi.org/10.1172/JCI62129

69. Castiello, L., Sestili, P., Schiavoni, G., Dattilo, R., Monque, D. M., Ciaffoni, F., Iezzi, M., Lamolinara, A., Sistigu, A., Moschella, F., Pacca, A. M., Macchia, D., Ferrantini, M., Zeuner, A., Biffoni, M., Proietti, E., Belardelli, F., & Arico, E. (2018). Disruption of IFN-I Signaling Promotes HER2/Neu Tumor Progression and Breast Cancer Stem Cells. *Cancer Immunol Res*, *6*(6), 658-670. https://doi.org/10.1158/2326-6066.CIR-17-0675

70. Celen, A. B., & Sahin, U. (2020). Sumoylation on its 25th anniversary: mechanisms, pathology, and emerging concepts. *FEBS J*, *287*(15), 3110-3140. https://doi.org/10.1111/febs.15319

71. Chalopin, D., & Volff, J. N. (2017). Analysis of the spotted gar genome suggests absence of causative link between ancestral genome duplication and transposable element diversification in teleost fish. *J Exp Zool B Mol Dev Evol*, *328*(7), 629-637. https://doi.org/10.1002/jez.b.22761

72. Chang, C. C., Naik, M. T., Huang, Y. S., Jeng, J. C., Liao, P. H., Kuo, H. Y., Ho, C. C., Hsieh, Y. L., Lin, C. H., Huang, N. J., Naik, N. M., Kung, C. C., Lin, S. Y., Chen, R. H., Chang, K. S., Huang, T. H., & Shih, H. M. (2011). Structural and functional roles of Daxx SIM phosphorylation in SUMO paralog-selective binding and apoptosis modulation. *Mol Cell*, *42*(1), 62-74. https://doi.org/10.1016/j.molcel.2011.02.022

73. Chang, H. R., Munkhjargal, A., Kim, M. J., Park, S. Y., Jung, E., Ryu, J. H., Yang, Y., Lim, J. S., & Kim, Y. (2018). The functional roles of PML nuclear bodies in genome maintenance. *Mutat Res*, *809*, 99-107. https://doi.org/10.1016/j.mrfmmm.2017.05.002

74. Chatterjee, N., & Walker, G. C. (2017). Mechanisms of DNA damage, repair, and mutagenesis. *Environ Mol Mutagen*, *58*(5), 235-263. https://doi.org/10.1002/em.22087

75. Chelbi-Alix, M. K., Pelicano, L., Quignon, F., Koken, M. H., Venturini, L., Stadler, M., Pavlovic, J., Degos, L., & de Thé, H. (1995). Induction of the PML protein by interferons in normal and APL cells. *Leukemia*, *9*(12), 2027-2033.

76. Chen, B., Li, C., Yao, J., Shi, L., Liu, W., Wang, F., Huo, S., Zhang, Y., Lu, Y., Ashraf, U., Ye, J., & Liu, X. (2020). Zebrafish NIK Mediates IFN Induction by Regulating Activation of IRF3 and NF-κB. *J Immunol*, *204*(7), 1881-1891. https://doi.org/10.4049/jimmunol.1900561

77. Chen, G. Q., Shi, X. G., Tang, W., Xiong, S. M., Zhu, J., Cai, X., Han, Z. G., Ni, J. H., Shi, G. Y., Jia, P. M., Liu, M. M., He, K. L., Niu, C., Ma, J., Zhang, P., Zhang, T. D., Paul, P., Naoe, T., Kitamura, K., . . . Chen, Z. (1997). Use of arsenic trioxide (As2O3) in the treatment of acute promyelocytic leukemia (APL): I. As2O3 exerts dose-dependent dual effects on APL cells. *Blood*, *89*(9), 3345-3353. https://www.ncbi.nlm.nih.gov/pubmed/9129041

78. Chen, J. H., Hales, C. N., & Ozanne, S. E. (2007). DNA damage, cellular senescence and organismal ageing: causal or correlative? *Nucleic Acids Res*, *35*(22), 7417-7428. https://doi.org/10.1093/nar/gkm681

79. Chen, M., Wan, L., Zhang, J., Zhang, J., Mendez, L., Clohessy, J. G., Berry, K., Victor, J., Yin, Q., Zhu, Y., Wei, W., & Pandolfi, P. P. (2018). Deregulated PP1alpha phosphatase activity towards MAPK activation is antagonized by a tumor suppressive failsafe mechanism. *Nat Commun*, *9*(1), 159. https://doi.org/10.1038/s41467-017-02272-y

80. Chen, M., Zhang, J., Sampieri, K., Clohessy, J. G., Mendez, L., Gonzalez-Billalabeitia, E., Liu, X. S., Lee, Y. R., Fung, J., Katon, J. M., Menon, A. V., Webster, K. A., Ng, C., Palumbieri, M. D., Diolombi, M. S., Breitkopf, S. B., Teruya-Feldstein, J., Signoretti, S., Bronson, R. T., . . . Pandolfi, P. P. (2018). An aberrant SREBP-dependent lipogenic program promotes metastatic prostate cancer. *Nat Genet*, *50*(2), 206-218. https://doi.org/10.1038/s41588-017-0027-2

81. Chen, Y., Wright, J., Meng, X., & Leppard, K. N. (2015). Promyelocytic Leukemia Protein Isoform II Promotes Transcription Factor Recruitment To Activate Interferon Beta and Interferon-Responsive Gene Expression. *Mol Cell Biol*, *35*(10), 1660-1672. https://doi.org/10.1128/MCB.01478-14

82. Chen, Y. C., Kappel, C., Beaudouin, J., Eils, R., & Spector, D. L. (2008). Live cell dynamics of promyelocytic leukemia nuclear bodies upon entry into and exit from mitosis. *Mol Biol Cell*, *19*(7), 3147-3162. https://doi.org/10.1091/mbc.e08-01-0035

83. Chen, Z., Zhao, W. L., Shen, Z. X., Li, J. M., Chen, S. J., Zhu, J., Lallemand-Breittenbach, V., Zhou, J., Guillemin, M. C., Vitoux, D., & de The, H. (2007). Arsenic trioxide and acute promyelocytic leukemia: clinical and biological. *Curr Top Microbiol Immunol*, *313*, 129-144. https://doi.org/10.1007/978-3-540-34594-7_8

84. Cheng, H. L., Lin, C. T., Huang, K. W., Wang, S., Lin, Y. T., Toh, S. I., & Hsiao, Y. Y. (2018). Structural insights into the duplex DNA processing of TREX2. *Nucleic Acids Res*, *46*(22), 12166-12176. https://doi.org/10.1093/nar/gky970

85. Cheng, X., & Kao, H. Y. (2012). Post-translational modifications of PML: consequences and implications. *Front Oncol*, *2*, 210. https://doi.org/10.3389/fonc.2012.00210

86. Cheng, X., Liu, Y., Chu, H., & Kao, H. Y. (2012). Promyelocytic leukemia protein (PML) regulates endothelial cell network formation and migration in response to tumor necrosis factor α (TNFα) and interferon α (IFNα). *J Biol Chem*, *287*(28), 23356-23367. https://doi.org/10.1074/jbc.M112.340505

87. Chernyavskaya, Y., Mudbhary, R., Zhang, C., Tokarz, D., Jacob, V., Gopinath, S., Sun, X., Wang, S., Magnani, E., Madakashira, B. P., Yoder, J. A., Hoshida, Y., & Sadler, K. C. (2017). Loss of DNA methylation in zebrafish embryos activates retrotransposons to trigger antiviral signaling. *Development*, *144*(16), 2925-2939. https://doi.org/10.1242/dev.147629

88. Ching, R. W., Dellaire, G., Eskiw, C. H., & Bazett-Jones, D. P. (2005). PML bodies: a meeting place for genomic loci? *J Cell Sci*, *118*(Pt 5), 847-854. https://doi.org/10.1242/jcs.01700

89. Cho, M.-G., Kumar, R. J., Lin, C.-C., Boyer, J. A., Shahir, J. A., Fagan-Solis, K., Simpson, D. A., Fan, C., Foster, C. E., & Goddard, A. M. (2022). Mre11 liberates cGAS from nucleosome sequestration during tumorigenesis. *bioRxiv*, 2022.2012. 2009.519750.

90. Choi, J., Hwang, S. Y., & Ahn, K. (2018). Interplay between RNASEH2 and MOV10 controls LINE-1 retrotransposition. *Nucleic Acids Res*, *46*(4), 1912-1926. https://doi.org/10.1093/nar/gkx1312

91. Choi, T.-Y., Choi, T.-I., Lee, Y.-R., Choe, S.-K., & Kim, C.-H. (2021). Zebrafish as an animal model for biomedical research. *Experimental & Molecular Medicine*, *53*(3), 310-317. https://doi.org/10.1038/s12276-021-00571-5

92. Christian, C. M., Sokolowski, M., deHaro, D., Kines, K. J., & Belancio, V. P. (2017). Involvement of Conserved Amino Acids in the C-Terminal Region of LINE-1 ORF2p in Retrotransposition. *Genetics*, *205*(3), 1139-1149. https://doi.org/10.1534/genetics.116.191403

93. Christoffels, A., Koh, E. G., Chia, J. M., Brenner, S., Aparicio, S., & Venkatesh, B. (2004). Fugu genome analysis provides evidence for a whole-genome duplication early during the evolution of ray-finned fishes. *Mol Biol Evol*, *21*(6), 1146-1151. https://doi.org/10.1093/molbev/msh114

94. Chung, I., Osterwald, S., Deeg, K. I., & Rippe, K. (2012). PML body meets telomere: the beginning of an ALTernate ending? *Nucleus*, *3*(3), 263-275. https://doi.org/10.4161/nucl.20326

95. Clements, A. P., & Singer, M. F. (1998). The human LINE-1 reverse transcriptase: effect of deletions outside the common reverse transcriptase domain. *Nucleic acids research*, *26*(15), 3528-3535.

96. Collins, P. L., Purman, C., Porter, S. I., Nganga, V., Saini, A., Hayer, K. E., Gurewitz, G. L., Sleckman, B. P., Bednarski, J. J., Bassing, C. H., & Oltz, E. M.

(2020). DNA double-strand breaks induce H2Ax phosphorylation domains in a contact-dependent manner. *Nat Commun*, *11*(1), 3158. https://doi.org/10.1038/s41467-020-16926-x

97. Condemine, W., Takahashi, Y., Le Bras, M., & de The, H. (2007). A nucleolar targeting signal in PML-I addresses PML to nucleolar caps in stressed or senescent cells. *J Cell Sci*, *120*(Pt 18), 3219-3227. https://doi.org/10.1242/jcs.007492

98. Condemine, W., Takahashi, Y., Le Bras, M., & de Thé, H. (2007). A nucleolar targeting signal in PML-I addresses PML to nucleolar caps in stressed or senescent cells. *J Cell Sci*, *120*(Pt 18), 3219-3227. https://doi.org/10.1242/jcs.007492

99. Condemine, W., Takahashi, Y., Zhu, J., Puvion-Dutilleul, F., Guegan, S., Janin, A., & de The, H. (2006). Characterization of endogenous human promyelocytic leukemia isoforms. *Cancer Res*, *66*(12), 6192-6198. https://doi.org/10.1158/0008-5472.CAN-05-3792

100. Coppe, J. P., Patil, C. K., Rodier, F., Sun, Y., Munoz, D. P., Goldstein, J., Nelson, P. S., Desprez, P. Y., & Campisi, J. (2008). Senescence-associated secretory phenotypes reveal cell-nonautonomous functions of oncogenic RAS and the p53 tumor suppressor. *PLoS Biol*, *6*(12), 2853-2868. https://doi.org/10.1371/journal.pbio.0060301

101. Corpet, A., Kleijwegt, C., Roubille, S., Juillard, F., Jacquet, K., Texier, P., & Lomonte, P. (2020). PML nuclear bodies and chromatin dynamics: catch me if you can! *Nucleic Acids Res*, *48*(21), 11890-11912. https://doi.org/10.1093/nar/gkaa828

102. Cost, G. J., Feng, Q., Jacquier, A., & Boeke, J. D. (2002). Human L1 element target-primed reverse transcription in vitro. *The EMBO journal*, *21*(21), 5899-5910.

103. Costantini, L. M., Fossati, M., Francolini, M., & Snapp, E. L. (2012). Assessing the tendency of fluorescent proteins to oligomerize under physiologic conditions. *Traffic*, *13*(5), 643-649. https://doi.org/10.1111/j.1600-0854.2012.01336.x

104. Courchaine, E. M., Barentine, A. E. S., Straube, K., Lee, D. R., Bewersdorf, J., & Neugebauer, K. M. (2021). DMA-tudor interaction modules control the specificity of in vivo condensates. *Cell*, *184*(14), 3612-3625 e3617. https://doi.org/10.1016/j.cell.2021.05.008

105. Crow, Y. J., Hayward, B. E., Parmar, R., Robins, P., Leitch, A., Ali, M., Black, D. N., van Bokhoven, H., Brunner, H. G., Hamel, B. C., Corry, P. C., Cowan, F. M., Frints, S. G., Klepper, J., Livingston, J. H., Lynch, S. A., Massey, R. F., Meritet, J. F., Michaud, J. L., . . . Lindahl, T. (2006). Mutations in the gene encoding the

3'-5' DNA exonuclease TREX1 cause Aicardi-Goutieres syndrome at the AGS1 locus. *Nat Genet*, *38*(8), 917-920. https://doi.org/10.1038/ng1845

106. Crow, Y. J., & Stetson, D. B. (2022). The type I interferonopathies: 10 years on. *Nature Reviews Immunology*, *22*(8), 471-483. https://doi.org/10.1038/s41577-021-00633-9

107. Cuchet-Lourenco, D., Boutell, C., Lukashchuk, V., Grant, K., Sykes, A., Murray, J., Orr, A., & Everett, R. D. (2011). SUMO pathway dependent recruitment of cellular repressors to herpes simplex virus type 1 genomes. *PLoS Pathog*, *7*(7), e1002123. https://doi.org/10.1371/journal.ppat.1002123

108. Cuchet-Lourenço, D., Boutell, C., Lukashchuk, V., Grant, K., Sykes, A., Murray, J., Orr, A., & Everett, R. D. (2011). SUMO pathway dependent recruitment of cellular repressors to herpes simplex virus type 1 genomes. *PLoS Pathog*, *7*(7), e1002123. https://doi.org/10.1371/journal.ppat.1002123

109. Cuchet-Lourenço, D., Vanni, E., Glass, M., Orr, A., & Everett, R. D. (2012). Herpes simplex virus 1 ubiquitin ligase ICP0 interacts with PML isoform I and induces its SUMO-independent degradation. *J Virol*, *86*(20), 11209-11222. https://doi.org/10.1128/jvi.01145-12

110. Da Silva-Ferrada, E., Lopitz-Otsoa, F., Lang, V., Rodriguez, M. S., & Matthiesen, R. (2012). Strategies to Identify Recognition Signals and Targets of SUMOylation. *Biochem Res Int*, *2012*, 875148. https://doi.org/10.1155/2012/875148

111. Dacks, J. B., Poon, P. P., & Field, M. C. (2008). Phylogeny of endocytic components yields insight into the process of nonendosymbiotic organelle evolution. *Proc Natl Acad Sci U S A*, *105*(2), 588-593. https://doi.org/10.1073/pnas.0707318105

112. Darnet, S., Dragalzew, A. C., Amaral, D. B., Sousa, J. F., Thompson, A. W., Cass, A. N., Lorena, J., Pires, E. S., Costa, C. M., Sousa, M. P., Frobisch, N. B., Oliveira, G., Schneider, P. N., Davis, M. C., Braasch, I., & Schneider, I. (2019). Deep evolutionary origin of limb and fin regeneration. *Proc Natl Acad Sci U S A*, *116*(30), 15106-15115. https://doi.org/10.1073/pnas.1900475116

113. Davalos, A. R., Coppe, J. P., Campisi, J., & Desprez, P. Y. (2010). Senescent cells as a source of inflammatory factors for tumor progression. *Cancer Metastasis Rev*, *29*(2), 273-283. https://doi.org/10.1007/s10555-010-9220-9

114. Davesne, D., Friedman, M., Schmitt, A. D., Fernandez, V., Carnevale, G., Ahlberg, P. E., Sanchez, S., & Benson, R. B. J. (2021). Fossilized cell structures identify an ancient origin for the teleost whole-genome duplication. *Proc Natl Acad Sci U S A*, *118*(30). https://doi.org/10.1073/pnas.2101780118

115. De Cecco, M., Ito, T., Petrashen, A. P., Elias, A. E., Skvir, N. J., Criscione, S. W., Caligiana, A., Brocculi, G., Adney, E. M., Boeke, J. D., Le, O., Beausejour, C., Ambati, J., Ambati, K., Simon, M., Seluanov, A., Gorbunova, V., Slagboom, P. E., Helfand, S. L., . . . Sedivy, J. M. (2019). L1 drives IFN in senescent cells and promotes age-associated inflammation. *Nature*, *566*(7742), 73-78. https://doi.org/10.1038/s41586-018-0784-9

116. De Cecco, M., Ito, T., Petrashen, A. P., Elias, A. E., Skvir, N. J., Criscione, S. W., Caligiana, A., Brocculi, G., Adney, E. M., Boeke, J. D., Le, O., Beauséjour, C., Ambati, J., Ambati, K., Simon, M., Seluanov, A., Gorbunova, V., Slagboom, P. E., Helfand, S. L., . . . Sedivy, J. M. (2019). L1 drives IFN in senescent cells and promotes age-associated inflammation. *Nature*, *566*(7742), 73-78. https://doi.org/10.1038/s41586-018-0784-9

117. de Oliveira Mann, C. C., Orzalli, M. H., King, D. S., Kagan, J. C., Lee, A. S. Y., & Kranzusch, P. J. (2019a). Modular Architecture of the STING C-Terminal Tail Allows Interferon and NF-kappaB Signaling Adaptation. *Cell Rep*, *27*(4), 1165-1175 e1165. https://doi.org/10.1016/j.celrep.2019.03.098

118. de Oliveira Mann, C. C., Orzalli, M. H., King, D. S., Kagan, J. C., Lee, A. S. Y., & Kranzusch, P. J. (2019b). Modular Architecture of the STING C-Terminal Tail Allows Interferon and NF-κB Signaling Adaptation. *Cell Rep*, *27*(4), 1165-1175.e1165. https://doi.org/10.1016/j.celrep.2019.03.098

119. de Silva, U., Choudhury, S., Bailey, S. L., Harvey, S., Perrino, F. W., & Hollis, T. (2007). The crystal structure of TREX1 explains the 3' nucleotide specificity and reveals a polyproline II helix for protein partnering. *J Biol Chem*, *282*(14), 10537-10543. https://doi.org/10.1074/jbc.M700039200

120. de Stanchina, E., Querido, E., Narita, M., Davuluri, R. V., Pandolfi, P. P., Ferbeyre, G., & Lowe, S. W. (2004). PML is a direct p53 target that modulates p53 effector functions. *Mol Cell*, *13*(4), 523-535. https://doi.org/10.1016/s1097-2765(04)00062-0

121. de The, H., Chomienne, C., Lanotte, M., Degos, L., & Dejean, A. (1990). The t(15;17) translocation of acute promyelocytic leukaemia fuses the retinoic acid receptor alpha gene to a novel transcribed locus. *Nature*, *347*(6293), 558-561. https://doi.org/10.1038/347558a0

122. Dellaire, G., & Bazett-Jones, D. P. (2004). PML nuclear bodies: dynamic sensors of DNA damage and cellular stress. *Bioessays*, *26*(9), 963-977. https://doi.org/10.1002/bies.20089

123. Dellaire, G., Ching, R. W., Ahmed, K., Jalali, F., Tse, K. C., Bristow, R. G., & Bazett-Jones, D. P. (2006). Promyelocytic leukemia nuclear bodies behave as DNA damage sensors whose response to DNA double-strand breaks is regulated by NBS1 and the kinases ATM, Chk2, and ATR. *J Cell Biol*, *175*(1), 55-66. https://doi.org/10.1083/jcb.200604009

124. Dellaire, G., Eskiw, C. H., Dehghani, H., Ching, R. W., & Bazett-Jones, D. P. (2006). Mitotic accumulations of PML protein contribute to the re-establishment of PML nuclear bodies in G1. *J Cell Sci*, *119*(Pt 6), 1034-1042. https://doi.org/10.1242/jcs.02817

125. Dellaire, G., Farrall, R., & Bickmore, W. A. (2003). The Nuclear Protein Database (NPD): sub-nuclear localisation and functional annotation of the nuclear proteome. *Nucleic Acids Res*, *31*(1), 328-330. https://doi.org/10.1093/nar/gkg018

126. Denis, J. F., Sader, F., Ferretti, P., & Roy, S. (2015). Culture and transfection of axolotl cells. *Methods Mol Biol*, *1290*, 187-196. https://doi.org/10.1007/978-1-4939-2495-0_15

127. Denli, A. M., Narvaiza, I., Kerman, B. E., Pena, M., Benner, C., Marchetto, M. C., Diedrich, J. K., Aslanian, A., Ma, J., Moresco, J. J., Moore, L., Hunter, T., Saghatelian, A., & Gage, F. H. (2015). Primate-specific ORF0 contributes to retrotransposon-mediated diversity. *Cell*, *163*(3), 583-593. https://doi.org/10.1016/j.cell.2015.09.025

128. Derynck, R., & Zhang, Y. E. (2003). Smad-dependent and Smad-independent pathways in TGF-β family signalling. *Nature*, *425*(6958), 577-584. https://doi.org/10.1038/nature02006

129. Deschamps, T., & Kalamvoki, M. (2017). Impaired STING Pathway in Human Osteosarcoma U2OS Cells Contributes to the Growth of ICP0-Null Mutant Herpes Simplex Virus. *J Virol*, *91*(9). https://doi.org/10.1128/JVI.00006-17

130. di Masi, A., Cilli, D., Berardinelli, F., Talarico, A., Pallavicini, I., Pennisi, R., Leone, S., Antoccia, A., Noguera, N. I., Lo-Coco, F., Ascenzi, P., Minucci, S., & Nervi, C. (2016). PML nuclear body disruption impairs DNA double-strand break sensing and repair in APL. *Cell Death Dis*, *7*(7), e2308. https://doi.org/10.1038/cddis.2016.115

131. Di Micco, R., Krizhanovsky, V., Baker, D., & d'Adda di Fagagna, F. (2021). Cellular senescence in ageing: from mechanisms to therapeutic opportunities. *Nat Rev Mol Cell Biol*, *22*(2), 75-95. https://doi.org/10.1038/s41580-020-00314-w

132. Diller, R. B., & Tabor, A. J. (2022). The Role of the Extracellular Matrix (ECM) in Wound Healing: A Review. *Biomimetics (Basel)*, *7*(3). https://doi.org/10.3390/biomimetics7030087

133. Diner, E. J., Burdette, D. L., Wilson, S. C., Monroe, K. M., Kellenberger, C. A., Hyodo, M., Hayakawa, Y., Hammond, M. C., & Vance, R. E. (2013). The innate immune DNA sensor cGAS produces a noncanonical cyclic dinucleotide that activates human STING. *Cell Rep*, *3*(5), 1355-1361. https://doi.org/10.1016/j.celrep.2013.05.009

134. Dion-Cote, A. M., & Barbash, D. A. (2017). Beyond speciation genes: an overview of genome stability in evolution and speciation. *Curr Opin Genet Dev*, *47*, 17-23. https://doi.org/10.1016/j.gde.2017.07.014

135. Dobbs, N., Burnaevskiy, N., Chen, D., Gonugunta, V. K., Alto, N. M., & Yan, N. (2015). STING Activation by Translocation from the ER Is Associated with Infection and Autoinflammatory Disease. *Cell Host Microbe*, *18*(2), 157-168. https://doi.org/10.1016/j.chom.2015.07.001

136. Dooley, K., & Zon, L. I. (2000). Zebrafish: a model system for the study of human disease. *Curr Opin Genet Dev*, *10*(3), 252-256. https://doi.org/10.1016/s0959-437x(00)00074-5

137. Drane, P., Ouararhni, K., Depaux, A., Shuaib, M., & Hamiche, A. (2010). The death-associated protein DAXX is a novel histone chaperone involved in the replication-independent deposition of H3.3. *Genes Dev*, *24*(12), 1253-1265. https://doi.org/10.1101/gad.566910

138. Du, H., Xiao, N., Zhang, S., Zhou, X., Zhang, Y., Lu, Z., Fu, Y., Huang, M., Xu, S., & Chen, Q. (2023). Suppression of TREX1 deficiency-induced cellular senescence and interferonopathies by inhibition of DNA damage response. *iScience*, *26*(7), 107090. https://doi.org/https://doi.org/10.1016/j.isci.2023.107090

139. Du, M., & Chen, Z. J. (2018). DNA-induced liquid phase condensation of cGAS activates innate immune signaling. *Science*, *361*(6403), 704-709. https://doi.org/10.1126/science.aat1022

140. Dunn, G. P., Bruce, A. T., Sheehan, K. C., Shankaran, V., Uppaluri, R., Bui, J. D., Diamond, M. S., Koebel, C. M., Arthur, C., White, J. M., & Schreiber, R. D. (2005). A critical function for type I interferons in cancer immunoediting. *Nat Immunol*, *6*(7), 722-729. https://doi.org/10.1038/ni1213

141. Dutrieux, J., Maarifi, G., Portilho, D. M., Arhel, N. J., Chelbi-Alix, M. K., & Nisole, S. (2015). PML/TRIM19-Dependent Inhibition of Retroviral Reverse-Transcription by Daxx. *PLoS Pathog*, *11*(11), e1005280. https://doi.org/10.1371/journal.ppat.1005280

142. Dwaraka, V. B., & Voss, S. R. (2021). Towards comparative analyses of salamander limb regeneration. *J Exp Zool B Mol Dev Evol*, *336*(2), 129-144. https://doi.org/10.1002/jez.b.22902

143. El-Asmi, F., El-Mchichi, B., Maroui, M. A., Dianoux, L., & Chelbi-Alix, M. K. (2019). TGF-β induces PML SUMOylation, degradation and PML nuclear body disruption. *Cytokine*, *120*, 264-272. https://doi.org/https://doi.org/10.1016/j.cyto.2019.05.008

144. El McHichi, B., Regad, T., Maroui, M. A., Rodriguez, M. S., Aminev, A., Gerbaud, S., Escriou, N., Dianoux, L., & Chelbi-Alix, M. K. (2010).

SUMOylation promotes PML degradation during encephalomyocarditis virus infection. *J Virol*, *84*(22), 11634-11645. https://doi.org/10.1128/JVI.01321-10

145. Eming, S. A., Martin, P., & Tomic-Canic, M. (2014). Wound repair and regeneration: mechanisms, signaling, and translation. *Sci Transl Med*, *6*(265), 265sr266. https://doi.org/10.1126/scitranslmed.3009337

146. Erdal, E., Haider, S., Rehwinkel, J., Harris, A. L., & McHugh, P. J. (2017). A prosurvival DNA damage-induced cytoplasmic interferon response is mediated by end resection factors and is limited by Trex1. *Genes & development*, *31*(4), 353-369.

147. Erdal, E., Haider, S., Rehwinkel, J., Harris, A. L., & McHugh, P. J. (2017). A prosurvival DNA damage-induced cytoplasmic interferon response is mediated by end resection factors and is limited by Trex1. *Genes Dev*, *31*(4), 353-369. https://doi.org/10.1101/gad.289769.116

148. Eskiw, C. H., Dellaire, G., & Bazett-Jones, D. P. (2004). Chromatin contributes to structural integrity of promyelocytic leukemia bodies through a SUMO-1-independent mechanism. *J Biol Chem*, *279*(10), 9577-9585. https://doi.org/10.1074/jbc.M312580200

149. Everett, R. D., & Chelbi-Alix, M. K. (2007). PML and PML nuclear bodies: implications in antiviral defence. *Biochimie*, *89*(6-7), 819-830. https://doi.org/10.1016/j.biochi.2007.01.004

150. Everett, R. D., Lomonte, P., Sternsdorf, T., van Driel, R., & Orr, A. (1999). Cell cycle regulation of PML modification and ND10 composition. *J Cell Sci*, *112 (Pt 24)*, 4581-4588. https://doi.org/10.1242/jcs.112.24.4581

151. Fagioli, M., Alcalay, M., Pandolfi, P. P., Venturini, L., Mencarelli, A., Simeone, A., Acampora, D., Grignani, F., & Pelicci, P. G. (1992). Alternative splicing of PML transcripts predicts coexpression of several carboxy-terminally different protein isoforms. *Oncogene*, *7*(6), 1083-1091.

152. Fasci, D., Anania, V. G., Lill, J. R., & Salvesen, G. S. (2015). SUMO deconjugation is required for arsenic-triggered ubiquitylation of PML. *Science Signaling*, *8*(380), ra56-ra56. https://doi.org/doi:10.1126/scisignal.aaa3929

153. Ferbeyre, G., de Stanchina, E., Querido, E., Baptiste, N., Prives, C., & Lowe, S. W. (2000). PML is induced by oncogenic ras and promotes premature senescence. *Genes Dev*, *14*(16), 2015-2027. https://www.ncbi.nlm.nih.gov/pubmed/10950866

154. Fischer, J. C., Bscheider, M., Eisenkolb, G., Lin, C. C., Wintges, A., Otten, V., Lindemans, C. A., Heidegger, S., Rudelius, M., Monette, S., Porosnicu Rodriguez, K. A., Calafiore, M., Liebermann, S., Liu, C., Lienenklaus, S., Weiss, S., Kalinke, U., Ruland, J., Peschel, C., . . . Poeck, H. (2017). RIG-I/MAVS and STING signaling promote gut integrity during irradiation- and immune-mediated

tissue injury. *Sci Transl Med*, *9*(386). https://doi.org/10.1126/scitranslmed.aag2513

155. Flasch, D. A., Macia, A., Sanchez, L., Ljungman, M., Heras, S. R., Garcia-Perez, J. L., Wilson, T. E., & Moran, J. V. (2019). Genome-wide de novo L1 Retrotransposition Connects Endonuclease Activity with Replication. *Cell*, *177*(4), 837-851 e828. https://doi.org/10.1016/j.cell.2019.02.050

156. Flotho, A., & Melchior, F. (2013). Sumoylation: a regulatory protein modification in health and disease. *Annu Rev Biochem*, *82*, 357-385. https://doi.org/10.1146/annurev-biochem-061909-093311

157. Fogal, V., Gostissa, M., Sandy, P., Zacchi, P., Sternsdorf, T., Jensen, K., Pandolfi, P. P., Will, H., Schneider, C., & Del Sal, G. (2000). Regulation of p53 activity in nuclear bodies by a specific PML isoform. *EMBO J*, *19*(22), 6185-6195. https://doi.org/10.1093/emboj/19.22.6185

158. Francica, B., Burdette, D., Clark, R., Cope, J., Freund, D., Holtz, A., Prasit, P., Whiting, C., & Dubensky, T. W. (2022). Abstract 2075: Systemic small molecule TREX1 inhibitors to selectively activate STING in the TME of metastatic disease. *Cancer Research*, *82*(12_Supplement), 2075-2075. https://doi.org/10.1158/1538-7445.AM2022-2075

159. Freund, A., Orjalo, A. V., Desprez, P. Y., & Campisi, J. (2010). Inflammatory networks during cellular senescence: causes and consequences. *Trends Mol Med*, *16*(5), 238-246. https://doi.org/10.1016/j.molmed.2010.03.003

160. Frisch, S. M., & MacFawn, I. P. (2020). Type I interferons and related pathways in cell senescence. *Aging Cell*, *19*(10), e13234. https://doi.org/10.1111/acel.13234

161. Fung, H. Y., & Chook, Y. M. (2014). Atomic basis of CRM1-cargo recognition, release and inhibition. *Semin Cancer Biol*, *27*, 52-61. https://doi.org/10.1016/j.semcancer.2014.03.002

162. Galanty, Y., Belotserkovskaya, R., Coates, J., Polo, S., Miller, K. M., & Jackson, S. P. (2009). Mammalian SUMO E3-ligases PIAS1 and PIAS4 promote responses to DNA double-strand breaks. *Nature*, *462*(7275), 935-939. https://doi.org/10.1038/nature08657

163. Galisson, F., Mahrouche, L., Courcelles, M., Bonneil, E., Meloche, S., Chelbi-Alix, M. K., & Thibault, P. (2011). A novel proteomics approach to identify SUMOylated proteins and their modification sites in human cells. *Mol Cell Proteomics*, *10*(2), M110.004796. https://doi.org/10.1074/mcp.M110.004796

164. Galon, J., & Bruni, D. (2019). Approaches to treat immune hot, altered and cold tumours with combination immunotherapies. *Nat Rev Drug Discov*, *18*(3), 197-218. https://doi.org/10.1038/s41573-018-0007-y

165. Gao, D., Li, T., Li, X. D., Chen, X., Li, Q. Z., Wight-Carter, M., & Chen, Z. J. (2015). Activation of cyclic GMP-AMP synthase by self-DNA causes autoimmune diseases. *Proc Natl Acad Sci U S A*, *112*(42), E5699-5705. https://doi.org/10.1073/pnas.1516465112

166. Garbati, M. R., Hays, L. E., Rathbun, R. K., Jillette, N., Chin, K., Al-Dhalimy, M., Agarwal, A., Newell, A. E., Olson, S. B., & Bagby, G. C., Jr. (2016). Cytokine overproduction and crosslinker hypersensitivity are unlinked in Fanconi anemia macrophages. *J Leukoc Biol*, *99*(3), 455-465. https://doi.org/10.1189/jlb.3A0515-201R

167. Garcia-Lepe, U. O., Cruz-Ramirez, A., & Bermudez-Cruz, R. M. (2021). DNA repair during regeneration in Ambystoma mexicanum. *Dev Dyn*, *250*(6), 788-799. https://doi.org/10.1002/dvdy.276

168. Garcia-Lepe, U. O., Torres-Dimas, E., Espinal-Centeno, A., Cruz-Ramirez, A., & Bermudez-Cruz, R. M. (2022). Evidence of requirement for homologous-mediated DNA repair during Ambystoma mexicanum limb regeneration. *Dev Dyn*, *251*(6), 1035-1053. https://doi.org/10.1002/dvdy.455

169. Garcia Perez, J. L., & Alarcon-Riquelme, M. E. (2017). The TREX1 Dinosaur Bites the Brain through the LINE. *Cell Stem Cell*, *21*(3), 287-288. https://doi.org/10.1016/j.stem.2017.08.010

170. Gärtner, A., & Muller, S. (2014). PML, SUMO, and RNF4: guardians of nuclear protein quality. *Mol Cell*, *55*(1), 1-3. https://doi.org/10.1016/j.molcel.2014.06.022

171. Gasior, S. L., Wakeman, T. P., Xu, B., & Deininger, P. L. (2006). The human LINE-1 retrotransposon creates DNA double-strand breaks. *J Mol Biol*, *357*(5), 1383-1393. https://doi.org/10.1016/j.jmb.2006.01.089

172. Gawriluk, T. R., Simkin, J., Hacker, C. K., Kimani, J. M., Kiama, S. G., Ezenwa, V. O., & Seifert, A. W. (2020). Complex Tissue Regeneration in Mammals Is Associated With Reduced Inflammatory Cytokines and an Influx of T Cells. *Front Immunol*, *11*, 1695. https://doi.org/10.3389/fimmu.2020.01695

173. Ge, R., Zhou, Y., Peng, R., Wang, R., Li, M., Zhang, Y., Zheng, C., & Wang, C. (2015). Conservation of the STING-Mediated Cytosolic DNA Sensing Pathway in Zebrafish. *J Virol*, *89*(15), 7696-7706. https://doi.org/10.1128/jvi.01049-15

174. Gehart, H., & Clevers, H. (2019). Tales from the crypt: new insights into intestinal stem cells. *Nat Rev Gastroenterol Hepatol*, *16*(1), 19-34. https://doi.org/10.1038/s41575-018-0081-y

175. Gehrke, N., Mertens, C., Zillinger, T., Wenzel, J., Bald, T., Zahn, S., Tuting, T., Hartmann, G., & Barchet, W. (2013). Oxidative damage of DNA confers resistance to cytosolic nuclease TREX1 degradation and potentiates STING-

dependent immune sensing. *Immunity*, *39*(3), 482-495. https://doi.org/10.1016/j.immuni.2013.08.004

176. Gentric, G., Kieffer, Y., Mieulet, V., Goundiam, O., Bonneau, C., Nemati, F., Hurbain, I., Raposo, G., Popova, T., Stern, M. H., Lallemand-Breitenbach, V., Muller, S., Caneque, T., Rodriguez, R., Vincent-Salomon, A., de The, H., Rossignol, R., & Mechta-Grigoriou, F. (2019). PML-Regulated Mitochondrial Metabolism Enhances Chemosensitivity in Human Ovarian Cancers. *Cell Metab*, *29*(1), 156-173 e110. https://doi.org/10.1016/j.cmet.2018.09.002

177. Geoffroy, M.-C., Jaffray, E. G., Walker, K. J., & Hay, R. T. (2010). Arsenic-Induced SUMO-Dependent Recruitment of RNF4 into PML Nuclear Bodies. *Molecular Biology of the Cell*, *21*(23), 4227-4239. https://doi.org/10.1091/mbc.e10-05-0449

178. Geoffroy, M. C., & Chelbi-Alix, M. K. (2011). Role of promyelocytic leukemia protein in host antiviral defense. *J Interferon Cytokine Res*, *31*(1), 145-158. https://doi.org/10.1089/jir.2010.0111

179. Giaimo, S., & d'Adda di Fagagna, F. (2012). Is cellular senescence an example of antagonistic pleiotropy? *Aging Cell*, *11*(3), 378-383. https://doi.org/10.1111/j.1474-9726.2012.00807.x

180. Giorgi, C., Ito, K., Lin, H. K., Santangelo, C., Wieckowski, M. R., Lebiedzinska, M., Bononi, A., Bonora, M., Duszynski, J., Bernardi, R., Rizzuto, R., Tacchetti, C., Pinton, P., & Pandolfi, P. P. (2010). PML regulates apoptosis at endoplasmic reticulum by modulating calcium release. *Science*, *330*(6008), 1247-1251. https://doi.org/10.1126/science.1189157

181. Glück, S., Guey, B., Gulen, M. F., Wolter, K., Kang, T. W., Schmacke, N. A., Bridgeman, A., Rehwinkel, J., Zender, L., & Ablasser, A. (2017). Innate immune sensing of cytosolic chromatin fragments through cGAS promotes senescence. *Nat Cell Biol*, *19*(9), 1061-1070. https://doi.org/10.1038/ncb3586

182. Godwin, J. (2014). The promise of perfect adult tissue repair and regeneration in mammals: Learning from regenerative amphibians and fish. *Bioessays*, *36*(9), 861-871. https://doi.org/https://doi.org/10.1002/bies.201300144

183. Godwin, J. W., Pinto, A. R., & Rosenthal, N. A. (2013). Macrophages are required for adult salamander limb regeneration. *Proc Natl Acad Sci U S A*, *110*(23), 9415-9420. https://doi.org/10.1073/pnas.1300290110

184. Gonzalez, A. C., Costa, T. F., Andrade, Z. A., & Medrado, A. R. (2016). Wound healing - A literature review. *An Bras Dermatol*, *91*(5), 614-620. https://doi.org/10.1590/abd1806-4841.20164741

185. Goodier, J. L. (2016). Restricting retrotransposons: a review. *Mob DNA*, *7*, 16. https://doi.org/10.1186/s13100-016-0070-z

186. Goss, R. J., & Holt, R. (1992). Epimorphic vs. tissue regeneration in Xenopus forelimbs. *Journal of Experimental Zoology*, *261*(4), 451-457. https://doi.org/https://doi.org/10.1002/jez.1402610412

187. Goubau, D., Deddouche, S., & Reis e Sousa, C. (2013). Cytosolic sensing of viruses. *Immunity*, *38*(5), 855-869. https://doi.org/10.1016/j.immuni.2013.05.007

188. Gray, E. E., Treuting, P. M., Woodward, J. J., & Stetson, D. B. (2015). Cutting edge: cGAS is required for lethal autoimmune disease in the Trex1-deficient mouse model of Aicardi–Goutières syndrome. *The Journal of Immunology*, *195*(5), 1939-1943.

189. Grignani, F., Fagioli, M., Ferrucci, P. F., Alcalay, M., & Pelicci, P. G. (1993). The molecular genetics of acute promyelocytic leukemia. *Blood Rev*, *7*(2), 87-93. https://doi.org/10.1016/s0268-960x(05)80018-9

190. Guan, D., Lim, J. H., Peng, L., Liu, Y., Lam, M., Seto, E., & Kao, H. Y. (2014). Deacetylation of the tumor suppressor protein PML regulates hydrogen peroxide-induced cell death. *Cell Death & Disease*, *5*(7), e1340-e1340. https://doi.org/10.1038/cddis.2014.185

191. Gulen, M. F., Samson, N., Keller, A., Schwabenland, M., Liu, C., Gluck, S., Thacker, V. V., Favre, L., Mangeat, B., Kroese, L. J., Krimpenfort, P., Prinz, M., & Ablasser, A. (2023). cGAS-STING drives ageing-related inflammation and neurodegeneration. *Nature*, *620*(7973), 374-380. https://doi.org/10.1038/s41586-023-06373-1

192. Guo, L., Giasson, B. I., Glavis-Bloom, A., Brewer, M. D., Shorter, J., Gitler, A. D., & Yang, X. (2014). A cellular system that degrades misfolded proteins and protects against neurodegeneration. *Mol Cell*, *55*(1), 15-30. https://doi.org/10.1016/j.molcel.2014.04.030

193. Gurrieri, C., Capodieci, P., Bernardi, R., Scaglioni, P. P., Nafa, K., Rush, L. J., Verbel, D. A., Cordon-Cardo, C., & Pandolfi, P. P. (2004). Loss of the tumor suppressor PML in human cancers of multiple histologic origins. *J Natl Cancer Inst*, *96*(4), 269-279. https://doi.org/10.1093/jnci/djh043

194. Hakem, R. (2008). DNA-damage repair; the good, the bad, and the ugly. *EMBO J*, *27*(4), 589-605. https://doi.org/10.1038/emboj.2008.15

195. Haller, M., Hock, A. K., Giampazolias, E., Oberst, A., Green, D. R., Debnath, J., Ryan, K. M., Vousden, K. H., & Tait, S. W. (2014). Ubiquitination and proteasomal degradation of ATG12 regulates its proapoptotic activity. *Autophagy*, *10*(12), 2269-2278.

196. Hamming, O. J., Lutfalla, G., Levraud, J. P., & Hartmann, R. (2011). Crystal structure of Zebrafish interferons I and II reveals conservation of type I interferon

structure in vertebrates. *J Virol*, *85*(16), 8181-8187. https://doi.org/10.1128/jvi.00521-11

197. Hancks, D. C., & Kazazian, H. H., Jr. (2016). Roles for retrotransposon insertions in human disease. *Mob DNA*, *7*, 9. https://doi.org/10.1186/s13100-016-0065-9

198. Hancock-Cerutti, W., Wu, Z., Xu, P., Yadavalli, N., Leonzino, M., Tharkeshwar, A. K., Ferguson, S. M., Shadel, G. S., & De Camilli, P. (2022). ER-lysosome lipid transfer protein VPS13C/PARK23 prevents aberrant mtDNA-dependent STING signaling. *J Cell Biol*, *221*(7). https://doi.org/10.1083/jcb.202106046

199. Handwerger, K. E., & Gall, J. G. (2006). Subnuclear organelles: new insights into form and function. *Trends Cell Biol*, *16*(1), 19-26. https://doi.org/10.1016/j.tcb.2005.11.005

200. Harding, S. M., Benci, J. L., Irianto, J., Discher, D. E., Minn, A. J., & Greenberg, R. A. (2017). Mitotic progression following DNA damage enables pattern recognition within micronuclei. *Nature*, *548*(7668), 466-470. https://doi.org/10.1038/nature23470

201. Hardy, K., Mansfield, L., Mackay, A., Benvenuti, S., Ismail, S., Arora, P., O'Hare, M. J., & Jat, P. S. (2005). Transcriptional networks and cellular senescence in human mammary fibroblasts. *Mol Biol Cell*, *16*(2), 943-953. https://doi.org/10.1091/mbc.e04-05-0392

202. Hasan, M., Fermaintt, C. S., Gao, N., Sakai, T., Miyazaki, T., Jiang, S., Li, Q. Z., Atkinson, J. P., Morse, H. C., 3rd, Lehrman, M. A., & Yan, N. (2015). Cytosolic Nuclease TREX1 Regulates Oligosaccharyltransferase Activity Independent of Nuclease Activity to Suppress Immune Activation. *Immunity*, *43*(3), 463-474. https://doi.org/10.1016/j.immuni.2015.07.022

203. Hasan, M., & Yan, N. (2014). Safeguard against DNA sensing: the role of TREX1 in HIV-1 infection and autoimmune diseases. *Front Microbiol*, *5*, 193. https://doi.org/10.3389/fmicb.2014.00193

204. Hason, M., & Bartůněk, P. (2019). Zebrafish Models of Cancer-New Insights on Modeling Human Cancer in a Non-Mammalian Vertebrate. *Genes (Basel)*, *10*(11). https://doi.org/10.3390/genes10110935

205. Hastie, K. M., King, L. B., Zandonatti, M. A., & Saphire, E. O. (2012). Structural basis for the dsRNA specificity of the Lassa virus NP exonuclease. *PLoS One*, *7*(8), e44211. https://doi.org/10.1371/journal.pone.0044211

206. Hattersley, N., Shen, L., Jaffray, E. G., & Hay, R. T. (2011). The SUMO protease SENP6 is a direct regulator of PML nuclear bodies. *Mol Biol Cell*, *22*(1), 78-90. https://doi.org/10.1091/mbc.E10-06-0504

207. Hayashi, Y., Kajikawa, M., Matsumoto, T., & Okada, N. (2014). Mechanism by which a LINE protein recognizes its 3' tail RNA. *Nucleic Acids Res*, *42*(16), 10605-10617. https://doi.org/10.1093/nar/gku753

208. He, L. Z., Guidez, F., Tribioli, C., Peruzzi, D., Ruthardt, M., Zelent, A., & Pandolfi, P. P. (1998). Distinct interactions of PML-RARalpha and PLZF-RARalpha with co-repressors determine differential responses to RA in APL. *Nat Genet*, *18*(2), 126-135. https://doi.org/10.1038/ng0298-126

209. He, X., Riceberg, J., Soucy, T., Koenig, E., Minissale, J., Gallery, M., Bernard, H., Yang, X., Liao, H., & Rabino, C. (2017). Probing the roles of SUMOylation in cancer cell biology by using a selective SAE inhibitor. *Nature chemical biology*, *13*(11), 1164-1171.

210. Hegde, P. S., & Chen, D. S. (2020). Top 10 Challenges in Cancer Immunotherapy. *Immunity*, *52*(1), 17-35. https://doi.org/10.1016/j.immuni.2019.12.011

211. Hegde, P. S., Karanikas, V., & Evers, S. (2016). The Where, the When, and the How of Immune Monitoring for Cancer Immunotherapies in the Era of Checkpoint Inhibition. *Clin Cancer Res*, *22*(8), 1865-1874. https://doi.org/10.1158/1078-0432.CCR-15-1507

212. Hemphill, W. O., & Perrino, F. W. (2019). Measuring TREX1 and TREX2 exonuclease activities. *Methods Enzymol*, *625*, 109-133. https://doi.org/10.1016/bs.mie.2019.05.004

213. Hemphill, W. O., Simpson, S. R., Liu, M., Salsbury, F. R., Jr., Hollis, T., Grayson, J. M., & Perrino, F. W. (2021). TREX1 as a Novel Immunotherapeutic Target. *Front Immunol*, *12*, 660184. https://doi.org/10.3389/fimmu.2021.660184

214. Hendriks, I. A., D'Souza, R. C., Yang, B., Verlaan-de Vries, M., Mann, M., & Vertegaal, A. C. (2014). Uncovering global SUMOylation signaling networks in a site-specific manner. *Nat Struct Mol Biol*, *21*(10), 927-936. https://doi.org/10.1038/nsmb.2890

215. Hendriks, I. A., Lyon, D., Su, D., Skotte, N. H., Daniel, J. A., Jensen, L. J., & Nielsen, M. L. (2018). Site-specific characterization of endogenous SUMOylation across species and organs. *Nat Commun*, *9*(1), 2456. https://doi.org/10.1038/s41467-018-04957-4

216. Henne, W. M., Reese, M. L., & Goodman, J. M. (2018). The assembly of lipid droplets and their roles in challenged cells. *EMBO J*, *37*(12). https://doi.org/10.15252/embj.201898947

217. Herbig, U., Ferreira, M., Condel, L., Carey, D., & Sedivy, J. M. (2006). Cellular senescence in aging primates. *Science*, *311*(5765), 1257. https://doi.org/10.1126/science.1122446

218. Herbst, R. S., Soria, J. C., Kowanetz, M., Fine, G. D., Hamid, O., Gordon, M. S., Sosman, J. A., McDermott, D. F., Powderly, J. D., Gettinger, S. N., Kohrt, H. E., Horn, L., Lawrence, D. P., Rost, S., Leabman, M., Xiao, Y., Mokatrin, A., Koeppen, H., Hegde, P. S., . . . Hodi, F. S. (2014). Predictive correlates of response to the anti-PD-L1 antibody MPDL3280A in cancer patients. *Nature*, *515*(7528), 563-567. https://doi.org/10.1038/nature14011

219. Herrmann, A., Wittmann, S., Thomas, D., Shepard, C. N., Kim, B., Ferreiros, N., & Gramberg, T. (2018). The SAMHD1-mediated block of LINE-1 retroelements is regulated by phosphorylation. *Mob DNA*, *9*, 11. https://doi.org/10.1186/s13100-018-0116-5

220. Herzner, A. M., Hagmann, C. A., Goldeck, M., Wolter, S., Kubler, K., Wittmann, S., Gramberg, T., Andreeva, L., Hopfner, K. P., Mertens, C., Zillinger, T., Jin, T., Xiao, T. S., Bartok, E., Coch, C., Ackermann, D., Hornung, V., Ludwig, J., Barchet, W., . . . Schlee, M. (2015). Sequence-specific activation of the DNA sensor cGAS by Y-form DNA structures as found in primary HIV-1 cDNA. *Nat Immunol*, *16*(10), 1025-1033. https://doi.org/10.1038/ni.3267

221. Hillestad, L. K. (1957). Acute promyelocytic leukemia. *Acta Med Scand*, *159*(3), 189-194. https://www.ncbi.nlm.nih.gov/pubmed/13508085

222. Hohjoh, H., & Singer, M. F. (1996). Cytoplasmic ribonucleoprotein complexes containing human LINE-1 protein and RNA. *EMBO J*, *15*(3), 630-639. https://www.ncbi.nlm.nih.gov/pubmed/8599946

223. Hoischen, C., Monajembashi, S., Weisshart, K., & Hemmerich, P. (2018). Multimodal Light Microscopy Approaches to Reveal Structural and Functional Properties of Promyelocytic Leukemia Nuclear Bodies. *Front Oncol*, *8*, 125. https://doi.org/10.3389/fonc.2018.00125

224. Hopfner, K.-P., & Hornung, V. (2020). Molecular mechanisms and cellular functions of cGAS–STING signalling. *Nature reviews Molecular cell biology*, *21*(9), 501-521.

225. Horio, T., Murai, M., Inoue, T., Hamasaki, T., Tanaka, T., & Ohgi, T. (2004). Crystal structure of human ISG20, an interferon-induced antiviral ribonuclease. *FEBS Lett*, *577*(1-2), 111-116. https://doi.org/10.1016/j.febslet.2004.09.074

226. Hsiao, Y. Y., Duh, Y., Chen, Y. P., Wang, Y. T., & Yuan, H. S. (2012). How an exonuclease decides where to stop in trimming of nucleic acids: crystal structures of RNase T-product complexes. *Nucleic Acids Res*, *40*(16), 8144-8154. https://doi.org/10.1093/nar/gks548

227. Hsiao, Y. Y., Nakagawa, A., Shi, Z., Mitani, S., Xue, D., & Yuan, H. S. (2009). Crystal structure of CRN-4: implications for domain function in apoptotic DNA degradation. *Mol Cell Biol*, *29*(2), 448-457. https://doi.org/10.1128/MCB.01006-08

228. Hu, M., Zhou, M., Bao, X., Pan, D., Jiao, M., Liu, X., Li, F., & Li, C. Y. (2021). ATM inhibition enhances cancer immunotherapy by promoting mtDNA leakage and cGAS/STING activation. *J Clin Invest*, *131*(3). https://doi.org/10.1172/JCI139333

229. Huang, K. W., Liu, T. C., Liang, R. Y., Chu, L. Y., Cheng, H. L., Chu, J. W., & Hsiao, Y. Y. (2018). Structural basis for overhang excision and terminal unwinding of DNA duplexes by TREX1. *PLoS Biol*, *16*(5), e2005653. https://doi.org/10.1371/journal.pbio.2005653

230. Ibáñez, M., Carbonell-Caballero, J., García-Alonso, L., Such, E., Jiménez-Almazán, J., Vidal, E., Barragán, E., López-Pavía, M., M, L. L., Martín, I., Gómez-Seguí, I., Montesinos, P., Sanz, M. A., Dopazo, J., & Cervera, J. (2016). The Mutational Landscape of Acute Promyelocytic Leukemia Reveals an Interacting Network of Co-Occurrences and Recurrent Mutations. *PLoS One*, *11*(2), e0148346. https://doi.org/10.1371/journal.pone.0148346

231. Iijima, K., Ohara, M., Seki, R., & Tauchi, H. (2008). Dancing on damaged chromatin: functions of ATM and the RAD50/MRE11/NBS1 complex in cellular responses to DNA damage. *J Radiat Res*, *49*(5), 451-464. https://doi.org/10.1269/jrr.08065

232. Iismaa, S. E., Kaidonis, X., Nicks, A. M., Bogush, N., Kikuchi, K., Naqvi, N., Harvey, R. P., Husain, A., & Graham, R. M. (2018). Comparative regenerative mechanisms across different mammalian tissues. *NPJ Regen Med*, *3*, 6. https://doi.org/10.1038/s41536-018-0044-5

233. Iismaa, S. E., Kaidonis, X., Nicks, A. M., Bogush, N., Kikuchi, K., Naqvi, N., Harvey, R. P., Husain, A., & Graham, R. M. (2018). Comparative regenerative mechanisms across different mammalian tissues. *npj Regenerative Medicine*, *3*(1), 6. https://doi.org/10.1038/s41536-018-0044-5

234. Ishikawa, H., & Barber, G. N. (2008). STING is an endoplasmic reticulum adaptor that facilitates innate immune signalling. *Nature*, *455*(7213), 674-678. https://doi.org/10.1038/nature07317

235. Ishov, A. M., Sotnikov, A. G., Negorev, D., Vladimirova, O. V., Neff, N., Kamitani, T., Yeh, E. T., Strauss, J. F., 3rd, & Maul, G. G. (1999). PML is critical for ND10 formation and recruits the PML-interacting protein daxx to this nuclear structure when modified by SUMO-1. *J Cell Biol*, *147*(2), 221-234. https://doi.org/10.1083/jcb.147.2.221

236. Ito, K., Bernardi, R., Morotti, A., Matsuoka, S., Saglio, G., Ikeda, Y., Rosenblatt, J., Avigan, D. E., Teruya-Feldstein, J., & Pandolfi, P. P. (2008). PML targeting eradicates quiescent leukaemia-initiating cells. *Nature*, *453*(7198), 1072-1078. https://doi.org/10.1038/nature07016

237. Ivanschitz, L., Takahashi, Y., Jollivet, F., Ayrault, O., Le Bras, M., & de The, H. (2015). PML IV/ARF interaction enhances p53 SUMO-1 conjugation, activation, and senescence. *Proc Natl Acad Sci U S A*, *112*(46), 14278-14283. https://doi.org/10.1073/pnas.1507540112

238. Jackson, S. P., & Bartek, J. (2009). The DNA-damage response in human biology and disease. *Nature*, *461*(7267), 1071-1078. https://doi.org/10.1038/nature08467

239. Jaillon, O., Aury, J. M., Brunet, F., Petit, J. L., Stange-Thomann, N., Mauceli, E., Bouneau, L., Fischer, C., Ozouf-Costaz, C., Bernot, A., Nicaud, S., Jaffe, D., Fisher, S., Lutfalla, G., Dossat, C., Segurens, B., Dasilva, C., Salanoubat, M., Levy, M., . . . Roest Crollius, H. (2004). Genome duplication in the teleost fish Tetraodon nigroviridis reveals the early vertebrate proto-karyotype. *Nature*, *431*(7011), 946-957. https://doi.org/10.1038/nature03025

240. Janer, A., Martin, E., Muriel, M. P., Latouche, M., Fujigasaki, H., Ruberg, M., Brice, A., Trottier, Y., & Sittler, A. (2006). PML clastosomes prevent nuclear accumulation of mutant ataxin-7 and other polyglutamine proteins. *J Cell Biol*, *174*(1), 65-76. https://doi.org/10.1083/jcb.200511045

241. Jauhari, A., Baranov, S. V., Suofu, Y., Kim, J., Singh, T., Yablonska, S., Li, F., Wang, X., Oberly, P., Minnigh, M. B., Poloyac, S. M., Carlisle, D. L., & Friedlander, R. M. (2020). Melatonin inhibits cytosolic mitochondrial DNA-induced neuroinflammatory signaling in accelerated aging and neurodegeneration. *J Clin Invest*, *130*(6), 3124-3136. https://doi.org/10.1172/JCI135026

242. Jensen, K., Shiels, C., & Freemont, P. S. (2001). PML protein isoforms and the RBCC/TRIM motif. *Oncogene*, *20*(49), 7223-7233. https://doi.org/10.1038/sj.onc.1204765

243. Jin, S., & Weaver, D. T. (1997). Double-strand break repair by Ku70 requires heterodimerization with Ku80 and DNA binding functions. *EMBO J*, *16*(22), 6874-6885. https://doi.org/10.1093/emboj/16.22.6874

244. Jul-Larsen, A., Grudic, A., Bjerkvig, R., & Boe, S. O. (2010). Subcellular distribution of nuclear import-defective isoforms of the promyelocytic leukemia protein. *BMC Mol Biol*, *11*, 89. https://doi.org/10.1186/1471-2199-11-89

245. Kahle, T., Volkmann, B., Eissmann, K., Herrmann, A., Schmitt, S., Wittmann, S., Merkel, L., Reuter, N., Stamminger, T., & Gramberg, T. (2015). TRIM19/PML Restricts HIV Infection in a Cell Type-Dependent Manner. *Viruses*, *8*(1). https://doi.org/10.3390/v8010002

246. Kakizuka, A., Miller, W. H., Jr., Umesono, K., Warrell, R. P., Jr., Frankel, S. R., Murty, V. V., Dmitrovsky, E., & Evans, R. M. (1991). Chromosomal translocation t(15;17) in human acute promyelocytic leukemia fuses RAR alpha with a novel putative transcription factor, PML. *Cell*, *66*(4), 663-674. https://doi.org/10.1016/0092-8674(91)90112-c

247. Kamashev, D., Vitoux, D., & De The, H. (2004). PML-RARA-RXR oligomers mediate retinoid and rexinoid/cAMP cross-talk in acute promyelocytic leukemia cell differentiation. *J Exp Med*, *199*(8), 1163-1174. https://doi.org/10.1084/jem.20032226

248. Kamitani, T., Kito, K., Nguyen, H. P., Wada, H., Fukuda-Kamitani, T., & Yeh, E. T. (1998). Identification of three major sentrinization sites in PML. *J Biol Chem*, *273*(41), 26675-26682. https://doi.org/10.1074/jbc.273.41.26675

249. Katlinskaya, Y. V., Katlinski, K. V., Yu, Q., Ortiz, A., Beiting, D. P., Brice, A., Davar, D., Sanders, C., Kirkwood, J. M., Rui, H., Xu, X., Koumenis, C., Diehl, J. A., & Fuchs, S. Y. (2016). Suppression of Type I Interferon Signaling Overcomes Oncogene-Induced Senescence and Mediates Melanoma Development and Progression. *Cell Rep*, *15*(1), 171-180. https://doi.org/10.1016/j.celrep.2016.03.006

250. Katlinski, K. V., Gui, J., Katlinskaya, Y. V., Ortiz, A., Chakraborty, R., Bhattacharya, S., Carbone, C. J., Beiting, D. P., Girondo, M. A., Peck, A. R., Pure, E., Chatterji, P., Rustgi, A. K., Diehl, J. A., Koumenis, C., Rui, H., & Fuchs, S. Y. (2017). Inactivation of Interferon Receptor Promotes the Establishment of Immune Privileged Tumor Microenvironment. *Cancer Cell*, *31*(2), 194-207. https://doi.org/10.1016/j.ccell.2017.01.004

251. Katoh, K., Misawa, K., Kuma, K., & Miyata, T. (2002). MAFFT: a novel method for rapid multiple sequence alignment based on fast Fourier transform. *Nucleic Acids Res*, *30*(14), 3059-3066. https://doi.org/10.1093/nar/gkf436

252. Khelifi, A. F., D'Alcontres, M. S., & Salomoni, P. (2005). Daxx is required for stress-induced cell death and JNK activation. *Cell Death Differ*, *12*(7), 724-733. https://doi.org/10.1038/sj.cdd.4401559

253. Kim, J., Han, K. Y., Khanna, N., Ha, T., & Belmont, A. S. (2019). Nuclear speckle fusion via long-range directional motion regulates speckle morphology after transcriptional inhibition. *J Cell Sci*, *132*(8). https://doi.org/10.1242/jcs.226563

254. Kim, J. M., Kee, Y., Gurtan, A., & D'Andrea, A. D. (2008). Cell cycle-dependent chromatin loading of the Fanconi anemia core complex by FANCM/FAAP24. *Blood*, *111*(10), 5215-5222. https://doi.org/10.1182/blood-2007-09-113092

255. Kim, K. I., Baek, S. H., & Chung, C. H. (2002). Versatile protein tag, SUMO: its enzymology and biological function. *J Cell Physiol*, *191*(3), 257-268. https://doi.org/10.1002/jcp.10100

256. Kim, S. H., Kim, G. H., Kemp, M. G., & Choi, J. H. (2022). TREX1 degrades the 3' end of the small DNA oligonucleotide products of nucleotide excision repair in human cells. *Nucleic Acids Res*, *50*(7), 3974-3984. https://doi.org/10.1093/nar/gkac214

257. Kirchmaier, S., Naruse, K., Wittbrodt, J., & Loosli, F. (2015). The genomic and genetic toolbox of the teleost medaka (Oryzias latipes). *Genetics*, *199*(4), 905-918. https://doi.org/10.1534/genetics.114.173849

258. Kirkwood, T. B., & Austad, S. N. (2000). Why do we age? *Nature*, *408*(6809), 233-238. https://doi.org/10.1038/35041682

259. Konno, H., Yamauchi, S., Berglund, A., Putney, R. M., Mule, J. J., & Barber, G. N. (2018). Suppression of STING signaling through epigenetic silencing and missense mutation impedes DNA damage mediated cytokine production. *Oncogene*, *37*(15), 2037-2051. https://doi.org/10.1038/s41388-017-0120-0

260. Korada, S. K., Johns, T. D., Smith, C. E., Jones, N. D., McCabe, K. A., & Bell, C. E. (2013). Crystal structures of Escherichia coli exonuclease I in complex with single-stranded DNA provide insights into the mechanism of processive digestion. *Nucleic Acids Res*, *41*(11), 5887-5897. https://doi.org/10.1093/nar/gkt278

261. Krokan, H. E., & Bjørås, M. (2013). Base excision repair. *Cold Spring Harb Perspect Biol*, *5*(4), a012583. https://doi.org/10.1101/cshperspect.a012583

262. Kubiczkova, L., Sedlarikova, L., Hajek, R., & Sevcikova, S. (2012). TGF-β – an excellent servant but a bad master. *Journal of Translational Medicine*, *10*(1), 183. https://doi.org/10.1186/1479-5876-10-183

263. Kucej, M., Fermaintt, C. S., Yang, K., Irizarry-Caro, R. A., & Yan, N. (2017). Mitotic Phosphorylation of TREX1 C Terminus Disrupts TREX1 Regulation of the Oligosaccharyltransferase Complex. *Cell Rep*, *18*(11), 2600-2607. https://doi.org/10.1016/j.celrep.2017.02.051

264. Kudo, N., Matsumori, N., Taoka, H., Fujiwara, D., Schreiner, E. P., Wolff, B., Yoshida, M., & Horinouchi, S. (1999). Leptomycin B inactivates CRM1/exportin 1 by covalent modification at a cysteine residue in the central conserved region. *Proc Natl Acad Sci U S A*, *96*(16), 9112-9117. https://doi.org/10.1073/pnas.96.16.9112

265. Kuilman, T., Michaloglou, C., Mooi, W. J., & Peeper, D. S. (2010). The essence of senescence. *Genes Dev*, *24*(22), 2463-2479. https://doi.org/10.1101/gad.1971610

266. Kumari, R., & Jat, P. (2021). Mechanisms of Cellular Senescence: Cell Cycle Arrest and Senescence Associated Secretory Phenotype. *Front Cell Dev Biol*, *9*, 645593. https://doi.org/10.3389/fcell.2021.645593

267. Kuo, H. Y., Chen, Y. C., Chang, H. Y., Jeng, J. C., Lin, E. H., Pan, C. M., Chang, Y. W., Wang, M. L., Chou, Y. T., Shih, H. M., & Wu, C. W. (2013). The PML isoform IV is a negative regulator of nuclear EGFR's transcriptional activity in lung cancer. *Carcinogenesis*, *34*(8), 1708-1716. https://doi.org/10.1093/carcin/bgt109

268. Kupsco, J. M., Wu, M. J., Marzluff, W. F., Thapar, R., & Duronio, R. J. (2006). Genetic and biochemical characterization of Drosophila Snipper: A promiscuous member of the metazoan 3'hExo/ERI-1 family of 3' to 5' exonucleases. *RNA*, *12*(12), 2103-2117. https://doi.org/10.1261/rna.186706

269. Kuriyama, Y., Shimizu, A., Kanai, S., Oikawa, D., Motegi, S.-i., Tokunaga, F., & Ishikawa, O. (2021). Coordination of retrotransposons and type I interferon with distinct interferon pathways in dermatomyositis, systemic lupus erythematosus and autoimmune blistering disease. *Scientific Reports*, *11*(1), 23146. https://doi.org/10.1038/s41598-021-02522-6

270. Labun, K., Montague, T. G., Krause, M., Torres Cleuren, Y. N., Tjeldnes, H., & Valen, E. (2019). CHOPCHOP v3: expanding the CRISPR web toolbox beyond genome editing. *Nucleic Acids Res*, *47*(W1), W171-W174. https://doi.org/10.1093/nar/gkz365

271. Lafarga, M., Berciano, M. T., Pena, E., Mayo, I., Castano, J. G., Bohmann, D., Rodrigues, J. P., Tavanez, J. P., & Carmo-Fonseca, M. (2002). Clastosome: a subtype of nuclear body enriched in 19S and 20S proteasomes, ubiquitin, and protein substrates of proteasome. *Mol Biol Cell*, *13*(8), 2771-2782. https://doi.org/10.1091/mbc.e02-03-0122

272. Lallemand-Breitenbach, V., & de The, H. (2010). PML nuclear bodies. *Cold Spring Harb Perspect Biol*, *2*(5), a000661. https://doi.org/10.1101/cshperspect.a000661

273. Lallemand-Breitenbach, V., Jeanne, M., Benhenda, S., Nasr, R., Lei, M., Peres, L., Zhou, J., Zhu, J., Raught, B., & de Thé, H. (2008). Arsenic degrades PML or PML-RARalpha through a SUMO-triggered RNF4/ubiquitin-mediated pathway. *Nat Cell Biol*, *10*(5), 547-555. https://doi.org/10.1038/ncb1717

274. Lam, Y. W., Ammerlaan, W., O, W. S., Kroese, F., & Opstelten, D. (1995). Cell type- and differentiation stage-dependent expression of PML domains in rat, detected by monoclonal antibody HIS55. *Exp Cell Res*, *221*(2), 344-356. https://doi.org/10.1006/excr.1995.1384

275. Lander, E. S., Linton, L. M., Birren, B., Nusbaum, C., Zody, M. C., Baldwin, J., Devon, K., Dewar, K., Doyle, M., FitzHugh, W., Funke, R., Gage, D., Harris, K., Heaford, A., Howland, J., Kann, L., Lehoczky, J., LeVine, R., McEwan, P., . . . The Wellcome, T. (2001). Initial sequencing and analysis of the human genome. *Nature*, *409*(6822), 860-921. https://doi.org/10.1038/35057062

276. Lavie, L., Maldener, E., Brouha, B., Meese, E. U., & Mayer, J. (2004). The human L1 promoter: variable transcription initiation sites and a major impact of upstream flanking sequence on promoter activity. *Genome Res*, *14*(11), 2253-2260. https://doi.org/10.1101/gr.2745804

277. Lavin, M. F., Kozlov, S., Gatei, M., & Kijas, A. W. (2015). ATM-Dependent Phosphorylation of All Three Members of the MRN Complex: From Sensor to Adaptor. *Biomolecules*, *5*(4), 2877-2902. https://doi.org/10.3390/biom5042877

278. Leblond, C. P. (1964). Classification of Cell Populations on the Basis of Their Proliferative Behavior. *Natl Cancer Inst Monogr*, *14*, 119-150. https://www.ncbi.nlm.nih.gov/pubmed/14147128

279. Lee-Kirsch, M. A., Gong, M., Chowdhury, D., Senenko, L., Engel, K., Lee, Y. A., de Silva, U., Bailey, S. L., Witte, T., Vyse, T. J., Kere, J., Pfeiffer, C., Harvey, S., Wong, A., Koskenmies, S., Hummel, O., Rohde, K., Schmidt, R. E., Dominiczak, A. F., . . . Hubner, N. (2007). Mutations in the gene encoding the 3'-5' DNA exonuclease TREX1 are associated with systemic lupus erythematosus. *Nat Genet*, *39*(9), 1065-1067. https://doi.org/10.1038/ng2091

280. Lee, D. S. W., Strom, A. R., & Brangwynne, C. P. (2022). The mechanobiology of nuclear phase separation. *APL Bioeng*, *6*(2), 021503. https://doi.org/10.1063/5.0083286

281. Lee, J., Salsman, J., Foster, J., Dellaire, G., & Ridgway, N. D. (2020). Lipid-associated PML structures assemble nuclear lipid droplets containing CCTalpha and Lipin1. *Life Sci Alliance*, *3*(8). https://doi.org/10.26508/lsa.202000751

282. Lehmann-Che, J., Bally, C., Letouzé, E., Berthier, C., Yuan, H., Jollivet, F., Ades, L., Cassinat, B., Hirsch, P., Pigneux, A., Mozziconacci, M. J., Kogan, S., Fenaux, P., & de Thé, H. (2018). Dual origin of relapses in retinoic-acid resistant acute promyelocytic leukemia. *Nat Commun*, *9*(1), 2047. https://doi.org/10.1038/s41467-018-04384-5

283. Lei, Y., VanPortfliet, J. J., Chen, Y. F., Bryant, J. D., Li, Y., Fails, D., Torres-Odio, S., Ragan, K. B., Deng, J., Mohan, A., Wang, B., Brahms, O. N., Yates, S. D., Spencer, M., Tong, C. W., Bosenberg, M. W., West, L. C., Shadel, G. S., Shutt, T. E., . . . West, A. P. (2023). Cooperative sensing of mitochondrial DNA by ZBP1 and cGAS promotes cardiotoxicity. *Cell*, *186*(14), 3013-3032.e3022. https://doi.org/10.1016/j.cell.2023.05.039

284. Lei, Z., Deng, M., Yi, Z., Sun, Q., Shapiro, R. A., Xu, H., Li, T., Loughran, P. A., Griepentrog, J. E., Huang, H., Scott, M. J., Huang, F., & Billiar, T. R. (2018). cGAS-mediated autophagy protects the liver from ischemia-reperfusion injury independently of STING. *Am J Physiol Gastrointest Liver Physiol*, *314*(6), G655-G667. https://doi.org/10.1152/ajpgi.00326.2017

285. Leibowitz, B. J., Zhao, G., Wei, L., Ruan, H., Epperly, M., Chen, L., Lu, X., Greenberger, J. S., Zhang, L., & Yu, J. (2021). Interferon b drives intestinal regeneration after radiation. *Sci Adv*, *7*(41), eabi5253. https://doi.org/10.1126/sciadv.abi5253

286. Lempiainen, H., & Halazonetis, T. D. (2009). Emerging common themes in regulation of PIKKs and PI3Ks. *EMBO J*, *28*(20), 3067-3073. https://doi.org/10.1038/emboj.2009.281

287. Ley, T. J., Miller, C., Ding, L., Raphael, B. J., Mungall, A. J., Robertson, A., Hoadley, K., Triche, T. J., Jr., Laird, P. W., Baty, J. D., Fulton, L. L., Fulton, R., Heath, S. E., Kalicki-Veizer, J., Kandoth, C., Klco, J. M., Koboldt, D. C., Kanchi, K. L., Kulkarni, S., . . . Eley, G. (2013). Genomic and epigenomic landscapes of adult de novo acute myeloid leukemia. *N Engl J Med*, *368*(22), 2059-2074. https://doi.org/10.1056/NEJMoa1301689

288. Li, H., Wei, X., Zhou, L., Zhang, W., Wang, C., Guo, Y., Li, D., Chen, J., Liu, T., Zhang, Y., Ma, S., Wang, C., Tan, F., Xu, J., Liu, Y., Yuan, Y., Chen, L., Wang, Q., Qu, J., . . . Xu, X. (2021). Dynamic cell transition and immune response landscapes of axolotl limb regeneration revealed by single-cell analysis. *Protein Cell*, *12*(1), 57-66. https://doi.org/10.1007/s13238-020-00763-1

289. Li, P., Du, J., Goodier, J. L., Hou, J., Kang, J., Kazazian, H. H., Jr., Zhao, K., & Yu, X. F. (2017a). Aicardi-Goutieres syndrome protein TREX1 suppresses L1 and maintains genome integrity through exonuclease-independent ORF1p depletion. *Nucleic Acids Res*, *45*(8), 4619-4631. https://doi.org/10.1093/nar/gkx178

290. Li, X., Zhang, J., Jia, R., Cheng, V., Xu, X., Qiao, W., Guo, F., Liang, C., & Cen, S. (2013). The MOV10 helicase inhibits LINE-1 mobility. *J Biol Chem*, *288*(29), 21148-21160. https://doi.org/10.1074/jbc.M113.465856

291. Li, Y., Ma, X., Chen, Z., Wu, H., Wang, P., Wu, W., Cheng, N., Zeng, L., Zhang, H., Cai, X., Chen, S. J., Chen, Z., & Meng, G. (2019). B1 oligomerization regulates PML nuclear body biogenesis and leukemogenesis. *Nat Commun*, *10*(1), 3789. https://doi.org/10.1038/s41467-019-11746-0

292. Li, Y., Ma, X., Wu, W., Chen, Z., & Meng, G. (2020). PML Nuclear Body Biogenesis, Carcinogenesis, and Targeted Therapy. *Trends Cancer*, *6*(10), 889-906. https://doi.org/10.1016/j.trecan.2020.05.005

293. Liang, C., Ke, Q., Liu, Z., Ren, J., Zhang, W., Hu, J., Wang, Z., Chen, H., Xia, K., Lai, X., Wang, Q., Yang, K., Li, W., Wu, Z., Wang, C., Yan, H., Jiang, X., Ji, Z., Ma, M., . . . Liu, G. H. (2022). BMAL1 moonlighting as a gatekeeper for LINE1 repression and cellular senescence in primates. *Nucleic Acids Res*, *50*(6), 3323-3347. https://doi.org/10.1093/nar/gkac146

294. Liang, Y.-C., Lee, C.-C., Yao, Y.-L., Lai, C.-C., Schmitz, M. L., & Yang, W.-M. (2016). SUMO5, a Novel Poly-SUMO Isoform, Regulates PML Nuclear Bodies. *Scientific Reports*, *6*(1), 26509. https://doi.org/10.1038/srep26509

295. Liang, Y. C., Lee, C. C., Yao, Y. L., Lai, C. C., Schmitz, M. L., & Yang, W. M. (2016). SUMO5, a Novel Poly-SUMO Isoform, Regulates PML Nuclear Bodies. *Sci Rep*, *6*, 26509. https://doi.org/10.1038/srep26509

296. Lin, D. I., Barbash, O., Kumar, K. G., Weber, J. D., Harper, J. W., Klein-Szanto, A. J., Rustgi, A., Fuchs, S. Y., & Diehl, J. A. (2006). Phosphorylation-dependent ubiquitination of cyclin D1 by the SCF(FBX4-alphaB crystallin) complex. *Mol Cell*, *24*(3), 355-366. https://doi.org/10.1016/j.molcel.2006.09.007

297. Lin, H. K., Bergmann, S., & Pandolfi, P. P. (2004). Cytoplasmic PML function in TGF-beta signalling. *Nature*, *431*(7005), 205-211. https://doi.org/10.1038/nature02783

298. Lindahl, T., Barnes, D. E., Yang, Y. G., & Robins, P. (2009). Biochemical properties of mammalian TREX1 and its association with DNA replication and inherited inflammatory disease. *Biochem Soc Trans*, *37*(Pt 3), 535-538. https://doi.org/10.1042/BST0370535

299. Lindic, N., Budic, M., Petan, T., Knisbacher, B. A., Levanon, E. Y., & Lovsin, N. (2013). Differential inhibition of LINE1 and LINE2 retrotransposition by vertebrate AID/APOBEC proteins. *Retrovirology*, *10*, 156. https://doi.org/10.1186/1742-4690-10-156

300. Lindič, N., Budič, M., Petan, T., Knisbacher, B. A., Levanon, E. Y., & Lovšin, N. (2013). Differential inhibition of LINE1 and LINE2 retrotransposition by vertebrate AID/APOBEC proteins. *Retrovirology*, *10*, 156. https://doi.org/10.1186/1742-4690-10-156

301. Liu, C., Yang, J., Zheng, J., Fu, J., Wang, W., Duan, L., Qian, X., & Yang, Y. (2023). Phase Separation in cGAS-STING Signaling: Cytosolic DNA Sensing and Regulatory Functions. *Chembiochem*, e202300147. https://doi.org/10.1002/cbic.202300147

302. Liu, D., Wu, H., Wang, C., Li, Y., Tian, H., Siraj, S., Sehgal, S. A., Wang, X., Wang, J., Shang, Y., Jiang, Z., Liu, L., & Chen, Q. (2019). STING directly activates autophagy to tune the innate immune response. *Cell Death Differ*, *26*(9), 1735-1749. https://doi.org/10.1038/s41418-018-0251-z

303. Liu, F., Bols, N. C., Pham, P. H., Secombes, C. J., & Zou, J. (2019). Evolution of IFN subgroups in bony fish-1: Group I-III IFN exist in early ray-finned fish, with group II IFN subgroups present in the Holostean spotted gar, Lepisosteus oculatus. *Fish & shellfish immunology*, *95*, 163-170.

304. Liu, F., Bols, N. C., Pham, P. H., Secombes, C. J., & Zou, J. (2019). Evolution of IFN subgroups in bony fish - 1:Group I-III IFN exist in early ray-finned fish, with group II IFN subgroups present in the Holostean spotted gar, Lepisosteus oculatus. *Fish & Shellfish Immunology*, *95*, 163-170. https://doi.org/https://doi.org/10.1016/j.fsi.2019.10.032

305. Liu, H., Ghosh, S., Vaidya, T., Bammidi, S., Huang, C., Shang, P., Nair, A. P., Chowdhury, O., Stepicheva, N. A., Strizhakova, A., Hose, S., Mitrousis, N., Gadde, S. G., Mb, T., Strassburger, P., Widmer, G., Lad, E. M., Fort, P. E., Sahel, J. A., . . . Sinha, D. (2023). Activated cGAS/STING signaling elicits endothelial cell senescence in early diabetic retinopathy. *JCI Insight*, *8*(12). https://doi.org/10.1172/jci.insight.168945

306. Liu, N., Pang, X., Zhang, H., & Ji, P. (2021). The cGAS-STING Pathway in Bacterial Infection and Bacterial Immunity. *Front Immunol*, *12*, 814709. https://doi.org/10.3389/fimmu.2021.814709

307. Liu, S., Atkinson, E., Paulucci-Holthauzen, A., & Wang, B. (2023). A CK2 and SUMO-dependent, PML NB-involved regulatory mechanism controlling BLM ubiquitination and G-quadruplex resolution. *Nature Communications*, *14*(1), 6111. https://doi.org/10.1038/s41467-023-41705-9

308. Liu, S., Cai, X., Wu, J., Cong, Q., Chen, X., Li, T., Du, F., Ren, J., Wu, Y. T., Grishin, N. V., & Chen, Z. J. (2015). Phosphorylation of innate immune adaptor proteins MAVS, STING, and TRIF induces IRF3 activation. *Science*, *347*(6227), aaa2630. https://doi.org/10.1126/science.aaa2630

309. Liu, S., Zhang, L., Quan, H., Tian, H., Meng, L., Yang, L., Feng, H., & Gao, Y. Q. (2018). From 1D sequence to 3D chromatin dynamics and cellular functions: a phase separation perspective. *Nucleic Acids Res*, *46*(18), 9367-9383. https://doi.org/10.1093/nar/gky633

310. Liu, S. B., Shen, Z. F., Guo, Y. J., Cao, L. X., & Xu, Y. (2017). PML silencing inhibits cell proliferation and induces DNA damage in cultured ovarian cancer cells. *Biomed Rep*, *7*(1), 29-35. https://doi.org/10.3892/br.2017.919

311. Liu, Z. F., Ji, J. F., Jiang, X. F., Shao, T., Fan, D. D., Jiang, X. H., Lin, A. F., Xiang, L. X., & Shao, J. Z. (2020). Characterization of cGAS homologs in innate and adaptive mucosal immunities in zebrafish gives evolutionary insights into cGAS-STING pathway. *FASEB J*, *34*(6), 7786-7809. https://doi.org/10.1096/fj.201902833R

312. Loe, T. K., Li, J. S. Z., Zhang, Y., Azeroglu, B., Boddy, M. N., & Denchi, E. L. (2020). Telomere length heterogeneity in ALT cells is maintained by PML-dependent localization of the BTR complex to telomeres. *Genes Dev*, *34*(9-10), 650-662. https://doi.org/10.1101/gad.333963.119

313. Longo, L., Pandolfi, P. P., Biondi, A., Rambaldi, A., Mencarelli, A., Lo Coco, F., Diverio, D., Pegoraro, L., Avanzi, G., Tabilio, A., & et al. (1990). Rearrangements and aberrant expression of the retinoic acid receptor alpha gene in acute promyelocytic leukemias. *J Exp Med*, *172*(6), 1571-1575. https://doi.org/10.1084/jem.172.6.1571

314. Lovejoy, C. A., & Cortez, D. (2009). Common mechanisms of PIKK regulation. *DNA Repair (Amst)*, *8*(9), 1004-1008. https://doi.org/10.1016/j.dnarep.2009.04.006

315. Lovšin, N., Gubenšek, F., & Kordi, D. (2001). Evolutionary Dynamics in a Novel L2 Clade of Non-LTR Retrotransposons in Deuterostomia. *Molecular Biology and Evolution*, *18*(12), 2213-2224. https://doi.org/10.1093/oxfordjournals.molbev.a003768

316. Low, J. T., Chandramohan, V., Bowie, M. L., Brown, M. C., Waitkus, M. S., Briley, A., Stevenson, K., Fuller, R., Reitman, Z. J., Muscat, A. M., Hariharan, S., Hostettler, J., Danehower, S., Baker, A., Khasraw, M., Wong, N. C., Gregory, S., Nair, S. K., Heimberger, A., . . . Ashley, D. M. (2022). Epigenetic STING silencing is developmentally conserved in gliomas and can be rescued by methyltransferase inhibition. *Cancer Cell*, *40*(5), 439-440. https://doi.org/10.1016/j.ccell.2022.04.009

317. Luan, D. D., Korman, M. H., Jakubczak, J. L., & Eickbush, T. H. (1993). Reverse transcription of R2Bm RNA is primed by a nick at the chromosomal target site: a mechanism for non-LTR retrotransposition. *Cell*, *72*(4), 595-605. https://doi.org/10.1016/0092-8674(93)90078-5

318. Luecke, S., Holleufer, A., Christensen, M. H., Jonsson, K. L., Boni, G. A., Sorensen, L. K., Johannsen, M., Jakobsen, M. R., Hartmann, R., & Paludan, S. R. (2017). cGAS is activated by DNA in a length-dependent manner. *EMBO Rep*, *18*(10), 1707-1715. https://doi.org/10.15252/embr.201744017

319. Lussier-Price, M., Wahba, H. M., Mascle, X. H., Cappadocia, L., Bourdeau, V., Gagnon, C., Igelmann, S., Sakaguchi, K., Ferbeyre, G., & Omichinski, James G. (2022). Zinc controls PML nuclear body formation through regulation of a paralog specific auto-inhibition in SUMO1. *Nucleic acids research*, *50*(14), 8331-8348. https://doi.org/10.1093/nar/gkac620

320. Lussier-Price, M., Wahba, H. M., Mascle, X. H., Cappadocia, L., Bourdeau, V., Gagnon, C., Igelmann, S., Sakaguchi, K., Ferbeyre, G., & Omichinski, J. G. (2022). Zinc controls PML nuclear body formation through regulation of a paralog specific auto-inhibition in SUMO1. *Nucleic Acids Res*, *50*(14), 8331-8348. https://doi.org/10.1093/nar/gkac620

321. Maciel-Baron, L. A., Morales-Rosales, S. L., Aquino-Cruz, A. A., Triana-Martinez, F., Galvan-Arzate, S., Luna-Lopez, A., Gonzalez-Puertos, V. Y., Lopez-Diazguerrero, N. E., Torres, C., & Konigsberg, M. (2016). Senescence associated secretory phenotype profile from primary lung mice fibroblasts depends on the senescence induction stimuli. *Age (Dordr)*, *38*(1), 26. https://doi.org/10.1007/s11357-016-9886-1

322. Mackenzie, K. J., Carroll, P., Lettice, L., Tarnauskaite, Z., Reddy, K., Dix, F., Revuelta, A., Abbondati, E., Rigby, R. E., Rabe, B., Kilanowski, F., Grimes, G.,

Fluteau, A., Devenney, P. S., Hill, R. E., Reijns, M. A., & Jackson, A. P. (2016). Ribonuclease H2 mutations induce a cGAS/STING-dependent innate immune response. *EMBO J*, *35*(8), 831-844. https://doi.org/10.15252/embj.201593339

323. Mallette, F. A., Goumard, S., Gaumont-Leclerc, M. F., Moiseeva, O., & Ferbeyre, G. (2004). Human fibroblasts require the Rb family of tumor suppressors, but not p53, for PML-induced senescence. *Oncogene*, *23*(1), 91-99. https://doi.org/10.1038/sj.onc.1206886

324. Mannan, A., Muhsen, I. N., Barragán, E., Sanz, M. A., Mohty, M., Hashmi, S. K., & Aljurf, M. (2020). Genotypic and Phenotypic Characteristics of Acute Promyelocytic Leukemia Translocation Variants. *Hematol Oncol Stem Cell Ther*, *13*(4), 189-201. https://doi.org/10.1016/j.hemonc.2020.05.007

325. Mao, Y. S., Zhang, B., & Spector, D. L. (2011). Biogenesis and function of nuclear bodies. *Trends Genet*, *27*(8), 295-306. https://doi.org/10.1016/j.tig.2011.05.006

326. Marechal, A., & Zou, L. (2013). DNA damage sensing by the ATM and ATR kinases. *Cold Spring Harb Perspect Biol*, *5*(9). https://doi.org/10.1101/cshperspect.a012716

327. Margolis, S. R., Wilson, S. C., & Vance, R. E. (2017). Evolutionary Origins of cGAS-STING Signaling. *Trends Immunol*, *38*(10), 733-743. https://doi.org/10.1016/j.it.2017.03.004

328. Maroui, M. A., Maarifi, G., McManus, F. P., Lamoliatte, F., Thibault, P., & Chelbi-Alix, M. K. (2018). Promyelocytic Leukemia Protein (PML) Requirement for Interferon-induced Global Cellular SUMOylation. *Mol Cell Proteomics*, *17*(6), 1196-1208. https://doi.org/10.1074/mcp.RA117.000447

329. Martin-Martin, N., Piva, M., Urosevic, J., Aldaz, P., Sutherland, J. D., Fernandez-Ruiz, S., Arreal, L., Torrano, V., Cortazar, A. R., Planet, E., Guiu, M., Radosevic-Robin, N., Garcia, S., Macias, I., Salvador, F., Domenici, G., Rueda, O. M., Zabala-Letona, A., Arruabarrena-Aristorena, A., . . . Carracedo, A. (2016). Stratification and therapeutic potential of PML in metastatic breast cancer. *Nat Commun*, *7*, 12595. https://doi.org/10.1038/ncomms12595

330. Martin, M., Hiroyasu, A., Guzman, R. M., Roberts, S. A., & Goodman, A. G. (2018). Analysis of Drosophila STING Reveals an Evolutionarily Conserved Antimicrobial Function. *Cell Rep*, *23*(12), 3537-3550.e3536. https://doi.org/10.1016/j.celrep.2018.05.029

331. Martin, S. L., & Bushman, F. D. (2001). Nucleic acid chaperone activity of the ORF1 protein from the mouse LINE-1 retrotransposon. *Mol Cell Biol*, *21*(2), 467-475. https://doi.org/10.1128/MCB.21.2.467-475.2001

332. Martin, S. L., Cruceanu, M., Branciforte, D., Wai-Lun Li, P., Kwok, S. C., Hodges, R. S., & Williams, M. C. (2005). LINE-1 retrotransposition requires the nucleic acid chaperone activity of the ORF1 protein. *J Mol Biol*, *348*(3), 549-561. https://doi.org/10.1016/j.jmb.2005.03.003

333. Massague, J. (2012). TGFbeta signalling in context. *Nat Rev Mol Cell Biol*, *13*(10), 616-630. https://doi.org/10.1038/nrm3434

334. Mathavarajah, S., Vergunst, K. L., Habib, E. B., Williams, S. K., He, R., Maliougina, M., Park, M., Salsman, J., Roy, S., Braasch, I., Roger, A. J., Langelaan, D. N., & Dellaire, G. (2023). PML and PML-like exonucleases restrict retrotransposons in jawed vertebrates. *Nucleic Acids Res*. https://doi.org/10.1093/nar/gkad152

335. Mathias, S. L., Scott, A. F., Kazazian Jr, H. H., Boeke, J. D., & Gabriel, A. (1991). Reverse transcriptase encoded by a human transposable element. *Science*, *254*(5039), 1808-1810.

336. Matic, I., Schimmel, J., Hendriks, I. A., van Santen, M. A., van de Rijke, F., van Dam, H., Gnad, F., Mann, M., & Vertegaal, A. C. (2010). Site-specific identification of SUMO-2 targets in cells reveals an inverted SUMOylation motif and a hydrophobic cluster SUMOylation motif. *Mol Cell*, *39*(4), 641-652. https://doi.org/10.1016/j.molcel.2010.07.026

337. Matsuoka, S., Ballif, B. A., Smogorzewska, A., McDonald, E. R., 3rd, Hurov, K. E., Luo, J., Bakalarski, C. E., Zhao, Z., Solimini, N., Lerenthal, Y., Shiloh, Y., Gygi, S. P., & Elledge, S. J. (2007). ATM and ATR substrate analysis reveals extensive protein networks responsive to DNA damage. *Science*, *316*(5828), 1160-1166. https://doi.org/10.1126/science.1140321

338. Matunis, M. J., Zhang, X. D., & Ellis, N. A. (2006). SUMO: the glue that binds. *Dev Cell*, *11*(5), 596-597. https://doi.org/10.1016/j.devcel.2006.10.011

339. Mazur, D. J., & Perrino, F. W. (1999). Identification and expression of the TREX1 and TREX2 cDNA sequences encoding mammalian 3'-->5' exonucleases. *J Biol Chem*, *274*(28), 19655-19660. https://doi.org/10.1074/jbc.274.28.19655

340. Mazur, D. J., & Perrino, F. W. (2001). Excision of 3' termini by the Trex1 and TREX2 3'-->5' exonucleases. Characterization of the recombinant proteins. *J Biol Chem*, *276*(20), 17022-17029. https://doi.org/10.1074/jbc.M100623200

341. Mazza, M., & Pelicci, P. G. (2013). Is PML a Tumor Suppressor? *Front Oncol*, *3*, 174. https://doi.org/10.3389/fonc.2013.00174

342. McKerrow, W., Wang, X., Mendez-Dorantes, C., Mita, P., Cao, S., Grivainis, M., Ding, L., LaCava, J., Burns, K. H., Boeke, J. D., & Fenyo, D. (2022). LINE-1 expression in cancer correlates with p53 mutation, copy number alteration, and S

phase checkpoint. *Proc Natl Acad Sci U S A*, *119*(8). https://doi.org/10.1073/pnas.2115999119

343. McLaughlin, H. M. G., Rathbone, M. P., Liversage, R. A., & McLaughlin, D. S. (1983). Levels of cyclic GMP and cyclic AMP in regenerating forelimbs of adult newts following denervation. *Journal of Experimental Zoology*, *225*(2), 175-185. https://doi.org/https://doi.org/10.1002/jez.1402250202

344. McNally, B. A., Trgovcich, J., Maul, G. G., Liu, Y., & Zheng, P. (2008). A Role for Cytoplasmic PML in Cellular Resistance to Viral Infection. *PLoS One*, *3*(5), e2277. https://doi.org/10.1371/journal.pone.0002277

345. McPhee, M. J., Lee, J., Dellaire, G., Pelech, S., & Ridgway, N. D. (2022). CTP:phosphocholine cytidylyltransferase alpha regulates nLD biogenesis in Caco2 cells. *The FASEB Journal*, *36*(S1). https://doi.org/https://doi.org/10.1096/fasebj.2022.36.S1.R5404

346. Meier, U. T. (2017). RNA modification in Cajal bodies. *RNA Biol*, *14*(6), 693-700. https://doi.org/10.1080/15476286.2016.1249091

347. Meng, X., Chen, Y., Macip, S., & Leppard, K. (2021). PML-II regulates ERK and AKT signal activation and IFNalpha-induced cell death. *Cell Commun Signal*, *19*(1), 70. https://doi.org/10.1186/s12964-021-00756-5

348. Menolfi, D., & Zha, S. (2020). ATM, ATR and DNA-PKcs kinases-the lessons from the mouse models: inhibition not equal deletion. *Cell Biosci*, *10*, 8. https://doi.org/10.1186/s13578-020-0376-x

349. Meroni, G. (2012). Genomics and evolution of the TRIM gene family. *Adv Exp Med Biol*, *770*, 1-9. https://doi.org/10.1007/978-1-4614-5398-7_1

350. Mijit, M., Caracciolo, V., Melillo, A., Amicarelli, F., & Giordano, A. (2020). Role of p53 in the Regulation of Cellular Senescence. *Biomolecules*, *10*(3). https://doi.org/10.3390/biom10030420

351. Mita, P., Sun, X., Fenyo, D., Kahler, D. J., Li, D., Agmon, N., Wudzinska, A., Keegan, S., Bader, J. S., Yun, C., & Boeke, J. D. (2020). BRCA1 and S phase DNA repair pathways restrict LINE-1 retrotransposition in human cells. *Nat Struct Mol Biol*, *27*(2), 179-191. https://doi.org/10.1038/s41594-020-0374-z

352. Mita, P., Wudzinska, A., Sun, X., Andrade, J., Nayak, S., Kahler, D. J., Badri, S., LaCava, J., Ueberheide, B., Yun, C. Y., Fenyo, D., & Boeke, J. D. (2018). LINE-1 protein localization and functional dynamics during the cell cycle. *Elife*, *7*. https://doi.org/10.7554/eLife.30058

353. Mohr, L., Toufektchan, E., von Morgen, P., Chu, K., Kapoor, A., & Maciejowski, J. (2021a). ER-directed TREX1 limits cGAS activation at micronuclei. *Mol Cell*, *81*(4), 724-738 e729. https://doi.org/10.1016/j.molcel.2020.12.037

354. Moran, J. V., Holmes, S. E., Naas, T. P., DeBerardinis, R. J., Boeke, J. D., & Kazazian, H. H., Jr. (1996). High frequency retrotransposition in cultured mammalian cells. *Cell*, *87*(5), 917-927. https://doi.org/10.1016/s0092-8674(00)81998-4

355. Morita, M., Stamp, G., Robins, P., Dulic, A., Rosewell, I., Hrivnak, G., Daly, G., Lindahl, T., & Barnes, D. E. (2004). Gene-targeted mice lacking the Trex1 (DNase III) 3'-->5' DNA exonuclease develop inflammatory myocarditis. *Mol Cell Biol*, *24*(15), 6719-6727. https://doi.org/10.1128/MCB.24.15.6719-6727.2004

356. Morozzi, G., Rothen, J., Toussaint, G., De Lange, K., Westritschnig, K., Doelemeyer, A., Ueberschlag, V. P., Kahle, P., Lambert, C., Obrecht, M., Beckmann, N., Ritter, V., Panesar, M., Stauffer, D., Garnier, I., Mueller, M., Guerini, D., Keller, C. G., Knehr, J., . . . Fornaro, M. (2021). STING regulates peripheral nerve regeneration and colony stimulating factor 1 receptor (CSF1R) processing in microglia. *iScience*, *24*(12), 103434. https://doi.org/10.1016/j.isci.2021.103434

357. Muckenfuss, H., Hamdorf, M., Held, U., Perkovic, M., Lower, J., Cichutek, K., Flory, E., Schumann, G. G., & Munk, C. (2006). APOBEC3 proteins inhibit human LINE-1 retrotransposition. *J Biol Chem*, *281*(31), 22161-22172. https://doi.org/10.1074/jbc.M601716200

358. Mullins, E. A., Shi, R., Parsons, Z. D., Yuen, P. K., David, S. S., Igarashi, Y., & Eichman, B. F. (2015). The DNA glycosylase AlkD uses a non-base-flipping mechanism to excise bulky lesions. *Nature*, *527*(7577), 254-258. https://doi.org/10.1038/nature15728

359. Nakamura, T., Gehrke, A. R., Lemberg, J., Szymaszek, J., & Shubin, N. H. (2016). Digits and fin rays share common developmental histories. *Nature*, *537*(7619), 225-228. https://doi.org/10.1038/nature19322

360. Nakano, Y., Takahashi-Fujigasaki, J., Sengoku, R., Kanemaru, K., Arai, T., Kanda, T., & Murayama, S. (2017). PML Nuclear Bodies Are Altered in Adult-Onset Neuronal Intranuclear Hyaline Inclusion Disease. *J Neuropathol Exp Neurol*, *76*(7), 585-594. https://doi.org/10.1093/jnen/nlx039

361. Nam, E. A., & Cortez, D. (2009). SOSS1/2: Sensors of single-stranded DNA at a break. *Mol Cell*, *35*(3), 258-259. https://doi.org/10.1016/j.molcel.2009.07.016

362. Nguyen, L. A., Pandolfi, P. P., Aikawa, Y., Tagata, Y., Ohki, M., & Kitabayashi, I. (2005). Physical and functional link of the leukemia-associated factors AML1 and PML. *Blood*, *105*(1), 292-300. https://doi.org/10.1182/blood-2004-03-1185

363. Nguyen, L. T., Schmidt, H. A., von Haeseler, A., & Minh, B. Q. (2015). IQ-TREE: a fast and effective stochastic algorithm for estimating maximum-

likelihood phylogenies. *Mol Biol Evol*, *32*(1), 268-274. https://doi.org/10.1093/molbev/msu300

364. Nisole, S., Maroui, M. A., Mascle, X. H., Aubry, M., & Chelbi-Alix, M. K. (2013). Differential Roles of PML Isoforms. *Front Oncol*, *3*, 125. https://doi.org/10.3389/fonc.2013.00125

365. Nogueira, A. F., Costa, C. M., Lorena, J., Moreira, R. N., Frota-Lima, G. N., Furtado, C., Robinson, M., Amemiya, C. T., Darnet, S., & Schneider, I. (2016). Tetrapod limb and sarcopterygian fin regeneration share a core genetic programme. *Nat Commun*, *7*, 13364. https://doi.org/10.1038/ncomms13364

366. Occhionorelli, M., Santoro, F., Pallavicini, I., Gruszka, A., Moretti, S., Bossi, D., Viale, A., Shing, D., Ronzoni, S., Muradore, I., Soncini, M., Pruneri, G., Rafaniello, P., Viale, G., Pelicci, P. G., & Minucci, S. (2011). The self-association coiled-coil domain of PML is sufficient for the oncogenic conversion of the retinoic acid receptor (RAR) alpha. *Leukemia*, *25*(5), 814-820. https://doi.org/10.1038/leu.2011.18

367. Ohsaki, Y., Kawai, T., Yoshikawa, Y., Cheng, J., Jokitalo, E., & Fujimoto, T. (2016). PML isoform II plays a critical role in nuclear lipid droplet formation. *J Cell Biol*, *212*(1), 29-38. https://doi.org/10.1083/jcb.201507122

368. Ohtani, N., Takahashi, A., Mann, D. J., & Hara, E. (2012). Cellular senescence: a double-edged sword in the fight against cancer. *Exp Dermatol*, *21 Suppl 1*, 1-4. https://doi.org/10.1111/j.1600-0625.2012.01493.x

369. Ohtani, N., Yamakoshi, K., Takahashi, A., & Hara, E. (2004). The p16INK4a-RB pathway: molecular link between cellular senescence and tumor suppression. *J Med Invest*, *51*(3-4), 146-153. https://doi.org/10.2152/jmi.51.146

370. Orban, T., Palczewska, G., & Palczewski, K. (2011). Retinyl ester storage particles (retinosomes) from the retinal pigmented epithelium resemble lipid droplets in other tissues. *J Biol Chem*, *286*(19), 17248-17258. https://doi.org/10.1074/jbc.M110.195198

371. Orebaugh, C. D., Fye, J. M., Harvey, S., Hollis, T., & Perrino, F. W. (2011). The TREX1 exonuclease R114H mutation in Aicardi-Goutières syndrome and lupus reveals dimeric structure requirements for DNA degradation activity. *J Biol Chem*, *286*(46), 40246-40254. https://doi.org/10.1074/jbc.M111.297903

372. Orebaugh, C. D., Fye, J. M., Harvey, S., Hollis, T., Wilkinson, J. C., & Perrino, F. W. (2013). The TREX1 C-terminal region controls cellular localization through ubiquitination. *J Biol Chem*, *288*(40), 28881-28892. https://doi.org/10.1074/jbc.M113.503391

373. Orecchini, E., Doria, M., Antonioni, A., Galardi, S., Ciafre, S. A., Frassinelli, L., Mancone, C., Montaldo, C., Tripodi, M., & Michienzi, A. (2017). ADAR1

restricts LINE-1 retrotransposition. *Nucleic Acids Res*, *45*(1), 155-168. https://doi.org/10.1093/nar/gkw834

374. Ostertag, E. M., & Kazazian, H. H., Jr. (2001). Biology of mammalian L1 retrotransposons. *Annu Rev Genet*, *35*, 501-538. https://doi.org/10.1146/annurev.genet.35.102401.091032

375. Palibrk, V., Lang, E., Lang, A., Schink, K. O., Rowe, A. D., & Boe, S. O. (2014). Promyelocytic leukemia bodies tether to early endosomes during mitosis. *Cell Cycle*, *13*(11), 1749-1755. https://doi.org/10.4161/cc.28653

376. Palibrk, V., Lång, E., Lång, A., Schink, K. O., Rowe, A. D., & Bøe, S. O. (2014). Promyelocytic leukemia bodies tether to early endosomes during mitosis. *Cell Cycle*, *13*(11), 1749-1755. https://doi.org/10.4161/cc.28653

377. Palla, V. V., Karaolanis, G., Katafigiotis, I., Anastasiou, I., Patapis, P., Dimitroulis, D., & Perrea, D. (2017). gamma-H2AX: Can it be established as a classical cancer prognostic factor? *Tumour Biol*, *39*(3), 1010428317695931. https://doi.org/10.1177/1010428317695931

378. Patel, D. J., Yu, Y., & Xie, W. (2023). cGAMP-activated cGAS-STING signaling: its bacterial origins and evolutionary adaptation by metazoans. *Nat Struct Mol Biol*, *30*(3), 245-260. https://doi.org/10.1038/s41594-023-00933-9

379. Patel, D. S., Misenko, S. M., Her, J., & Bunting, S. F. (2017). BLM helicase regulates DNA repair by counteracting RAD51 loading at DNA double-strand break sites. *J Cell Biol*, *216*(11), 3521-3534. https://doi.org/10.1083/jcb.201703144

380. Patton, E. E., Zon, L. I., & Langenau, D. M. (2021). Zebrafish disease models in drug discovery: from preclinical modelling to clinical trials. *Nat Rev Drug Discov*, *20*(8), 611-628. https://doi.org/10.1038/s41573-021-00210-8

381. Pearl, L. H., Schierz, A. C., Ward, S. E., Al-Lazikani, B., & Pearl, F. M. (2015). Therapeutic opportunities within the DNA damage response. *Nat Rev Cancer*, *15*(3), 166-180. https://doi.org/10.1038/nrc3891

382. Pearson, M., & Pelicci, P. G. (2001). PML interaction with p53 and its role in apoptosis and replicative senescence. *Oncogene*, *20*(49), 7250-7256. https://doi.org/10.1038/sj.onc.1204856

383. Perrino, F. W., Miller, H., & Ealey, K. A. (1994). Identification of a 3'-->5'-exonuclease that removes cytosine arabinoside monophosphate from 3' termini of DNA. *J Biol Chem*, *269*(23), 16357-16363.

384. Perry, J. J., Yannone, S. M., Holden, L. G., Hitomi, C., Asaithamby, A., Han, S., Cooper, P. K., Chen, D. J., & Tainer, J. A. (2006). WRN exonuclease structure

and molecular mechanism imply an editing role in DNA end processing. *Nat Struct Mol Biol*, *13*(5), 414-422. https://doi.org/10.1038/nsmb1088

385. Piazza, F., Gurrieri, C., & Pandolfi, P. P. (2001). The theory of APL. *Oncogene*, *20*(49), 7216-7222. https://doi.org/10.1038/sj.onc.1204855

386. Pinder, J., Salsman, J., & Dellaire, G. (2015). Nuclear domain 'knock-in' screen for the evaluation and identification of small molecule enhancers of CRISPR-based genome editing. *Nucleic Acids Res*, *43*(19), 9379-9392. https://doi.org/10.1093/nar/gkv993

387. Piskareva, O., Ernst, C., Higgins, N., & Schmatchenko, V. (2013). The carboxy-terminal segment of the human LINE-1 ORF2 protein is involved in RNA binding. *FEBS Open Bio*, *3*, 433-437. https://doi.org/10.1016/j.fob.2013.09.005

388. Piskareva, O., & Schmatchenko, V. (2006). DNA polymerization by the reverse transcriptase of the human L1 retrotransposon on its own template in vitro. *FEBS Lett*, *580*(2), 661-668. https://doi.org/10.1016/j.febslet.2005.12.077

389. Podhorecka, M., Skladanowski, A., & Bozko, P. (2010). H2AX Phosphorylation: Its Role in DNA Damage Response and Cancer Therapy. *J Nucleic Acids*, *2010*. https://doi.org/10.4061/2010/920161

390. Pokatayev, V., Hasin, N., Chon, H., Cerritelli, S. M., Sakhuja, K., Ward, J. M., Morris, H. D., Yan, N., & Crouch, R. J. (2016). RNase H2 catalytic core Aicardi-Goutieres syndrome-related mutant invokes cGAS-STING innate immune-sensing pathway in mice. *J Exp Med*, *213*(3), 329-336. https://doi.org/10.1084/jem.20151464

391. Ponente, M., Campanini, L., Cuttano, R., Piunti, A., Delledonne, G. A., Coltella, N., Valsecchi, R., Villa, A., Cavallaro, U., Pattini, L., Doglioni, C., & Bernardi, R. (2017). PML promotes metastasis of triple-negative breast cancer through transcriptional regulation of HIF1A target genes. *JCI Insight*, *2*(4), e87380. https://doi.org/10.1172/jci.insight.87380

392. Qiu, L., Meng, Y., & Han, J. (2022). STING cg16983159 methylation: a key factor for glioblastoma immunosuppression. *Signal Transduct Target Ther*, *7*(1), 228. https://doi.org/10.1038/s41392-022-01093-w

393. Ranjha, L., Howard, S. M., & Cejka, P. (2018). Main steps in DNA double-strand break repair: an introduction to homologous recombination and related processes. *Chromosoma*, *127*(2), 187-214. https://doi.org/10.1007/s00412-017-0658-1

394. Ravi, V., & Venkatesh, B. (2018). The Divergent Genomes of Teleosts. *Annu Rev Anim Biosci*, *6*, 47-68. https://doi.org/10.1146/annurev-animal-030117-014821

395. Redmond, A. K., Zou, J., Secombes, C. J., Macqueen, D. J., & Dooley, H. (2019). Discovery of All Three Types in Cartilaginous Fishes Enables Phylogenetic

Resolution of the Origins and Evolution of Interferons. *Front Immunol*, *10*, 1558. https://doi.org/10.3389/fimmu.2019.01558

396. Rego, E. M., Wang, Z. G., Peruzzi, D., He, L. Z., Cordon-Cardo, C., & Pandolfi, P. P. (2001). Role of promyelocytic leukemia (PML) protein in tumor suppression. *J Exp Med*, *193*(4), 521-529. https://doi.org/10.1084/jem.193.4.521

397. Reuter, H., Perner, B., Wahl, F., Rohde, L., Koch, P., Groth, M., Buder, K., & Englert, C. (2022). Aging Activates the Immune System and Alters the Regenerative Capacity in the Zebrafish Heart. *Cells*, *11*(3). https://doi.org/10.3390/cells11030345

398. Rice, G., Patrick, T., Parmar, R., Taylor, C. F., Aeby, A., Aicardi, J., Artuch, R., Montalto, S. A., Bacino, C. A., Barroso, B., Baxter, P., Benko, W. S., Bergmann, C., Bertini, E., Biancheri, R., Blair, E. M., Blau, N., Bonthron, D. T., Briggs, T., . . . Crow, Y. J. (2007). Clinical and Molecular Phenotype of Aicardi-Goutières Syndrome. *The American Journal of Human Genetics*, *81*(4), 713-725. https://doi.org/https://doi.org/10.1086/521373

399. Rio, P., & Bueren, J. A. (2008). FA core complex moves to chromatin. *Blood*, *111*(10), 4837-4838. https://doi.org/10.1182/blood-2008-01-134668

400. Riva, L., Ronchini, C., Bodini, M., Lo-Coco, F., Lavorgna, S., Ottone, T., Martinelli, G., Iacobucci, I., Tarella, C., Cignetti, A., Volorio, S., Bernard, L., Russo, A., Melloni, G. E., Luzi, L., Alcalay, M., Dellino, G. I., & Pelicci, P. G. (2013). Acute promyelocytic leukemias share cooperative mutations with other myeloid-leukemia subgroups. *Blood Cancer J*, *3*(9), e147. https://doi.org/10.1038/bcj.2013.46

401. Rodier, F., Coppe, J. P., Patil, C. K., Hoeijmakers, W. A., Munoz, D. P., Raza, S. R., Freund, A., Campeau, E., Davalos, A. R., & Campisi, J. (2009). Persistent DNA damage signalling triggers senescence-associated inflammatory cytokine secretion. *Nat Cell Biol*, *11*(8), 973-979. https://doi.org/10.1038/ncb1909

402. Rodriguez-Martin, B., Alvarez, E. G., Baez-Ortega, A., Zamora, J., Supek, F., Demeulemeester, J., Santamarina, M., Ju, Y. S., Temes, J., Garcia-Souto, D., Detering, H., Li, Y., Rodriguez-Castro, J., Dueso-Barroso, A., Bruzos, A. L., Dentro, S. C., Blanco, M. G., Contino, G., Ardeljan, D., . . . Consortium, P. (2020). Pan-cancer analysis of whole genomes identifies driver rearrangements promoted by LINE-1 retrotransposition. *Nature Genetics*, *52*(3), 306-319. https://doi.org/10.1038/s41588-019-0562-0

403. Ronchini, C., Brozzi, A., Riva, L., Luzi, L., Gruszka, A. M., Melloni, G. E. M., Scanziani, E., Dharmalingam, G., Mutarelli, M., Belcastro, V., Lavorgna, S., Rossi, V., Spinelli, O., Biondi, A., Rambaldi, A., Lo-Coco, F., di Bernardo, D., & Pelicci, P. G. (2017). PML-RARA-associated cooperating mutations belong to a transcriptional network that is deregulated in myeloid leukemias. *Leukemia*, *31*(9), 1975-1986. https://doi.org/10.1038/leu.2016.386

404. Ronco, C., Martin, A. R., Demange, L., & Benhida, R. (2017). ATM, ATR, CHK1, CHK2 and WEE1 inhibitors in cancer and cancer stem cells. *Medchemcomm*, *8*(2), 295-319. https://doi.org/10.1039/c6md00439c

405. Roos, W. P., & Kaina, B. (2006). DNA damage-induced cell death by apoptosis. *Trends Mol Med*, *12*(9), 440-450. https://doi.org/10.1016/j.molmed.2006.07.007

406. Rossi, M. L., Ghosh, A. K., & Bohr, V. A. (2010). Roles of Werner syndrome protein in protection of genome integrity. *DNA Repair (Amst)*, *9*(3), 331-344. https://doi.org/10.1016/j.dnarep.2009.12.011

407. Rowley, J. D., Golomb, H. M., & Dougherty, C. (1977). 15/17 translocation, a consistent chromosomal change in acute promyelocytic leukaemia. *Lancet*, *1*(8010), 549-550. https://doi.org/10.1016/s0140-6736(77)91415-5

408. Sahin, U., de The, H., & Lallemand-Breitenbach, V. (2022). Sumoylation in Physiology, Pathology and Therapy. *Cells*, *11*(5). https://doi.org/10.3390/cells11050814

409. Sahin, U., Ferhi, O., Jeanne, M., Benhenda, S., Berthier, C., Jollivet, F., Niwa-Kawakita, M., Faklaris, O., Setterblad, N., de The, H., & Lallemand-Breitenbach, V. (2014). Oxidative stress-induced assembly of PML nuclear bodies controls sumoylation of partner proteins. *J Cell Biol*, *204*(6), 931-945. https://doi.org/10.1083/jcb.201305148

410. Saint-Germain, E., Mignacca, L., Vernier, M., Bobbala, D., Ilangumaran, S., & Ferbeyre, G. (2017). SOCS1 regulates senescence and ferroptosis by modulating the expression of p53 target genes. *Aging (Albany NY)*, *9*(10), 2137-2162. https://doi.org/10.18632/aging.101306

411. Saitoh, T., Fujita, N., Hayashi, T., Takahara, K., Satoh, T., Lee, H., Matsunaga, K., Kageyama, S., Omori, H., Noda, T., Yamamoto, N., Kawai, T., Ishii, K., Takeuchi, O., Yoshimori, T., & Akira, S. (2009). Atg9a controls dsDNA-driven dynamic translocation of STING and the innate immune response. *Proc Natl Acad Sci U S A*, *106*(49), 20842-20846. https://doi.org/10.1073/pnas.0911267106

412. Salama, R., Sadaie, M., Hoare, M., & Narita, M. (2014). Cellular senescence and its effector programs. *Genes Dev*, *28*(2), 99-114. https://doi.org/10.1101/gad.235184.113

413. Salomoni, P. (2013). The PML-Interacting Protein DAXX: Histone Loading Gets into the Picture. *Front Oncol*, *3*, 152. https://doi.org/10.3389/fonc.2013.00152

414. Salsman, J., Rapkin, L. M., Margam, N. N., Duncan, R., Bazett-Jones, D. P., & Dellaire, G. (2017). Myogenic differentiation triggers PML nuclear body loss and DAXX relocalization to chromocentres. *Cell Death Dis*, *8*(3), e2724. https://doi.org/10.1038/cddis.2017.151

415. Scaglioni, P. P., Yung, T. M., Cai, L. F., Erdjument-Bromage, H., Kaufman, A. J., Singh, B., Teruya-Feldstein, J., Tempst, P., & Pandolfi, P. P. (2006). A CK2-Dependent Mechanism for Degradation of the PML Tumor Suppressor. *Cell*, *126*(2), 269-283. https://doi.org/https://doi.org/10.1016/j.cell.2006.05.041

416. Schärer, O. D. (2013). Nucleotide excision repair in eukaryotes. *Cold Spring Harb Perspect Biol*, *5*(10), a012609. https://doi.org/10.1101/cshperspect.a012609

417. Scherer, M., & Stamminger, T. (2016). Emerging Role of PML Nuclear Bodies in Innate Immune Signaling. *J Virol*, *90*(13), 5850-5854. https://doi.org/10.1128/jvi.01979-15

418. Schilling, E. M., Scherer, M., Reuter, N., Schweininger, J., Muller, Y. A., & Stamminger, T. (2017). The Human Cytomegalovirus IE1 Protein Antagonizes PML Nuclear Body-Mediated Intrinsic Immunity via the Inhibition of PML De Novo SUMOylation. *J Virol*, *91*(4). https://doi.org/10.1128/JVI.02049-16

419. Schmitz, C. R. R., Maurmann, R. M., Guma, F., Bauer, M. E., & Barbe-Tuana, F. M. (2023). cGAS-STING pathway as a potential trigger of immunosenescence and inflammaging. *Front Immunol*, *14*, 1132653. https://doi.org/10.3389/fimmu.2023.1132653

420. Schmitz, C. R. R., Maurmann, R. M., Guma, F., Bauer, M. E., & Barbé-Tuana, F. M. (2023). cGAS-STING pathway as a potential trigger of immunosenescence and inflammaging. *Front Immunol*, *14*, 1132653. https://doi.org/10.3389/fimmu.2023.1132653

421. Schumann, T., Ramon, S. C., Schubert, N., Mayo, M. A., Hega, M., Maser, K. I., Ada, S. R., Sydow, L., Hajikazemi, M., Badstubner, M., Muller, P., Ge, Y., Shakeri, F., Buness, A., Rupf, B., Lienenklaus, S., Utess, B., Muhandes, L., Haase, M., . . . Behrendt, R. (2023). Deficiency for SAMHD1 activates MDA5 in a cGAS/STING-dependent manner. *J Exp Med*, *220*(1). https://doi.org/10.1084/jem.20220829

422. Scrima, A., Konickova, R., Czyzewski, B. K., Kawasaki, Y., Jeffrey, P. D., Groisman, R., Nakatani, Y., Iwai, S., Pavletich, N. P., & Thoma, N. H. (2008). Structural basis of UV DNA-damage recognition by the DDB1-DDB2 complex. *Cell*, *135*(7), 1213-1223. https://doi.org/10.1016/j.cell.2008.10.045

423. Seamon, K. J., Sun, Z., Shlyakhtenko, L. S., Lyubchenko, Y. L., & Stivers, J. T. (2015). SAMHD1 is a single-stranded nucleic acid binding protein with no active site-associated nuclease activity. *Nucleic Acids Res*, *43*(13), 6486-6499. https://doi.org/10.1093/nar/gkv633

424. Secombes, C. J., & Zou, J. (2017). Evolution of Interferons and Interferon Receptors. *Front Immunol*, *8*, 209. https://doi.org/10.3389/fimmu.2017.00209

425. Sellaththurai, S., Jung, S., Kim, M. J., Nadarajapillai, K., Ganeshalingam, S., Jeong, J. B., & Lee, J. (2023). CRISPR/Cas9-Induced Knockout of Sting Increases Susceptibility of Zebrafish to Bacterial Infection. *Biomolecules*, *13*(2). https://doi.org/10.3390/biom13020324

426. Shao, F., Han, M., & Peng, Z. (2019). Evolution and diversity of transposable elements in fish genomes. *Scientific Reports*, *9*(1), 15399. https://doi.org/10.1038/s41598-019-51888-1

427. Sharma, A., Singh, K., & Almasan, A. (2012). Histone H2AX phosphorylation: a marker for DNA damage. *Methods Mol Biol*, *920*, 613-626. https://doi.org/10.1007/978-1-61779-998-3_40

428. Sharma, R., Rodic, N., Burns, K. H., & Taylor, M. S. (2016). Immunodetection of Human LINE-1 Expression in Cultured Cells and Human Tissues. *Methods Mol Biol*, *1400*, 261-280. https://doi.org/10.1007/978-1-4939-3372-3_17

429. Sharma, S., tenOever, B. R., Grandvaux, N., Zhou, G. P., Lin, R., & Hiscott, J. (2003). Triggering the interferon antiviral response through an IKK-related pathway. *Science*, *300*(5622), 1148-1151. https://doi.org/10.1126/science.1081315

430. Shastrula, P. K., Sierra, I., Deng, Z., Keeney, F., Hayden, J. E., Lieberman, P. M., & Janicki, S. M. (2019). PML is recruited to heterochromatin during S phase and represses DAXX-mediated histone H3.3 chromatin assembly. *J Cell Sci*, *132*(6). https://doi.org/10.1242/jcs.220970

431. Shaw, A. E., Hughes, J., Gu, Q., Behdenna, A., Singer, J. B., Dennis, T., Orton, R. J., Varela, M., Gifford, R. J., Wilson, S. J., & Palmarini, M. (2017). Fundamental properties of the mammalian innate immune system revealed by multispecies comparison of type I interferon responses. *PLoS Biol*, *15*(12), e2004086. https://doi.org/10.1371/journal.pbio.2004086

432. Shen, T. H., Lin, H. K., Scaglioni, P. P., Yung, T. M., & Pandolfi, P. P. (2006). The mechanisms of PML-nuclear body formation. *Mol Cell*, *24*(3), 331-339. https://doi.org/10.1016/j.molcel.2006.09.013

433. Shen, W. J., Azhar, S., & Kraemer, F. B. (2016). Lipid droplets and steroidogenic cells. *Exp Cell Res*, *340*(2), 209-214. https://doi.org/10.1016/j.yexcr.2015.11.024

434. Sil, S., Keegan, S., Ettefa, F., Denes, L. T., Boeke, J. D., & Holt, L. J. (2023). Condensation of LINE-1 is critical for retrotransposition. *Elife*, *12*, e82991.

435. Simmer, J. P., Hu, J. C., Hu, Y., Zhang, S., Liang, T., Wang, S. K., Kim, J. W., Yamakoshi, Y., Chun, Y. H., Bartlett, J. D., & Smith, C. E. (2021). A genetic model for the secretory stage of dental enamel formation. *J Struct Biol*, *213*(4), 107805. https://doi.org/10.1016/j.jsb.2021.107805

436. Simon, A., & Tanaka, E. M. (2013). Limb regeneration. *Wiley Interdiscip Rev Dev Biol*, *2*(2), 291-300. https://doi.org/10.1002/wdev.73

437. Simpson, S. R., Hemphill, W. O., Hudson, T., & Perrino, F. W. (2020). TREX1 - Apex predator of cytosolic DNA metabolism. *DNA Repair (Amst)*, *94*, 102894. https://doi.org/10.1016/j.dnarep.2020.102894

438. Singh, R. S., Vidhyasagar, V., Yang, S., Arna, A. B., Yadav, M., Aggarwal, A., Aguilera, A. N., Shinriki, S., Bhanumathy, K. K., & Pandey, K. (2022). DDX41 is required for cGAS-STING activation against DNA virus infection. *Cell reports*, *39*(8).

439. Sistigu, A., Yamazaki, T., Vacchelli, E., Chaba, K., Enot, D. P., Adam, J., Vitale, I., Goubar, A., Baracco, E. E., Remedios, C., Fend, L., Hannani, D., Aymeric, L., Ma, Y., Niso-Santano, M., Kepp, O., Schultze, J. L., Tuting, T., Belardelli, F., . . . Zitvogel, L. (2014). Cancer cell-autonomous contribution of type I interferon signaling to the efficacy of chemotherapy. *Nat Med*, *20*(11), 1301-1309. https://doi.org/10.1038/nm.3708

440. Slade, D. (2020). PARP and PARG inhibitors in cancer treatment. *Genes Dev*, *34*(5-6), 360-394. https://doi.org/10.1101/gad.334516.119

441. Sladitschek-Martens, H. L., Guarnieri, A., Brumana, G., Zanconato, F., Battilana, G., Xiccato, R. L., Panciera, T., Forcato, M., Bicciato, S., Guzzardo, V., Fassan, M., Ulliana, L., Gandin, A., Tripodo, C., Foiani, M., Brusatin, G., Cordenonsi, M., & Piccolo, S. (2022). YAP/TAZ activity in stromal cells prevents ageing by controlling cGAS-STING. *Nature*, *607*(7920), 790-798. https://doi.org/10.1038/s41586-022-04924-6

442. Slavik, K. M., Morehouse, B. R., Ragucci, A. E., Zhou, W., Ai, X., Chen, Y., Li, L., Wei, Z., Bähre, H., König, M., Seifert, R., Lee, A. S. Y., Cai, H., Imler, J. L., & Kranzusch, P. J. (2021). cGAS-like receptors sense RNA and control 3'2'-cGAMP signalling in Drosophila. *Nature*, *597*(7874), 109-113. https://doi.org/10.1038/s41586-021-03743-5

443. Sliter, D. A., Martinez, J., Hao, L., Chen, X., Sun, N., Fischer, T. D., Burman, J. L., Li, Y., Zhang, Z., Narendra, D. P., Cai, H., Borsche, M., Klein, C., & Youle, R. J. (2018). Parkin and PINK1 mitigate STING-induced inflammation. *Nature*, *561*(7722), 258-262. https://doi.org/10.1038/s41586-018-0448-9

444. Smolka, M. B., Albuquerque, C. P., Chen, S. H., & Zhou, H. (2007). Proteome-wide identification of in vivo targets of DNA damage checkpoint kinases. *Proc Natl Acad Sci U S A*, *104*(25), 10364-10369. https://doi.org/10.1073/pnas.0701622104

445. Sołtysik, K., Ohsaki, Y., & Fujimoto, T. (2019). Duo in a Mystical Realm—Nuclear Lipid Droplets and the Inner Nuclear Membrane. *Contact*, *2*, 2515256419896965. https://doi.org/10.1177/2515256419896965

446. Song, J., Durrin, L. K., Wilkinson, T. A., Krontiris, T. G., & Chen, Y. (2004). Identification of a SUMO-binding motif that recognizes SUMO-modified proteins. *Proc Natl Acad Sci U S A*, *101*(40), 14373-14378. https://doi.org/10.1073/pnas.0403498101

447. Song, X., Aw, J. T. M., Ma, F., Cheung, M. F., Leung, D., & Herrup, K. (2021). DNA Repair Inhibition Leads to Active Export of Repetitive Sequences to the Cytoplasm Triggering an Inflammatory Response. *J Neurosci*, *41*(45), 9286-9307. https://doi.org/10.1523/JNEUROSCI.0845-21.2021

448. Soto-Gamez, A., & Demaria, M. (2017). Therapeutic interventions for aging: the case of cellular senescence. *Drug Discov Today*, *22*(5), 786-795. https://doi.org/10.1016/j.drudis.2017.01.004

449. Sousounis, K., Bryant, D. M., Martinez Fernandez, J., Eddy, S. S., Tsai, S. L., Gundberg, G. C., Han, J., Courtemanche, K., Levin, M., & Whited, J. L. (2020). Eya2 promotes cell cycle progression by regulating DNA damage response during vertebrate limb regeneration. *Elife*, *9*. https://doi.org/10.7554/eLife.51217

450. Stachura, D. L., Reyes, J. R., Bartunek, P., Paw, B. H., Zon, L. I., & Traver, D. (2009). Zebrafish kidney stromal cell lines support multilineage hematopoiesis. *Blood*, *114*(2), 279-289. https://doi.org/10.1182/blood-2009-02-203638

451. Stadler, M., Chelbi-Alix, M. K., Koken, M. H., Venturini, L., Lee, C., Saïb, A., Quignon, F., Pelicano, L., Guillemin, M. C., Schindler, C., & et al. (1995). Transcriptional induction of the PML growth suppressor gene by interferons is mediated through an ISRE and a GAS element. *Oncogene*, *11*(12), 2565-2573.

452. Stavropoulos, D. J., Bradshaw, P. S., Li, X., Pasic, I., Truong, K., Ikura, M., Ungrin, M., & Meyn, M. S. (2002). The Bloom syndrome helicase BLM interacts with TRF2 in ALT cells and promotes telomeric DNA synthesis. *Human Molecular Genetics*, *11*(25), 3135-3144. https://doi.org/10.1093/hmg/11.25.3135

453. Stetson, D. B., Ko, J. S., Heidmann, T., & Medzhitov, R. (2008). Trex1 prevents cell-intrinsic initiation of autoimmunity. *Cell*, *134*(4), 587-598. https://doi.org/10.1016/j.cell.2008.06.032

454. Stixova, L., Matula, P., Kozubek, S., Gombitova, A., Cmarko, D., Raska, I., & Bartova, E. (2012). Trajectories and nuclear arrangement of PML bodies are influenced by A-type lamin deficiency. *Biol Cell*, *104*(7), 418-432. https://doi.org/10.1111/boc.201100053

455. Stocum, D. L. (1979). Stages of forelimb regeneration in Ambystoma maculatum. *Journal of Experimental Zoology*, *209*(3), 395-416. https://doi.org/https://doi.org/10.1002/jez.1402090306

456. Stokes, M. P., Rush, J., Macneill, J., Ren, J. M., Sprott, K., Nardone, J., Yang, V., Beausoleil, S. A., Gygi, S. P., Livingstone, M., Zhang, H., Polakiewicz, R. D., &

Comb, M. J. (2007). Profiling of UV-induced ATM/ATR signaling pathways. *Proc Natl Acad Sci U S A*, *104*(50), 19855-19860. https://doi.org/10.1073/pnas.0707579104

457. Storer, M., Mas, A., Robert-Moreno, A., Pecoraro, M., Ortells, M. C., Di Giacomo, V., Yosef, R., Pilpel, N., Krizhanovsky, V., Sharpe, J., & Keyes, W. M. (2013). Senescence is a developmental mechanism that contributes to embryonic growth and patterning. *Cell*, *155*(5), 1119-1130. https://doi.org/10.1016/j.cell.2013.10.041

458. Stoyek, M. R., Rog-Zielinska, E. A., & Quinn, T. A. (2018). Age-associated changes in electrical function of the zebrafish heart. *Progress in Biophysics and Molecular Biology*, *138*, 91-104. https://doi.org/https://doi.org/10.1016/j.pbiomolbio.2018.07.014

459. Streetz, K. L., Luedde, T., Manns, M. P., & Trautwein, C. (2000). Interleukin 6 and liver regeneration. *Gut*, *47*(2), 309-312. https://doi.org/10.1136/gut.47.2.309

460. Stuurman, N., de Graaf, A., Floore, A., Josso, A., Humbel, B., de Jong, L., & van Driel, R. (1992). A monoclonal antibody recognizing nuclear matrix-associated nuclear bodies. *J Cell Sci*, *101 (Pt 4)*, 773-784. https://doi.org/10.1242/jcs.101.4.773

461. Sugano, T., Kajikawa, M., & Okada, N. (2006). Isolation and characterization of retrotransposition-competent LINEs from zebrafish. *Gene*, *365*, 74-82. https://doi.org/10.1016/j.gene.2005.09.037

462. Sun, H., Leverson, J. D., & Hunter, T. (2007). Conserved function of RNF4 family proteins in eukaryotes: targeting a ubiquitin ligase to SUMOylated proteins. *The EMBO journal*, *26*(18), 4102-4112.

463. Sun, J., Xu, H., Subramony, S. H., & Hebert, M. D. (2005). Interactions between coilin and PIASy partially link Cajal bodies to PML bodies. *J Cell Sci*, *118*(Pt 21), 4995-5003. https://doi.org/10.1242/jcs.02613

464. Sun, L., Wu, J., Du, F., Chen, X., & Chen, Z. J. (2013). Cyclic GMP-AMP synthase is a cytosolic DNA sensor that activates the type I interferon pathway. *Science*, *339*(6121), 786-791. https://doi.org/10.1126/science.1232458

465. Susaki, Etsuo A., Tainaka, K., Perrin, D., Kishino, F., Tawara, T., Watanabe, Tomonobu M., Yokoyama, C., Onoe, H., Eguchi, M., Yamaguchi, S., Abe, T., Kiyonari, H., Shimizu, Y., Miyawaki, A., Yokota, H., & Ueda, Hiroki R. (2014). Whole-Brain Imaging with Single-Cell Resolution Using Chemical Cocktails and Computational Analysis. *Cell*, *157*(3), 726-739. https://doi.org/10.1016/j.cell.2014.03.042

466. Syed, A., & Tainer, J. A. (2018). The MRE11-RAD50-NBS1 Complex Conducts the Orchestration of Damage Signaling and Outcomes to Stress in DNA

Replication and Repair. *Annu Rev Biochem*, *87*, 263-294. https://doi.org/10.1146/annurev-biochem-062917-012415

467. Szostecki, C., Guldner, H. H., Netter, H. J., & Will, H. (1990). Isolation and characterization of cDNA encoding a human nuclear antigen predominantly recognized by autoantibodies from patients with primary biliary cirrhosis. *J Immunol*, *145*(12), 4338-4347. https://www.ncbi.nlm.nih.gov/pubmed/2258622

468. Takahashi, A., Loo, T. M., Okada, R., Kamachi, F., Watanabe, Y., Wakita, M., Watanabe, S., Kawamoto, S., Miyata, K., Barber, G. N., Ohtani, N., & Hara, E. (2018). Downregulation of cytoplasmic DNases is implicated in cytoplasmic DNA accumulation and SASP in senescent cells. *Nat Commun*, *9*(1), 1249. https://doi.org/10.1038/s41467-018-03555-8

469. Tanaka, Y., & Chen, Z. J. (2012). STING specifies IRF3 phosphorylation by TBK1 in the cytosolic DNA signaling pathway. *Sci Signal*, *5*(214), ra20. https://doi.org/10.1126/scisignal.2002521

470. Tao, X., Song, J., Song, Y., Zhang, Y., Yang, J., Zhang, P., Zhang, D., Chen, D., & Sun, Q. (2022). Ku proteins promote DNA binding and condensation of cyclic GMP-AMP synthase. *Cell reports*, *40*(10).

471. Tatham, M. H., Geoffroy, M. C., Shen, L., Plechanovova, A., Hattersley, N., Jaffray, E. G., Palvimo, J. J., & Hay, R. T. (2008). RNF4 is a poly-SUMO-specific E3 ubiquitin ligase required for arsenic-induced PML degradation. *Nat Cell Biol*, *10*(5), 538-546. https://doi.org/10.1038/ncb1716

472. Tatham, M. H., Jaffray, E., Vaughan, O. A., Desterro, J. M., Botting, C. H., Naismith, J. H., & Hay, R. T. (2001). Polymeric chains of SUMO-2 and SUMO-3 are conjugated to protein substrates by SAE1/SAE2 and Ubc9. *J Biol Chem*, *276*(38), 35368-35374. https://doi.org/10.1074/jbc.M104214200

473. Teame, T., Zhang, Z., Ran, C., Zhang, H., Yang, Y., Ding, Q., Xie, M., Gao, C., Ye, Y., Duan, M., & Zhou, Z. (2019). The use of zebrafish (Danio rerio) as biomedical models. *Animal Frontiers*, *9*(3), 68-77. https://doi.org/10.1093/af/vfz020

474. Thomas, C. A., Tejwani, L., Trujillo, C. A., Negraes, P. D., Herai, R. H., Mesci, P., Macia, A., Crow, Y. J., & Muotri, A. R. (2017). Modeling of TREX1-Dependent Autoimmune Disease using Human Stem Cells Highlights L1 Accumulation as a Source of Neuroinflammation. *Cell Stem Cell*, *21*(3), 319-331 e318. https://doi.org/10.1016/j.stem.2017.07.009

475. Tomlinson, B. L., Tomlinson, D. E., & Tassava, R. A. (1985). Pattern-deficient forelimb regeneration in adult bullfrogs. *Journal of Experimental Zoology*, *236*(3), 313-326. https://doi.org/https://doi.org/10.1002/jez.1402360309

476. Toufektchan, E., & Maciejowski, J. (2021). Purification of micronuclei from cultured cells by flow cytometry. *STAR Protocols*, *2*(1), 100378. https://doi.org/https://doi.org/10.1016/j.xpro.2021.100378

477. Tsai, S. L., Baselga-Garriga, C., & Melton, D. A. (2019). Blastemal progenitors modulate immune signaling during early limb regeneration. *Development*, *146*(1), dev169128.

478. Tsuchida, T., Zou, J., Saitoh, T., Kumar, H., Abe, T., Matsuura, Y., Kawai, T., & Akira, S. (2010). The ubiquitin ligase TRIM56 regulates innate immune responses to intracellular double-stranded DNA. *Immunity*, *33*(5), 765-776. https://doi.org/10.1016/j.immuni.2010.10.013

479. Tucker, J. B., Bonema, S. C., García-Varela, R., Denu, R. A., Hu, Y., McGregor, S. M., Burkard, M. E., & Weaver, B. A. (2023). Misaligned Chromosomes are a Major Source of Chromosomal Instability in Breast Cancer. *Cancer Res Commun*, *3*(1), 54-65. https://doi.org/10.1158/2767-9764.Crc-22-0302

480. Turelli, P., Doucas, V., Craig, E., Mangeat, B., Klages, N., Evans, R., Kalpana, G., & Trono, D. (2001). Cytoplasmic recruitment of INI1 and PML on incoming HIV preintegration complexes: interference with early steps of viral replication. *Mol Cell*, *7*(6), 1245-1254. https://doi.org/10.1016/s1097-2765(01)00255-6

481. Ugge, M., Simoni, M., Fracassi, C., & Bernardi, R. (2022). PML isoforms: a molecular basis for PML pleiotropic functions. *Trends Biochem Sci*, *47*(7), 609-619. https://doi.org/10.1016/j.tibs.2022.02.002

482. Ulbricht, T., Alzrigat, M., Horch, A., Reuter, N., von Mikecz, A., Steimle, V., Schmitt, E., Kramer, O. H., Stamminger, T., & Hemmerich, P. (2012). PML promotes MHC class II gene expression by stabilizing the class II transactivator. *J Cell Biol*, *199*(1), 49-63. https://doi.org/10.1083/jcb.201112015

483. Valcourt, U., Kowanetz, M., Niimi, H., Heldin, C. H., & Moustakas, A. (2005). TGF-beta and the Smad signaling pathway support transcriptomic reprogramming during epithelial-mesenchymal cell transition. *Mol Biol Cell*, *16*(4), 1987-2002. https://doi.org/10.1091/mbc.e04-08-0658

484. Van Damme, E., Laukens, K., Dang, T. H., & Van Ostade, X. (2010). A manually curated network of the PML nuclear body interactome reveals an important role for PML-NBs in SUMOylation dynamics. *Int J Biol Sci*, *6*(1), 51-67. https://doi.org/10.7150/ijbs.6.51

485. Vancurova, M., Hanzlikova, H., Knoblochova, L., Kosla, J., Majera, D., Mistrik, M., Burdova, K., Hodny, Z., & Bartek, J. (2019). PML nuclear bodies are recruited to persistent DNA damage lesions in an RNF168-53BP1 dependent manner and contribute to DNA repair. *DNA Repair (Amst)*, *78*, 114-127. https://doi.org/10.1016/j.dnarep.2019.04.001

486. Varejao, N., Lascorz, J., Li, Y., & Reverter, D. (2020). Molecular mechanisms in SUMO conjugation. *Biochem Soc Trans*, *48*(1), 123-135. https://doi.org/10.1042/BST20190357

487. Vernier, M., Bourdeau, V., Gaumont-Leclerc, M. F., Moiseeva, O., Begin, V., Saad, F., Mes-Masson, A. M., & Ferbeyre, G. (2011). Regulation of E2Fs and senescence by PML nuclear bodies. *Genes Dev*, *25*(1), 41-50. https://doi.org/10.1101/gad.1975111

488. Vertegaal, A. C., Andersen, J. S., Ogg, S. C., Hay, R. T., Mann, M., & Lamond, A. I. (2006). Distinct and overlapping sets of SUMO-1 and SUMO-2 target proteins revealed by quantitative proteomics. *Mol Cell Proteomics*, *5*(12), 2298-2310. https://doi.org/10.1074/mcp.M600212-MCP200

489. Villagra, N. T., Navascues, J., Casafont, I., Val-Bernal, J. F., Lafarga, M., & Berciano, M. T. (2006). The PML-nuclear inclusion of human supraoptic neurons: a new compartment with SUMO-1- and ubiquitin-proteasome-associated domains. *Neurobiol Dis*, *21*(1), 181-193. https://doi.org/10.1016/j.nbd.2005.07.003

490. Vizioli, M. G., Liu, T., Miller, K. N., Robertson, N. A., Gilroy, K., Lagnado, A. B., Perez-Garcia, A., Kiourtis, C., Dasgupta, N., Lei, X., Kruger, P. J., Nixon, C., Clark, W., Jurk, D., Bird, T. G., Passos, J. F., Berger, S. L., Dou, Z., & Adams, P. D. (2020). Mitochondria-to-nucleus retrograde signaling drives formation of cytoplasmic chromatin and inflammation in senescence. *Genes Dev*, *34*(5-6), 428-445. https://doi.org/10.1101/gad.331272.119

491. von Zglinicki, T., Saretzki, G., Ladhoff, J., d'Adda di Fagagna, F., & Jackson, S. P. (2005). Human cell senescence as a DNA damage response. *Mech Ageing Dev*, *126*(1), 111-117. https://doi.org/10.1016/j.mad.2004.09.034

492. Walther, T. C., Chung, J., & Farese, R. V., Jr. (2017). Lipid Droplet Biogenesis. *Annu Rev Cell Dev Biol*, *33*, 491-510. https://doi.org/10.1146/annurev-cellbio-100616-060608

493. Wang, C., Nan, J., Holvey-Bates, E., Chen, X., Wightman, S., Latif, M. B., Zhao, J., Li, X., Sen, G. C., Stark, G. R., & Wang, Y. (2023). STAT2 hinders STING intracellular trafficking and reshapes its activation in response to DNA damage. *Proc Natl Acad Sci U S A*, *120*(16), e2216953120. https://doi.org/10.1073/pnas.2216953120

494. Wang, L., & Jordan, I. K. (2018). Transposable element activity, genome regulation and human health. *Curr Opin Genet Dev*, *49*, 25-33. https://doi.org/10.1016/j.gde.2018.02.006

495. Wang, M., Wang, L., Qian, M., Tang, X., Liu, Z., Lai, Y., Ao, Y., Huang, Y., Meng, Y., Shi, L., Peng, L., Cao, X., Wang, Z., Qin, B., & Liu, B. (2020). PML2-

mediated thread-like nuclear bodies mark late senescence in Hutchinson-Gilford progeria syndrome. *Aging Cell*, *19*(6), e13147. https://doi.org/10.1111/acel.13147

496. Wang, P., Benhenda, S., Wu, H., Lallemand-Breitenbach, V., Zhen, T., Jollivet, F., Peres, L., Li, Y., Chen, S. J., Chen, Z., de The, H., & Meng, G. (2018). RING tetramerization is required for nuclear body biogenesis and PML sumoylation. *Nat Commun*, *9*(1), 1277. https://doi.org/10.1038/s41467-018-03498-0

497. Wang, Q., Liu, X., Cui, Y., Tang, Y., Chen, W., Li, S., Yu, H., Pan, Y., & Wang, C. (2014). The E3 ubiquitin ligase AMFR and INSIG1 bridge the activation of TBK1 kinase by modifying the adaptor STING. *Immunity*, *41*(6), 919-933. https://doi.org/10.1016/j.immuni.2014.11.011

498. Wang, X., Schoenhals, J. E., Li, A., Valdecanas, D. R., Ye, H., Zang, F., Tang, C., Tang, M., Liu, C. G., Liu, X., Krishnan, S., Allison, J. P., Sharma, P., Hwu, P., Komaki, R., Overwijk, W. W., Gomez, D. R., Chang, J. Y., Hahn, S. M., . . . Welsh, J. W. (2017). Suppression of Type I IFN Signaling in Tumors Mediates Resistance to Anti-PD-1 Treatment That Can Be Overcome by Radiotherapy. *Cancer Res*, *77*(4), 839-850. https://doi.org/10.1158/0008-5472.CAN-15-3142

499. Wang, X., Yang, C., Wang, X., Miao, J., Chen, W., Zhou, Y., Xu, Y., An, Y., Cheng, A., Ye, W., Chen, M., Song, D., Yuan, X., Wang, J., Qian, P., Wu, A. R., Zhang, Z. Y., & Liu, K. (2023). Driving axon regeneration by orchestrating neuronal and non-neuronal innate immune responses via the IFNgamma-cGAS-STING axis. *Neuron*, *111*(2), 236-255 e237. https://doi.org/10.1016/j.neuron.2022.10.028

500. Wang, X., Zhang, J. B., He, K. J., Wang, F., & Liu, C. F. (2021). Advances of Zebrafish in Neurodegenerative Disease: From Models to Drug Discovery. *Front Pharmacol*, *12*, 713963. https://doi.org/10.3389/fphar.2021.713963

501. Wang, Y., Lian, Q., Yang, B., Yan, S., Zhou, H., He, L., Lin, G., Lian, Z., Jiang, Z., & Sun, B. (2015). TRIM30alpha Is a Negative-Feedback Regulator of the Intracellular DNA and DNA Virus-Triggered Response by Targeting STING. *PLoS Pathog*, *11*(6), e1005012. https://doi.org/10.1371/journal.ppat.1005012

502. Wang, Y. T., Chen, J., Chang, C. W., Jen, J., Huang, T. Y., Chen, C. M., Shen, R., Liang, S. Y., Cheng, I. C., Yang, S. C., Lai, W. W., Cheng, K. H., Hsieh, T. S., Lai, M. Z., Cheng, H. C., Wang, Y. C., & Chen, R. H. (2017). Ubiquitination of tumor suppressor PML regulates prometastatic and immunosuppressive tumor microenvironment. *J Clin Invest*, *127*(8), 2982-2997. https://doi.org/10.1172/JCI89957

503. Wang, Z. G., Delva, L., Gaboli, M., Rivi, R., Giorgio, M., Cordon-Cardo, C., Grosveld, F., & Pandolfi, P. P. (1998). Role of PML in cell growth and the retinoic acid pathway. *Science*, *279*(5356), 1547-1551. https://doi.org/10.1126/science.279.5356.1547

504. Wang, Z. G., Ruggero, D., Ronchetti, S., Zhong, S., Gaboli, M., Rivi, R., & Pandolfi, P. P. (1998). PML is essential for multiple apoptotic pathways. *Nat Genet*, *20*(3), 266-272. https://doi.org/10.1038/3073

505. Wang, Z. Y., & Chen, Z. (2008). Acute promyelocytic leukemia: from highly fatal to highly curable. *Blood*, *111*(5), 2505-2515. https://doi.org/10.1182/blood-2007-07-102798

506. Wei, W., Gilbert, N., Ooi, S. L., Lawler, J. F., Ostertag, E. M., Kazazian, H. H., Boeke, J. D., & Moran, J. V. (2001). Human L1 retrotransposition: cis preference versus trans complementation. *Mol Cell Biol*, *21*(4), 1429-1439. https://doi.org/10.1128/MCB.21.4.1429-1439.2001

507. Wei, X., Wang, Z., Hinson, C., & Yang, K. (2022). Human TDP1, APE1 and TREX1 repair 3′-DNA–peptide/protein cross-links arising from abasic sites in vitro. *Nucleic acids research*, *50*(7), 3638-3657. https://doi.org/10.1093/nar/gkac185

508. Weichenrieder, O., Repanas, K., & Perrakis, A. (2004). Crystal structure of the targeting endonuclease of the human LINE-1 retrotransposon. *Structure*, *12*(6), 975-986.

509. Weidtkamp-Peters, S., Lenser, T., Negorev, D., Gerstner, N., Hofmann, T. G., Schwanitz, G., Hoischen, C., Maul, G., Dittrich, P., & Hemmerich, P. (2008). Dynamics of component exchange at PML nuclear bodies. *Journal of Cell Science*, *121*(16), 2731-2743. https://doi.org/10.1242/jcs.031922

510. Weindel, C. G., Bell, S. L., Vail, K. J., West, K. O., Patrick, K. L., & Watson, R. O. (2020). LRRK2 maintains mitochondrial homeostasis and regulates innate immune responses to Mycobacterium tuberculosis. *Elife*, *9*. https://doi.org/10.7554/eLife.51071

511. Williams, G. (1957). Pleiotropy, natural selection, and the evolution of senescence. Evolution (NY) 11: 398. In.

512. Wu, J., Sun, L., Chen, X., Du, F., Shi, H., Chen, C., & Chen, Z. J. (2013). Cyclic GMP-AMP is an endogenous second messenger in innate immune signaling by cytosolic DNA. *Science*, *339*(6121), 826-830. https://doi.org/10.1126/science.1229963

513. Wu, Q., Hu, H., Lan, J., Emenari, C., Wang, Z., Chang, K. S., Huang, H., & Yao, X. (2009). PML3 Orchestrates the Nuclear Dynamics and Function of TIP60. *J Biol Chem*, *284*(13), 8747-8759. https://doi.org/10.1074/jbc.M807590200

514. Wu, W. S., Vallian, S., Seto, E., Yang, W. M., Edmondson, D., Roth, S., & Chang, K. S. (2001). The growth suppressor PML represses transcription by functionally and physically interacting with histone deacetylases. *Mol Cell Biol*, *21*(7), 2259-2268. https://doi.org/10.1128/MCB.21.7.2259-2268.2001

515. Wu, X., Wu, F. H., Wang, X., Wang, L., Siedow, J. N., Zhang, W., & Pei, Z. M. (2014). Molecular evolutionary and structural analysis of the cytosolic DNA sensor cGAS and STING. *Nucleic Acids Res*, *42*(13), 8243-8257. https://doi.org/10.1093/nar/gku569

516. Xia, T., Konno, H., Ahn, J., & Barber, G. N. (2016). Deregulation of STING Signaling in Colorectal Carcinoma Constrains DNA Damage Responses and Correlates With Tumorigenesis. *Cell Rep*, *14*(2), 282-297. https://doi.org/10.1016/j.celrep.2015.12.029

517. Xiao, N., Wei, J., Xu, S., Du, H., Huang, M., Zhang, S., Ye, W., Sun, L., & Chen, Q. (2019). cGAS activation causes lupus-like autoimmune disorders in a TREX1 mutant mouse model. *J Autoimmun*, *100*, 84-94. https://doi.org/10.1016/j.jaut.2019.03.001

518. Xu, Z.-X., Timanova-Atanasova, A., Zhao, R.-X., & Chang, K.-S. (2003). PML Colocalizes with and Stabilizes the DNA Damage Response Protein TopBP1. *Molecular and Cellular Biology*, *23*(12), 4247-4256. https://doi.org/10.1128/MCB.23.12.4247-4256.2003

519. Xue, C., Salunkhe, S. J., Tomimatsu, N., Kawale, A. S., Kwon, Y., Burma, S., Sung, P., & Greene, E. C. (2022). Bloom helicase mediates formation of large single-stranded DNA loops during DNA end processing. *Nat Commun*, *13*(1), 2248. https://doi.org/10.1038/s41467-022-29937-7

520. Yan, J., Zhao, Y., Du, J., Wang, Y., Wang, S., Wang, Q., Zhao, X., Xu, W., & Zhao, K. (2022). RNA sensor MDA5 suppresses LINE-1 retrotransposition by regulating the promoter activity of LINE-1 5'-UTR. *Mob DNA*, *13*(1), 10. https://doi.org/10.1186/s13100-022-00268-0

521. Yang, H., Wang, H., Ren, J., Chen, Q., & Chen, Z. J. (2017). cGAS is essential for cellular senescence. *Proc Natl Acad Sci U S A*, *114*(23), E4612-E4620. https://doi.org/10.1073/pnas.1705499114

522. Yang, H., Wang, H., Ren, J., Chen, Q., & Chen, Z. J. (2017). cGAS is essential for cellular senescence. *Proceedings of the National Academy of Sciences*, *114*(23), E4612-E4620.

523. Yang, K., Wei, X., Le, J., & Rodriguez, N. (2022). Human TREX1 Repairs 3′-End DNA Lesions in Vitro. *Chemical Research in Toxicology*, *35*(6), 935-939. https://doi.org/10.1021/acs.chemrestox.2c00087

524. Yang, W. (2011). Nucleases: diversity of structure, function and mechanism. *Q Rev Biophys*, *44*(1), 1-93. https://doi.org/10.1017/S0033583510000181

525. Yu, L., & Liu, P. (2021). Cytosolic DNA sensing by cGAS: regulation, function, and human diseases. *Signal Transduction and Targeted Therapy*, *6*(1), 170. https://doi.org/10.1038/s41392-021-00554-y

526. Yu, Q., Walters, H. E., Pasquini, G., Singh, S. P., Lachnit, M., Oliveira, C., León-Periñán, D., Petzold, A., Kesavan, P., Subiran, C., Garteizgogeascoa, I., Knapp, D., Wagner, A., Bernardos, A., Alfonso, M., Nadar, G., Graf, A. M., Troyanovskiy, K. E., Dahl, A., . . . Yun, M. H. (2023). Cellular senescence promotes progenitor cell expansion during axolotl limb regeneration. *bioRxiv*, 2022.2009.2001.506196. https://doi.org/10.1101/2022.09.01.506196

527. Yuan, F., Dutta, T., Wang, L., Song, L., Gu, L., Qian, L., Benitez, A., Ning, S., Malhotra, A., Deutscher, M. P., & Zhang, Y. (2015). Human DNA Exonuclease TREX1 Is Also an Exoribonuclease That Acts on Single-stranded RNA. *J Biol Chem*, *290*(21), 13344-13353. https://doi.org/10.1074/jbc.M115.653915

528. Yuan, W. C., Lee, Y. R., Huang, S. F., Lin, Y. M., Chen, T. Y., Chung, H. C., Tsai, C. H., Chen, H. Y., Chiang, C. T., Lai, C. K., Lu, L. T., Chen, C. H., Gu, D. L., Pu, Y. S., Jou, Y. S., Lu, K. P., Hsiao, P. W., Shih, H. M., & Chen, R. H. (2011). A Cullin3-KLHL20 Ubiquitin ligase-dependent pathway targets PML to potentiate HIF-1 signaling and prostate cancer progression. *Cancer Cell*, *20*(2), 214-228. https://doi.org/10.1016/j.ccr.2011.07.008

529. Yue, X., Bai, C., Xie, D., Ma, T., & Zhou, P. K. (2020). DNA-PKcs: A Multi-Faceted Player in DNA Damage Response. *Front Genet*, *11*, 607428. https://doi.org/10.3389/fgene.2020.607428

530. Zevini, A., Olagnier, D., & Hiscott, J. (2017). Crosstalk between Cytoplasmic RIG-I and STING Sensing Pathways. *Trends Immunol*, *38*(3), 194-205. https://doi.org/10.1016/j.it.2016.12.004

531. Zhang, J., Hu, M. M., Wang, Y. Y., & Shu, H. B. (2012). TRIM32 protein modulates type I interferon induction and cellular antiviral response by targeting MITA/STING protein for K63-linked ubiquitination. *J Biol Chem*, *287*(34), 28646-28655. https://doi.org/10.1074/jbc.M112.362608

532. Zhang, X., Bai, X.-c., & Chen, Z. J. (2020). Structures and Mechanisms in the cGAS-STING Innate Immunity Pathway. *Immunity*, *53*(1), 43-53. https://doi.org/https://doi.org/10.1016/j.immuni.2020.05.013

533. Zhang, X., Shi, H., Wu, J., Zhang, X., Sun, L., Chen, C., & Chen, Z. J. (2013). Cyclic GMP-AMP containing mixed phosphodiester linkages is an endogenous high-affinity ligand for STING. *Mol Cell*, *51*(2), 226-235. https://doi.org/10.1016/j.molcel.2013.05.022

534. Zhang, X. P., Liu, F., & Wang, W. (2010). Coordination between cell cycle progression and cell fate decision by the p53 and E2F1 pathways in response to DNA damage. *J Biol Chem*, *285*(41), 31571-31580. https://doi.org/10.1074/jbc.M110.134650

535. Zhang, X. W., Yan, X. J., Zhou, Z. R., Yang, F. F., Wu, Z. Y., Sun, H. B., Liang, W. X., Song, A. X., Lallemand-Breitenbach, V., Jeanne, M., Zhang, Q. Y., Yang,

H. Y., Huang, Q. H., Zhou, G. B., Tong, J. H., Zhang, Y., Wu, J. H., Hu, H. Y., de The, H., . . . Chen, Z. (2010). Arsenic trioxide controls the fate of the PML-RARalpha oncoprotein by directly binding PML. *Science*, *328*(5975), 240-243. https://doi.org/10.1126/science.1183424

536. Zhao, A., Qin, H., & Fu, X. (2016). What Determines the Regenerative Capacity in Animals? *BioScience*, *66*(9), 735-746. https://doi.org/10.1093/biosci/biw079

537. Zhao, N., Hao, F., Qu, T., Zuo, Y. G., & Wang, B. X. (2008). A novel mutation of the WRN gene in a Chinese patient with Werner syndrome. *Clin Exp Dermatol*, *33*(3), 278-281. https://doi.org/10.1111/j.1365-2230.2007.02641.x

538. Zhao, Q., Xie, Y., Zheng, Y., Jiang, S., Liu, W., Mu, W., Liu, Z., Zhao, Y., Xue, Y., & Ren, J. (2014). GPS-SUMO: a tool for the prediction of sumoylation sites and SUMO-interaction motifs. *Nucleic Acids Res*, *42*(Web Server issue), W325-330. https://doi.org/10.1093/nar/gku383

539. Zhao, X., Zhao, Y., Du, J., Gao, P., & Zhao, K. (2021). The Interplay Among HIV, LINE-1, and the Interferon Signaling System. *Front Immunol*, *12*, 732775. https://doi.org/10.3389/fimmu.2021.732775

540. Zhong, B., Zhang, L., Lei, C., Li, Y., Mao, A. P., Yang, Y., Wang, Y. Y., Zhang, X. L., & Shu, H. B. (2009). The ubiquitin ligase RNF5 regulates antiviral responses by mediating degradation of the adaptor protein MITA. *Immunity*, *30*(3), 397-407. https://doi.org/10.1016/j.immuni.2009.01.008

541. Zhong, S., Hu, P., Ye, T.-Z., Stan, R., Ellis, N. A., & Pandolfi, P. P. (1999). A role for PML and the nuclear body in genomic stability. *Oncogene*, *18*(56), 7941-7947.

542. Zhong, S., Muller, S., Ronchetti, S., Freemont, P. S., Dejean, A., & Pandolfi, P. P. (2000). Role of SUMO-1-modified PML in nuclear body formation. *Blood*, *95*(9), 2748-2752. https://www.ncbi.nlm.nih.gov/pubmed/10779416

543. Zhou, B. B., & Elledge, S. J. (2000). The DNA damage response: putting checkpoints in perspective. *Nature*, *408*(6811), 433-439. https://doi.org/10.1038/35044005

544. Zhou, M., Cheng, X., Zhu, W., Jiang, J., Zhu, S., Wu, X., Liu, M., & Fang, Q. (2022). Activation of cGAS-STING pathway - A possible cause of myofiber atrophy/necrosis in dermatomyositis and immune-mediated necrotizing myopathy. *J Clin Lab Anal*, *36*(10), e24631. https://doi.org/10.1002/jcla.24631

545. Zhou, W., Cheng, L., Shi, Y., Ke, S. Q., Huang, Z., Fang, X., Chu, C. W., Xie, Q., Bian, X. W., Rich, J. N., & Bao, S. (2015). Arsenic trioxide disrupts glioma stem cells via promoting PML degradation to inhibit tumor growth. *Oncotarget*, *6*(35), 37300-37315. https://doi.org/10.18632/oncotarget.5836

546. Zhou, W., Mohr, L., Maciejowski, J., & Kranzusch, P. J. (2021a). cGAS phase separation inhibits TREX1-mediated DNA degradation and enhances cytosolic DNA sensing. *Mol Cell*, *81*(4), 739-755 e737. https://doi.org/10.1016/j.molcel.2021.01.024

547. Zhou, W., Mohr, L., Maciejowski, J., & Kranzusch, P. J. (2021b). cGAS phase separation inhibits TREX1-mediated DNA degradation and enhances cytosolic DNA sensing. *Mol Cell*, *81*(4), 739-755.e737. https://doi.org/10.1016/j.molcel.2021.01.024

548. Zhou, W., Richmond-Buccola, D., Wang, Q., & Kranzusch, P. J. (2022). Structural basis of human TREX1 DNA degradation and autoimmune disease. *Nat Commun*, *13*(1), 4277. https://doi.org/10.1038/s41467-022-32055-z

549. Zhu, J., Zhu, S., Guzzo, C. M., Ellis, N. A., Sung, K. S., Choi, C. Y., & Matunis, M. J. (2008). Small ubiquitin-related modifier (SUMO) binding determines substrate recognition and paralog-selective SUMO modification. *J Biol Chem*, *283*(43), 29405-29415. https://doi.org/10.1074/jbc.M803632200

550. Zou, L., & Elledge, S. J. (2003). Sensing DNA damage through ATRIP recognition of RPA-ssDNA complexes. *Science*, *300*(5625), 1542-1548. https://doi.org/10.1126/science.1083430

551. Zuo, Y., & Deutscher, M. P. (2001). Exoribonuclease superfamilies: structural analysis and phylogenetic distribution. *Nucleic Acids Res*, *29*(5), 1017-1026. https://doi.org/10.1093/nar/29.5.1017

Appendix A – Copyright agreements

"Mathavarajah, S., Vergunst, K.L., Habib, E.B., Williams, S.K., He, R., Maliougina, M., Park, M., Salsman, J., Roy, S., Braasch, I. and Roger, A.J., 2023. PML and PML-like exonucleases restrict retrotransposons in jawed vertebrates. *Nucleic Acids Research*, *51*(7), pp.3185-3204."

OXFORD UNIVERSITY PRESS LICENSE
TERMS AND CONDITIONS

Sep 05, 2023

This Agreement between Dalhousie University -- Sabateeshan Mathavarajah ("You") and Oxford University Press ("Oxford University Press") consists of your license details and the terms and conditions provided by Oxford University Press and Copyright Clearance Center.

License Number	5622640668803
License date	Sep 05, 2023
Licensed content publisher	Oxford University Press
Licensed content publication	Nucleic Acids Research
Licensed content title	PML and PML-like exonucleases restrict retrotransposons in jawed vertebrates
Licensed content author	Mathavarajah, Sabateeshan; Vergunst, Kathleen L
Licensed content date	Mar 13, 2023
Type of Use	Thesis/Dissertation
Institution name	
Title of your work	The molecular evolution of DEDDh exonucleases reveals novel functions in innate immune signalling
Publisher of your work	Dalhousie University

Expected publication date	Nov 2023
Permissions cost	0.00 USD
Value added tax	0.00 USD
Total	0.00 USD
Title	The molecular evolution of DEDDh exonucleases reveals novel functions in innate immune signalling
Institution name	Dalhousie University
Expected presentation date	Nov 2023
Requestor Location	Dalhousie University 5850 College Street Sir Charles Tupper Medical Building, 11G Halifax, Nova Scotia, Canada Halifax, NS B3H 4R2 Canada Attn: Dalhousie University
Publisher Tax ID	GB125506730
Total	0.00 USD

Terms and Conditions

STANDARD TERMS AND CONDITIONS FOR REPRODUCTION OF MATERIAL FROM AN OXFORD UNIVERSITY PRESS JOURNAL

1. Use of the material is restricted to the type of use specified in your order details.

2. This permission covers the use of the material in the **English** language in the following territory: *world*. If you have requested additional permission to translate this material, the terms and conditions of this reuse will be set out in clause 12.

3. This permission is limited to the particular use authorized in (1) above and does not allow you to sanction its use elsewhere in any other format other than specified above, nor does it

apply to quotations, images, artistic works etc that have been reproduced from other sources which may be part of the material to be used.

4. No alteration, omission or addition is made to the material without our written consent. Permission **must** be re-cleared with Oxford University Press if/when you decide to reprint.

5. The following credit line appears wherever the material is used: author, title, journal, year, volume, issue number, pagination, by permission of Oxford University Press or the sponsoring society if the journal is a society journal. Where a journal is being published on behalf of a learned society, the details of that society **must** be included in the credit line.

6. For the reproduction of a full article from an Oxford University Press journal for whatever purpose, the corresponding author of the material concerned should be informed of the proposed use. Contact details for the corresponding authors of all Oxford University Press journal contact can be found alongside either the abstract or full text of the article concerned, accessible from www.oxfordjournals.org Should there be a problem clearing these rights, please contact journals.permissions@oup.com

7. If the credit line or acknowledgement in our publication indicates that any of the figures, images or photos was reproduced, drawn or modified from an earlier source it will be necessary for you to clear this permission with the original publisher as well. If this permission has not been obtained, please note that this material cannot be included in your publication/photocopies.

8. While you may exercise the rights licensed immediately upon issuance of the license at the end of the licensing process for the transaction, provided that you have disclosed complete and accurate details of your proposed use, no license is finally effective unless and until full payment is received from you (either by Oxford University Press or by Copyright Clearance Center (CCC)) as provided in CCC's Billing and Payment terms and conditions. If full payment is not received on a timely basis, then any license preliminarily granted shall be deemed automatically revoked and shall be void as if never granted. Further, in the event that you breach any of these terms and conditions or any of CCC's Billing and Payment terms and conditions, the license is automatically revoked and shall be void as if never granted. Use of materials as described in a revoked license, as well as any use of the materials beyond the scope of an unrevoked license, may constitute copyright infringement and Oxford University Press reserves the right to take any and all action to protect its copyright in the materials.

9. This license is personal to you and may not be sublicensed, assigned or transferred by you to any other person without Oxford University Press's written permission.

10. Oxford University Press reserves all rights not specifically granted in the combination of (i) the license details provided by you and accepted in the course of this licensing transaction, (ii) these terms and conditions and (iii) CCC's Billing and Payment terms and conditions.

11. You hereby indemnify and agree to hold harmless Oxford University Press and CCC, and their respective officers, directors, employs and agents, from and against any and all claims arising out of your use of the licensed material other than as specifically authorized pursuant to this license.

12. Unless otherwise specified, inclusion under a Creative Commons license or any other Open Access license allowing onward reuse is prohibited.

13. Where permission to translate has been agreed, the credit line and any copyright/disclaimer notices provided by OUP shall be included on the same page as the Material, translated into the language of the new work, except for trademark names:

Translated and reproduced by permission of Oxford University Press on behalf of the <Society Name>. Translation Disclaimer: OUP and the <Society Name> are not responsible or in any way liable for the accuracy of the translation. The Licensee is solely responsible for the translation in this publication/reprint.

14. Other Terms and Conditions:

v1.5

Questions? customercare@copyright.com.

Mathavarajah, Sabateeshan, and Graham Dellaire. "LINE-1: an emerging initiator of cGAS-STING signalling and inflammation that is dysregulated in disease." *Biochemistry and Cell Biology* (2023). e-First.

This is a License Agreement between Sabateeshan Mathavarajah ("User") and Copyright Clearance Center, Inc. ("CCC") on behalf of the Rightsholder identified in the order details below. The license consists of the order details, the Marketplace Permissions General Terms and Conditions below, and any Rightsholder Terms and Conditions which are included below.

All payments must be made in full to CCC in accordance with the Marketplace Permissions General Terms and Conditions below.

Order Date	12-Oct-2023
Order License ID	1406178-1
ISSN	0829-8211
Type of Use	Republish in a thesis/dissertation
Publisher	Canadian Science Publishing
Portion	Chapter/article

LICENSED CONTENT

Publication Title	Biochemistry and cell biology
Article Title	LINE-1: an emerging initiator of cGAS-STING signalling and inflammation that is dysregulated in disease.
Date	01/01/1986
Language	French
Country	Canada
Rightsholder	Canadian Science Publishing
Publication Type	Journal

REQUEST DETAILS

Portion Type	Chapter/article
Page Range(s)	1-9
Total Number of Pages	9
Format (select all that apply)	Print, Electronic
Who Will Republish the Content?	Academic institution
Duration of Use	Life of current edition
Lifetime Unit Quantity	More than 2,000,000
Rights Requested	Main product
Distribution	Canada
Translation	Original language of publication
Copies for the Disabled?	No
Minor Editing Privileges?	Yes
Incidental Promotional Use?	No
Currency	CAD

NEW WORK DETAILS

Title	The molecular evolution of DEDDh exonucleases reveals novel functions in innate immune signalling
Instructor Name	Sabateeshan Mathavarajah
Institution Name	Dalhousie University
Expected Presentation Date	2023-10-13

ADDITIONAL DETAILS

Order Reference Number	N/A
The Requesting Person/Organization to Appear on the License	Sabateeshan Mathavarajah

REQUESTED CONTENT DETAILS

Title, Description or Numeric Reference of the Portion(s)	LINE-1: an emerging initiator of cGAS-STING signalling and inflammation that is dysregulated in disease
Editor of Portion(s)	Mathavarajah, Sabateeshan; Dellaire, Graham
Volume / Edition	e-First
Page or Page Range of Portion	1-9
Title of the Article/Chapter the Portion Is From	LINE-1: an emerging initiator of cGAS-STING signalling and inflammation that is dysregulated in disease.
Author of Portion(s)	Mathavarajah, Sabateeshan; Dellaire, Graham
Issue, if Republishing an Article From a Serial	N/A
Publication Date of Portion	2023-08-29

Marketplace Permissions General Terms and Conditions

The following terms and conditions ("General Terms"), together with any applicable Publisher Terms and Conditions, govern User's use of Works pursuant to the Licenses granted by Copyright Clearance Center, Inc. ("CCC") on behalf of the applicable Rightsholders of such Works through CCC's applicable Marketplace transactional licensing services (each, a "Service").

1) **Definitions.** For purposes of these General Terms, the following definitions apply:

"License" is the licensed use the User obtains via the Marketplace platform in a particular licensing transaction, as set forth in the Order Confirmation.

"Order Confirmation" is the confirmation CCC provides to the User at the conclusion of each Marketplace transaction. "Order Confirmation Terms" are additional terms set forth on specific Order Confirmations not set forth in the General Terms that can include terms applicable to a particular CCC transactional licensing service and/or any Rightsholder-specific terms.

"Rightsholder(s)" are the holders of copyright rights in the Works for which a User obtains licenses via the Marketplace platform, which are displayed on specific Order Confirmations.

"Terms" means the terms and conditions set forth in these General Terms and any additional Order Confirmation Terms collectively.

"User" or "you" is the person or entity making the use granted under the relevant License. Where the person accepting the Terms on behalf of a User is a freelancer or other third party who the User authorized to accept the General Terms on the User's behalf, such person shall be deemed jointly a User for purposes of such Terms.

"Work(s)" are the copyright protected works described in relevant Order Confirmations.

2) **Description of Service.** CCC's Marketplace enables Users to obtain Licenses to use one or more Works in accordance with all relevant Terms. CCC grants Licenses as an agent on behalf of the copyright rightsholder identified in the relevant Order Confirmation.

3) **Applicability of Terms.** The Terms govern User's use of Works in connection with the relevant License. In the event of any conflict between General Terms and Order Confirmation Terms, the latter shall govern. User acknowledges that Rightsholders have complete discretion whether to grant any permission, and whether to place any limitations on any grant, and that CCC has no right to supersede or to modify any such discretionary act by a Rightsholder.

4) **Representations; Acceptance.** By using the Service, User represents and warrants that User has been duly authorized by the User to accept, and hereby does accept, all Terms.

5) **Scope of License; Limitations and Obligations.** All Works and all rights therein, including copyright rights, remain the sole and exclusive property of the Rightsholder. The License provides only those rights expressly set forth in the terms and conveys no other rights in any Works

6) **General Payment Terms.** User may pay at time of checkout by credit card or choose to be invoiced. If the User chooses to be invoiced, the User shall: (i) remit payments in the manner identified on specific invoices, (ii) unless otherwise specifically stated in an Order Confirmation or separate written agreement, Users shall remit payments upon receipt of the relevant invoice from CCC, either by delivery or notification of availability of the invoice via the Marketplace platform, and (iii) if the User does not pay the invoice within 30 days of receipt, the User may incur a service charge of 1.5% per month or the maximum rate allowed by applicable law, whichever is less. While User may exercise the rights in the License immediately upon receiving the Order Confirmation, the License is automatically revoked and is null and void, as if it had never been issued, if CCC does not receive complete payment on a timely basis.

7) **General Limits on Use.** Unless otherwise provided in the Order Confirmation, any grant of rights to User (i) involves only the rights set forth in the Terms and does not include subsequent or additional uses, (ii) is non-exclusive and non-transferable, and (iii) is subject to any and all limitations and restrictions (such as, but not limited to, limitations on duration of use or circulation) included in the Terms. Upon completion of the licensed use as set forth in the Order Confirmation, User shall either secure a new permission for further use of the Work(s) or immediately cease any new use of the Work(s) and shall render inaccessible (such as by deleting or by removing or severing links or other locators) any further copies of the Work. User may only make alterations to the Work if and as expressly set forth in the Order Confirmation. No Work may be used in any way that is unlawful, including without limitation if such use would violate applicable sanctions laws or regulations, would be defamatory, violate the rights of third parties (including such third parties' rights of copyright, privacy, publicity, or other tangible or intangible property), or is otherwise illegal, sexually explicit, or obscene. In addition, User may not conjoin a Work with any other material that may result in damage to the reputation of the Rightsholder. Any unlawful use will render any licenses hereunder null and void. User agrees to inform CCC if it becomes aware of any infringement of any rights in a Work and to cooperate with any reasonable request of CCC or the Rightsholder in connection therewith.

8) **Third Party Materials.** In the event that the material for which a License is sought includes third party materials (such as photographs, illustrations, graphs, inserts and similar materials) that are identified in such material as having been used by permission (or a similar indicator), User is responsible for identifying, and seeking separate licenses (under this Service, if available, or otherwise) for any of such third party materials; without a separate license, User may not use such third party materials via the License.

9) **Copyright Notice.** Use of proper copyright notice for a Work is required as a condition of any License granted under the Service. Unless otherwise provided in the Order Confirmation, a proper copyright notice will read substantially as follows: "Used with permission of [Rightsholder's name], from [Work's title, author, volume, edition number and year of copyright]; permission conveyed through Copyright Clearance Center, Inc." Such notice must be provided in a reasonably legible font size and must be placed either on a cover page or in another location that any person, upon gaining access to the material which is the subject of a permission, shall see, or in the case of republication Licenses, immediately adjacent to the Work as used (for example, as part of a by-line or footnote) or in the place where substantially all other credits or notices for the new work containing the republished Work are located. Failure to include the required notice results in loss to the Rightsholder and CCC, and the User shall be liable to pay liquidated damages for each such failure equal to twice the use fee specified in the Order Confirmation, in addition to the use fee itself and any other fees and charges specified.

10) **Indemnity.** User hereby indemnifies and agrees to defend the Rightsholder and CCC, and their respective employees and directors, against all claims, liability, damages, costs, and expenses, including legal fees and expenses, arising out of any use of a Work beyond the scope of the rights granted herein and in the Order Confirmation, or any use of a Work which has been altered in any unauthorized way by User, including claims of defamation or infringement of rights of copyright, publicity, privacy, or other tangible or intangible property.

11) **Limitation of Liability.** UNDER NO CIRCUMSTANCES WILL CCC OR THE RIGHTSHOLDER BE LIABLE FOR ANY DIRECT, INDIRECT, CONSEQUENTIAL, OR INCIDENTAL DAMAGES (INCLUDING WITHOUT LIMITATION DAMAGES FOR LOSS OF BUSINESS PROFITS OR INFORMATION, OR FOR BUSINESS INTERRUPTION) ARISING OUT OF THE USE OR INABILITY TO USE A WORK, EVEN IF ONE OR BOTH OF THEM HAS BEEN ADVISED OF THE POSSIBILITY OF SUCH DAMAGES. In any event, the total liability of the Rightsholder and CCC (including their respective employees and directors) shall not exceed the total amount actually paid by User for the relevant License. User assumes full liability for the actions and omissions of its principals, employees, agents, affiliates, successors, and assigns.

12) **Limited Warranties.** THE WORK(S) AND RIGHT(S) ARE PROVIDED "AS IS." CCC HAS THE RIGHT TO GRANT TO USER THE RIGHTS GRANTED IN THE ORDER CONFIRMATION DOCUMENT. CCC AND THE RIGHTSHOLDER DISCLAIM ALL OTHER WARRANTIES RELATING TO THE WORK(S) AND RIGHT(S), EITHER EXPRESS OR IMPLIED, INCLUDING WITHOUT LIMITATION IMPLIED WARRANTIES OF MERCHANTABILITY OR FITNESS FOR A PARTICULAR PURPOSE. ADDITIONAL RIGHTS MAY BE REQUIRED TO USE ILLUSTRATIONS, GRAPHS, PHOTOGRAPHS, ABSTRACTS, INSERTS, OR OTHER PORTIONS OF THE WORK (AS OPPOSED TO THE ENTIRE WORK) IN A MANNER CONTEMPLATED BY USER; USER UNDERSTANDS AND AGREES THAT NEITHER CCC NOR THE RIGHTSHOLDER MAY HAVE SUCH ADDITIONAL RIGHTS TO GRANT.

13) **Effect of Breach.** Any failure by User to pay any amount when due, or any use by User of a Work beyond the scope of the License set forth in the Order Confirmation and/or the Terms, shall be a material breach of such License. Any breach not cured within 10 days of written notice thereof shall result in immediate termination of such License without further notice. Any unauthorized (but licensable) use of a Work that is terminated immediately upon notice thereof may be liquidated by payment of the Rightsholder's ordinary license price therefor; any unauthorized (and unlicensable) use that is not terminated immediately for any reason (including, for example, because materials containing the Work cannot reasonably be recalled) will be subject to all remedies available at law or in equity, but in no event to a payment of less than three times the Rightsholder's ordinary license price for the most closely analogous licensable use plus Rightsholder's and/or CCC's costs and expenses incurred in collecting such payment.

14) **Additional Terms for Specific Products and Services.** If a User is making one of the uses described in this Section 14, the additional terms and conditions apply:

a) ***Print Uses of Academic Course Content and Materials (photocopies for academic coursepacks or classroom handouts).*** For photocopies for academic coursepacks or classroom handouts the following additional terms apply:

i) The copies and anthologies created under this License may be made and assembled by faculty members individually or at their request by on-campus bookstores or copy centers, or by off-campus copy shops and other similar entities.

ii) No License granted shall in any way: (i) include any right by User to create a substantively non-identical copy of the Work or to edit or in any other way modify the Work (except by means of deleting material immediately preceding or following the entire portion of the Work copied) (ii) permit "publishing ventures" where any particular anthology would be systematically marketed at multiple institutions.

iii) Subject to any Publisher Terms (and notwithstanding any apparent contradiction in the Order Confirmation arising from data provided by User), any use authorized under the academic pay-per-use service is limited as follows:

A) any License granted shall apply to only one class (bearing a unique identifier as assigned by the institution, and thereby including all sections or other subparts of the class) at one institution;

B) use is limited to not more than 25% of the text of a book or of the items in a published collection of essays, poems or articles;

C) use is limited to no more than the greater of (a) 25% of the text of an issue of a journal or other periodical or (b) two articles from such an issue;

D) no User may sell or distribute any particular anthology, whether photocopied or electronic, at more than one institution of learning;

E) in the case of a photocopy permission, no materials may be entered into electronic memory by User except in order to produce an identical copy of a Work before or during the academic term (or analogous period) as to which any particular permission is granted. In the event that User shall choose to retain materials that are the subject of a photocopy permission in electronic memory for purposes of producing identical copies more than one day after such retention (but still within the scope of any permission granted), User must notify CCC of such fact in the applicable permission request and such retention shall constitute one copy actually sold for purposes of calculating permission fees due; and

F) any permission granted shall expire at the end of the class. No permission granted shall in any way include any right by User to create a substantively non-identical copy of the Work or to edit or in any other way modify the Work (except by means of deleting material immediately preceding or following the entire portion of the Work copied).

iv) Books and Records; Right to Audit. As to each permission granted under the academic pay-per-use Service, User shall maintain for at least four full calendar years books and records sufficient for CCC to determine the numbers of copies made by User under such permission. CCC and any representatives it may designate shall have the right to audit such books and records at any time during User's ordinary business hours, upon two days' prior notice. If any such audit shall determine that User shall have underpaid for, or underreported, any photocopies sold or by three percent (3%) or more, then User shall bear all the costs of any such audit; otherwise, CCC shall bear the costs of any such audit. Any amount determined by such audit to have been underpaid by User shall immediately be paid to CCC by User, together with interest thereon at the rate of 10% per annum from the date such amount was originally due. The provisions of this paragraph shall survive the termination of this License for any reason.

b) ***Digital Pay-Per-Uses of Academic Course Content and Materials (e-coursepacks, electronic reserves, learning management systems, academic institution intranets).*** For uses in e-coursepacks, posts in electronic reserves, posts in learning management systems, or posts on academic institution intranets, the following additional terms apply:

i) The pay-per-uses subject to this Section 14(b) include:

A) **Posting e-reserves, course management systems, e-coursepacks for text-based content,** which grants authorizations to import requested material in electronic format, and allows electronic access to this material to members of a designated college or university class, under the direction of an instructor designated by the college or university, accessible only under appropriate electronic controls (e.g., password);

B) **Posting e-reserves, course management systems, e-coursepacks for material consisting of photographs or other still images not embedded in text,** which grants not only the authorizations described in Section 14(b)(i)(A) above, but also the following authorization: to include the requested material in course materials for use consistent with Section 14(b)(i)(A) above, including any necessary resizing, reformatting or modification of the resolution of such requested material (provided that such modification does not alter the underlying editorial content or meaning of the requested material, and provided that the resulting modified content is used solely within the scope of, and in a manner consistent with, the particular authorization described in the Order Confirmation and the Terms), but not including any other form of manipulation, alteration or editing of the requested material;

C) **Posting e-reserves, course management systems, e-coursepacks or other academic distribution for audiovisual content,** which grants not only the authorizations described in Section 14(b)(i)(A) above, but also the following authorizations: (i) to include the requested material in course materials for use consistent with Section 14(b)(i)(A) above; (ii) to display and perform the requested material to such members of such class in the physical classroom or remotely by means of streaming media or other video formats; and (iii) to "clip" or reformat the requested material for purposes of time or content management or ease of delivery, provided that such "clipping" or reformatting does not alter the underlying editorial content or meaning of the requested material and that the resulting material is used solely within the scope of, and in a manner consistent with, the particular authorization described in the Order Confirmation and the Terms. Unless expressly set forth in the relevant Order Conformation, the License does not authorize any other form of manipulation, alteration or editing of the requested material.

ii) Unless expressly set forth in the relevant Order Confirmation, no License granted shall in any way: (i) include any right by User to create a substantively non-identical copy of the Work or to edit or in any other way modify the Work (except by means of deleting material immediately preceding or following the entire portion of the Work copied or, in the case of Works subject to Sections 14(b)(1)(B) or (C) above, as described in such Sections) (ii) permit "publishing ventures" where any particular course materials would be systematically marketed at multiple institutions.

iii) Subject to any further limitations determined in the Rightsholder Terms (and notwithstanding any apparent contradiction in the Order Confirmation arising from data provided by User), any use authorized under the electronic course content pay-per-use service is limited as follows:

A) any License granted shall apply to only one class (bearing a unique identifier as assigned by the institution, and thereby including all sections or other subparts of the class) at one institution;

B) use is limited to not more than 25% of the text of a book or of the items in a published collection of essays, poems or articles;

C) use is limited to not more than the greater of (a) 25% of the text of an issue of a journal or other periodical or (b) two articles from such an issue;

D) no User may sell or distribute any particular materials, whether photocopied or electronic, at more than one institution of learning;

E) electronic access to material which is the subject of an electronic-use permission must be limited by means of electronic password, student identification or other control permitting access solely to students and instructors in the class;

F) User must ensure (through use of an electronic cover page or other appropriate means) that any person, upon gaining electronic access to the material, which is the subject of a permission, shall see:

- a proper copyright notice, identifying the Rightsholder in whose name CCC has granted permission,
- a statement to the effect that such copy was made pursuant to permission,
- a statement identifying the class to which the material applies and notifying the reader that the material has been made available electronically solely for use in the class, and
- a statement to the effect that the material may not be further distributed to any person outside the class, whether by copying or by transmission and whether electronically or in paper form, and User must also ensure that such cover page or other means will print out in the event that the person accessing the material chooses to print out the material or any part thereof.

G) any permission granted shall expire at the end of the class and, absent some other form of authorization, User is thereupon required to delete the applicable material from any electronic storage or to block electronic access to the applicable material.

iv) Uses of separate portions of a Work, even if they are to be included in the same course material or the same university or college class, require separate permissions under the electronic course content pay-per-use Service. Unless otherwise provided in the Order Confirmation, any grant of rights to User is limited to use completed no later than the end of the academic term (or analogous period) as to which any particular permission is granted.

v) Books and Records; Right to Audit. As to each permission granted under the electronic course content Service, User shall maintain for at least four full calendar years books and records sufficient for CCC to determine the numbers of copies made by User under such permission. CCC and any representatives it may designate shall have the right to audit such books and records at any time during User's ordinary business hours, upon two days' prior notice. If any such audit shall determine that User shall have underpaid for, or underreported, any electronic copies used by three percent (3%) or more, then User shall bear all the costs of any such audit; otherwise, CCC shall bear the costs of any such audit. Any amount determined by such audit to have been underpaid by User shall immediately be paid to CCC by User, together with interest thereon at the rate of 10% per annum from the date such amount was originally due. The provisions of this paragraph shall survive the termination of this license for any reason.

c) ***Pay-Per-Use Permissions for Certain Reproductions (Academic photocopies for library reserves and interlibrary loan reporting) (Non-academic internal/external business uses and commercial document delivery).*** The License expressly excludes the uses listed in Section (c)(i)-(v) below (which must be subject to separate license from the applicable Rightsholder) for: academic photocopies for library reserves and interlibrary loan reporting; and non-academic internal/external business uses and commercial document delivery.

i) electronic storage of any reproduction (whether in plain-text, PDF, or any other format) other than on a transitory basis;

ii) the input of Works or reproductions thereof into any computerized database;

iii) reproduction of an entire Work (cover-to-cover copying) except where the Work is a single article;

iv) reproduction for resale to anyone other than a specific customer of User;

v) republication in any different form. Please obtain authorizations for these uses through other CCC services or directly from the rightsholder.

Any license granted is further limited as set forth in any restrictions included in the Order Confirmation and/or in these Terms.

d) ***Electronic Reproductions in Online Environments (Non-Academic-email, intranet, internet and extranet).*** For "electronic reproductions", which generally includes e-mail use (including instant messaging or other electronic transmission to a defined group of recipients) or posting on an intranet, extranet or Intranet site (including any display or performance incidental thereto), the following additional terms apply:

i) Unless otherwise set forth in the Order Confirmation, the License is limited to use completed within 30 days for any use on the Internet, 60 days for any use on an intranet or extranet and one year for any other use, all as measured from the "republication date" as identified in the Order Confirmation, if any, and otherwise from the date of the Order Confirmation.

i) Unless otherwise set forth in the Order Confirmation, the License is limited to use completed within 30 days for any use on the Internet, 60 days for any use on an intranet or extranet and one year for any other use, all as measured from the "republication date" as identified in the Order Confirmation, if any, and otherwise from the date of the Order Confirmation.

ii) User may not make or permit any alterations to the Work, unless expressly set forth in the Order Confirmation (after request by User and approval by Rightsholder); provided, however, that a Work consisting of photographs or other still images not embedded in text may, if necessary, be resized, reformatted or have its resolution modified without additional express permission, and a Work consisting of audiovisual content may, if necessary, be "clipped" or reformatted for purposes of time or content management or ease of delivery (provided that any such resizing, reformatting, resolution modification or "clipping" does not alter the underlying editorial content or meaning of the Work used, and that the resulting material is used solely within the scope of, and in a manner consistent with, the particular License described in the Order Confirmation and the Terms.

15) **Miscellaneous.**

a) User acknowledges that CCC may, from time to time, make changes or additions to the Service or to the Terms, and that Rightsholder may make changes or additions to the Rightsholder Terms. Such updated Terms will replace the prior terms and conditions in the order workflow and shall be effective as to any subsequent Licenses but shall not apply to Licenses already granted and paid for under a prior set of terms.

b) Use of User-related information collected through the Service is governed by CCC's privacy policy, available online at www.copyright.com/about/privacy-policy/.

c) The License is personal to User. Therefore, User may not assign or transfer to any other person (whether a natural person or an organization of any kind) the License or any rights granted thereunder; provided, however, that, where applicable, User may assign such License in its entirety on written notice to CCC in the event of a transfer of all or substantially all of User's rights in any new material which includes the Work(s) licensed under this Service.

d) No amendment or waiver of any Terms is binding unless set forth in writing and signed by the appropriate parties, including, where applicable, the Rightsholder. The Rightsholder and CCC hereby object to any terms contained in any writing prepared by or on behalf of the User or its principals, employees, agents or affiliates and purporting to govern or otherwise relate to the License described in the Order Confirmation, which terms are in any way inconsistent with any Terms set forth in the Order Confirmation, and/or in CCC's standard operating procedures, whether such writing is prepared prior to, simultaneously with or subsequent to the Order Confirmation, and whether such writing appears on a copy of the Order Confirmation or in a separate instrument.

e) The License described in the Order Confirmation shall be governed by and construed under the law of the State of New York, USA, without regard to the principles thereof of conflicts of law. Any case, controversy, suit, action, or proceeding arising out of, in connection with, or related to such License shall be brought, at CCC's sole discretion, in any federal or state court located in the County of New York, State of New York, USA, or in any federal or state court whose geographical jurisdiction covers the location of the Rightsholder set forth in the Order Confirmation. The parties expressly submit to the personal jurisdiction and venue of each such federal or state court.

Last updated October 2022